Universiteit Leiden
The Netherlands

The good? The bad? The mutant! Characterization of cancer-related somatic mutations and identification of a selectivity hotspot in adenosine receptor
Wang, X.

The Good? The Bad? The Mutant!

Characterization of cancer-related somatic mutations and identification of a selectivity hotspot in adenosine receptors

The Good? The Bad? The Mutant!

Characterization of cancer-related somatic mutations and identification of a selectivity hotspot in adenosine receptors

Proefschrift

ter verkrijging van de graad van doctor aan de Universiteit Leiden,

op gezag van rector magnificus prof.dr.ir. H. Bijl,

volgens besluit van het college voor promoties

te verdedigen op dinsdag 20 september 2022

klokke 16.15 uur

door

Xuesong Wang

geboren te Xi'an, Shaanxi, China

in 1992

Promotores:

Prof. dr. A.P. IJzerman

Prof. dr. L.H. Heitman

Prof. dr. G.J.P. van Westen

Promotiecommissie:

Prof. dr. H. Irth

Prof. dr. J.A. Bouwstra

Prof. dr. E.H.J. Danen

Prof. dr. K. Ye (Xi'an Jiaotong University)

Dr. L. May (Monash University)

Dr. M.H. Siderius (VU Amsterdam)

Contents

Chapter 1

General Introduction

G protein-coupled receptors (GPCRs) are a family of membrane-bound proteins with approximately 800 members that have seven-transmembrane (7-TM) domains, an extracellular amino terminus and an intracellular carboxyl terminus[1,2]. According to sequence homology and phylogenetic analysis, human GPCRs can be classified into 5 main families, glutamate family (class C), rhodopsin family (class A), adhesion family, frizzled/taste2 and secretin family (class B), shorten as GRAFS[2,3]. The majority of GPCRs belongs to the class A subfamily resembling the visual pigment rhodopsin. GPCRs are responsive to a diverse set of physiological endogenous ligands including hormones and neurotransmitters. Upon activation, GPCRs induce a signal transduction cascade inside the cell via heterotrimeric G proteins, which consist of three subunits, α, β and γ[4,5]. Due to the various GPCR binding domains and their sensitivities to a diverse array of ligands, these proteins have shown to be very 'druggable' as they are the main target for an estimated 30% of approved drugs[6].

Mutations occurring in GPCRs can severely alter their normal function, including cell surface expression, basal activity, ligand binding and receptor – G protein interaction (Figure 1)[7], and may ultimately trigger their physiological roles to pathological ones. Mutations in 55 GPCR genes have been reported as causal link to 66 human monogenic diseases[8]. Different diseases can result from a single GPCR gene, due to the possibility of inactivating and activating mutations. Therapeutical approaches have been developed for the treatment of pathologies caused by GPCR malfunctions. For instance, symptomatic therapies with pharmacological and/or surgical intervention have been established to aim at the symptoms of the GPCR variants-linked diseases[9,10]. In addition, direct targeting of malfunctional GPCRs via genome editing approaches or small molecules could also be suitable strategies toward personalized therapeutics in GPCR pathologies[11,12]. Genetic variants in drug-targeted GPCRs, especially variants located in functional sites of GPCR structures, have been identified with altered drug responses[13]. Therefore, characterization of these GPCR variants is of great importance with respect to possibly impaired drug efficacy and undesired side effects.

In preclinical oncology the primary focus has mostly been on kinases due to their central role in the cell cycle[4,14]. However, a growing body of evidence shows a prominent role of GPCRs in all phases of cancer. Malignant cells can e.g., hijack GPCRs to increase proliferation or metastasis formation to distant tissue (Figure 2)[14]. In addition to an increased understanding of the role of GPCRs in cancer, recent investigations have shown that these proteins, present in patient isolates, are sensitive to mutation[15,16]. More specifically, it has been found that GPCRs are the second most mutated protein class with a mutations frequency of an estimated 20% of all cancers[17]. Higher mutations rates are often observed for certain conserved residues, and given the (evolutionary) importance of these residues the exact impact of these mutations in receptor pharmacology warrants considerable investigation[17,18].

1

One particular class of rhodopsin-like GPCRs included in this thesis are the adenosine receptors (ARs). This GPCR family consists of 4 subtypes, A_1AR, $A_{2A}AR$, $A_{2B}AR$, and A_3AR, which share the common local hormone adenosine as ligand[19]. Adenosine is a purine nucleoside that serves several important roles in a physiological context including DNA synthesis, a precursor in energy transfer (adenosine tri-phosphate, ATP) and secondary messenger (cyclic adenosine monophosphate, cAMP)[20]. Activation of A_1AR and A_3AR inhibits the activity of adenylyl cyclase via the $G_{\alpha i}$ protein, leading to decreased levels of intracellular cAMP[21,22]. The $A_{2A}AR$ and $A_{2B}AR$ are coupled to the $G_{\alpha s}$ protein upon activation, resulting in an increased production of intracellular cAMP[23,24]. The adenosine receptors are expressed throughout the body and are under investigation as drug targets in different disorders, including Parkinson's disease and Alzheimer's disease[25–27]. However, these GPCRs are also of interest in the context of cancer research due to the evidence of adenosine accumulation in the tumor microenvironment[28], which has been supported by several studies in immune cells[29]. In short, all the adenosine receptors might be targets for the development of novel approaches to the treatment of cancer, which will be further elaborated on in **Chapter 3** of this thesis.

Combining background knowledge on the role of GPCRs in cancer with the increased understanding of mutational patterns, it stands to reason that targeting GPCRs with drugs may have a beneficial effect on cancer in patients in general. More specifically, the group of adenosine receptors might form an interesting focus area for cancer treatment via GPCRs. For each of the four subtypes, a number of somatic mutations have been identified in patient isolates.
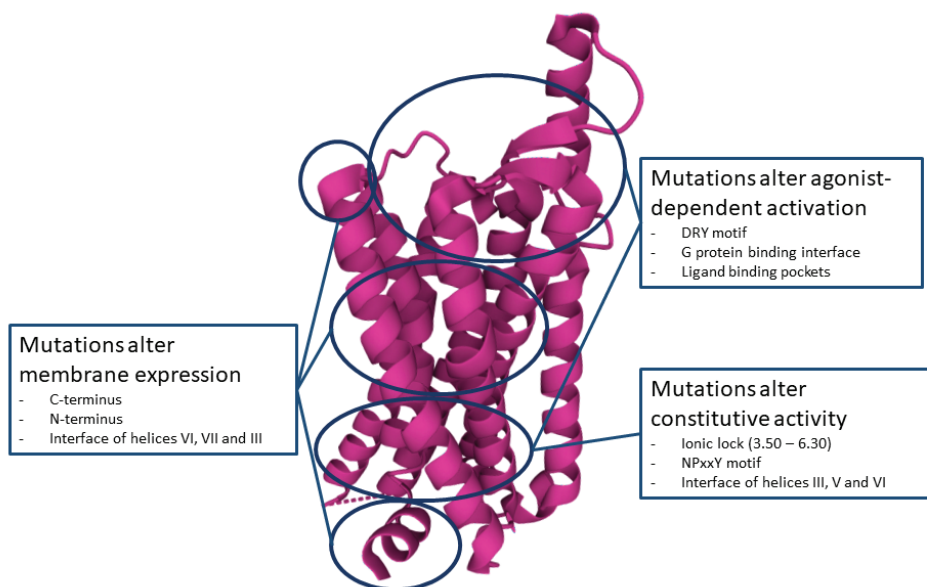
Figure 1. General consequences of class A GPCR mutations in receptor pharmacology. The 3D structure is adapted from A_1AR (PDB 7LD4).
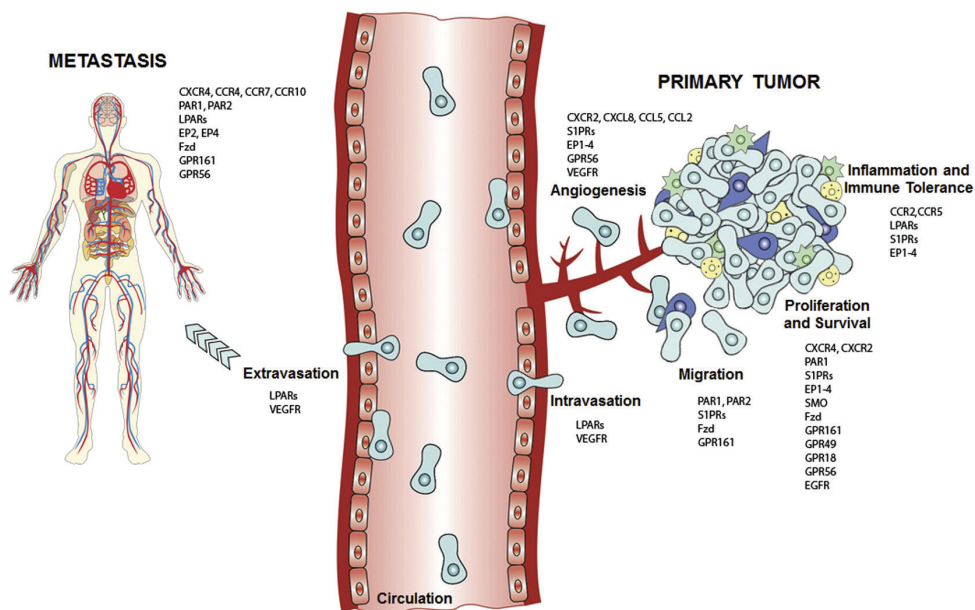

Figure 2. Examples of GPCRs and their roles in cancer progression[30]. Reproduced with permission.

Aim and outline of this thesis

To establish the role of cancer-related AR mutations at the molecular level in this thesis, we decided to express and study these in a yeast strain devoid of GPCRs and in some cases in a mammalian cell system. Here, we examined them using reference adenosine receptor ligands on receptor activation and ligand binding, and determined the impact mutations have on these pharmacological readouts.

Chapter 2 summarizes the strategies of using yeast systems in human GPCR studies with a focus on adenosine receptors. **Chapter 3** provides an overview of GPCRs and their mutations involved in cancer progression. Furthermore, evidence for adenosine receptors in cancer development is discussed in detail. As mutations of adenosine receptor have been identified from cancer patient isolates, **Chapter 4**, **5** and **6** provide information on the impact of these mutations in receptor functionality. **Chapter 4** focuses on receptor expression and activation of A_{2B} receptors using the engineered yeast system. The effects of cancer-related mutations in A_1 receptors on receptor activation and ligand binding are described in **Chapter 5** and **6**. **Chapter 5** describes mutations located at the loop regions, while **Chapter 6** focuses on mutations positioned in the 7-TM domains. **Chapter 7** reports the approach for the identification of a stereoselectivity hotspot in A_{2B} receptor antagonist recognition from both computational and experimental aspects. Finally, **Chapter 8** summarizes the results of the work described in this thesis, as well as future prospects and challenges that emerge from this thesis. Hopefully, this thesis will enrich the view of cancer-related mutations in GPCR pharmacology and ultimately contribute to novel strategies for the modulation of their activity using medicinal products.

References

1. Vassilatis, D. K. *et al.* The G protein-coupled receptor repertoires of human and mouse. *Proc. Natl. Acad. Sci.* **100**, 4903–4908 (2003).
2. Fredriksson, R., Lagerström, M. C., Lundin, L.-G. & Schiöth, H. B. The G-protein-coupled receptors in the human genome form five main families. Phylogenetic analysis, paralogon groups, and fingerprints. *Mol. Pharmacol.* **63**, 1256–72 (2003).
3. Kolakowski, L. F. J. GCRDb: a G-protein-coupled receptor database. *Receptors Channels* **2**, 1–7 (1994).
4. Lefkowitz, R. J., Cotecchia, S., Samama, P. & Costa, T. Constitutive activity of receptors coupled to guanine nucleotide regulatory proteins. *Trends Pharmacol. Sci.* **14**, 303–307 (1993).
5. Dorsam, R. T. & Gutkind, J. S. G-protein-coupled receptors and cancer. *Nat. Rev. Cancer* **7**, 79–94 (2007).
6. Overington, J. P., Al-Lazikani, B. & Hopkins, A. L. How many drug targets are there? *Nat. Rev. Drug Discov.* **5**, 993–996 (2006).
7. Stoy, H. & Gurevich, V. V. How genetic errors in GPCRs affect their function: Possible therapeutic strategies. *Genes Dis.* **2**, 108–132 (2015).
8. Schöneberg, T. & Liebscher, I. Mutations in g protein–coupled receptors: Mechanisms, pathophysiology and potential therapeutic approaches. *Pharmacol. Rev.* **73**, 89–119 (2021).
9. Bautista, R. M. *et al.* Cutaneous pharmacologic cAMP induction induces melanization of the skin and improves recovery from ultraviolet injury in melanocortin 1 receptor-intact or heterozygous skin. *Pigment Cell Melanoma Res.* **33**, 30–40 (2020).
10. Olesen, E. T. B., Rützler, M. R., Moeller, H. B., Praetorius, H. A. & Fenton, R. A. Vasopressin-independent targeting of aquaporin-2 by selective E-prostanoid receptor agonists alleviates nephrogenic diabetes insipidus. *Proc. Natl. Acad. Sci. U. S. A.* **108**, 12949–12954 (2011).
11. Bradley, E. C. *et al.* In vivo identification of small molecules mediating gpr126/adgrg6 signaling during schwann cell development. in *Annals of the New York Academy of Sciences* **1456**, 44–63 (Blackwell Publishing Inc., 2019).
12. O'Reilly, M. *et al.* RNA interference-mediated suppression and replacement of human rhodopsin in vivo. *Am. J. Hum. Genet.* **81**, 127–135 (2007).
13. Hauser, A. S. *et al.* Pharmacogenomics of GPCR Drug Targets. *Cell* **172**, 41-54.e19 (2018).
14. Lappano, R. & Maggiolini, M. GPCRs and cancer. *Acta Pharmacol. Sin.* **33**, 351–362 (2012).

15. Watson, I. R., Takahashi, K., Futreal, P. A. & Chin, L. Emerging patterns of somatic mutations in cancer. *Nat. Rev. Genet.* **14**, 703–18 (2013).
16. Kan, Z. *et al.* Diverse somatic mutation patterns and pathway alterations in human cancers. *Nature* **466**, 869–73 (2010).
17. O'Hayre, M. *et al.* The emerging mutational landscape of G proteins and G-protein-coupled receptors in cancer. *Nat. Rev. Cancer* **13**, 412–24 (2013).
18. Finch, A. M., Sarramegna, V. & Graham, R. M. Ligand Binding, Activation, and Agonist Trafficking. in *The Adrenergic Receptors* 25–85 (Humana Press, 2006). doi:10.1385/1-59259-931-1:025
19. Fredholm, B. B., IJzerman, A. P., Jacobson, K. a, Linden, J. & Müller, C. E. International Union of Basic and Clinical Pharmacology. LXXXI. Nomenclature and Classification of Adenosine Receptors—An Update. *Pharmacol. Rev.* **63**, 1–34 (2011).
20. Knowles, J. R. Enzyme-Catalyzed Phosphoryl Transfer Reactions. *Annu. Rev. Biochem.* **49**, 877–919 (1980).
21. Freund, S., Ungerer, M. & Lohse, M. J. A_1 adenosine receptors expressed in CHO-cells couple to adenylyl cyclase and to phospholipase C. *Naunyn. Schmiedebergs. Arch. Pharmacol.* **350**, 49–56 (1994).
22. Zhou, Q.-Y. *et al.* Molecular cloning and characterization of an adenosine receptor: the A_3 adenosine receptor. *Proc. Natl. Acad. Sci.* **89**, 7432–7436 (1992).
23. Schulte, G. & Fredholm, B. B. The Gs-coupled adenosine A_{2B} receptor recruits divergent pathways to regulate ERK1/2 and p38□. *Exp. Cell Res.* **290**, 168–176 (2003).
24. Hirano, D. *et al.* Functional coupling of adenosine A_{2a} receptor to inhibition of the mitogen-activated protein kinase cascade in Chinese hamster ovary cells. *Biochem. J.* **316**, 81–86 (1996).
25. Fredholm, B. B. Adenosine receptors as drug targets. *Exp. Cell Res.* **316**, 1284–1288 (2010).
26. Laurent, C. *et al.* A_{2A} adenosine receptor deletion is protective in a mouse model of Tauopathy. *Mol. Psychiatry* **21**, 97–107 (2016).
27. Cellai, L. *et al.* The adenosinergic signaling: A complex but promising therapeutic target for Alzheimer's disease. *Front. Neurosci.* **12**, 1–9 (2018).
28. Gessi, S., Merighi, S., Sacchetto, V., Simioni, C. & Borea, P. A. Adenosine receptors and cancer. *Biochim. Biophys. Acta* **1808**, 1400–1412 (2011).
29. Merighi, S. *et al.* A glance at adenosine receptors: novel target for antitumor therapy. *Pharmacol. Ther.* **100**, 31–48 (2003).
30. Nieto Gutierrez, A. & McDonald, P. H. GPCRs: Emerging anti-cancer drug targets. *Cell. Signal.* **41**, 65–74 (2018).

Chapter 2

G protein-coupled receptors expressed and studied in yeast.
The adenosine receptor as prime example.

Abstract

G protein-coupled receptors (GPCRs) are the largest class of membrane proteins with around 800 members in the human genome/proteome. Extracellular signals such as hormones and neurotransmitters regulate various biological processes via GPCRs, with GPCRs being the bodily target of 30–40% of current drugs on the market. Complete identification and understanding of GPCR functionality will provide opportunities for novel drug discovery. Yeast expresses three different endogenous GPCRs regulating pheromone and sugar sensing, with the pheromone pathway offering perspectives for the characterization of heterologous GPCR signaling. Moreover, yeast offers a "null" background for studies on mammalian GPCRs, including GPCR activation and signaling, ligand identification, and characterization of disease-related mutations. This review focuses on modifications of the yeast pheromone signaling pathway for functional GPCR studies, and on opportunities and usage of the yeast system as a platform for human GPCR studies. Finally, this review discusses in some further detail studies of adenosine receptors heterologously expressed in yeast.

Introduction

G protein-coupled receptors (GPCRs) are the largest family of membrane-bound proteins with approximately 800 members identified from the human genome[1,2]. They share a common basic architecture of seven-transmembrane (7TM) α-helices, linked by three intracellular (IL) and three extracellular (EL) loops, an extracellular amino terminus, and an intracellular carboxyl terminus[2]. According to their sequence homology, human GPCRs can be classified into five main families according to the GRAFS system: glutamate, rhodopsin, adhesion, frizzled/taste, and secretin[3]. Alternatively, GPCRs are divided in three main classes (A, B, and C)[4].

GPCRs respond to a wide diversity of extracellular endogenous ligands, including neurotransmitters and hormones. Intracellularly, GPCRs are coupled to different families of heterotrimeric G proteins, which contain three subunits, α, β, and γ[2]. Upon extracellular stimulation, conformational changes in GPCRs leads to the replacement of GDP for GTP at the G_α subunit resulting in the dissociation of the $G_{\beta\gamma}$ subunit from G_α and further interactions with effector proteins in the cell[5,6]. Based on sequence similarity and functionality, the G_α-subunit family is divided into four major subfamilies, $G_{\alpha s}$, $G_{\alpha i}$, $G_{\alpha q/11}$ and $G_{\alpha 12/13}$[7,8].

GPCRs play a crucial role in human physiology due to their abundant distribution and numerous GPCR-related downstream pathways. Moreover, they are substantially involved in human pathophysiology[6]. During the past decades, GPCRs have thus been investigated as pharmacological targets with the focus on their extracellular ligand binding site[9]. The major disease indications for GPCR modulators have shifted over the years from high blood pressure to metabolic diseases, as well as several central nervous system disorders, and more recently also to tumor initiation and progression[6–8,10–12]. Their role in both physiological and pathophysiological conditions have made GPCRs the target of approximately 30% of therapeutic drugs to date[9]. Thereby, ongoing further characterization of GPCR functionality will offer new opportunities for drug discovery. However, due to the complexity of mammalian GPCR signaling pathways, using mammalian cells as the host for investigating GPCR signaling is relatively time-consuming and can result in ambiguous output. The latter can be problematic due to the wide distribution and variety of endogenous receptors and their ligands in such cells, and also expensive. In this case, engineered yeast systems provide a relatively cost-effective and useful model system to analyze human GPCRs.

In this review, we will discuss strategies to link human GPCR expression and functionality to the endogenous yeast pheromone mating pathway in *Saccharomyces cerevisiae* (*S. cerevisiae*) as well as expression strategies in *Pichia Pastoris* (*P. pastoris*). Finally, we will focus on functional studies on adenosine receptor signaling using yeast reporter systems.

General features of yeast

Among the many yeast species *S. cerevisiae* and *P. pastoris* have been genetically well characterized as a model system. The first crystal structures of recombinant mammalian membrane proteins were obtained by their overexpression in these two yeast species[13,14]. Since then, yeast expression has been frequently used for harvesting, purifying and subsequently obtaining crystal structures of membrane proteins deposited in the ProteinDataBank[15].

P. pastoris, as a recombinant expression host system, is an engineered methylotrophic microorganism using methanol as carbon and energy source[16]. The strain Y-11430 (wild-type) is not used for heterologous protein expression due to low transformation efficiency, while the GS115 strain is one of the most commonly used expression systems particularly for industry[17]. The *P. pastoris* system shows high similarity to advanced eukaryotic expression systems like CHO and HEK293 cell lines, as cotranslational and posttranslational modifications also occur[18]. However, this inexpensive yeast system constitutes a more rapid expression platform, and *P. pastoris* does not overglycosylate therapeutic proteins in comparison to *S. cerevisiae*[18].

The budding yeast *S. cerevisiae* expresses three different endogenous GPCRs involved in sugar and pheromone sensing[19]. Glucose sensing is mediated via the yeast G protein-coupled receptor-1 (Gpr1) and the G_α protein Gpa2 (Figure 1A)[20,21], and pheromone sensing via GPCRs α-factor receptor (Ste2) and a-factor receptor (Ste3), as well as the G_α protein Gpa1 (Figure 1B)[22]. During the past decades the yeast pheromone pathway has been the most extensively studied GPCR signaling cascade[23,24]. Similar to mammalian GPCR signaling, Ste2 or Ste3, couples to the yeast trimeric G protein upon activation by a- or α-factor pheromones, consisting of Gpa1(α subunit), Ste4 (β subunit) and Ste18 (γ subunit)[19,25]. Activation of the receptor results in the dissociation of the βγ-dimer from the α-subunit. The βγ-dimer further couples and induces mating-specific responses by activating the mitogen-activated protein kinase (MAPK) signaling cascade[26]. Ultimately, the translocation of the transcription factor Ste12 mediated by activation of the MAPK cascade further regulates the expression of numerous mating pathway target promotors[27–29]. Based on the similarity between the yeast mating pathway and mammalian GPCR signaling pathways, human GPCRs have been expressed and further coupled to a reporter gene output in order to more broadly study GPCR signaling[23].

Modifications in engineered yeast system

Yeast has been used as a vehicle for more than three decades for the structural and functional characterization of endogenously and heterologously expressed GPCRs[23,30,31], for the discovery of novel GPCR ligands (deorphanization)[32,33], for metabolic engineering purposes[34,35], and for the minimization of GPCR signaling

complexity[36]. With the deletion of yeast GPCRs, the yeast system provides a synthetic 'null' GPCR background for investigating non-native receptors[23,25,37]. In comparison to mammalian systems, shorter doubling time and simple cell culture are among the benefits when studying GPCRs in yeast[38]. The yeast mating pathway with its resemblance to mammalian GPCR signaling pathways, therefore, offers a framework with multiple engineering possibilities to link heterologous GPCRs to a reporter output[36]. Hereby, we will discuss the modifications of the natural yeast pathway to investigate GPCR signaling and deorphanization (Figure 1C).
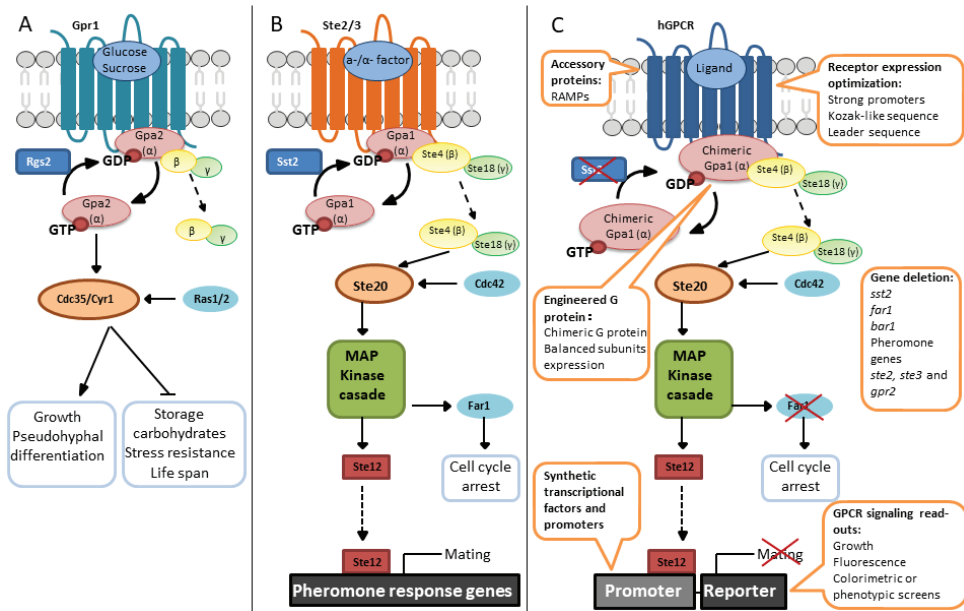
Figure 1. Overview of GPCR signaling pathways in *S. cerevisiae*, adapted from Versele *et al.* (2001)[19] and Lengger *et al.* (2020)[63]. A) Glucose signaling via Gpr1, B) pheromone signaling via Ste2 and Ste 3 and C) modifications of pheromone signaling pathway for coupling to human GPCRs.

Engineered G proteins

In general, heterologous GPCRs show preferences in G protein coupling depending on their native G_a coupling[39]. Although it has been reported that heterologous GPCRs can couple to the endogenous Gpa1 subunit[34], higher coupling efficiency has been achieved by using chimeric G_a subunits, which are thus commonly preferred[37,40]. In the chimeric G_a subunits, the last five amino acids of the C-terminus have been transplanted based on the mammalian G_a sequence to improve receptor recognition[41,42]. Apart from identifying matching GPCRs, optimization of G protein subunit expression is crucial for successfully engineering and restoring GPCR signaling. It has been computationally and experimentally confirmed that optimally balanced levels of G protein subunits maintain high pathway output but low basal activity[36,43,44].

Gene deletions

The yeast pheromone pathway regulates mating initiation[19], however, there is no requirement of mating genes for studying GPCR signaling. Instead, they may even intervene with functional studies of heterologous GPCRs. In order to boost GPCR signaling strength, certain pheromone pathway-related genes were thus eliminated, for example through knock-out of the three native GPCRs, down regulation of Gpa1 and SST2 expression, as well as deletion of the FAR1 gene, a cell cycle arrest inducer during mating[34,38,40,45,46]. More recently, deletion of BAR1 and pheromone genes has been proven to (further) minimize the pheromone response[32]. Moreover, yeast proteases may target intracellular loops of GPCRs resulting in receptor degradation. Thus, deletion of the central portion of the intracellular loops of heterologous GPCRs and the usage of a protease-deficient yeast strain have been shown to increase receptor amounts[47–49]. In addition, targeted insertion of defined sequences at the deletion sites allows re-introduction of key signaling genes, which provides a highly tunable GPCR signaling pathway in the yeast system[36].

Optimization of receptor expression

Multiple GPCRs have been successfully expressed in yeast cells, while the development of expressing functional GPCRs is still ongoing. In *P. pastoris*, GPCRs are typically and deliberately truncated at the C-terminus to prevent degradation, which increases the expression and stability of receptor[16,50]. Besides, strong constitutive promoters, such as TDH3 or PGK1, have also been reported to increase GPCR levels[32,51]. Additionally, agonist-mediated fluorescence reporter intensity could be dramatically increased by the upstream insertion of the Kozak-like sequence (-AAAAAAAUGUCU-) to a neurotensin GPCR open reading frame[51,52].

To increase GPCR expression by expanding the post-translational processing, the fusion of a leader sequence to the N-terminus of the receptor has been shown to assist the plasma membrane insertion of the receptor[53]. An early study on the β_2-adrenoreceptor suggested that replacing part of the receptor N-terminus with the corresponding sequence of Ste2 supported the expression and functionalization of the β_2-adrenoreceptor[54]. Moreover, the addition of a hydrophobic pre-prosequence resulted in higher expression and better insertion into the membrane for 12 different human GPCRs in a GPCR fusion study[55]. Although all these 12 GPCRs were successfully expressed with high yields, all except the adenosine A_{2A} receptor were primarily observed within the cells and detected with intact or partially cleaved leader sequences, indicating the problem of improper ER translocation and thus the limiting step of human GPCR production in *S. cerevisiae*[55].

Accessory proteins

Despite the transcriptional and post-transcriptional controls discussed above, lack of accessory proteins also hampers the development of functional GPCR assays in yeast[40,55,56]. Co-expression of human odorant receptor OR7D4 with an accessory

protein, receptor-transporting protein, have been reported to increase receptor transportation to the yeast membrane[57]. Other accessory proteins, such as receptor-activity modifying proteins (RAMPs), can dimerize with GPCRs and modulate their activity, including ligand selectivity, transport to the cell surface, internalization and even downstream signaling[58].

Synthetic transcriptional factors and promoters

MAPK cascade-mediated Ste12 translocation regulates the expression of endogenous mating pathway target promoters in yeast cells[29]. Thus, the use of Ste12 as a controller for reporter gene expression via the FUS1, FUS2 and FIG1 promoters is the most commonly used design for studying GPCR signaling in yeast[59–62]. However, the expression strength of Ste12 needs to be limited to prevent impaired cell growth[36]. Therefore, in this case, coupling heterologous GPCR signaling to a synthetic transcription factor is able to target the reporter gene without influencing yeast mating target promoters[63]. For instance, compared to the FIG1 promoter, using the synthetic promoter PLexA(4x) results in a 7-fold increase of green fluorescent protein (GFP) expression upon the activation of olfactory OR1G1 GPCR in response to decanoic acid[34].

GPCR signaling read-outs

Functional GPCR screening assays often involve cell growth, fluorescence, and/or colorimetric or phenotypic screens[36,64,65]. A growth assay coupling GPCRs to a HIS3 reporter gene was designed for ligand screening of inverse agonists and weak partial agonists[66,67]. Complementarily, inverted reporter systems coupling to CAN1 and FUI, encoding permeases, can only survive with the addition of agonists and have been used to investigate non-functional GPCRs, such as mutant GPCRs with abolished receptor activation[67–69]. Moreover, GPCR antagonists have been investigated using the inverted reporter system with fluorescent read-outs[70]. Overall, the usage and optimization of novel sensitive fluorescent markers with high signal-to-noise ratio have become the trend for functional assays of GPCR signaling in yeast[51,71,72].

GPCR studies in yeast

As mentioned above, *P. pastoris* is a preferred platform for GPCR production due to its high expression capacity[31]. Functional characterization of GPCR signaling has been extensively studied employing the *S. cerevisiae* mating pathway[23,25,37]. In this section, we will discuss some examples in which yeast systems are used as a crucial platform in the development of GPCR purification and signaling characterization, as well as for GPCR deorphanization studies (Table 1).

Purification of GPCRs

Crystal structures of GPCRs in complex with various ligands and/or G proteins

nowadays provide numerous initial models for drug design and discovery[6]. However, large quantities of high-quality pure protein are always required for X-ray crystallography, which constitutes a major hurdle in GPCR expression and purification. Therefore, relatively cheap and easy-to-handle yeast systems are used as expression systems for GPCRs, also to improve expression and stability of the receptors[31,73].

S. cerevisiae has been developed as a chassis for rapid expression and characterization of four functional human GPCRs and their variants as a starting point for X-ray crystallography, viz. β_2-adrenoreceptor, acetylcholine M_2 receptor, histamine H_1 receptor and neurotensin NTS_1 receptor[73]. In this study, the expression of a stabilized H_1 receptor variant was scaled up to 65 pmol/mg in *P. pastoris* and successfully purified for crystallization trials, indicating that the combined strategy of using *S. cerevisiae* for rapid screening and *P. pastoris* for high expression could be effective for GPCR structural studies[73]. Human smoothened receptor with an N-terminal purification tag has been successfully expressed, visualized, and purified from the *S. cerevisiae* system[74]. High expression levels of N-terminal histidine-tagged β_2-adrenoreceptor were successfully achieved in *P. pastoris* with optimized codon usage and further purified with hydroxyapatite and gel-filtration columns[75]. In fact the *P. pastoris* expression system has been specifically used to produce membrane proteins, such as calcium and potassium channels, nitrate and phosphate transporters, and the H_1 histamine receptor[31]. The fusion of T4 lysozyme (T4L) into the third intracellular loop of GPCR favors GPCR stabilization and crystallization[76]. *P. pastoris* was also used to express the H_1 receptor-T4L fusion protein, which was later used for a crystallographic study of the receptor in complex with doxepin, a first-generation H_1 receptor antagonist[77,78]. Furthermore, functional cannabinoid receptors (both CB_1 and CB_2 receptors) with a c-myc epitope and a hexahistidine tag at the C-terminus were successfully expressed and purified in the *P. pastoris* system[79,80]. However, non-homogenous glycosylation and the presence of unprocessed α-factor sequence were detected at the N-terminus of the CB_2 receptor expressed in the same *P. pastoris* system, where this unprocessed α-factor appeared to be the cause of poor ligand binding at the CB_2 receptor[81]. Hence, it makes yeast suitable for CB_2 receptor purification, but less or unsuitable for functional characterization of the protein.

Characterization of novel ligands and GPCR signaling

The human β_2-adrenoreceptor was the first functional heterologously expressed GPCR in yeast responding to its agonist isoproterenol[54]. Since then, many more human GPCRs have been linked to the yeast pheromone pathway for functional studies[24]. Most sub-families of class A and few receptors of class B GPCRs have shown successful expression in yeast[34,37,38,47,54,66,82–93].

A comparative study between the *S. cerevisiae* and a mammalian system with respect to the $P2Y_1$ receptor indicated that the reporter gene HIS3-coupled yeast system

was suitable for screening both agonists and antagonists of the P2Y$_1$ receptor[94]. Wild-type and the constitutively active mutant (N119S) CXCR4 chemokine receptor were expressed in *S. cerevisiae* coupled to the FUS1 promoter controlling reporter genes HIS3, FUI, and lacZ, and tested for receptor signaling mediated by T140 derivatives[67]. Of note, relatively high concentrations of chemokine were needed to obtain a response in the yeast system, as compared to more conventional mammalian functional assays. Besides, novel allosteric CXCR4 antagonists were identified from a screening a library of 160,000 known chemokine receptor ligands using the *S. cerevisiae* system coupled to reporter genes HIS3 and lacZ[95]. Propionate and further short-chain carboxylic acids were identified as agonists on orphan receptors GPR41 and GPR43 from routine ligand bank screening using the yeast system coupled to β-galactosidase activity[96]. Similarly, yeast-based screening assays on GPR68 suggested the benzodiazepine lorazepam as a non-selective agonist of this orphan receptor[85]. For GPR119 a novel agonist PSN375963 was identified with a similar potency to the reported endogenous ligand, oleoylethanolamide[97–99]. The usage of yeast systems with different G protein modifications for glucagon-like peptide-1 receptor revealed the importance of the co-expression of receptor activity-modifying protein-2 (RAMP-2) with the receptor in ligand binding and G protein selectivity experiments[56].

The lacZ reporter gene was used as functional read-out of acetylcholine M$_3$ receptor ligands in *S. cerevisiae* strains containing different chimeric G proteins, indicating functional selectivity of this receptor upon coupling to different G$_\alpha$ subunits[100]. The same reporter gene was coupled to P2Y$_{12}$ receptors expressed in *S. cerevisiae* as a functional read-out of agonist-induced activation, revealing similar functional pharmacological properties between human and murine P2Y$_{12}$ receptors[101]. Functional chimeras of P2Y$_1$, P2Y$_2$ and/or leukotriene BLT$_1$ receptors have been successfully expressed in an *S. cerevisiae* system with the lacZ reporter gene to define regions required for ligand-induced activation. This provided a new approach to study receptors with low coupling efficiency in the given system[102]. A mutagenesis study of complement peptide C5a$_1$ receptor has been done in an *S. cerevisiae* system with the HIS3 reporter gene, demonstrating a particular role of the WXFG motif in the first extracellular loop during C5a$_1$ receptor activation[103]. In order to characterize antagonists and analyze mutations of 5-hydroxytryptamine receptor 1A, a high-sensitivity yeast system was developed with an engineered G$_\alpha$ subunit and coupled to a fluorescent reporter, ZsGreen[104]. Additionally, yeast strains coupling human GPCR activation to the HIS3 reporter gene were used in a mutagenesis study for the investigation of the role of the C-terminus in G protein activation by the human hydroxycarboxylic acid receptors 2 and 3[86]. Recently, light-sensing human rhodopsin has been coupled to the yeast mating pathway with successful expression and characterization of disease-causing mutations, enabling cost-efficient ligand screening in a semi-high-throughput format[38,105].

Biosensors

For the investigation of the neurotensin NTS$_1$ receptor, a fluorescence-based microbial yeast biosensor has been constructed to monitor receptor activation stimulated by agonists, which is also a promising approach in the diagnosis of NTS$_1$ receptor-related diseases and agonist development[106]. For the angiotensin AT$_1$ receptor, a fluorescence-based yeast biosensor was also developed with the yeast-human chimeric G$_\alpha$ for the introduction of single mutations into the receptor to screen agonistic peptides[107]. In this system, the engineered yeast cells produced and secreted the autocrine Ang II peptide and an analog, which activated AT$_1$ receptors expressed in the same system[107]. Engineered human P2Y$_{14}$ receptors with different ligand specificities and efficacies expressed in *S. cerevisiae* in combination with a fluorescent read-out were suitable biosensors for detecting ligands in complex mixtures, and for differentiating among (stereo)chemically related ligands[108]. Moreover, an olfactory biosensor has been developed in engineered *S. cerevisiae* yeast cells expressing human olfactory receptor OR17-40 to detect odorants with a high sensitivity and selectivity[109].

Deorphanization

In an early deorphanization study in yeast, the olfactory receptor KIAA0001, now known as P2Y$_{14}$ receptor, was expressed and coupled to different G$_\alpha$ subunits, which ultimately identified UDP-glucose as a specific agonist[82]. Human receptor OSGPR1116, now known as GPR119, has been identified with fatty-acid ethanolamides as agonists in a yeast system[97]. Recently, seven human orphan olfactory receptors were expressed in a yeast system, their presence determined by immunofluorescence microscopy, and eventually screened with 57 chemicals, suggesting the value of yeast-based screening systems for olfactory receptor deorphanization[33].

Adenosine receptor studies in yeast

The adenosine receptors belong to Class A, rhodopsin-like GPCRs and exist of four subtypes, A$_1$, A$_{2A}$, A$_{2B}$ and A$_3$. They have attracted much attention in recent years as therapeutic targets[3]. Depending on the adenosine receptor subtype, binding of extracellular adenosine leads to activation of different downstream signaling cascades[110–115]. The A$_1$ and A$_3$ receptors inhibit adenylate cyclase and reduce cAMP levels mainly via G$_i$-coupling[112,113]. Conversely, A$_{2A}$ and A$_{2B}$ receptors are mainly coupled to G$_s$ proteins and increase the levels of cAMP[114,115]. The A$_1$ receptor, abundant in the central nervous system (CNS) and identified in numerous peripheral tissues, plays a pivotal role in neuronal, renal and cardiac processes[116–119]. Thus, the A$_1$ receptor has been under investigation as a drug target for brain pathologies, such as pain, depression and memory disorders[120–123]. High expression levels of A$_{2A}$ receptor are found in the CNS and the immune system[124]. The A$_{2A}$ receptor is therefore involved in CNS disorders,

Table 1. Examples of human GPCR studies in yeast systems.

Receptors	Yeast species	Applications	Read-outs	Reference
5-hydroxytryptamine receptor 1A	S. cerevisiae	Characterization of ligand and site-directed mutants	Fluorescence (ZsGreen)	[104]
Acetylcholine M$_2$ receptor	S. cerevisiae	Crystallization	-	[73]
Acetylcholine M$_3$ receptor	S. cerevisiae	Functional selectivity	Fluorescence (β-galactosidase)	[100]
Adenosine A$_1$ receptor	S. cerevisiae	Ligand characterization	Fluorescence (β-galactosidase)	[134]
	S. cerevisiae	Structural characterization	Growth (HIS3)	[135]
Adenosine A$_{2A}$ receptor	P. pastoris	Crystallization	-	[146]
	P. pastoris	Purification	-	[147–149]
	S. cerevisiae	Expression purpose	Radioligand binding; fluorescence (GFP)	[55,142–145]
	S. cerevisiae	Thermostabilizing mutation screening	Growth (HIS3); fluorescence (β-galactosidase)	[136]
Adenosine A$_{2B}$ receptor	S. cerevisiae	Structural characterization	Growth (HIS3)	[137–141]
	S. cerevisiae	Characterization of cancer-related mutations	Growth (HIS3)	[151]
Adenosine A$_3$ receptor	S. cerevisiae	Expression purpose	Fluorescence (mCitrine)	[150]
Angiotensin AT$_1$ receptor	S. cerevisiae	Microbial biosensor	Fluorescence (GFP)	[107]
Cannabinoid CB$_1$ receptor	P. pastoris	Purification	-	[80]
Cannabinoid CB$_2$ receptor	P. pastoris	Purification	-	[79,81]
Complement peptide C5a$_1$ receptor	S. cerevisiae	Structural characterization	Growth (HIS3)	[103]
CXCR4	S. cerevisiae	Ligand screening	Growth (HIS3 and FUI); fluorescence (β-galactosidase)	[67,95]
Glucagon-like peptide-1 receptor	S. cerevisiae	Ligand screening and G protein selectivity	Fluorescence (β-galactosidase)	[56]
GPR119	S. cerevisiae	Ligand screening and deorphanization	Fluorescence (β-galactosidase)	[97–99]
GPR41 and GPR43	S. cerevisiae	Ligand screening	Fluorescence (β-galactosidase)	[96]
GPR68	S. cerevisiae	Ligand screening	Growth (HIS3)	[84]
Histamine H$_1$ receptor	P. pastoris	Crystallization (fused with T4L)	-	[76-78]
	S. cerevisiae	Crystallization	-	[73]
Hydroxycarboxylic acid receptors 2 and 3	S. cerevisiae	Structural characterization	Growth (HIS3)	[86]
Leukotriene BLT$_1$ receptor	S. cerevisiae	Functional characterization of receptor chimeras	Fluorescence (β-galactosidase)	[102]
Neurotensin NTS$_1$ receptor	S. cerevisiae	Purification	-	[73]
Olfactory receptor	S. cerevisiae	Microbial biosensor	Fluorescence (GFP)	[106]
Olfactory receptor 10S1	S. cerevisiae	Microbial biosensor	Conductance	[109]
Olfactory receptor 2T4	S. cerevisiae	Deorphanization	Fluorescence (GFP)	[33]
	S. cerevisiae	Deorphanization	Fluorescence (GFP)	[33]
P2Y$_1$ receptor	S. cerevisiae	Ligand screening	Growth (HIS3)	[94]
P2Y$_1$ and P2Y$_2$ receptors	S. cerevisiae	Functional characterization of receptor chimeras	Fluorescence (β-galactosidase)	[102]
P2Y$_{12}$ receptor	S. cerevisiae	Characterization of murine receptor in comparison to human receptor	Fluorescence (β-galactosidase)	[101]
P2Y$_{14}$ receptor	S. cerevisiae	Deorphanization	Fluorescence (β-galactosidase)	[82]
	S. cerevisiae	Biosensor	Fluoresence (β-galactosidase)	[108]
Rhodopsin	S. cerevisiae	Functional characterization of disease-causing mutations	Fluorescence (GFP, mCherry)	[38,105]
Smoothened receptor	S. cerevisiae	Purification	-	[74]
β$_1$-adrenoreceptor	P. pastoris	Purification	-	[73,75]
β$_2$-adrenoreceptor	S. cerevisiae	Expression and functional characterization of the wild-type receptor	Radioligand binding; fluorescence (β-galactosidase)	[54]

inflammation, pain and drug addiction[116,125,126]. The A_{2B} receptor is ubiquitously expressed in many organs, as well as on microvascular, endothelial and immune cells[127,128]. This receptor is only activated by high concentrations of adenosine and is known to modulate inflammation and immune responses in several pathological conditions, such as cancer, diabetes and lung diseases[129,130]. The A_3 receptor is suggested to mediate allergic responses, airway contraction and apoptotic events in certain cell types[117,118]. High expression levels of A_3 receptor have been determined in tumor cells compared to healthy cells, demonstrating its potential role as a tumor marker[131]. In the tumor microenvironment adenosine accumulation is mediated via the catabolism of extracellular ATP to adenosine by CD38, CD39, and CD73, which suppresses anti-tumor immune responses via the activation of adenosine receptors[132]. Therefore, multiple antagonistic antibodies and small molecule inhibitors targeting adenosine receptors have been developed as new strategies in cancer immunotherapy and display therapeutic efficacy in clinical trials against different solid tumors[133]. During the past years, it has become clear that activation of adenosine receptors not only depends on the ligand binding and G protein coupling sites, but also on other, more distant regions in the receptor architecture[134–141]. Yeast systems, in this case, have been used as a host for adenosine receptors for receptor purification and the characterization of ligands, receptor structure and function, and disease-related mutations (Table 1).

Expression and purification of adenosine receptors

The first functional human adenosine receptor expressed in a yeast system was the A_{2A} receptor using *S. cerevisiae* and confirmed by a radioligand binding assay[142]. In this study, the expression and functionality of A_{2A} receptors were not altered by the co-overexpression of several ER-resident proteins, suggesting that interactions with these proteins did not decrease human GPCR expression in yeast[142]. Later on, the A_{2A} receptor with a C-terminal GFP tag was expressed and analyzed in *S. cerevisiae*, and the obtained results suggested that limited heterologous GPCR expression was caused by translational or post-translational events[143]. The same team also obtained and selected a yeast strain with a high expression level using flow cytometry, which was eventually used to purify the A_{2A} receptor[144]. Further optimizations were performed by fusing a purification tag to the A_{2A} receptor, as well as developing a suitable purification scheme, resulting in large enough quantities for spectroscopic characterization[145]. Furthermore, in order to better understand the improper trafficking and inactivation of GPCRs in heterologous expression systems, 12 human GPCRs with a GFP tag were transformed in *S. cerevisiae*[55]. Among these GPCRs, only the A_{2A} receptor proved active and was located primarily at the plasma membrane with proper leader sequence processing, indicating a crucial role of translocation in producing active human GPCRs in *S. cerevisiae*[55]. A crystal structure of the A_{2A} receptor with the complete third intracellular loop and an allosteric inverse-agonist antibody was obtained using *P. pastoris* as the expression host of the receptor[146]. Moreover, the A_{2A} receptor was expressed in *P. pastoris* and encapsulated into

styrene maleic acid lipid particles (SMALPs) to increase thermostability, which enabled purification procedures without the requirement of detergent[147]. The same combination of *P. pastoris*-expressed human A$_{2A}$ receptor and SMALPs has recently been used to characterize the binding capability[148], and to investigate ligand-induced conformational changes of the A$_{2A}$ receptor in response to an inverse agonist and full agonist[149].

More recently, the A$_3$ receptor was successfully expressed in *S. cerevisiae* in which the C-terminus was replaced by the corresponding tail of the A$_{2A}$ receptor[150]. The A$_3$/A$_{2A}$ chimeric receptor significantly increased receptor expression and decreased unfolded protein in comparison to wild-type A$_3$ receptor. Thus, chimeric receptor variants can be used as a strategy to produce "difficult-to-express" receptors in yeast for further drug discovery[150].

Functional characterization of adenosine receptors

In order to characterize both antagonists and agonists of the A$_1$ receptor, *S. cerevisiae* strains expressing the receptor and different human-yeast chimeric G proteins were used in combination with a lacZ reporter gene[134]. In this study, β-galactosidase activity was measured as a read-out of receptor activation, suggesting that R-PIA was an agonist with high efficacy when coupling to G$_{\alpha o}$, G$_{\alpha i1/2}$, and G$_{\alpha i3}$ proteins, while VCP-189 was an agonist with low efficacy selectively coupling to the G$_{\alpha i1/2}$, and G$_{\alpha i3}$ proteins[134]. Besides, results obtained in a mammalian system were in general agreement with those in the yeast system, except for VCP-189 which also activated G$_{\alpha o}$ coupling in mammalian cells[134]. The role of extracellular loops in receptor activation and allosteric modulation was examined in another study in which the adenosine A$_1$ receptor was expressed in yeast[135]. Here, receptor signaling was coupled to yeast growth via a chimeric Gpa1/G$_{\alpha i3}$ protein, and single alanine mutations were introduced to the extracellular loops of the receptor via site-directed mutagenesis. Results obtained from this study implicated the importance of many residues located at the second and third extracellular loops in receptor activation, and identified two residues, W156[EL2] and E164[EL2], regulating the effect of the allosteric modulator[135].

Screening of thermostabilizing mutations in the adenosine A$_{2A}$ receptor was performed in a yeast system with an engineered G protein and HIS3 and lacZ reporter genes[136]. Alanine mutation of residues R199 and L208 completely abolished the constitutive activity of the A$_{2A}$ receptor. Besides, decreased potency was observed on mutant receptor R199A while reduced efficacy was displayed on mutant receptor L208A, supporting key roles of these residues in receptor signaling[136].

Several mutagenesis studies have been performed on the A$_{2B}$ receptor in a yeast system with engineered G protein and HIS3 reporter gene[137–141]. Inverse agonists of the A$_{2B}$ receptor were discovered using constitutively active mutants (CAMs) expressed in the yeast system[139]. In this study, CAMs with different constitutive activity levels were used to determine the relative intrinsic efficacy of the three inverse agonists,

DPCPX, MRS1706, and ZM241385[139]. Two high-level CAMs were identified to lock the receptor in the active state and to be irresponsive to these inverse agonists[139]. In a study focusing on the interaction between the A_{2B} receptor and the C-terminus of G_{α} subunits, wild-type and mutant receptors were investigated in eight yeast strains expressing different chimeric G proteins[137]. Three residues, R103, I107 and L236, were revealed to be important in receptor activation via altering G protein interaction and activation[137]. Besides, key residues in the NPxxY(x)$_{5,6}$F motif and helix 8 of the receptor were screened in the yeast system with chimeric Gpa1/$G_{\alpha i3}$ protein[138]. Four mutants P287A, Y290A, R293A and I304A were identified with a complete loss of function, and eight more residues, N286, V289, Y292, N294, F297, R298, H302 and R307, were also found to be vital in receptor activation[138]. A random mutagenesis study on the first extracellular loop of the adenosine A_{2B} receptor expressed in an *S. cerevisiae* strain demonstrated the necessity of a polar residue at position 74[140]. Various mutations at residues 71 and 74 were able to dramatically influence receptor activation, suggesting that the first extracellular loop of A_{2B} receptor is (also) essential for receptor activation (Figure 2)[140]. Furthermore, random mutagenesis on the fragment encoding the second extracellular loop flanked by the fourth and
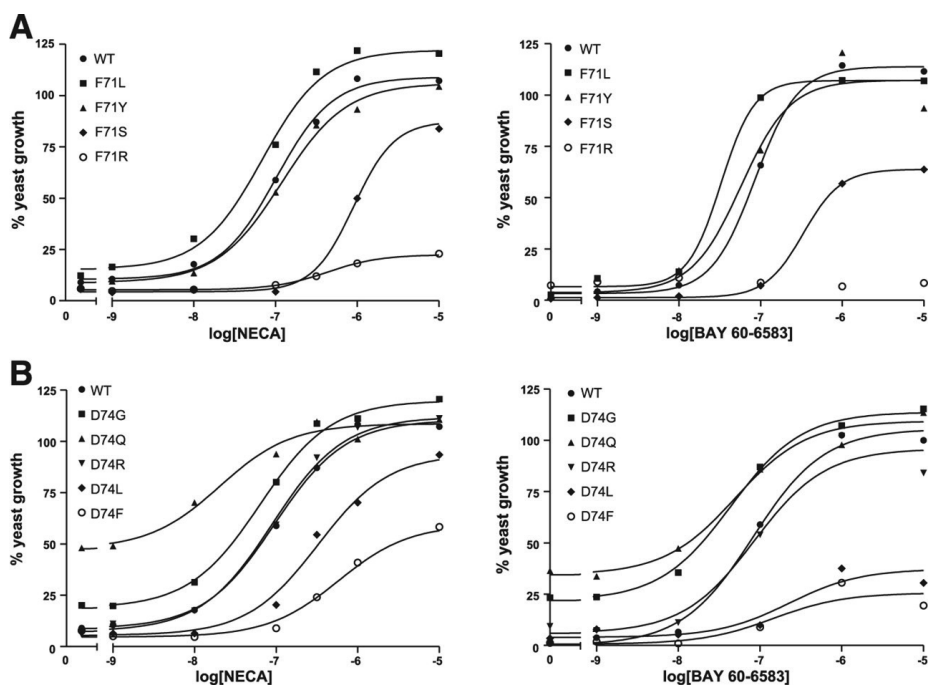
Figure 2. Representative concentration-growth curves of wild-type and A) mutant adenosine A_{2B} receptors of residue F71 and B) mutant A_{2B} receptors of residue D74 in response to the ribose agonist NECA or the non-ribose agonist BAY 60-6583. The maximum activation level of wild-type A_{2B} receptors was set at 100%, the background of the selection medium was set at 0%. Mutations are shown in the numbering of the A_{2B} receptors amino acid sequencing. WT in the figures represents wild-type. Reproduced with permission from Peeters *et al*. (2011)[140].

fifth transmembrane helices resulted in 22 different single and double mutant receptors with decreased constitutive activity and agonist potency[141]. Comparing these constitutively inactive mutants (CIMs) and CAMs previously identified from the same fragment, six residues were found in both CAM and CIM screening, indicating their crucial roles in both activation and inactivation of the A_{2B} receptor (Figure 3)[141]. Recently, the same yeast strain was used in characterizing cancer-related somatic mutations in the A_{2B} receptor[151], as described in **Chapter 4**. These mutations might even be cancer-specific as they did not match any point mutations identified from the natural variance set[151]. Several of these cancer-related mutations caused significantly altered receptor pharmacology (Figure 4)[151].

Conclusion

A considerable number of human GPCRs has been investigated in a yeast platform with different purposes, including protein purification, investigation of receptor activation and signaling, as well as ligand identification. *P. pastoris* yeast strains can be highly efficient and cost-effective expression systems for GPCRs of interest for the purpose of protein purification and eventually crystallization/ structure elucidation. The pheromone signaling pathway of the budding yeast *S. cerevisiae* has been engineered with various modifications to provide a robust platform for functional studies on human GPCRs, both wild-type and mutated. Therefore, these yeast platforms are a very useful and attractive addition to the more commonly employed mammalian cell lines for receptor expression, such as CHO and HEK293 cells.
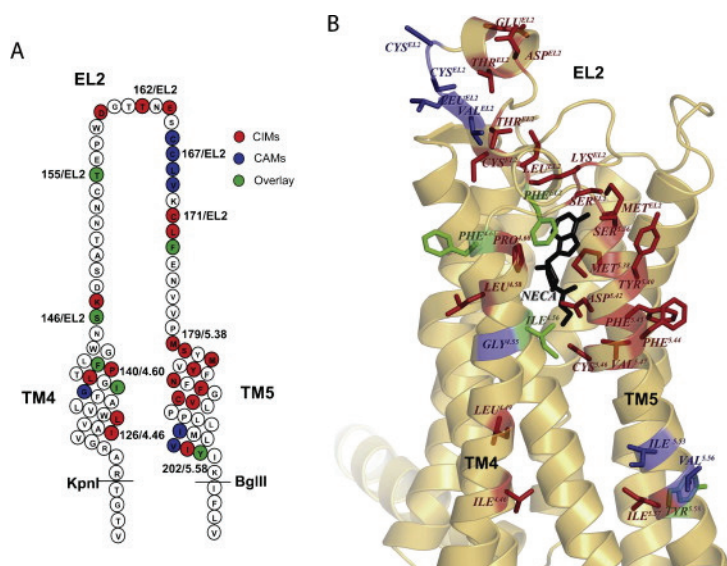
Figure 3. Location of constitutively inactive mutants (CIMs) and constitutively active mutants (CAMs) in the human adenosine A_{2B} receptor. (A) A snake-plot structure of the fragment used in the CIMs and CAMs screening. The positions are shown in the numbering of the A_{2B} receptors amino acid sequencing as well as according to the Ballesteros–Weinstein numbering[152]. (B) Based on the multiple sequence alignment, the mutated residues identified from the screen were mapped onto the crystal structure of the A_{2A} receptor (PDB: 3YDV). The positions are labeled according to the Ballesteros–Weinstein numbering[152]. The CIMs are shown in red, CAMs in blue, and positions identified in both screens are shown in green (overlay). Reproduced with permission from Peeters *et al*. (2014)[141].
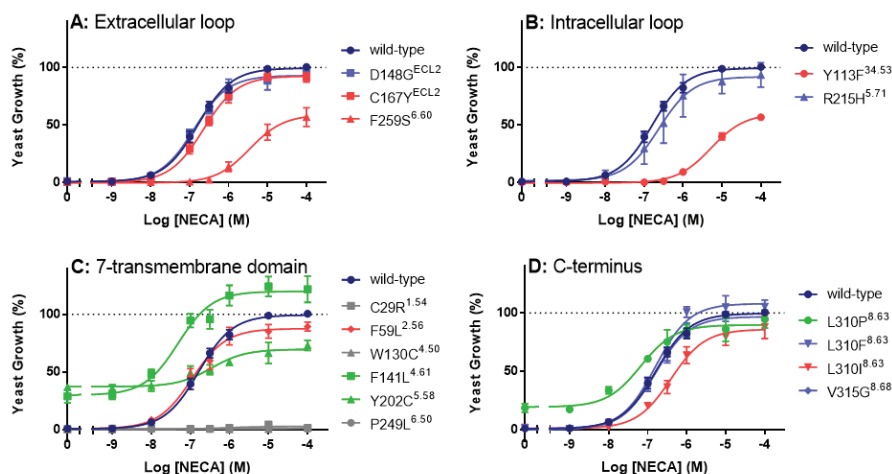
Figure 4. Concentration-growth curves for the wild-type and 15 cancer-related mutant A_{2B} receptors in response to the reference full agonist NECA. The maximum activation level of wild-type A_{2B} receptors was set at 100%, the background of the selection medium was set at 0%. The mutations are shown in the numbering of the A_{2B} receptors amino acid sequencing as well as according to the Ballesteros–Weinstein numbering[152]. The no-effect mutants are shown in blue, less active mutants in red, constitutively active mutants in green and loss of function mutants in grey. Reproduced with permission from Wang *et al*. (2020)[151].

Reference

1. Rask-Andersen, M., Masuram, S. & Schiöth, H. B. The druggable genome: Evaluation of drug targets in clinical trials suggests major shifts in molecular class and indication. *Annu. Rev. Pharmacol. Toxicol.* **54**, 9–26 (2014).
2. Vassilatis, D. K. *et al.* The G protein-coupled receptor repertoires of human and mouse. *Proc. Natl. Acad. Sci.* **100**, 4903–4908 (2003).
3. Fredriksson, R., Lagerström, M. C., Lundin, L.-G. & Schiöth, H. B. The G-protein-coupled receptors in the human genome form five main families. Phylogenetic analysis, paralogon groups, and fingerprints. *Mol. Pharmacol.* **63**, 1256–72 (2003).
4. Kolakowski, L. F. J. GCRDb: a G-protein-coupled receptor database. *Receptors Channels* **2**, 1–7 (1994).
5. Simon, M., Strathmann, M. & Gautam, N. Diversity of G proteins in signal transduction. *Science (80-.).* **252**, 802–808 (1991).
6. Hauser, A. S., Attwood, M. M., Rask-Andersen, M., Schiöth, H. B. & Gloriam, D. E. Trends in GPCR drug discovery: New agents, targets and indications. *Nat. Rev. Drug Discov.* **16**, 829–842 (2017).
7. Hollenberg, M. D. *et al.* Biased signalling and proteinase-activated receptors (PARs): Targeting inflammatory disease. *Br. J. Pharmacol.* **171**, 1180–1194 (2014).
8. Kenakin, T. The potential for selective pharmacological therapies through biased receptor signaling. *BMC Pharmacol. Toxicol.* **13**, 1–8 (2012).
9. Lagerström, M. C. & Schiöth, H. B. Structural diversity of G protein-coupled receptors and significance for drug discovery. *Nat. Rev. Drug Discov.* **7**, 339–57 (2008).
10. Lynch, J. R. & Wang, J. Y. G protein-coupled receptor signaling in stem cells and cancer. *Int. J. Mol. Sci.* **17**, 707-725 (2016).
11. O'Hayre, M., Degese, M. S. & Gutkind, J. S. Novel insights into G protein and G protein-coupled receptor signaling in cancer. *Curr. Opin. Cell Biol.* **27**, 126–135 (2014).
12. Sever, R. & Brugge, J. S. Signal transduction in cancer. *Cold Spring Harb. Perspect. Med.* **5**, a006098 (2015).
13. Jidenko, M. *et al.* Crystallization of a mammalian membrane protein overexpressed in Saccharomyces cerevisiae. *Proc. Natl. Acad. Sci. U. S. A.* **102**, 11687–11691 (2005).
14. Long, S. B., Campbell, E. B. & MacKinnon, R. Crystal structure of mammalian voltage-dependent shaker family K+ channel. *Science.* **309**, 897–903 (2005).
15. Zorman, S., Botte, M., Jiang, Q., Collinson, I. & Schaffitzel, C. Advances and challenges of membrane-protein complex production. *Curr. Opin. Struct. Biol.* **32**, 123–130 (2015).
16. Cereghino, G. P. L., Cereghino, J. L., Ilgen, C. & Cregg, J. M. Production of recombinant proteins in fermenter cultures of the yeast Pichia pastoris. *Curr. Opin. Biotechnol.* **13**, 329–332 (2002).
17. Julien, C. Production of Humanlike Recombinant Proteins in Pichia pastoris. *BioProcess Tech.* **4**, 22–31 (2006).
18. Karbalaei, M., Rezaee, S. A. & Farsiani, H. Pichia pastoris: A highly successful expression system for optimal synthesis of heterologous proteins. *J. Cell. Physiol.* **235**, 5867–5881 (2020).
19. Versele, M., Lemaire, K. & Thevelein, J. M. Sex and sugar in yeast: two distinct GPCR systems. *EMBO Rep.* **2**, 574–579 (2001).
20. Colombo, S. *et al.* Involvement of distinct G-proteins, Gpa2 and Ras, in glucose- and intracellular acidification-induced cAMP signalling in the yeast Saccharomyces cerevisiae. *EMBO J.* **17**, 3326–3341 (1998).
21. Kraakman, L. *et al.* A Saccharomyces cerevisiae G-protein coupled receptor, Gpr1, is specifically required for glucose activation of the cAMP pathway during the transition to growth on glucose. *Mol. Microbiol.* **32**, 1002–1012 (1999).
22. Nakayama, N., Miyajima, A. & Arai, K. Nucleotide sequences of STE2 and STE3 , cell type-specific sterile genes from Saccharomyces cerevisiae . *EMBO J.* **4**, 2643–2648 (1985).
23. Dohlman, H. G., Thorner, J., Caron, M. G. & Lefkowitz, R. J. Model systems for the study of seven-transmembrane-segment receptors. *Annu. Rev. Biochem.* **60**, 653–688 (1991).
24. Liu, R., Wong, W. & IJzerman, A. P. Human G protein-coupled receptor studies in Saccharomyces cerevisiae. *Biochem. Pharmacol.* **114**, 103–115 (2016).
25. Pausch, M. H. G-protein-coupled receptors in high-throughput screening assays for drug discovery. *Trends Biotechnol.* **15**, 487–494 (1997).
26. Leberer, E., Dignard, D., Harcus, D., Thomas, D. Y. & Whiteway, M. The protein kinase homologue Ste20p is required to link the yeast pheromone response G-protein βγ subunits to downstream signalling components. *EMBO J.* **11**, 4815–4824 (1992).
27. Hung, W., Olson, K. A., Breitkreutz, A. & Sadowski, I. Characterization of the basal and pheromone-stimulated phosphorylation states of Ste12p. *Eur. J. Biochem.* **245**, 241–251 (1997).
28. Bardwell, L. A walk-through of the yeast mating pheromone response pathway. *Peptides* **26**, 339–350 (2005).
29. Roberts, C. J. *et al.* Signaling and circuitry of multiple MAPK pathways revealed by a matrix of global gene expression profiles. *Science.* **287**, 873–880 (2000).
30. Ladds, G., Goddard, A. & Davey, J. Functional analysis of heterologous GPCR signalling pathways in yeast. *Trends Biotechnol.* **23**, 367–373 (2005).
31. Byrne, B. Pichia pastoris as an expression host for membrane protein structural biology. *Curr. Opin. Struct. Biol.* **32**, 9–17 (2015).
32. Billerbeck, S. *et al.* A scalable peptide-GPCR language for engineering multicellular communication. *Nat. Commun.* **9**, (2018).
33. Yasi, E. A. *et al.* Rapid Deorphanization of Human Olfactory Receptors in Yeast. *Biochemistry* **58**, 2160–2166 (2019).
34. Mukherjee, K., Bhattacharyya, S. & Peralta-Yahya, P. GPCR-Based Chemical Biosensors for Medium-Chain Fatty Acids. *ACS Synth. Biol.* **4**, 1261–1269 (2015).
35. Ehrenworth, A. M., Claiborne, T. & Peralta-Yahya, P. Medium-Throughput Screen of Microbially Produced Serotonin via a G-Protein-Coupled Receptor-Based Sensor. *Biochemistry* **56**, 5471–5475 (2017).
36. Shaw, W. M. *et al.* Engineering a Model Cell for Rational Tuning of GPCR Signaling. *Cell* **177**, 782-796.e27 (2019).
37. Brown, A. J. *et al.* Functional coupling of mammalian receptors to the yeast mating pathway using novel yeast/mammalian G protein α-subunit chimeras. *Yeast* **16**, 11–22 (2000).
38. Scott, B. M. *et al.* Screening of Chemical Libraries Using a Yeast Model of Retinal Disease. *SLAS Discov.* **24**, 969–977 (2019).
39. Syrovatkina, V., Alegre, K. O., Dey, R. & Huang, X. Y. Regulation, Signaling, and Physiological Functions of G-Proteins. *J. Mol. Biol.* **428**, 3850–3868 (2016).
40. Erlenbach, I. *et al.* Single Amino Acid Substitutions and Deletions That Alter the G Protein Coupling Properties of the V2 Vasopressin Receptor Identified in Yeast by Receptor Random Mutagenesis. *J. Biol. Chem.* **276**, 29382–29392

(2001).

41. Liu, J., Conklin, B. R., Blin, N., Yun, J. & Wess, J. Identification of a receptor/G-protein contact site critical for signaling specificity and G-prptein activation. *Proc. Natl. Acad. Sci. U. S. A.* **92**, 11642–11646 (1995).

42. Conklin, B. R., Farfel, Z., Lustig, K. D., Julius, D. & Bourne, H. R. Substitution of three amino acids switches receptor specificity of Gqα to that of Giα. *Nature* **363**, 274–276 (1993).

43. Bush, A. *et al.* Yeast GPCR signaling reflects the fraction of occupied receptors, not the number . *Mol. Syst. Biol.* **12**, 898-918 (2016).

44. Bridge, L. J., Mead, J., Frattini, E., Winfield, I. & Ladds, G. Modelling and simulation of biased agonism dynamics at a G protein-coupled receptor. *J. Theor. Biol.* **442**, 44–65 (2018).

45. Dohlman, H. G., Song, J., Ma, D., Courchesne, W. E. & Thorner, J. Sst2, a negative regulator of pheromone signaling in the yeast Saccharomyces cerevisiae: expression, localization, and genetic interaction and physical association with Gpa1 (the G-protein alpha subunit). *Mol. Cell. Biol.* **16**, 5194–5209 (1996).

46. Leplatois, P. *et al.* Neurotensin induces mating in Saccharomyces cerevisiae cells that express human neurotensin receptor type 1 in place of the endogenous pheromone receptor. *Eur. J. Biochem.* **268**, 4860–4867 (2001).

47. Erlenbach, I. *et al.* Functional expression of M1, M3 and M5 muscarinic acetylcholine receptors in yeast. *J. Neurochem.* **77**, 1327–1337 (2001).

48. Routledge, S. J. *et al.* The synthesis of recombinant membrane proteins in yeast for structural studies. *Methods* **95**, 26–37 (2016).

49. Sander, P. *et al.* Heterologous Expression of the Human D_{2S} Dopamine Receptor in Protease-Deficient Saccharomyces cerevisiae Strains. *Eur. J. Biochem.* **226**, 697–705 (1994).

50. Singh, S. *et al.* A purified C-terminally truncated human adenosine A_{2A} receptor construct is functionally stable and degradation resistant. *Protein Expr. Purif.* **74**, 80–87 (2010).

51. Hashi, H., Nakamura, Y., Ishii, J. & Kondo, A. Modifying Expression Modes of Human Neurotensin Receptor Type 1 Alters Sensing Capabilities for Agonists in Yeast Signaling Biosensor. *Biotechnol. J.* **13**, 1–11 (2018).

52. Hamilton, R., Watanabe, C. K. & de Boer, H. A. Compilation and comparison of the sequence context around the AUG startcodons in Saccharomyces cerevisiae mRNAs. *Nucleic Acids Res.* **15**, 3581–3593 (1987).

53. Seraj Uddin, M., Hauser, M., Naider, F. & Becker, J. M. The N-terminus of the yeast G protein-coupled receptor Ste2p plays critical roles in surface expression, signaling, and negative regulation. *Biochim. Biophys. Acta - Biomembr.* **1858**, 715–724 (2016).

54. King, K., Dohlman, H. G., Thorner, J., Caron, M. G. & Lefkowitz, R. J. Control of yeast mating signal transduction by a mammalian β2-adrenergic receptor and Gs α subunit. *Science (80-.).* **250**, 121–123 (1990).

55. O'Malley, M. A. *et al.* Progress toward heterologous expression of active G-protein-coupled receptors in Saccharomyces cerevisiae: Linking cellular stress response with translocation and trafficking. *Protein Sci.* **18**, 2356–2370 (2009).

56. Weston, C. *et al.* Modulation of glucagon receptor pharmacology by receptor activity-modifying protein-2 (RAMP2). *J. Biol. Chem.* **290**, 23009–23022 (2015).

57. Fukutani, Y. *et al.* Improving the odorant sensitivity of olfactory receptor-expressing yeast with accessory proteins. *Anal. Biochem.* **471**, 1–8 (2015).

58. Klein, K. R., Matson, B. C. & Caron, K. M. The expanding repertoire of receptor activity modifying protein (RAMP) function. *Crit. Rev. Biochem. Mol. Biol.* **51**, 66–71 (2016).

59. Muller, E. M., Mackin, N. A., Erdman, S. E. & Cunningham, K. W. Fig1p facilitates Ca^{2+} influx and cell fusion during mating of Saccharomyces cerevisiae. *J. Biol. Chem.* **278**, 38461–38469 (2003).

60. Alvaro, C. G. & Thorner, J. Heterotrimeric G protein-coupled receptor signaling in yeast mating pheromone response. *J. Biol. Chem.* **291**, 7785–7798 (2016).

61. Trueheart, J. & Fink, G. R. The yeast cell fusion protein FUS1 is O-glycosylated and spans the plasma membrane. *Proc. Natl. Acad. Sci. U. S. A.* **86**, 9916–9920 (1989).

62. Trueheart, J., Boeke, J. D. & Fink, G. R. Two genes required for cell fusion during yeast conjugation: evidence for a pheromone-induced surface protein. *Mol. Cell. Biol.* **7**, 2316–2328 (1987).

63. Lengger, B. & Jensen, M. K. Engineering G protein-coupled receptor signalling in yeast for biotechnological and medical purposes. *FEMS Yeast Res.* **20**, 1–13 (2020).

64. Price, L. A., Kajkowski, E. M., Hadrock, J. R., Ozenberger, B. A. & Pausch, M. H. Functional coupling of a mammalian somatostatin receptor to the yeast pheromone response pathway. *Mol. Cell. Biol.* **15**, 6188–6195 (1995).

65. Ostrov, N. *et al.* A modular yeast biosensor for low-cost point-of-care pathogen detection. *Sci. Adv.* **3**, e1603221 (2017).

66. Zhang, W. B. *et al.* A point mutation that confers constitutive activity to CXCR4 reveals that T140 is an inverse agonist and that AMD3100 and ALX40-4C are weak partial agonists. *J. Biol. Chem.* **277**, 24515–24521 (2002).

67. Evans, B. J. *et al.* Expression of CXCR4, a G-Protein-Coupled Receptor for CXCL12 in Yeast. Identification of New-Generation Inverse Agonists. *Methods in Enzymology* **460**, 399-412 (2009).

68. Li, B. *et al.* Rapid identification of functionally critical amino acids in a G protein-coupled receptor. *Nat. Methods* **4**, 169–174 (2007).

69. Scarselli, M., Li, B., Kim, S. K. & Wess, J. Multiple residues in the second extracellular loop are critical for M3 muscarinic acetylcholine receptor activation. *J. Biol. Chem.* **282**, 7385–7396 (2007).

70. Fukuda, N., Ishii, J., Kaishima, M. & Kondo, A. Amplification of agonist stimulation of human G-protein-coupled receptor signaling in yeast. *Anal. Biochem.* **417**, 182–187 (2011).

71. Kaishima, M., Ishii, J., Matsuno, T., Fukuda, N. & Kondo, A. Expression of varied GFPs in *Saccharomyces cerevisiae*: Codon optimization yields stronger than expected expression and fluorescence intensity. *Sci. Rep.* **6**, 1–15 (2016).

72. Nakamura, Y., Ishii, J. & Kondo, A. Bright Fluorescence Monitoring System Utilizing Zoanthus sp. Green Fluorescent Protein (ZsGreen) for Human G-Protein-Coupled Receptor Signaling in Microbial Yeast Cells. *PLoS One* **8**, e82237 (2013).

73. Shiroishi, M. *et al.* Platform for the rapid construction and evaluation of GPCRs for crystallography in *Saccharomyces cerevisiae*. *Microb. Cell Fact.* **11**, 1–11 (2012).

74. Nehmé, R. *et al.* Stability study of the human G-protein coupled receptor, Smoothened. *Biochim. Biophys. Acta - Biomembr.* **1798**, 1100–1110 (2010).

75. Noguchi, S. & Satow, Y. Purification of Human β2-Adrenergic Receptor Expressed in Methylotrophic Yeast *Pichia pastoris*. *J. Biochem.* **140**, 799–804 (2006).

76. Mathew, E., Ding, F. X., Naider, F. & Dumont, M. E. Functional fusions of T4 lysozyme in the third intracellular loop of a G protein-coupled receptor identified by a random screening approach in yeast. *Protein Eng. Des. Sel.* **26**, 59–71 (2013).

77. Shiroishi, M. *et al.* Production of the stable human histamine H_1 receptor in *Pichia pastoris* for structural determination. *Methods* **55**, 281–286 (2011).

78. Shimamura, T. *et al.* Structure of the human histamine H_1 receptor complex with doxepin. *Nature* **475**, 65–72 (2011).

79. Feng, W., Cai, J., Pierce, W. M. & Song, Z. H. Expression of CB2 cannabinoid receptor in *Pichia pastoris*. *Protein Expr. Purif.* **26**, 496–505 (2002).
80. Kim, T. K. *et al.* Expression and characterization of human CB1 cannabinoid receptor in methylotrophic yeast *Pichia pastoris*. *Protein Expr. Purif.* **40**, 60–70 (2005).
81. Zhang, R. *et al.* Biochemical and mass spectrometric characterization of the human CB2 cannabinoid receptor expressed in *Pichia pastoris*-Importance of correct processing of the N-terminus. *Protein Expr. Purif.* **55**, 225–235 (2007).
82. Chambers, J. K. *et al.* A G protein-coupled receptor for UDP-glucose. *J. Biol. Chem.* **275**, 10767–10771 (2000).
83. Arias, D. A., Navenot, J. M., Zhang, W. B., Broach, J. & Peiper, S. C. Constitutive activation of CCR5 and CCR2 induced by conformational changes in the conserved TXP motif in transmembrane helix 2. *J. Biol. Chem.* **278**, 36513–36521 (2003).
84. Brown, N. A., Schrevens, S., van Dijck, P. & Goldman, G. H. Fungal G-protein-coupled receptors: mediators of pathogenesis and targets for disease control. *Nat. Microbiol.* **3**, 402–414 (2018).
85. Huang, X. *et al.* Allosteric ligands for the pharmacologically dark receptors GPR68 and GPR65. *Nature* **527**, 477–483 (2015).
86. Liu, R., Van Veldhoven, J. P. D. & IJzerman, A. P. The role of the C-terminus of the human hydroxycarboxylic acid receptors 2 and 3 in G protein activation using Gα-engineered yeast cells. *Eur. J. Pharmacol.* **770**, 70–77 (2016).
87. Kajkowski, E. M., Price, L. A., Pausch, M. H., Young, K. H. & Ozenberger, B. A. Investigation of growth hormone releasing hormone receptor structure and activity using yeast expression technologies. *J. Recept. Signal Transduct. Res.* **17**, 293–303 (1997).
88. Miret, J. J., Rakhilina, L., Silverman, L. & Oehlen, B. Functional expression of heteromeric calcitonin gene-related peptide and adrenomedullin receptors in yeast. *J. Biol. Chem.* **277**, 6881–6887 (2002).
89. Ladds, G., Davis, K., Hillhouse, E. W. & Davey, J. Modified yeast cells to investigate the coupling of G protein-coupled receptors to specific G proteins. *Mol. Microbiol.* **47**, 781–792 (2003).
90. Bass, R. T. *et al.* Identification and characterization of novel somatostatin antagonists. *Mol. Pharmacol.* **50**, 709–715 (1996).
91. Baranski, T. J. *et al.* C5a Receptor Activation face other helices in a modeled seven-helix bundle. *Biochemistry* **274**, 15757–15765 (1999).
92. Kokkola, T. *et al.* Mutagenesis of human Mel(1a) melatonin receptor expressed in yeast reveals domains important for receptor function. *Biochem. Biophys. Res. Commun.* **249**, 531–536 (1998).
93. Campbell, R. M. *et al.* Selective A$_1$-adenosine receptor antagonists identified using yeast *Saccharomyces cerevisiae* functional assays. *Bioorganic Med. Chem. Lett.* **9**, 2413–2418 (1999).
94. Niebauer, R. T., Gao, Z. G., Li, B., Wess, J. & Jacobson, K. A. Signaling of the human P2Y1 receptor measured by a yeast growth assay with comparisons to assays of phospholipase C and calcium mobilization in 1321N1 human astrocytoma cells. *Purinergic Signal.* **1**, 241–247 (2005).
95. Sachpatzidis, A. *et al.* Identification of allosteric peptide agonists of CXCR4. *J. Biol. Chem.* **278**, 896–907 (2003).
96. Brown, A. J. *et al.* The orphan G protein-coupled receptors GPR41 and GPR43 are activated by propionate and other short chain carboxylic acids. *J. Biol. Chem.* **278**, 11312–11319 (2003).
97. Overton, H. A. *et al.* Deorphanization of a G protein-coupled receptor for oleoylethanolamide and its use in the discovery of small-molecule hypophagic agents. *Cell Metab.* **3**, 167–175 (2006).
98. Brown, A. J. Novel cannabinoid receptors. *Br. J. Pharmacol.* **152**, 567–575 (2007).
99. Overton, H. A., Fyfe, M. C. T. & Reynet, C. GPR119, a novel G protein-coupled receptor target for the treatment of type 2 diabetes and obesity. *Br. J. Pharmacol.* **153**, 76–81 (2008).
100. Stewart, G. D., Sexton, P. M. & Christopoulos, A. Detection of novel functional selectivity at M$_3$ muscarinic acetylcholine receptors using a *saccharomyces cerevisiae* platform. *ACS Chem. Biol.* **5**, 365–375 (2010).
101. Pausch, M. H. *et al.* Functional expression of human and mouse P2Y12 receptors in *Saccharomyces cerevisiae*. *Biochem. Biophys. Res. Commun.* **324**, 171–177 (2004).
102. Gearing, K. L. *et al.* Complex chimeras to map ligand binding sites of GPCRs. *Protein Eng.* **16**, 365–372 (2003).
103. Klco, J. M., Nikiforovich, G. V. & Baranski, T. J. Genetic analysis of the first and third extracellular loops of the C5a receptor reveals an essential WXFG motif in the first loop. *J. Biol. Chem.* **281**, 12010–12019 (2006).
104. Nakamura, Y., Ishii, J. & Kondo, A. Applications of yeast-based signaling sensor for characterization of antagonist and analysis of site-directed mutants of the human serotonin 1A receptor. *Biotechnol. Bioeng.* **112**, 1906–1915 (2015).
105. Scott, B. M. *et al.* Coupling of human rhodopsin to a yeast signaling pathway enables characterization of mutations associated with retinal disease. *Genetics* **211**, 597–615 (2019).
106. Ishii, J. *et al.* Microbial fluorescence sensing for human neurotensin receptor type 1 using Gα-engineered yeast cells. *Anal. Biochem.* **446**, 37–43 (2014).
107. Nakamura, Y., Ishii, J. & Kondo, A. Construction of a yeast-based signaling biosensor for human angiotensin II type 1 receptor via functional coupling between Asn295-mutated receptor and Gpa1/Gi3 chimeric Gα. *Biotechnol. Bioeng.* **111**, 2220–2228 (2014).
108. Ault, A. D. & Broach, J. R. Creation of GPCR-based chemical sensors by directed evolution in yeast. *Protein Eng. Des. Sel.* **19**, 1–8 (2006).
109. Marrakchi, M., Vidic, J., Jaffrezic-Renault, N., Martelet, C. & Pajot-Augy, E. A new concept of olfactory biosensor based on interdigitated microelectrodes and immobilized yeasts expressing the human receptor OR17-40. *Eur. Biophys. J.* **36**, 1015–1018 (2007).
110. Jockers, R. *et al.* Species difference in the G protein selectivity of the human and bovine A$_1$-adenosine receptor. *J. Biol. Chem.* **269**, 32077–32084 (1994).
111. Palmer, T. M., Gettys, T. W. & Stiles, G. L. Differential interaction with and regulation of multiple G-proteins by the rat A$_3$ adenosine receptor. *J. Biol. Chem.* **270**, 16895–16902 (1995).
112. Freund, S., Ungerer, M. & Lohse, M. J. A$_1$ adenosine receptors expressed in CHO-cells couple to adenylyl cyclase and to phospholipase C. *Naunyn. Schmiedebergs. Arch. Pharmacol.* **350**, 49–56 (1994).
113. Zhou, Q.-Y. *et al.* Molecular cloning and characterization of an adenosine receptor: the A$_3$ adenosine receptor. *Proc. Natl. Acad. Sci.* **89**, 7432–7436 (1992).
114. Schulte, G. & Fredholm, B. B. The Gs-coupled adenosine A$_{2B}$ receptor recruits divergent pathways to regulate ERK1/2 and p38. *Exp. Cell Res.* **290**, 168–176 (2003).
115. HIRANO, D. *et al.* Functional coupling of adenosine A$_{2a}$ receptor to inhibition of the mitogen-activated protein kinase cascade in Chinese hamster ovary cells. *Biochem. J.* **316**, 81–86 (1996).
116. Yaar, R., Jones, M. R., Chen, J.-F. & Ravid, K. Animal models for the study of adenosine receptor function. *J. Cell. Physiol.* **202**, 9–20 (2005).
117. Palmer, T. M. & Stiles, G. L. Adenosine receptors. *Neuropharmacology* **34**, 683–694 (1995).
118. Fredholm, B. B., IJzerman, A. P., Jacobson, K. a, Klotz, K. N. & Linden, J. International Union of Pharmacology. XXV.

Nomenclature and classification of adenosine receptors. *Pharmacol. Rev.* **53**, 527–52 (2001).
119. Glukhova, A. *et al.* Structure of the Adenosine A$_1$ Receptor Reveals the Basis for Subtype Selectivity. *Cell* **168**, 867–877.e13 (2017).
120. Dunwiddie, T. V. The Physiological Role of Adenosine In The Central Nervous System. *Int. Rev. Neurobiol.* **27**, 63–139 (1985).
121. Johnston, J. B. *et al.* Diminished adenosine A$_1$ receptor expression on macrophages in brain and blood of patients with multiple sclerosis. *Ann. Neurol.* **49**, 650–658 (2001).
122. Nascimento, F. P. *et al.* Adenosine A$_1$ Receptor-Dependent Antinociception Induced by Inosine in Mice: Pharmacological, Genetic and Biochemical Aspects. *Mol. Neurobiol.* **51**, 1368–1378 (2015).
123. De Mendonça, A. & Ribeiro, J. A. Influence of metabotropic glutamate receptor agonists on the inhibitory effects of adenosine A$_1$ receptor activation in the rat hippocampus. *Br. J. Pharmacol.* **121**, 1541–1548 (1997).
124. De Lera Ruiz, M., Lim, Y. H. & Zheng, J. Adenosine A$_{2A}$ receptor as a drug discovery target. *J. Med. Chem.* **57**, 3623–3650 (2014).
125. Fredholm, B. B., Irenius, E., Kull, B. & Schulte, G. Comparison of the potency of adenosine as an agonist at human adenosine receptors expressed in Chinese hamster ovary cells. *Biochem. Pharmacol.* **61**, 443–8 (2001).
126. El Yacoubi, M., Costentin, J. & Vaugeois, J.-M. Adenosine A$_{2A}$ receptors and depression. *Neurology* **61**, S82 LP-S87 (2003).
127. Klotz, K. N. Adenosine receptors and their ligands. *Naunyn. Schmiedebergs. Arch. Pharmacol.* **362**, 382–391 (2000).
128. Franco, R. *et al.* Partners for adenosine A$_1$ receptors. *J. Mol. Neurosci.* **26**, 221–231 (2005).
129. Fredholm, B. B. Adenosine receptors as drug targets. *Exp. Cell Res.* **316**, 1284–1288 (2010).
130. Borea, P. A., Gessi, S., Merighi, S., Vincenzi, F. & Varani, K. Pharmacology of Adenosine Receptors: The State of the Art. *Physiol. Rev.* **98**, 1591–1625 (2018).
131. Gessi, S., Merighi, S., Sacchetto, V., Simioni, C. & Borea, P. A. Adenosine receptors and cancer. *Biochim. Biophys. Acta* **1808**, 1400–1412 (2011).
132. Merighi, S. *et al.* A glance at adenosine receptors: novel target for antitumor therapy. *Pharmacol. Ther.* **100**, 31–48 (2003).
133. Sek, K. *et al.* Targeting Adenosine Receptor Signaling in Cancer Immunotherapy. *Int. J. Mol. Sci.* **19**, 3837 (2018).
134. Stewart, G. D. *et al.* Determination of adenosine A$_1$ receptor agonist and antagonist pharmacology using *Saccharomyces cerevisiae*: Implications for ligand screening and functional selectivity. *J. Pharmacol. Exp. Ther.* **331**, 277–286 (2009).
135. Peeters, M. C. *et al.* The role of the second and third extracellular loops of the adenosine A$_1$ receptor in activation and allosteric modulation. *Biochem. Pharmacol.* **84**, 76–87 (2012).
136. Bertheleme, N., Strege, A., Bunting, S. E., Dowell, S. J. & Byrne, B. Arginine 199 and Leucine 208 have key roles in the control of adenosine A$_{2A}$ receptor signalling function. *PLoS One* **9**, 1–7 (2014).
137. Liu, R., Groenewoud, N. J. A., Peeters, M. C., Lenselink, E. B. & IJzerman, A. P. A yeast screening method to decipher the interaction between the adenosine A$_{2B}$ receptor and the C-terminus of different G protein α-subunits. *Purinergic Signal.* **10**, 441–453 (2014).
138. Liu, R., Nahon, D., le Roy, B., Lenselink, E. B. & IJzerman, A. P. Scanning mutagenesis in a yeast system delineates the role of the NPxxY(x)5,6F motif and helix 8 of the adenosine A$_{2B}$ receptor in G protein coupling. *Biochem. Pharmacol.* **95**, 290–300 (2015).
139. Li, Q. *et al.* ZM241385, DPCPX, MRS1706 Are Inverse Agonists with Different Relative Intrinsic Efficacies on Constitutively Active Mutants of the Human Adenosine A$_{2B}$ Receptor. *J. Pharmacol. Exp. Ther.* **320**, 637–645 (2007).
140. Peeters, M. C. *et al.* GPCR structure and activation: an essential role for the first extracellular loop in activating the adenosine A$_{2B}$ receptor. *FASEB J.* **25**, 632–43 (2011).
141. Peeters, M. C. *et al.* Domains for activation and inactivation in G protein-coupled receptors – A mutational analysis of constitutive activity of the adenosine A$_{2B}$ receptor. *Biochem. Pharmacol.* **92**, 348–357 (2014).
142. Butz, J. A., Niebauer, R. T. & Robinson, A. S. Co-expression of molecular chaperones does not improve the heterologous expression of mammalian G-protein coupled receptor expression in yeast. *Biotechnol. Bioeng.* **84**, 292–304 (2003).
143. Niebauer, R. T., Wedekind, A. & Robinson, A. S. Decreases in yeast expression yields of the human adenosine A$_{2a}$ receptor are a result of translational or post-translational events. *Protein Expr. Purif.* **37**, 134–143 (2004).
144. Niebauer, R. T. & Robinson, A. S. Exceptional total and functional yields of the human adenosine (A$_{2a}$) receptor expressed in the yeast *Saccharomyces cerevisiae*. *Protein Expr. Purif.* **46**, 204–211 (2006).
145. O'Malley, M. A., Lazarova, T., Britton, Z. T. & Robinson, A. S. High-level expression in *Saccharomyces cerevisiae* enables isolation and spectroscopic characterization of functional human adenosine A$_{2a}$ receptor. *J. Struct. Biol.* **159**, 166–178 (2007).
146. Hino, T. *et al.* G-protein-coupled receptor inactivation by an allosteric inverse-agonist antibody. *Nature* **482**, 237–240 (2012).
147. Jamshad, M. *et al.* G-protein coupled receptor solubilization and purification for biophysical analysis and functional studies, in the total absence of detergent. *Biosci. Rep.* **35**, 1–10 (2015).
148. Grime, R. L. *et al.* Single molecule binding of a ligand to a G-protein-coupled receptor in real time using fluorescence correlation spectroscopy, rendered possible by nano-encapsulation in styrene maleic acid lipid particles. *Nanoscale* **12**, 11518–11525 (2020).
149. Routledge, S. J. *et al.* Ligand-induced conformational changes in a SMALP-encapsulated GPCR. *Biochim. Biophys. Acta - Biomembr.* **1862**, 183235 (2020).
150. Jain, A. R. & Robinson, A. S. Functional Expression of Adenosine A$_3$ Receptor in Yeast Utilizing a Chimera with the A$_{2A}$R C-Terminus. *Int. J. Mol. Sci.* **21**, 4547 (2020).
151. Wang, X. *et al.* Characterization of cancer-related somatic mutations in the adenosine A$_{2B}$ receptor. *Eur. J. Pharmacol.* **880**, 173126 (2020).
152. Ballesteros, J. A. & Weinstein, H. Integrated methods for the construction of three-dimensional models and computational probing of structure-function relations in G protein-coupled receptors. in *Methods in Neurosciences* **25**, 366–428 (1995).

Chapter 3

G protein-coupled receptors and their mutations in cancer - a focus on adenosine receptors.

Chapter 3

Abstract

G protein-coupled receptors (GPCRs) are the most intensively studied drug targets due to their ubiquitous involvement in human (patho)physiology. However, less attention has been paid to their role in oncology (tumorigenesis and metastasis) and is the main subject of this work. We will first discuss the involvement of those GPCRs for which existing evidence of "cancer" involvement is available. Subsequently, we will focus our scope on the effect of GPCR mutations in cancer progression. Nearly 20% of human tumors harbor GPCR mutations, which may alter the pharmacological function of the receptor by affecting e.g., their ligand binding, cell surface expression, GPCR-G protein interaction and/or constitutive activity. To illustrate this context we will take one subfamily of GPCRs, i.e. adenosine receptors, as a prominent example. Adenosine accumulation has been reported in the hypoxic tumor micro-environment. Adenosine regulates apoptosis, angiogenesis, metastasis and immune suppression as hallmarks in cancer via adenosine receptors. Cancer-related mutations of these receptors potentially alter adenosine receptor pharmacology, for which evidence will be presented. These studies suggest that these and other GPCRs and their cancer-specific mutations, together with linked signaling circuitry, represent novel biomarkers as well as therapeutic targets for cancer prevention and treatment.

3

Introduction

Drug development is mostly geared towards members of one of the following five protein families: kinases, G protein-coupled receptors (GPCRs), nuclear hormone receptors, ion channels or proteases[1]. GPCRs are the largest family of membrane-bound proteins, and include approximately 800 members accounting for around 4% of encoded human genes[2]. They can be subdivided in five main families: glutamate, rhodopsin, adhesion, frizzled/taste, and secretin (GRAFS)[3]. An alternative subdivision is in three main classes (A, B, and C)[4].

GPCRs share a common structure that consists of seven-transmembrane (7TM) helices, connected by three intracellular (IL) and three extracellular (EL) loops, an extracellular amino terminus, and an intracellular carboxyl terminus[2]. GPCRs respond to a wide diversity of physiological endogenous ligands, including neurotransmitters and hormones. GPCRs are coupled to different families of heterotrimeric G proteins, which consist of three subunits, α, β, and γ[2]. Extracellular signaling leads to conformational changes in GPCRs, causing the replacement of GDP for GTP at the G_α subunit. This exchange makes the $G_{\beta\gamma}$ subunit dissociate from G_α, which leads to interaction with effector proteins in the cell (Figure 1)[5,6]. Based on sequence similarity, the G_α-subunit family is divided into four major subfamilies, $G_{\alpha s}$, $G_{\alpha i}$, $G_{\alpha q/11}$ and $G_{\alpha12/13}$. Downstream signaling pathways can be regulated through both G_α subunits and $G_{\beta\gamma}$-dimers of G proteins by coupling to different effector molecules, such as phospholipase C (activated by $G_{\alpha q}$ or $G_{\alpha11}$), or adenylyl cyclase (activated or inhibited by $G_{\alpha s}$ and $G_{\alpha i}$). More downstream cellular signaling cascades involve second messengers, namely intracellular Ca^{2+} ($G_{\alpha q}$ or $G_{\alpha11}$) and cyclic adenosine monophosphate (cAMP) ($G_{\alpha s}$ or $G_{\alpha i}$)[7,8]. Once the receptor is activated, this is often followed by receptor desensitization and internalization via G protein-coupled receptor kinase (GRK)-mediated phosphorylation of the agonist-occupied receptor. GPCR phosphorylation regulates β-arrestin recruitment from the cytosol to the receptor, resulting in the termination of G protein-mediated signaling[9,10].

GPCRs are distributed throughout the human body and in combination with these various GPCR-related downstream pathways they have a crucial role in numerous physiological functions. However, GPCRs also make a substantial contribution to human pathophysiology[6]. This protein family has thus been investigated as pharmacological targets for decades, focusing on their ligand binding site that often can be accessed from the cell surface[11]. The major disease indications for GPCR modulators have shifted over the years from e.g., high blood pressure to metabolic diseases such as diabetes and obesity, as well as several central nervous system disorders[6]. Recently, GPCRs have become the targets for new indications, such as smoking cessation, hypocalcaemia, short bowel syndrome/Crohn's disease and multiple sclerosis. More recently, they are also seen as regulators of tumor initiation and progression including cell death, cell proliferation, invasion, angiogenesis, metastasis, stress signaling and immune evasion, making GPCRs attractive cancer drug targets[7,8,12–14]. Therefore, intervening with GPCRs and their distant

regulatory pathways provide an opportunity for developing approaches for cancer prevention, diagnosis and treatment[15]. Examples of anti-cancer drugs targeting GPCRs undergoing clinical trials are summarized in Table 1, though this table is not exhaustive.

Crystal structures of GPCRs in complex with various ligands and/or G proteins provide numerous templates for structure-based drug design and discovery[6]. Hauser *et al.* have recently reviewed all GPCR approved agents and drugs in clinical trials, which accounts for 475 chemical entities acting at 108 unique GPCRs[6]. Although around 30% of currently used therapeutic drugs are targeting GPCRs, only around 10% of the superfamily is being addressed and only few GPCRs are being explored as oncology drug targets[11], leaving many opportunities for cancer drug discovery.
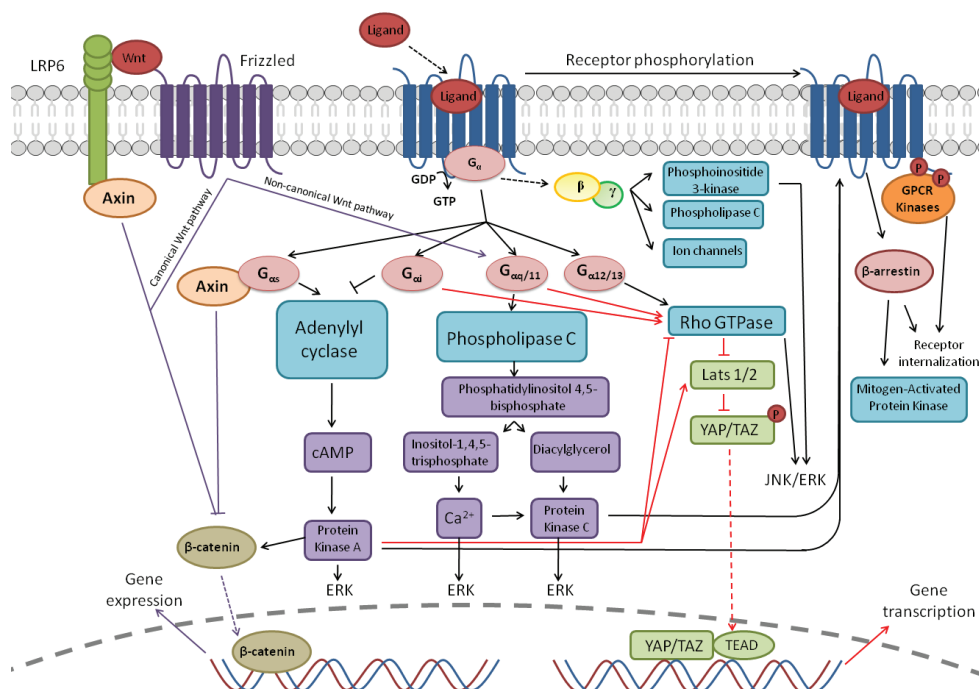
Figure 1. GPCR signaling from extracellular to intracellular. Upon receptor activation, GPCRs interact with G proteins, resulting in the dissociation of the α and βγ subunits and subsequent activation of downstream signaling effectors (black arrows). Subsequently, protein kinase A and protein kinase C regulate receptor phosphorylation and turn off the G protein signaling. GPCR kinases phosphorylation GPCR leads to β-arrestin recruitment and eventually receptor desensitization and internalization. β-arrestin engagement with the receptor also initiates the activation of β-arrestin–mediated signaling. Hippo signaling pathway can be activated by GPCR activation via several G proteins (red arrows). The Wnt pathway is mainly regulated by Frizzled receptors (purple arrows), where canonical and non-canonical signaling pathways can be activated.

Table 1. Examples of anti-cancer drugs and antibodies currently under clinical trials targeting GPCRs[273]. Adapted and updated from Usman et al. (2018)[274].

Receptor	Cancer type	Drug	Type of molecule	Phase	Sponsor
Adenosine receptors	Prostatic cancer	AB928	Small molecule	I (combined with zimberelimab)	Acrus Biosciences
Androgen receptor	Prostatic cancer	Apalutamide	Small molecule	I	Jansen Research & Development
CCR2	Pancreatic cancer	CCX872	Small molecule	I	ChemoCentryx
CCR2	Melanoma	Plozalizumab	Humanized monoclonal antibody	I	Millennium Pharmaceuticals
CCR4	Adult T-cell leukemia and lymphoma	Mogamulizumab (KW-0761)	Humanized, afucosylated monoclonal antibody	II	Kyowa Hakko Kirin
Cholecystokinin-2 receptor	Pancreatic cancer	G17DT	immunogen	III	Cancer Advances
CXCR4	Multiple myeloma	Ulocuplumab (BMS-936564)	Fully human monoclonal antibody	I	Bristol-Myers Squibb
CXCR4	Advanced or Metastatic cancer	LY-2624587	Monoclonal antibody	I	Eli Lilly
Dopamine D2 receptor	Endometrial cancer	ONC201	Small molecule	II	Fox Chase Cancer Center with Oncoceutics
Endothelin A receptor		Zibotentan (ZD4054)	Small molecule	I, II, III	AstraZeneca / Abbott
Endothelin A receptor	Prostate cancer	Atrasentan (ABT-627)	Small molecule	II; III (combined with docetaxel and prednisone)	Southwest Oncology Group
Endothelin-1 receptor	Ovarian cancer	GDC-0449 (Vismodegib) TALAZOPARIB	Small molecule	II	Genentech
	Breast cancer	Atezolizumab	Small molecule; Monoclonal antibody	II	Pfizer / Renske Altena
Epidermal growth factor receptor 2	Metastatic colorectal cancer	KL-140	Small molecule	II	Sichuan Kelun Pharmaceutical Research Institute
	Non-small cell lung cancer	Osimertinib (AZD9291)	Small molecule	III (combined with antibody); III	AstraZeneca
GPR20	Gastrointestinal stromal tumors	DS-6157a	Antibody-drug conjugate	I	Daiichi Sankyo
Frizzled receptor (FZD1, 2, 5, 7, 8)	Metastatic breast cancer	Vantictumab (OMP-18R5)	Human monoclonal antibody	I (combined with paclitaxel)	OncoMed Pharmaceuticals
	Non small cell lung carcinoma	Vantictumab (OMP-18R5)	Human monoclonal antibody	I (combined with Docetaxel)	OncoMed Pharmaceuticals
Frizzled receptor FZD7	Pancreatic cancer	Vantictumab (OMP-18R5)	Human monoclonal antibody	I (combined with Nab-Paclitaxel and Gemcitabine)	OncoMed Pharmaceuticals
Prostaglandin E2 receptor 4	Advanced solid tumors	AAT-007	Small molecule	II	University of Maryland
Smoothened receptor	Head and neck cancer	GDC-0449 (Vismodegib) Propranolol (β-adrenergic receptor antagonists)	Small molecule	II	Private person in collaboration with Genentech
	Ovarian cancer	β-adrenergic receptor antagonists	Small molecule	I	Washington University School of Medicine
β-adrenergic receptor	Metastatic breast cancer	β-adrenergic receptor antagonists	Small molecule	II	Columbia University

3

GPCRs and cancer

Cancer development consists of multiple steps, where the hallmarks of cancer comprise ten biological aspects, i.e. sustaining proliferative signaling, enabling replicative immortality, resisting cell death, evading growth suppressors, activating invasion and metastasis, avoiding immune destruction, inducing angiogenesis, tumor-promoting inflammation, deregulating cellular energetics, and genome instability and mutation[16]. GPCRs are traditionally connected to many physiological functions demonstrated by post-mitotic, differentiated cells, but are also present on proliferating cells, and involved in cancer development and cancer metastasis[15,17]. Current treatments are targeted towards only a small portion of the GPCR family (Table 1). Therefore, fundamental research is essential to obtain further insight in the roles of GPCRs in this disease area[17]. In the next paragraphs we will discuss GPCRs and their signaling pathways for which a role in tumor biology has been firmly established (Figure 2).

GPCR signaling in cancer

Following GPCR activation, several mechanisms and modulatory proteins are involved in preventing hyperactivation of GPCR signaling, including GTP hydrolysis,
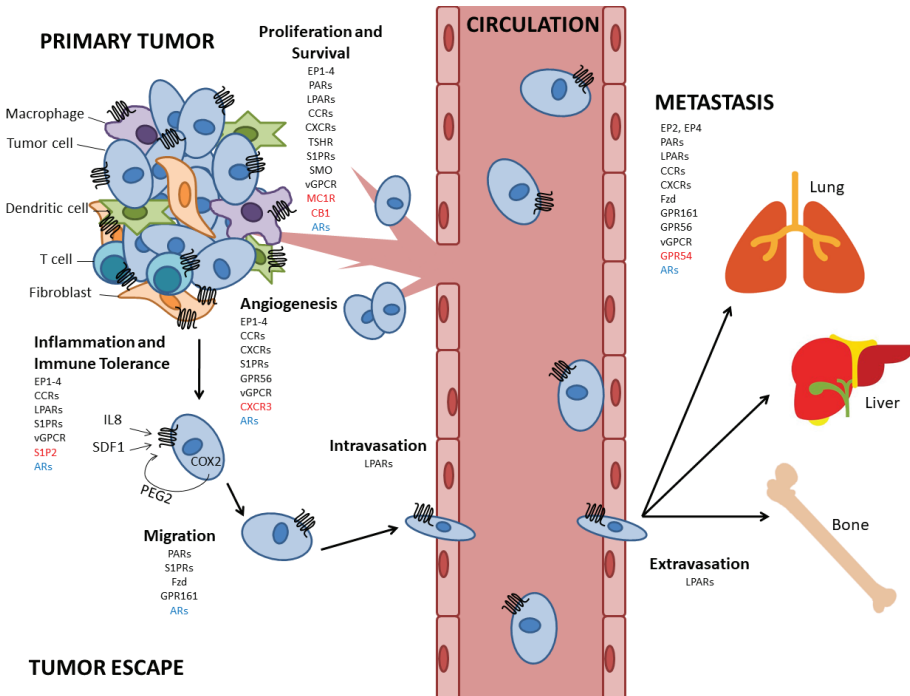

Figure 2. GPCRs and their roles in cancer hallmarks, adapted from Nieto Gutierrez *et al.* (2018)[51] and Dorsam *et al.* (2007)[15]. GPCRs with stimulating effects are marked in black, while GPCRs with suppressive effects are marked in red. Of note, adenosine receptors (blue) have both pro- and anti-tumoral effects depending on cancer type.

second messenger-related protein kinases, G protein-coupled receptor kinases (GRKs), and arrestins (Figure 1)[18]. As a result of phosphorylation of specific serine and threonine residues in the C-terminus of GPCRs, GPCR-mediated activity is abolished by GRKs followed by β-arrestin recruitment, which precedes cytosolic internalization and degradation of GPCRs by lysosomes[19]. Based on sequence similarity, mammalian GRKs have been classified into three subgroups, namely the rhodopsin kinases (GRK1 and GRK7), the β-ARK subgroup (GRK2 and GRK3), as well as the GRK4 subgroup (GRK4, GRK5, and GRK6)[20,21]. GRKs, acting as negative regulators of GPCR activity, may participate in cancer progression and tumor vascularization in a cell type-dependent manner[22–26]. Specifically, GRK1/7 is involved in cancer-associated retinopathy found in lung cancer patient via the interaction with recoverin, although direct evidence of reduced GRK1/7 activity in cancer progression has not yet been established[27].

In contrast, the involvement of GRK2 in cancer has been well-characterized with opposing effects in different cancer types. Poor survival rates and a high tumor stage of patients with pancreatic cancer are correlated with high GRK2 expression in clinical studies[28]. Overexpressed GRK2 in differentiated thyroid carcinoma reduces cancer cell proliferation through rapid desensitization of the thyroid-stimulating hormone receptor (TSHR)[29]. GRK2 acts as a negative regulator of cell cycle progression in human hepatocellular carcinoma HepG2 cells (HCCs)[23,30]. Besides, GRK2 participates in inhibiting Kaposi's associated sarcoma herpes virus (KSHV/HHV-8)-associated tumor progression as well as breast cancer and gastric cancer progression[31–33]. The role for GRK3 in breast cancer progression has been implicated to regulate CXCL12-mediated CXCR4 activation[34]. In prostate cancer GRK3 is overexpressed in both primary tumor and metastatic cells[35]. Moreover, decreased GRK3 levels may be beneficial for cancer cell survival by increasing stress adaptation in cancer cells[36]. GRK4 is mainly expressed in the testis, kidney, brain, ovaries and myometrium, although further research is warranted to characterize the role of GRK4 in cancer[37,38]. GRK5 plays diverse roles during tumorigenesis. In thyroid carcinoma, GRK5 inhibits the desensitization of TSHR[29]. GRK5 expression in glioblastoma cells is associated with a worsened prognosis in patients with stage II to IV glioblastoma[39]. It has been reported that induced expression of GRK5 is linked with oncogenesis and tumorigenesis via the regulation of cell cycle progression in prostate cancer[40]. GRK6 might be a promising biomarker for the early diagnosis of hepatocellular carcinoma[41].

Frizzled (Fzd) receptors, a subgroup of GPCRs, regulate normal development, tissue homeostasis and pathological processes, such as in cancer, through the interaction with Wnt proteins[42]. It is known that one single Wnt ligand is able to bind multiple different Fzd receptors. Moreover, the Wnt signaling pathway, highly conserved among species, regulates critical aspects of cell proliferation, polarity, cell fate determination and development, and stem cell differentiation[43,44]. The canonical Wnt signaling pathway involves β-catenin (Figure 1), and this pathway

has long been implicated in cancer, including colon cancer, ovarian carcinomas, hepatocellular carcinomas, melanomas and prostate cancers[42]. Wnt signaling via Fzd receptors is known to stabilize β-catenin and the low-density lipoprotein-related protein 6 receptor (LRP6) complex that inhibits β-catenin degradation[45]. Stabilized β-catenin, expressed in a wide range of cancers, is translocated to the cell nucleus and functions as a co-transcription factor[46,47]. In a diverse set of cancer types, the most commonly upregulated Wnt receptor, Fzd7, is therefore an attractive target for anti-cancer therapeutic strategy[48]. Non-canonical Wnt signaling consists of both the planar cell polarity pathway mediated via JNK signaling and the Ca^{2+}/PKC pathway via $G_{\alpha q/11}$ (Figure 1)[49,50]. The Wnt family also plays a prominent role in cancer stem cell (CSC) function, suggesting that deviant Wnt signaling might lead to tumorigenesis[46]. Taken together, blockage of the Wnt pathway may eventually inhibit tumor growth and tumor initiation[48]. Targeting the Wnt pathway-related Fzd receptor family members is therefore a potential anti-cancer strategy.

GPCRs are known as one of the multiple upstream modulators of the recently discovered Hippo signaling pathway that plays a crucial role in coordinating cell proliferation, autophagy, cell growth and apoptosis to establish and maintain particular control of organ size[51]. The mammalian Hippo signaling pathway commonly consists of serine/threonine kinase mammalian Ste2-like kinases 1 and 2 (MST1 and 2) that activate large tumor suppressor kinase 1/2 (LATS1 and 2), which phosphorylate the transcriptional coactivators Yes-associated protein (YAP) and transcriptional coactivator with PDZ-binding motif (TAZ)[51]. Phosphorylated YAP and TAZ are kept in the cytosol thereby preventing their access to the nucleus and inhibiting their transcriptional activity[52,53]. Overgrowth of both tissue and organ always involves unwanted inhibition or loss of function of Hippo signaling, which is associated with a wide variety of cancers[54–56]. YAP and TAZ functionality can either be induced or blocked depending on the different type of G protein that is coupled to a GPCR (Figure 1)[57,58]. In general, $G_{\alpha s}$ coupled GPCRs induce YAP phosphorylation preventing YAP-mediated transcriptional activation and YAP accumulation in nuclei, while $G_{\alpha 12/13}$, $G_{\alpha q/11}$, or $G_{\alpha i/o}$ coupled GPCRs result in dephosphorylation of YAP[59]. Therefore, the regulation of the Hippo signaling pathway via GPCRs may be a useful strategy in the treatment of certain cancer types.

Taken together, research on GPCR signaling networks is warranted to provide a better understanding of the involvement of these networks in cancer progression.

Inflammatory role of GPCRs in cancer

GPCRs are known to play an important role in the modulation of key inflammatory mediators[60], thus suggesting a possible link between cancer and chronic inflammation (Figure 2). Additionally, GPCRs have a crucial role in tumor-induced angiogenesis and migration of cancer cells to cause tumor metastasis[15]. Angiogenic factors produced from solid tumors are known to promote the proliferation of endothelial cells, therefore leading to the formation of tumor vascularization to increase oxygen

and nutrients supply for the tumor cells and routes for invasion and metastasis[13]. GPCRs and their related ligands are known to enhance angiogenesis by either directly inducing endothelial cell proliferation or indirectly by promoting release of vascular endothelial growth factor (VEGF) and other angiogenic factors from immune, stromal, or cancer cells[15].

Chemokines and chemokine (CC and CXC) receptors play an essential role in regulating the function of the immune system[61]. Notably, most chemokine receptors have been reported to bind several chemokines, while some are more selective, namely CXCR4, which only binds to CXCL12[62]. In cancer, they participate either in several steps of the antitumor immunity or in the coordination of the release of several mediators to promote angiogenesis, thus facilitating tumor development[63]. For instance, CCL2 recruits CCR2-bearing tumor-associated macrophages, which are known to modulate tumor vascularization and growth[62,64]. A similar effect has been suggested for CCL5, the chemokine ligand for CCR5, which is also related to macrophage recruitment as well as the recruitment of various other leukocytes into inflammatory sites including eosinophils, T cells, and basophils[65]. Furthermore, CCL5/CCR5 interactions may regulate tumor development in several ways, e.g. by stimulating angiogenesis, acting as growth factors, modulating the extracellular matrix, and taking part in immune evasion mechanisms[66]. Moreover, killing of tumor cells can be promoted by some immune cells; therefore, the presenting chemokine in the tumor microenvironment (TME) may help tumor cells escape the immune surveillance system through a less effective humoral response[62,64]. CXCL12, among other CXC-chemokines, is known to alter the local immune response and is a potent chemoattractant for pre-B lymphocytes, T cells, and dendritic cells. One of the receptors of CXCL12, CXCR4, is expressed on monocytes, T lymphocytes, endothelial cells, and neutrophils. This chemokine produced by various cell types in the TME regulates the activity of immunosuppressive cells and thus contributes to tumor progression[63]. Therefore, the characterization of the different chemokine networks in various cancer types may provide a better understanding of the immune-related mechanisms in cancer development.

The interaction between prostaglandin (PG) production and tumor progression is one of the most intensively investigated among the effectors linking inflammation and cancer. Cyclooxygenases (COX-1 and COX-2) produce PGs and thromboxane A_2 (TXA_2), and the pro-inflammatory effects of COX-1/2 are mediated upon binding of PGs to their respective GPCRs. Therefore, in numerous cancer types, inhibiting COX-1/2 using nonsteroidal anti-inflammatory drugs (NSAIDs) can reduce the incidence and risk of cancer[67,68]. For instance, NSAIDs inhibiting COX-2 can reduce the overall size and amount of adenomas in colorectal cancer patients. Furthermore, these drugs are used as a chemopreventive approach for colon cancer in healthy individuals[67,68]. Therefore, for early and advanced cancer, the effect of COX-2 inhibition in cancer prevention is under investigation in many clinical trials[69–71]. However, due to the potential cardiovascular complications of COX-2 inhibitors[72],

the (downstream/direct) inhibition of prostanoid receptors, yet another subfamily of GPCRs, might serve as an alternative strategy for cancer prevention and treatment.

Prostaglandin E_2 (PGE$_2$) and its GPCRs, E prostanoid receptors (EP$_1$–EP$_4$), are involved in tumor progression[73–75]. The EP$_1$ receptor is abundantly expressed, while the EP$_3$ receptor is only expressed at high level in certain tissues, such as pancreas, adipose tissues, vena cava and kidney. The EP$_4$ receptor is mainly expressed in the uterus, gastrointestinal tract, skin and hematopoietic tissues, while the EP$_2$ receptor is the least abundantly expressed EP receptor although widely distributed in many tissues[51]. In colon cancer, using an EP$_1$ receptor knockout mice model, EP$_1$ receptors were shown to play an essential role in cancer progression, and similar results were obtained in wild-type mice treated with an EP$_1$ receptor antagonist[76]. The involvement of EP4 receptors is widely established in tumorigenesis of multiple malignancies[77]. Together, COX-2 overexpression and PGE$_2$-mediated activation of EP$_2$ and EP$_4$ receptors contribute to the abnormal growth, and metastatic and angiogenesis potential of many highly prevalent cancers other than colon cancer[70,78–80]. PGE$_2$ and antigen presenting cell (APC)-regulated mechanisms are also known to be intimately related. APC inactivation is known as an early event in progression of colon cancer, which results in β-catenin stabilization in cytoplasm[75,81]. Similar to Wnt/Fzd receptors, PGE$_2$ stimulates the β-catenin pathway through the EP$_2$ receptor in colon cancer cells[82,83]. Even the EP$_2$ receptor is also involved in VEGF expression to promote angiogenesis[84]. The least commonly cancer-linked EP receptor, EP$_3$ receptor, may indirectly modulate pathways involved in tumor angiogenesis[85–87].

Moreover, PGE$_2$ initiates cross-talk with other GPCRs. For instance, the endogenous ligand of the endothelin 1 receptor, endothelin 1, is expressed at a high level in over 80% of colon cancers and can rescue colon cells from apoptosis by β-catenin inhibition as it is also a downstream transcriptional target of β-catenin[69].

Investigation of cancer-related inflammation and the role of GPCRs therein may thus provide insights in the immune-related mechanisms of cancer progression and suggest novel strategies in cancer immunotherapy.

Aberrant expression of GPCRs in cancer

Overexpression of many GPCRs occurs in a wide variety of cancer types, suggesting their contribution to tumor cell growth upon activation of their ligands whether produced locally or circulating. Among these, chemokine receptors, protease-activated receptors (PARs), as well as receptors for bio-active lipids (sphingosine-1-phosphate receptors (S1PRs) and lysophosphatidic acid receptors (LPARs)), increase cell proliferation in a wide array of cancer cells[15].

In highly invasive breast carcinomas PAR1 overexpression has been observed, and this increased expression in mammary glands in a mouse model results in premalignant atypical intraductal hyperplasia[88]. The increase of PAR1 expression is also seen in advanced stage prostate cancer[89].

Quite often the altered expression of chemokine receptors in cancer cells together with the release of chemokines from secondary organs causes organ-specific metastasis[15]. High expression levels of CXCR4 in prostate cancer cells increase blood-vessel density and muscle invasion[90]. CCR10, the receptor for CCL27 and CCL28, has been found expressed in human melanoma cells. In a common site of metastasis for melanoma, i.e. skin, CCL27 and CCL28 are highly expressed[91]. Constitutive production of CXCL1 and CXCL8 is observed in melanoma cells. Furthermore, the same cell types also highly express the receptor of these chemokines, CXCR2, and stimulation of autocrine chemokine increases proliferation, migration and survival of tumor cells[92]. Many different tumor cells aberrantly express CXCR4 and cancer cells with a high level of CXCR4 expression are more prone to undergo metastases[93]. In some cancer types, CXCR4 is co-expressed with other CC or CXC chemokine receptors on cancer cells and the combination has been suggested to be related to cancer progression[94].

In ovarian cancer, LPA is one of the most potent mitogens secreted by cancer cells to the ascites fluid. The effect of LPA in promoting growth, survival and resistance to chemotherapy is via the stimulation of the LPARs that are frequently overexpressed in ovarian cancer cells[95].

S1P regulates central cellular processes and affects all steps of tumor growth and metastasis[96]. S1P has been shown to be important in the metastatic behavior of aggressive thyroid tumors, where the expression of S1P receptors is up-regulated[97]. High expression of S1P together with up-regulation of S1P receptors, is observed in the human prostate cancer cell line PC3, where together they protect cells from apoptosis induced by camptothecin, a topoisomerase inhibitor[98]. The pathological diversities in gastric cancers are largely dependent on the expression profiles of the S1P receptor subtype and thus therapeutic interventions targeting each S1P receptor might be clinically effective in preventing metastasis[99].

Therefore, overexpression of a certain GPCR may serve as a biomarker for diagnostic purposes in some cancer types and a target for cancer treatment.

Role of GPCRs in cancer cell proliferation and metastasis

Metastasis, as one of the more serious challenges for cancer therapy, significantly reduces life quality and overall long-term survival of patients with malignancies[100]. Cancer cells metastasize to specific organs with a much greater incidence than would be expected from the primary tumor site and the secondary organs (Figure 2). GPCRs are considered as attractive targets to prevent and treat metastasis.

PARs are activated by a unique proteolytic cleavage mechanism of their N-terminus, leading to the activation of a diverse network of signals[101]. PARs sense and respond to proteases activated in the tumor microenvironment, and are thus pivotally involved in tumor invasion and metastatic efficiency[101]. In an animal melanoma model PAR1 knock-down led to reduced tumor growth and metastases to the lung[51]. Expression

of both PAR1 and PAR2 has been established in different types of cancer cells, and evidence suggests the contribution of PAR2 in tumor development. For example, in a mouse model with PAR2 deletion breast tumor development was delayed with decreased metastasis formation[102]. A similar observation was noted in breast xenograft models in which inhibitory antibodies of PAR2 weakened tumor growth and metastasis[103].

Chemokines and chemokine receptors also direct the traffic of leukocytes and their progenitor cells between the lymphoid organs and the blood and the migration of leukocytes to sites of inflammation[62]. As mentioned before multiple chemokine receptors are expressed in tumor cells, and are activated in response to released chemokines in the tumor microenvironment from tumor-infiltrating leukocytes, macrophages, stromal cells and even cancer cells, thus promoting the survival and motility of cancer cells in both an autocrine and paracrine pattern[62]. Although few studies comprehensively characterized all chemokine receptors present on cancer cells, one single chemokine receptor is still able to influence the spreading direction of a cancer cell. Multiple chemokine receptors possibly participate in metastases of the same cancer to different sites[94]. CXCR4 is highly expressed in many tumor cells, and CXCR4 activation stimulates directed cancer cell migration and induces their filtration through bone marrow stromal cells, endothelial cells and fibroblasts[94]. Breast tumors with high CXCR4 expression showed more extended metastasis in comparison to tumors with low expression of CXCR4, but no significant correlation was found with blood-born metastasis[104]. Furthermore, CXCR4-mediated metastasis was observed from melanoma cells to the lungs[105]. Pancreatic cancer cells with CCR6 expression show enhanced proliferation in response to CCL20[106]. CCR7 has been found expressed in some cancer types, which was correlated to metastatic potential and poor prognosis. The ligand of CCR7, CCL12, has been found at high levels in the lymph nodes that connect many cancers[91].

Similar to chemokine receptors LPARs are reported to have proliferative, pro-survival and pro-migratory effects in ovarian cancer cells, while LPARs also stimulate further LPA release[95]. In this case, an autocrine loop occurs to drive the unrestricted ovarian cancer cell growth[95,107].

As the GPCRs described above promote cancer cell proliferation and metastasis, inhibitors of these (and potentially several other) GPCRs have the potential of decreasing the survival, uncontrolled proliferation and organ-specific metastasis of cancer cells.

Viral GPCRs in cancer

In the examples above, human GPCRs played a role in cancer development. However, many human cancer-associated viruses hijack GPCR signaling to enhance their life cycle[108]. Among them, herpes viruses can set up life-long persistent infection in humans with normal immune response. Particularly, re-activation of

herpes viruses in patients with an impaired immune system may cause severe morbidity and mortality[109,110]. These viral GPCRs, sharing sequence homology with human chemokine receptors, are able to direct immune cells to the inflammation site; they are also actively involved in different pathological processes, including tumor growth, survival and metastasis (Figure 2)[62,63]. Different from predominantly $G_{\alpha i}$ coupled human chemokine receptors, viral GPCRs may activate different downstream signaling pathways through several G_α proteins even in the absence of ligand activation, meaning they are constitutively activated[108,111]. Moreover, viral GPCRs promiscuously respond to a wide array of chemokines, indicating that they can utilize the immune system of the host to modulate viral dissemination as part of the immunopathology of the viral infection[112]. Early studies of virally encoded oncogenes have provided evidence that at least seven human viruses, hepatitis B virus (HBV), Epstein-Barr virus (EBV/HHV-4), human papilloma virus (HPV), human T-cell lymphotropic virus (HTLV-1), hepatitis C virus (HCV), Merkel cell polyomavirus, and Kaposi's associated sarcoma herpes virus (KSHV/HHV-8), are involved in 10–15% of cancers[113,114]. Interestingly, open reading frames encoding GPCRs have been observed in the viral genomes of many human viruses, suggesting that replicative success benefits from these signaling pathways[115]. For instance, human cytomegalovirus (HCMV/HHV-5) regulates the expression of at least four GPCRs (US27, US28, UL33 and UL78), and EBV encodes one GPCR (BILF1). The receptor expressed by KSHV, commonly known as KSHV vGPCR (or ORF74), shares similar structure and functionality to CXCR1 and CXCR2[116]. Constitutive activity of KSHV vGPCR gives it potent transforming and pro-angiogenic properties, and contributes to Kaposi's sarcoma development[117]. It promotes the function of a complex signaling network to induce sarcomagenesis. KSHV vGPCR-expressing cells activate the dysregulated growth of distant and surrounding endothelial cells, thus representing an example of paracrine neoplasia[117]. Hence, inhibition of vGPCRs and their downstream signaling networks may provide new potential treatment for KSHV-associated cancers.

Role of GPCRs in tumor suppression

GPCRs mainly show pro-tumoral effects, but in certain malignancies some GPCRs and related G proteins may actually show tumor suppressive effects (Figure 2). As an example, inactivating mutations of the melanocortin 1 receptor (MC1R) increase the risk of melanoma development[118], suggesting the wild-type receptor to be tumor suppressive. CXCR3 ligands suppress tumor progression by indirectly mediating anti-angiogenic effects, while in gliomas, colorectal, skin, and breast cancer the cannabinoid receptors (CB1 and CB2) play tumor suppressive roles[119]. In addition, SIP_2 receptor signaling via $G_{\alpha 13}$ acts as a tumor suppressor in diffuse large B cell lymphoma (DLBCL)[120]. Lastly, *KiSS1*-derived peptide receptor (GPR54) suppresses metastasis in melanoma and breast cancer cells[121]. These are certainly not the only anti-tumorigenic GPCR/G protein signaling pathways in different cancers[13], and many anti-tumoral GPCRs are likely to be discovered in the near future.

GPCR mutations in cancer

Large scale sequencing efforts of cancer genomes combined with unbiased systematic approaches, have identified a large number of mutations in GPCRs and G proteins, Specifically, it was found that in approximately 20% of all cancers GPCRs are mutated[122,123], making research into the potential oncogenic effects of GPCR mutations paramount. Cancer-related mutation data have for example been collected in The Cancer Genome Atlas (TCGA)[124] and the National Cancer Institute Genomic Data Commons (GDC)[125]. Of note, higher mutation rates are often observed for certain conserved residues, and given the (evolutionary) importance of these residues the exact impact of these mutations in receptor pharmacology warrants considerable investigation[122,126]. In tumor samples, analysis of GPCR somatic mutation rates in comparison with the background mutation rates has identified several frequently mutated GPCRs, suggesting their involvement in cancer[122]. In this section, we will first discuss the general consequences of a mutation for receptor behavior (Figure 3), be it somatic or experimentally induced. Thereafter, we will discuss in depth some of the naturally occurring mutations in cancer tissue.
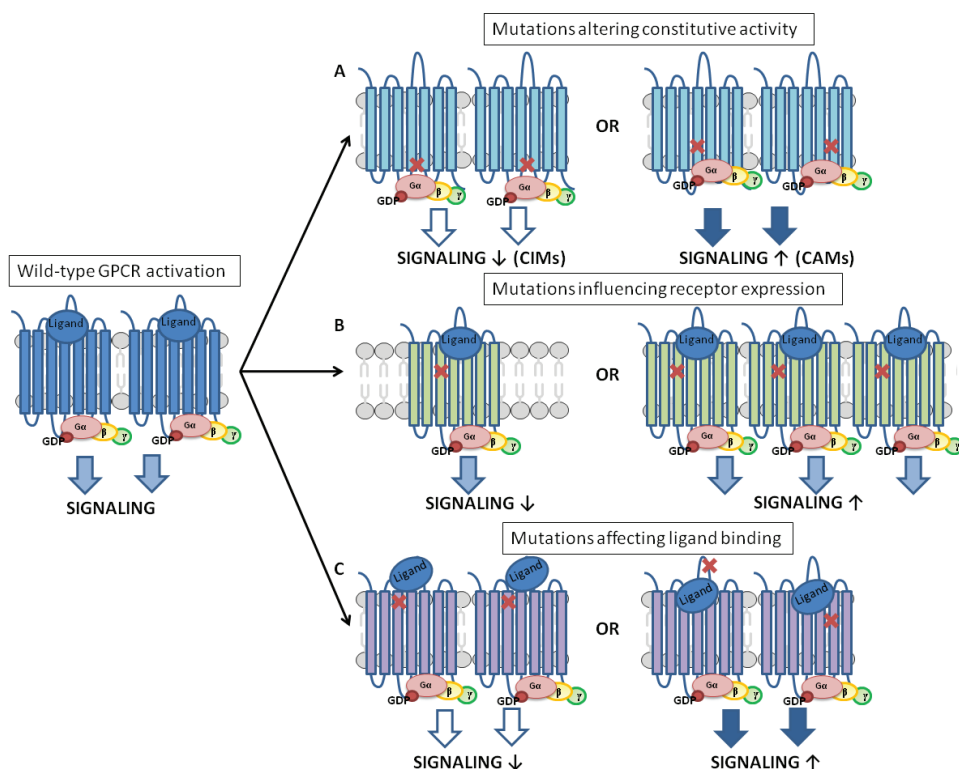

Figure 3. Effects of GPCR mutations on receptor pharmacology, such as A) constitutive activity, B) receptor expression and C) ligand binding and their concomitant effect on receptor signaling. Red crosses indicate potential mutation sites.

GPCR mutations affecting constitutive activity

Several detailed three-dimensional structures of various GPCRs in different activation states have been published, providing us with an unprecedented understanding of GPCR structure and function[127]. GPCRs harbor various signaling states and structural conformations[128]. Based on the simplified two-state-receptor model, all states that are unfavorable for G protein binding are referred to as inactive (R), and all states that couple to G proteins as "active" (R*)[129]. Since GPCRs are flexible, the equilibrium between R and R* states provides room for the presence of the R* state even without agonist binding. This brings constitutive or basal activity into play, which varies highly among wild-type GPCRs and has physiological importance in many cases. Both decreased and increased constitutive activity are known to cause disease phenotypes, such as neuropsychiatric and cardiovascular diseases[130]. Mutant receptors that show induced basal activity in the absence of an agonist, are referred as constitutively active mutants (CAMs), while those with decreased basal activity are termed constitutively inactive mutants (CIMs) (Figure 3)[131]. In many GPCRs an aspartate acid residue in TM6 (Asp6.30) and an arginine in the TM3 DRY motif (Arg3.50) form a salt bridge, also called "ionic lock", which has been linked to the modulation of basal activity by limiting GPCR flexibility[132–134]. This salt bridge can be disrupted by mutation of the aspartate acid at residue 6.30 into different amino acids, resulting in increased constitutive activity in several GPCRs[135–138]. This increased flexibility in GPCRs can preclude the necessity for ligand binding to open the cavity of G protein-binding.

In general, at the amino acid side chains within the helical bundle a mutation with increased hydrophilicity can destabilize the receptor[139]. Increasing the size of the amino acid side chain may lead to clashes with surroundings, which leads to small conformational changes in the immediate surroundings. This is especially important for the residues located around the kink area in TM6, where a small conformational change can cause the movement of the helix and open up the cavity for G protein coupling[140,141]. Several CAMs are caused by an altered charge of the affected amino acid, either a change from negative to neutral or from negative to positive. In general, charged side chains in the helical bundle likely participate in electrostatic interactions. Therefore, mutations with charge-altered side chain break these interactions, releasing a constraint that otherwise keeps the receptor in the R state[142]. Mutations leading to decreased basal activity have also been found in many GPCRs by restraining interactions, while most of them also cause other defects, such as impaired agonist binding, impaired G protein coupling, or a generally decreased response to agonist-mediated activation[142].

GPCR mutations affect receptor expression

GPCR mutations can affect receptor expression (Figure 3B). Although increased GPCR expression in cancer is regularly reported (see above), it is yet unclear if mutations play a role in this. In contrast, amongst all impacts of GPCR mutations

the most common defect is impaired receptor expression[143]. Even though the biosynthesis of mutant receptors does not seem to be much affected, the trafficking of mutant receptors has been altered in that nascent receptors with misfolded structures are not moved to the Golgi apparatus, but instead, transported to lysosomes for degradation[144,145]. Any mutation causing disturbance of the disulfide bridge between the second extracellular loop and residue Cys3.25 in TM3 has been suggested to cause receptor malfunction and instability[146]. Other causes of faulty trafficking are the deletion or disruption of signal peptide motifs. For example in the follicle-stimulating hormone receptor, a motif within the C-terminal tail has been reported to be important for targeting the plasma membrane, and mutations found in this motif often result in intracellular retention[147]. Thus, mutations altering receptor expression may also affect the functionality of a GPCR.

GPCR mutations affect agonist-dependent activation

Upon ligand binding, a GPCR mutation can modify the response by altering agonist affinity, efficacy and/or receptor selectivity (Figure 3). During receptor activation, the conformation of intracellular parts of TMs 5 and 6 change considerably to generate an interaction with G protein and to process activation[139]. It is possible that a mutation located in or near key positions, including micro-switches, GPCR-G protein interaction interface and ligand-dependent trigger residues, can partially mimic this process, resulting in altered receptor functionality. Residues directly and indirectly essential for agonist binding are usually found within the ELs and in the (top half of the) 7TM domains, and are expected to modulate affinity[133,146]. Upon agonist binding, a mutation facilitating the R* state formation of the receptor, provides a more preferred interface interaction for G-protein activation and thus increases agonist affinity and efficacy. However, depending on the type of ligand and receptor, GPCRs can engage a G-protein and/or β-arrestin, or prefer one over the other. This ability of a ligand is called functional selectivity or biased signaling, which directs a GPCR towards a specific conformation selectively linked to a particular activation pathway[128]. In general, mutations located within the 7TM domain can be expected to disrupt the energy barrier for agonist-mediated activation, thereby modulating functional selectivity of the receptor[142]. Residues along TM6 are especially interesting, as these residues experience the most dramatic structural/spatial change upon receptor activation[148]. Moreover, the residues located around the kink area of TM6, including clusters between TMs 6 and 7 and between TMs 3 and 6, have been suggested in movement regulation[146]. Taken together, agonist-dependent activation of mutant GPCRs and changes in the basal activity of such receptors (as described in the preceding paragraph) are inextricably linked.

Role of GPCR mutations in cancer

One of the most frequently mutated GPCRs in tumors is smoothened (SMO), a class F GPCR, for which the twelve-transmembrane receptor Patched (PTCH) acts as a negative regulator[149,150]. This SMO inhibition is relieved upon the binding Hedgehog

(Hh) to PTCH, which results in downstream stimulation of the transcription factor glioma-associated oncogene (GLI)[149,150]. Mutations in PTCH and SMO have been suggested to initiate sporadic basal cell carcinoma[151–153]. An activating mutation of SMO, W535L located at the bottom part of TM7, initially identified from basal-cell carcinoma, has recently also been found in meningiomas[154,155]. In addition, mutations of SMO have been identified in colon cancer and cancers in the central nervous system, and emerging evidence strongly supports continuous SMO signaling is involved in tumor progression[156].

The second most frequently mutated GPCRs are the metabotropic glutamate receptor (mGlu) family members, mGlu1–8, which have a significant cancer-specific distribution[122]. Mutations in mGlu8, mGlu1 and mGlu3 have been identified in squamous non-small cell lung cancer (NSCLC), melanomas, and NSCLC adenocarcinomas, respectively[122]. Mutated mGlu8 was found in 8% of NSCLCs of the squamous subtype, while mutated mGlu1 was found in 7% of NSCLC adenocarcinomas[123]. However, the impact of these mutations at a molecular and cellular level still needs to be fully characterized to understand their subsequent effects on tumor progression[13]. Mutated mGlu3 has been found in 16% of examined melanomas in a study in which endogenously expressed mutant GPCRs were linked to the progression of melanoma by using a systematic exon-capture analysis together with a massively parallel sequencing approach on 734 GPCRs[157]. The mGlu receptor family is of particular interest due to the increased availability of glutamate, its endogenous ligand, in the tumor microenvironment[158]. Together, this suggests that at the surface of tumor cells both wild-type and mutant mGlu receptors may be expressed and activated.

The GPCR adhesion receptor family, consisting of 33 members, also presents frequent mutations. The adhesion receptors, including GPR98, GPR112 and brain-specific angiogenesis inhibitor (BAI) members, are involved in regulating cell-cell and cell-matrix interactions[159]. Among these receptors, the most frequently mutated GPCR in cancer is GPR98[122], for instance in melanoma progression it was mutated in 28% of the melanomas examined[157].

Syndromes caused by unrestrained hormonal secretion often involve activating mutations in GPCRs, which are also found in endocrine tumors[15]. For instance, TSHR mutations with activating effects are found in around 80% of thyroid adenomas and in some thyroid carcinomas, and TSHR mutations in germ cells result in familial non-autoimmune hyperthyroidism[72]. In thyroid cancer TSHR is found to be the most frequently mutated GPCR, while it is also mutated in ovarian, lung and large intestine cancers. These TSHR variants need further investigation to unravel their precise role[122]. Mutations in the TSHR are located throughout the receptor structure. The effects of these variants vary from completely abolished to slightly decreased TSH response, to those with increased constitutive activity[72]. The activating TSHR mutants promote the constant activation of adenylate cyclase via $G_{\alpha s}$, leading to hyperfunctional thyroid adenomas[72]. A close homologue of TSHR, luteinizing hormone

receptor (LHCGR), is particularly evident in colon, lung and breast cancers, whereas another related GPCR, follicle-stimulating hormone receptor (FSHR), is known to be mutated in large intestine cancers[122]. Some subtypes of adult stem cells particularly express other TSHR-related receptors, such as leucine-rich repeat-containing GPCR 4 (LGR4), LGR5 and LGR6[160]. Mutations of these receptors have also been identified in melanoma and in colon carcinoma. This implicates that these stem cell populations play a potential role in cancer initiation. Taken together, cancer-specific GPCR mutations offer a novel approach for the development of strategies that target both cancer prevention and treatment.

Adenosine receptors and cancer

The adenosine receptors (ARs) belong to Class A, rhodopsin-like GPCRs and there are four subtypes, A_1AR, $A_{2A}AR$, $A_{2B}AR$ and A_3AR. ARs have attracted much attention in the recent years as therapeutic targets[3]. As they play an important role in both physiological and pathophysiological conditions, in-depth investigation of these GPCRs is required. Additionally, all four AR subtypes have been detected in different human tumor tissues[161]. Dependent on the adenosine receptor subtype, extracellular binding of adenosine leads to activation of different downstream signaling cascades (Figure 1). Through G_i-coupling, the A_1AR and A_3AR inhibit adenylate cyclase and reduce cAMP levels[162–165]. $A_{2A}AR$ and $A_{2B}AR$ are coupled to G_S proteins and increase the levels of cAMP[166,167]. In addition, $A_{2B}AR$ can also couple to G_q proteins, which causes the activation of phospholipase C and mobilization of calcium[168,169]. We will first briefly discuss the general (patho)physiological roles of ARs and their sometimes contradicting roles, i.e. pro- and anti-tumoral effects in cancer cells, as well as their involvement in the TME. Then we will discuss potential cancer treatments targeting ARs. Afterwards, we will take $A_{2B}AR$ as an example to discuss the effect of cancer-related mutations in receptor pharmacology.

Distribution and (patho)physiological roles of adenosine receptors

The A_1AR is abundant in the central nervous system (CNS), with high expression levels in the hippocampus, cerebral cortex, thalamus, cerebellum, spinal cord and brain stem. The A_1AR has also been identified in numerous peripheral tissues, including testis, vas deferens, stomach, white adipose tissue, pituitary, spleen, heart, adrenal gland, aorta, bladder, eye and liver. In tissues such as kidney, lung and small intestine, A_1AR is expressed at low levels[170–172]. A_1AR has a pivotal role in neuronal, renal and cardiac processes[173]. Based on the receptors involved or the site of application, adenosine causes either pro- or anti-nociceptive effects on pain. A_1AR is mostly suggested to be involved in pain pathways, and has been reported in animal models of inflammatory and neuropathic pain[174]. Moreover, during periods of decreased sleep duration and sustained wakefulness, accumulated adenosine acts as a natural sleep-promoting agent[175]. Indeed, A_1ARs expressed in the suprachiasmatic

nucleus regulate the circadian clock response to light[176]. Endogenous adenosine, via A_1AR activation, regulates long-term synaptic plasticity phenomena, such as depotentiation, long-term depression and long-term potentiation[177], Moreover, A_1AR antagonists have been suggested to be beneficial in memory disorders. In the CNS, acute administration of A_1AR agonists is neuroprotective, while A_1AR antagonists promote the death of neuronal cells in ischemic models[178]. In addition, selective agonists of A_1AR may be utilized as pharmacologic preconditioning agents for lung transplantation to prevent ischemia-reperfusion injury, as well as other forms of pulmonary vascular ischemia[179].

In the CNS the $A_{2A}AR$ is expressed at high levels in the olfactory tubercle and striatum[171]. It is also highly expressed in blood platelets, leucocytes, spleen and thymus in the periphery. Intermediate expression levels of $A_{2A}AR$ have been found in blood vessels, heart, and lung[169,170]. The $A_{2A}AR$ is involved in the onset of vasodilation, exploratory activity, aggressiveness, hypoalgesia and inhibition of platelet aggregation[170]. Additionally, $A_{2A}AR$ is involved in the progression of Parkinson's disease, Alzheimer's disease, Huntington's disease, and in the attenuation of neuroprotection, ischaemia and inflammation, particularly in peripheral tissues[169,170]. More recently, $A_{2A}AR$ antagonists have been suggested for the management of chronic pain[180]. For example, in two acute thermal pain tests, the $A_{2A}AR$ selective antagonist SCH 58261 produced antinociception[181]. The impact of $A_{2A}ARs$ in controlling neuronal damage was first proposed in a cerebral ischemic injury model[181]. Studies have shown that either the genetic elimination or the pharmacological blockade of $A_{2A}ARs$ in brain ischemia animal models provided robust neuroprotection[181]. Furthermore, the excessive activity of the thalamic cortex can be reduced through blockage of $A_{2A}ARs$ on striato-pallidal neurons. This is known to restore balance between striatopallidal and striatonigral neurons and consequently influence the efficacy of $A_{2A}AR$ antagonist in Parkinson's disease[182]. Several lines of evidence support a role for $A_{2A}AR$ in abuse substance pathologies, thereby suggesting this receptor as a possible target for the treatment of drug addiction[183].

$A_{2B}ARs$ receptors are expressed in many organs, including kidney, colon, lung and spleen, and the vasculature is the primary site of expression in all of these organs. In addition, endothelial cells, macrophages and smooth muscle cells display a high level of $A_{2B}AR$ expression[184], and colonic epithelial cells also express this receptor[185]. $A_{2B}AR$ expressions has been shown in isolated primary cells, as well as cell lines for other cell types, such as dendritic cells, lymphocytes and mast cells[185–187]. It has long been implicated that extracellular adenosine is related to adaptation to hypoxic conditions and $A_{2B}ARs$ play an essential role in inhibiting hypoxia-induced vascular leak *in vivo*[188]. In addition, extracellular adenosine stimulates cell death of human arterial smooth muscle cells through a cAMP-dependent pathway mediated by $A_{2B}AR$[189].

The A_3AR is expressed at relatively low levels in the CNS, particularly in the thalamus and the hypothalamus[187]. Liver and lung express A_3AR with the highest reported

levels, while the aorta expresses A_3AR at intermediate levels[171]. Additionally, the A_3AR has been found in mast cells, eosinophils, kidney, testis, heart, placenta, spleen, bladder, uterus, aorta, jejunum, eye and proximal colon, although with differences in expression level, and among species[170–172]. The A_3AR is suggested to mediate apoptotic events in certain cell types, allergic responses, and airway inflammation[171,172]. Despite the low expression in the brain, the involvement of A_3AR in both normal and pathological conditions in the CNS has been of considerable interest[190]. Furthermore, higher expression levels of A_3ARs have been determined in tumor cells than in healthy cells, demonstrating its potential role as a tumor marker[191].

Role of adenosine receptors in cancer cells

ARs have been associated with carcinogenesis, where both pro- and anti-tumoral effects have been identified (Figure 4). Although multiple studies addressed the role of A_1AR in cancer progression, its precise role has not been fully characterized. Increased expression levels of the A_1AR have been observed in diverse cancer cells, such as colorectal adenocarcinomas, leukemia Jurkat and melanoma A375 cell lines[192–194]. Overexpression of A_1AR in MDA-MB-468 breast cancer cells enhances cell growth, survival, and proliferation[193]. In renal cell carcinoma, blockage of A_1AR signaling inhibits cell proliferation and migration by regulating the ERK/JNK signaling pathway (Figure 1)[192]. Lastly, it has been shown that adenosine-mediated tumor cell chemotaxis could be inhibited by an A_1AR antagonist[195]. On the other hand, in CW2 colonic cancer cells and rat astrocytoma cells, adenosine induces cell death through activation of caspases 3 and 9 via A_1AR[196,197]. It has been shown that activation of A_1AR causes increased apoptosis and thus inhibits tumor growth in MCF7 breast cancer cell lines[194]. In breast tumor cell lines T74D and HS578T, leukemia MOLT-4 and human LoVo metastatic cell lines, stimulation of A_1AR inhibits cell proliferation[161,198]. In addition, activation of A_1AR expressed on microglia dampens the growth of glioblastoma[199].

As $A_{2A}AR$ has been discovered on the cell surface of diverse human tumor cells, this receptor is expected to play a role in cancer[200,201]. $A_{2A}AR$ is involved in promotion of angiogenesis inducing endothelial cell proliferation and migration, as well as synthesis of important angiogenic growth factors such as VEGF[202,203]. Adenosine-mediated $A_{2A}AR$ activation produces cAMP and inhibits the destruction of cancer cells initiated by lymphokine-activated killer cells[204]. Activation of $A_{2A}AR$ also stimulates cell proliferation of endothelial and melanoma cells[205]. Under both normal and hypoxic conditions in hepatocellular carcinoma cells (Hep3B) *in vitro* and *in vivo*, $A_{2A}AR$ activation has been shown to increase erythropoietin production, resulting in increased cell survival[206,207]. Additionally, an $A_{2A}AR$ agonist induces proliferation of MCF-7 breast cancer cells and interferes with the ethanol-induced activation of estrogen receptor signal transduction[200]. In contrast, adenosine promotes cell death via $A_{2A}AR$ by activating caspase 3 and 9 in association with mitochondrial damage in the Caco-2 colon cancer cell line[208]. $A_{2A}AR$ activation in human A375 melanoma cells has been shown to promote cell death[205].
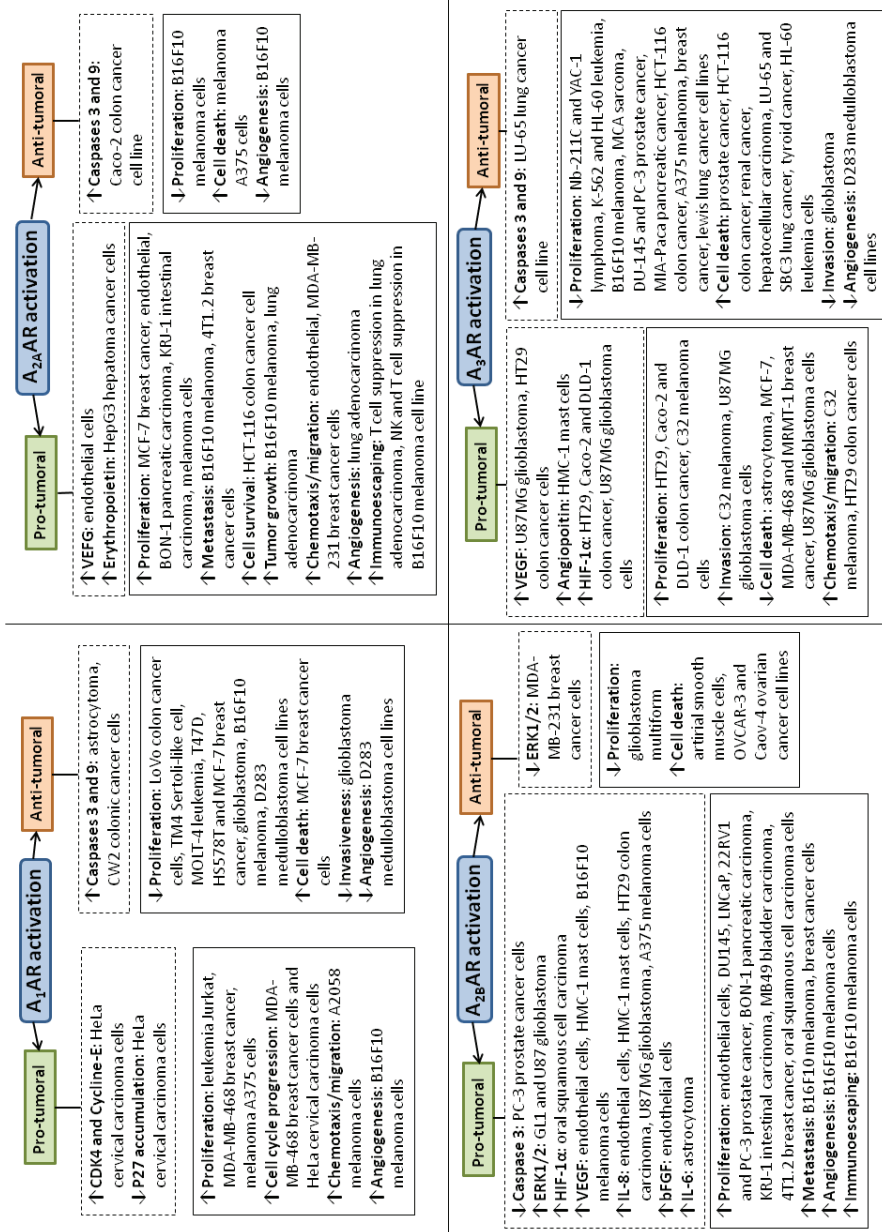
Figure 4. Pro- and anti-tumoral effects of adenosine receptors, A$_1$AR, A$_{2A}$AR, A$_{2B}$AR and A$_3$AR adapted from Gessi *et al.* (2011)[191] and Kazemi *et al.* (2018)[272]. Effects on cellular levels are shown in dashed boxes and effects in cancer hallmarks are shown in solid boxes.

$A_{2B}AR$ has been reported to be expressed in many tissues and cell types, and is only activated by high concentrations of adenosine, such as are present in certain pathological conditions[209,210]. In HT29 human colon cancer cells activation of $A_{2B}AR$ via adenosine increased IL-8 expression, thus promoting angiogenesis[211,212]. In a triple negative breast cancer model with MDA-MD-231 cells, adenosine increased proliferation and migration via activation of the $A_{2B}AR$[213]. Besides, it has been shown that proangiogenic dendritic cells can develop an anomalous phenotype via the stimulation of $A_{2B}AR$[214]. In mouse cancer models experimental and spontaneous metastasis formation has been induced by activation of $A_{2B}AR$, which is also known to worsen the efficacy of classical chemotherapy drugs[215]. Additionally, $A_{2B}AR$-stimulated metastasis has been observed in melanoma, breast, ovarian and blood carcinomas[216,217]. In contrast, $A_{2B}AR$ activation inhibits the ERK1/2 pathway, which results in an antiproliferative effect in MDA-MB-231 breast cancer cells[218]. A_3AR has been investigated for its role in diverse types of cancer cells. The receptor is involved in both pro- and antiproliferative effects, as well as in cell migration and cell death[219–222]. It has been shown that A_3AR activation leads to induced expression of angiopoietin 2 in HMC-1 human mastocytoma cancer cells and melanoma cells[223,224], resulting in a pro-tumoral effect. In addition, in glioblastoma cells an increase in expression of multidrug resistance-associated protein 1 via A_3AR activation was inhibited by A_3AR antagonist administration, which also increased the anti-tumoral effect of the chemotherapy drug vincristine[225]. On the other hand, A_3AR is also involved in controlling the cell cycle and inhibiting tumor growth both *in vitro* and *in vivo*[170]. Experimental animal studies have validated the therapeutic efficacy of orally administered A_3AR agonists in multiple pathological models, including xenograft, syngeneic, metastatic and orthotopic models of melanoma, hepatocellular, prostate, and colon carcinomas. It was shown that these drugs decreased cell proliferation in murine melanoma of both syngeneic and lung metastatic models[226]. In summary, as all four subtypes of ARs regulate cancer progression in diverse type of cancers, the incorporation of adenosine ligands and pharmacological inhibitors of AR signaling into preclinical studies may provide for novel therapeutic approaches for cancer treatment.

Roles of adenosine receptors in the tumor micro-environment

In addition to their role(s) in cancer cells, all four AR subtypes are involved in the control of inflammatory responses within the cancer cell environment. For example, $A_{2A}AR$ and $A_{2B}AR$ are known to exert immunosuppression during conditions of inflammation, hypoxia and cellular stress, when endogenous adenosine accumulates extracellularly[227–229]. In conjunction, the TME exhibits high concentrations of adenosine produced by stromal and immune cells, inflammation and tissue disruption. Due to the lack of perfusion hypoxia is a predominant driver that can cause cellular stress[230,231], and secretion of a large amount of ATP[232]. CD39 catalyzes the conversion of ATP and ADP into AMP, whereas CD73 catalyzes the irreversible conversion of AMP into adenosine[233]. CD38 generates cyclic ADP-ribose from NAD^+, which is essential for

the regulation of intracellular Ca^{2+} [234]. Tumor cells, NK cells and T cells all express CD38 which can promote adenosine generation and ultimately suppression of T cell proliferation and function[235]. Adenosine and enzymatically active CD39/CD73 are also carried by tumor-derived exosomes (TEX), which promote cancer progression via angiogenesis stimulation[236]. Thus, the accumulation of adenosine in the TME is predominantly via the catabolism of extracellular ATP to adenosine by CD38, CD39, and CD73, and suppression of anti-tumor immunity is via the activation of ARs[237]. Furthermore, accumulation of adenosine causes a reduced anti-tumoral immune response via adenosine receptors in hypoxic tumoral environments[238]. This promotes hypoxic tumor cell survival and immunoescape[161].

Although the exact inflammatory roles of A_1AR have not been fully characterized in the TME, deletion of A_1AR has recently been demonstrated to up-regulate the expression of programmed death-ligand 1 (PD-L1 or CD274)[239]. Therapeutic strategies on blocking the interaction between PD-L1 and its receptor, programmed cell death protein 1 (PD-1), have been developed for multiple tumor types[240,241]. Moreover, the combination of PD-1 monoclonal antibody and selective A_1AR antagonist induces the activity of $CD8^+$ T cells, resulting in increased treatment efficacy for melanoma and NSCLC[239].

It has been proven in a large number of studies that adenosine, through the activation of $A_{2A}AR$, also participates in T cell anergy induction, Treg response stimulation and the inhibition of natural killer cell activity. Combined this results in enhanced escape of tumor cells from the immune system with subsequent metastasis formation[242,243]. In large solid tumors where extracellular adenosine accumulates under hypoxic conditions, $A_{2A}AR$ expressed on the T cell surface inhibits incoming antitumor cytotoxic T lymphocytes from destroying the tumor[244]. Recently, $A_{2A}ARs$ have also been described to protect tumors from anti-tumor T cells, which may form the framework for an $A_{2A}AR$ antagonist-based cancer immunotherapy to prevent the inhibition of anti-tumor T cells in the TME[245].

Similar to $A_{2A}AR$, $A_{2B}AR$ abrogates immune responses by stimulating the production of cAMP, and thus promoting immunoescape[216]. The pro-tumoral effect of $A_{2B}AR$ is in the activation of myeloid-derived suppressor cells and M2 macrophages, which are essential for proliferation, angiogenesis and metastasis[216,246]. Besides, adenosine produced by TEX promotes angiogenesis via $A_{2B}AR$[236]. Under hypoxic conditions high levels of adenosine in the TME lead to the release of angiogenic factors via an $A_{2B}AR$ response which further promotes tumor growth[247].

The involvement of the A_3AR in hypoxia, typical of solid tumors[248], has been reported in the TME in an *in vitro* model as well as solid tumors *in vivo*[209]. One of the first lines of evidence showed that activation of A_3AR in mast cells was responsible for the release of allergic mediators and mast cell degranulation[249]. As a result, all these subtypes of ARs provide protection against excessive inflammation and tissue injury. Thus, AR antagonists may be useful for increasing the immune response in the TME

and provide a potential approach for cancer treatment, which will be discussed in more details in the next paragraph.

Potential anti-cancer therapies targeting adenosine receptors

Multiple antagonistic antibodies and small molecule inhibitors against adenosine receptors have been developed and display therapeutic efficacy in clinical trials against different solid tumors (Table 1)[237]. Several $A_{2A}AR$ antagonists have shown promising anti-cancer effects in preclinical models of melanoma, renal cell cancer, TNBC, colorectal, bladder and prostate cancers[250,251], which will be discussed below. Interestingly, $A_{2A}AR$ agonists are also being evaluated as a novel pharmacological approach to improve drug delivery to the brain due to their ability to transiently increase BBB permeability, especially for drugs targeting brain tumors[252]. Specifically, using microdialysis in glioblastoma patients regadenoson was tested clinically with increasing doses of the anti-cancer drug temozolomide in the brain interstitium[253]. Therefore, to reduce neurological side effects, anti-cancer molecules targeting $A_{2A}AR$ should be unable to cross the blood-brain barrier[254].

Although the majority of clinical development has targeted $A_{2A}AR$, compounds targeting other subtypes of ARs are also being obtained. Inhibiting the $A_{2B}AR$ receptor with antagonists has been reported to reduce tumor metastasis load and to inhibit the growth of melanoma, breast and prostate cancer in mouse models[215,255,256]. Whereas the importance of $A_{2A}AR$ and $A_{2B}AR$ compounds in chemotherapy has slowly emerged, the potential role of A_1AR or A_3AR agonists/antagonists still remains to be elucidated in preclinical studies, either on their own or in combination treatment.

Cancer immunotherapies are now considered as a pillar of cancer treatment[237]. Blockade of checkpoint receptor can cause durable responses in various cancers, however, this treatment does not work for all patients. Further investigations are needed to unravel the mechanisms of tumor evasion and to identify other potential targets that can overcome these 'brakes' on the immune response[237]. Adenosine is known as a negative regulator of NK cell and T cell responses in the TME via $A_{2A}AR$, thus, targeting this $A_{2A}AR$-involved pathway in the clinic may be beneficial for increasing the efficacy of immunotherapies. This hypothesis was substantiated in a study showing that in an $A_{2A}AR$ knock-out mouse model the activation or increase of T cells in the TME was induced, leading to potently induced anti-tumoral effects[257,258]. The combination of anti-PD-1 with inhibition of CD73, $A_{2A}AR$ or CD38 leads to stimulated anti-tumor T cell responses mediated by induced expression of Granzyme B and IFNγ in CD8+ T cells[216,259,260]. To further increase anti-tumoral effects, dual checkpoint blockade was combined with $A_{2A}AR$ knock-out in T cells, which led to better penetration into hypoxic tumors[230]. The majority of combination approaches have long been focused on blocking the function of adenosine in order to increase T cell responses within the TME, while the adenosine axis within NK cells can also be targeted[216]. Hence, future combination approaches may explore compounds that stimulate other subtypes of immune cells modulated by adenosine,

potentially via one of the other adenosine receptor subtypes.

Adenosine receptor mutations in cancer

Although abnormal functions of the ARs are observed in cancer tissues, the role of AR mutations present in human cancers is not well characterized yet. Herein, we will take the $A_{2B}AR$ as an example to discuss the effects of cancer-related mutations on receptor pharmacology.

3

To gather a selection of interesting cancer-related mutations, insight in the ligand-receptor and receptor-G protein interaction of these receptors is essential. Previous studies focusing on site-directed mutagenesis and docking studies of the A_1AR, $A_{2A}AR$ and $A_{2B}AR$ have identified residues involved in functional activity and ligand recognition[148,261–268]. Alanine scanning is generally used to examine the contribution of a single amino acid to receptor pharmacology. Substitution by alanine represents a replacement of the side chain at the β-carbon by a methyl group, thus removing the properties and functionality of the original amino acid[269]. Although alanine scanning is a useful tool to identify pharmacologically important positions[270], cancer-related mutations rarely involve a simple alanine substitution. Therefore, the influence of cancer-related somatic mutations on ligand binding and functional activity is likely more intricate.

As described in **Chapter 4**, cancer-related mutations of $A_{2B}AR$, derived from the Cancer Genome Atlas, have been characterized in an engineered yeast system[271]. Mutations with dramatic impact in receptor pharmacology were found in highly conserved residues, as well as residues that were directly involved in receptor-ligand and receptor-G protein interaction. Interestingly, none of these cancer-related mutations were found to match the natural variants of $A_{2B}AR$ existing in the human population, indicating that they could indeed be cancer-specific. Yet, data obtained from yeast assays might not be representative for mammalian species. Therefore, further studies in mammalian cells are needed to provide insight in receptor pharmacology and ligand binding of these cancer-related mutations in physiological and/or pathological conditions. Since adenosine, as pointed out above, is an anti-inflammatory stimulus in the tumor microenvironment[191], both wild-type and mutant adenosine receptors may play an important, yet largely undefined role in cancer progression, which eventually may be modulated with medicinal products.

Conclusions

Although a large amount of evidence supports the role of GPCRs in all stages of cancer progression, the knowledge of genetically altered variants in G proteins and GPCRs was initially limited to only a few neoplastic lesions, mainly endocrine tumors. Currently, GPCRs together with their downstream signaling pathways have been directly targeted for anti-cancer treatments. However, a pharmacological characterization is still needed to improve anti-cancer drug design. Investigation of cancer-related inflammation and GPCRs involved therein will provide a better

understanding of the immune-related mechanisms of cancer development. In numerous different cancer types GPCRs as well as viral GPCRs have been shown to be involved in multiple hallmarks of cancer, suggesting their importance in cancer progression. As an example, adenosine and adenosine receptors are known to regulate the immune response in the TME, while they are also directly involved in cancer hallmarks. Additionally, cancer-specific mutations influencing receptor pharmacology may also alter the cancer-related roles of GPCRs. Thus, drug discovery targeting both wild-type and mutant (adenosine) receptors might be a novel cancer-therapeutic approach. Overall, while being targets of many drugs on the market already, GPCRs are promising targets for developing novel strategies for cancer prevention and treatment.

References

1. Rask-Andersen, M., Masuram, S. & Schiöth, H. B. The druggable genome: Evaluation of drug targets in clinical trials suggests major shifts in molecular class and indication. *Annu. Rev. Pharmacol. Toxicol.* **54**, 9–26 (2014).
2. Vassilatis, D. K. *et al.* The G protein-coupled receptor repertoires of human and mouse. *Proc. Natl. Acad. Sci.* **100**, 4903–4908 (2003).
3. Fredriksson, R., Lagerström, M. C., Lundin, L.-G. & Schiöth, H. B. The G-protein-coupled receptors in the human genome form five main families. Phylogenetic analysis, paralogon groups, and fingerprints. *Mol. Pharmacol.* **63**, 1256–72 (2003).
4. Kolakowski, L. F. J. GCRDb: a g-protein-coupled receptor database. *Receptors Channels* **2**, 1–7 (1994).
5. Simon, M., Strathmann, M. & Gautam, N. Diversity of G proteins in signal transduction. *Science.* **252**, 802–808 (1991).
6. Hauser, A. S., Attwood, M. M., Rask-Andersen, M., Schiöth, H. B. & Gloriam, D. E. Trends in GPCR drug discovery: New agents, targets and indications. *Nat. Rev. Drug Discov.* **16**, 829–842 (2017).
7. Hollenberg, M. D. *et al.* Biased signalling and proteinase-activated receptors (PARs): Targeting inflammatory disease. *Br. J. Pharmacol.* **171**, 1180–1194 (2014).
8. Kenakin, T. The potential for selective pharmacological therapies through biased receptor signaling. *BMC Pharmacol. Toxicol.* **13**, 1–8 (2012).
9. Cattaneo, F. *et al.* Cell-surface receptors transactivation mediated by G protein-coupled receptors. *Int. J. Mol. Sci.* **15**, 19700–19728 (2014).
10. Heitzler, D. *et al.* Towards a systems biology approach of G protein-coupled receptor signalling: Challenges and expectations. *Comptes Rendus - Biol.* **332**, 947–957 (2009).
11. Lagerström, M. C. & Schiöth, H. B. Structural diversity of G protein-coupled receptors and significance for drug discovery. *Nat. Rev. Drug Discov.* **7**, 339–57 (2008).
12. Lynch, J. R. & Wang, J. Y. G protein-coupled receptor signaling in stem cells and cancer. *Int. J. Mol. Sci.* **17**, (2016).
13. O'Hayre, M., Degese, M. S. & Gutkind, J. S. Novel insights into G protein and G protein-coupled receptor signaling in cancer. *Curr. Opin. Cell Biol.* **27**, 126–135 (2014).
14. Sever, R. & Brugge, J. S. Signal transduction in cancer. *Cold Spring Harb. Perspect. Med.* **5**, a006098 (2015).
15. Dorsam, R. T. & Gutkind, J. S. G-protein-coupled receptors and cancer. *Nat. Rev. Cancer* **7**, 79–94 (2007).
16. Hanahan, D. & Weinberg, R. A. Hallmarks of cancer: The next generation. *Cell* **144**, 646–674 (2011).
17. Lappano, R. & Maggiolini, M. G protein-coupled receptors: novel targets for drug discovery in cancer. *Nat. Rev. Drug Discov.* **10**, 47–60 (2011).
18. Yu, S., Sun, L., Jiao, Y. & Lee, L. T. O. The role of G protein-coupled receptor kinases in cancer. *Int. J. Biol. Sci.* **14**, 189–203 (2018).
19. Audet, M. & Bouvier, M. Restructuring G-protein-coupled receptor activation. *Cell* **151**, 14–23 (2012).
20. Premont, R. T. *et al.* Characterization of the G protein-coupled receptor kinase GRK4: Identification of four splice vaeiants. *J. Biol. Chem.* **271**, 6403–6410 (1996).
21. Hall, R. A. *et al.* G protein-coupled receptor kinase 6A phosphorylates the Na^+/H^+ exchanger regulatory factor via a PDZ domain-mediated interaction. *J. Biol. Chem.* **274**, 24328–24334 (1999).
22. Penela, P., Murga, C., Ribas, C., Lafarga, V. & Mayor, F. The complex G protein-coupled receptor kinase 2 (GRK2) interactome unveils new physiopathological targets. *Br. J. Pharmacol.* **160**, 821–832 (2010).
23. Ma, Y., Han, C. C., Huang, Q., Sun, W. Y. & Wei, W. GRK2 overexpression inhibits IGF1-induced proliferation and migration of human hepatocellular carcinoma cells by downregulating EGR1. *Oncol. Rep.* **35**, 3068–3074 (2016).
24. Miyagawa, Y. *et al.* Aberrantly expressed recoverin is functionally associated with G-protein-coupled receptor kinases in cancer cell lines. *Biochem. Biophys. Res. Commun.* **300**, 669–673 (2003).
25. Billard, M. J. *et al.* G protein coupled receptor kinase 3 regulates breast cancer migration, invasion, and metastasis. *PLoS One* **11**, 1–23 (2016).
26. Gurevich, E. V., Tesmer, J. J. G., Mushegian, A. & Gurevich, V. V. G protein-coupled receptor kinases: More than just kinases and not only for GPCRs. *Pharmacol. Ther.* **133**, 40–69 (2012).
27. Maeda, T. *et al.* Mechanisms of photoreceptor cell death in cancer-associated retinopathy. *Investig. Ophthalmol. Vis. Sci.* **42**, 705–712 (2001).
28. Zhou, L. *et al.* G-protein-coupled receptor kinase 2 in pancreatic cancer: clinicopathologic and prognostic significance. *Hum. Pathol.* **56**, 171–177 (2016).
29. Métayé, T., Menet, E., Guilhot, J. & Kraimps, J. L. Expression and activity of G protein-coupled receptor kinases in differentiated thyroid carcinoma. *J. Clin. Endocrinol. Metab.* **87**, 3279–3286 (2002).
30. Wei, Z. *et al.* GRK2 negatively regulates IGF-1R signaling pathway and cyclins' expression in HepG2 cells. *J. Cell.*

Physiol. **228**, 1897–1901 (2013).

31. Hu, M. *et al.* A KSHV microRNA Directly Targets G Protein-Coupled Receptor Kinase 2 to Promote the Migration and Invasion of Endothelial Cells by Inducing CXCR2 and Activating AKT Signaling. *PLoS Pathog.* **11**, 1–27 (2015).
32. Nogués, L. *et al.* G Protein-coupled Receptor Kinase 2 (GRK2) Promotes Breast Tumorigenesis Through a HDAC6-Pin1 Axis. *EBioMedicine* **13**, 132–145 (2016).
33. Nakata, H. *et al.* Involvement of β-Adrenergic Receptor Kinase-1 in Homologous Desensitization of Histamine H_2 Receptors in Human Gastric Carcinoma Cell Line MKN-45. *Digestion* **57**, 406–410 (1996).
34. Fitzhugh, D. J. *et al.* G Protein Coupled Receptor Kinase 3 (GRK3) Negatively Regulates CXCL12/CXCR4 Signaling and Tumor Migration in Breast Cancer. *J. Allergy Clin. Immunol.* **127**, AB230 (2011).
35. Li, W. *et al.* GRK3 is essential for metastatic cells and promotes prostate tumor progression. *Proc. Natl. Acad. Sci. U. S. A.* **111**, 1521–1526 (2014).
36. Dautzenberg, F. M., Braun, S. & Hauger, R. L. GRK3 mediates desensitization of CRF1 receptors: A potential mechanism regulating stress adaptation. *Am. J. Physiol. - Regul. Integr. Comp. Physiol.* **280**, R935-R946 (2001).
37. Brenninkmeijer, C. B. A. P., Price, S. A., López Bernal, A. & Phaneuf, S. Expression of G-protein-coupled receptor kinases in pregnant term and non-pregnant human myometrium. *J. Endocrinol.* **162**, 401–408 (1999).
38. King, D. W. *et al.* Differential Expression of GRK Isoforms in Nonmalignant and Malignant Human Granulosa Cells. *Endocrine* **22**, 135–141 (2003).
39. Kaur, G. *et al.* G-protein coupled receptor kinase (GRK)-5 regulates proliferation of glioblastoma-derived stem cells. *J. Clin. Neurosci.* **20**, 1014–1018 (2013).
40. Malbon, C. C. Frizzleds: new members of the superfamily of G-protein-coupled-receptors. *Front. Biosci.* **9**, 1048–1058 (2004).
41. Li, Y. P. GRK6 expression in patients with hepatocellular carcinoma. *Asian Pac. J. Trop. Med.* **6**, 220–223 (2013).
42. Behrens, J. & Lustig, B. The Wnt connection to tumorigenesis. *Int. J. Dev. Biol.* **48**, 477–487 (2004).
43. Zhan, T., Rindtorff, N. & Boutros, M. Wnt signaling in cancer. *Oncogene* **36**, 1461–1473 (2017).
44. Anastas, J. N. & Moon, R. T. WNT signalling pathways as therapeutic targets in cancer. *Nat. Rev. Cancer* **13**, 11–26 (2013).
45. Bar-Shavit, R. *et al.* G Protein-Coupled Receptors in Cancer. *Int. J. Mol. Sci.* **17**, 1320 (2016).
46. Nusse, R. Wnt signaling in disease and in development. *Cell Res.* **15**, 28–32 (2005).
47. Korinek, V. *et al.* Constitutive transcriptional activation by a β-catenin-Tcf complex in APC$^{-/-}$ colon carcinoma. *Science* **275**, 1784–1787 (1997).
48. Gurney, A. *et al.* Wnt pathway inhibition via the targeting of Frizzled receptors results in decreased growth and tumorigenicity of human tumors. *Proc. Natl. Acad. Sci. U. S. A.* **109**, 11717–11722 (2012).
49. O'Connell, M. P. & Weeraratna, A. T. Hear the wnt ror: How melanoma cells adjust to changes in Wnt. *Pigment Cell Melanoma Res.* **22**, 724–739 (2009).
50. Chien, A. J., Conrad, W. H. & Moon, R. T. A wnt survival guide: From flies to human disease. *J. Invest. Dermatol.* **129**, 1614–1627 (2009).
51. Nieto Gutierrez, A. & McDonald, P. H. GPCRs: Emerging anti-cancer drug targets. *Cell. Signal.* **41**, 65–74 (2018).
52. Praskova, M., Xia, F. & Avruch, J. MOBKL1A/MOBKL1B Phosphorylation by MST1 and MST2 Inhibits Cell Proliferation. *Curr. Biol.* **18**, 311–321 (2008).
53. Wu, S., Huang, J., Dong, J. & Pan, D. hippo encodes a Ste-20 family protein kinase that restricts cell proliferation and promotes apoptosis in conjunction with salvador and warts. *Cell* **114**, 445–456 (2003).
54. Mo, J.-S., Park, H. W. & Guan, K.-L. The hippo signaling pathway and cancer. *EMBO Rep.* **15**, 642–656 (2014).
55. Zeng, Q. & Hong, W. The Emerging Role of the Hippo Pathway in Cell Contact Inhibition, Organ Size Control, and Cancer Development in Mammals. *Cancer Cell* **13**, 188–192 (2008).
56. Zanconato, F., Cordenonsi, M. & Piccolo, S. YAP/TAZ at the Roots of Cancer. *Cancer Cell* **29**, 783–803 (2016).
57. Guo, L. & Teng, L. YAP/TAZ for cancer therapy: Opportunities and challenges (Review). *Int. J. Oncol.* **46**, 1444–1452 (2015).
58. Yu, F. X. *et al.* Regulation of the Hippo-YAP pathway by G-protein-coupled receptor signaling. *Cell* **150**, 780–791 (2012).
59. Bao, Y. *et al.* A cell-based assay to screen stimulators of the Hippo pathway reveals the inhibitory effect of dobutamine on the YAP-dependent gene transcription. *J. Biochem.* **150**, 199–208 (2011).
60. Mantovani, A., Allavena, P., Sica, A. & Balkwill, F. Cancer-related inflammation. *Nature* **454**, 436–444 (2008).
61. Balkwill, F. & Mantovani, A. Inflammation and cancer: back to Virchow? *Lancet* **357**, 539–45 (2001).
62. Balkwill, F. Cancer and the chemokine network. *Nat. Rev. Cancer* **4**, 540–550 (2004).
63. Barbieri, F., Bajetto, A. & Florio, T. Role of chemokine network in the development and progression of ovarian cancer: A potential novel pharmacological target. *J. Oncol.* **2010** (2010).
64. Rollins, B. J. Inflammatory chemokines in cancer growth and progression. *Eur. J. Cancer* **42**, 760–767 (2006).
65. Aldinucci, D. & Colombatti, A. The Inflammatory Chemokine CCL5 and Cancer Progression. *Mediators Inflamm.* **2014**, 1–12 (2014).
66. Kershaw, M. H., Westwood, J. A. & Darcy, P. K. Gene-engineered T cells for cancer therapy. *Nat. Rev. Cancer* **13**, 525–541 (2013).
67. Brown, J. R. & DuBois, R. N. COX-2: A molecular target for colorectal cancer prevention. *J. Clin. Oncol.* **23**, 2840–2855 (2005).
68. Gupta, R. A. & Dubois, R. N. Colorectal Cancer Prevention of Cyclooxygenase-2. *Nat. Rev. Cancer* **1**, 11–21 (2001).
69. Kim, T. H., Xiong, H., Zhang, Z. & Ren, B. β-Catenin Activates the Growth Factor Endothelin-1 in Colon Cancer Cells. *Oncogene* **24**, 597–604 (2005).
70. Mazhar, D., Ang, R. & Waxman, J. COX inhibitors and breast cancer. *Br. J. Cancer* **94**, 346–350 (2006).
71. Lin, D. T., Subbaramaiah, K., Shah, J. P., Dannenberg, A. J. & Boyle, J. O. Cyclooxygenase-2: A novel molecular target for the prevention and treatment of head and neck cancer. *Head Neck* **24**, 792–799 (2002).
72. Bresalier, R. S. *et al.* Cardiovascular events associated with rofecoxib in a colorectal adenoma chemoprevention trial: Commentary. *Dis. Colon Rectum* **48**, 1330–1331 (2005).
73. Hull, M. A., Ko, S. C. W. & Hawcroft, G. Prostaglandin EP receptors: Targets for treatment and prevention of colorectal cancer? *Mol. Cancer Ther.* **3**, 1031–1039 (2004).
74. Hansen-Petrik, M. B. *et al.* Prostaglandin E(2) protects intestinal tumors from nonsteroidal anti-inflammatory drug-induced regression in Apc(Min/+) mice. *Cancer Res.* **62**, 403–408 (2002).
75. Sonoshita, M. *et al.* Acceleration of intestinal polyposis through prostaglandin receptor EP2 in Apc(Δ716) knockout mice. *Nat. Med.* **7**, 1048–1051 (2001).
76. Watanabe, K. *et al.* Inhibitory effect of a prostaglandin E receptor subtype EP1 selective antagonist, ONO-8713, on development of azoxymethane-induced aberrant crypt foci in mice. *Cancer Lett.* **156**, 57–61 (2000).
77. Kim, J. II, Lakshmikanthan, V., Frilot, N. & Daaka, Y. Prostaglandin E2 promotes lung cancer cell migration via EP4-βArrestin1-c-Src signalsome. *Mol. Cancer Res.* **8**, 569–577 (2010).

78. Hida, T. *et al.* Increased expression of cyclooxygenase 2 occurs frequently in human lung cancers, specifically in adenocarcinomas. *Cancer Res.* **58**, 3761–3764 (1998).
79. Chang, S. H., Ai, Y., Breyer, R. M., Lane, T. F. & Hla, T. The prostaglandin E2 receptor EP2 is required for cyclooxygenase 2-mediated mammary hyperplasia. *Cancer Res.* **65**, 4496–4499 (2005).
80. Liu, C. H. *et al.* Overexpression of Cyclooxygenase-2 is Sufficient to Induce Tumorigenesis in Transgenic Mice. *J. Biol. Chem.* **276**, 18563–18569 (2001).
81. Kikuchi, A. Tumor formation by genetic mutations in the components of the Wnt signaling pathway. *Cancer Sci.* **94**, 225–229 (2003).
82. Castellone, M. D., Teramoto, H., Williams, B. O., Druey, K. M. & Gutkind, J. S. Prostaglandin E2 promotes colon cancer cell growth through a Gs-axin-β-catenin signaling axis. *Science.* **310**, 1504–1510 (2005).
83. Shao, J., Jung, C., Liu, C. & Sheng, H. Prostaglandin E2 stimulates the β-catenin/T cell factor-dependent transcription in colon cancer. *J. Biol. Chem.* **280**, 26565–26572 (2005).
84. Kamiyama, M. *et al.* EP2, a receptor for PGE2, regulates tumor angiogenesis through direct effects on endothelial cell motility and survival. *Oncogene* **25**, 7019–7032 (2006).
85. Taniguchi, T., Fujino, H., Israel, D. D., Regan, J. W. & Murayama, T. Human EP3I prostanoid receptor induces VEGF and VEGF receptor-1 mRNA expression. *Biochem. Biophys. Res. Commun.* **377**, 1173–1178 (2008).
86. Kubo, H. *et al.* Host prostaglandin EP3 receptor signaling relevant to tumor-associated lymphangiogenesis. *Biomed. Pharmacother.* **64**, 101–106 (2010).
87. Amano, H. *et al.* Roles of a prostaglandin E-type receptor, EP3, in upregulation of matrix metalloproteinase-9 and vascular endothelial growth factor during enhancement of tumor metastasis. *Cancer Sci.* **100**, 2318–2324 (2009).
88. Even-Ram, S. *et al.* Thrombin receptor overexpression in malignant and physiological invasion processes. *Nat. Med.* **4**, 909–914 (1998).
89. Daaka, Y. G proteins in cancer: the prostate cancer paradigm. *Sci. STKE* **2004**, 1–11 (2004).
90. Darash-Yahana, M. *et al.* Role of high expression levels of CXCR4 in tumor growth, vascularization, and metastasis. *FASEB J.* **18**, 1240–1242 (2004).
91. Müller, A. *et al.* Involvement of chemokine receptors in breast cancer metastasis. *Nature* **410**, 50–56 (2001).
92. Dhawan, P. & Richmond, A. Role of CXCL1 in tumorigenesis of melanoma. *J. Leukoc. Biol.* **72**, 9–18 (2002).
93. Balkwill, F. The significance of cancer cell expression of the chemokine receptor CXCR4. *Semin. Cancer Biol.* **14**, 171–179 (2004).
94. Kakinuma, T. Chemokines, chemokine receptors, and cancer metastasis. *J. Leukoc. Biol.* **79**, 639–651 (2006).
95. Mills, G. B. & Moolenaar, W. H. The emerging role of lysophosphatidic acid in cancer. *Nat. Rev. Cancer* **3**, 582–591 (2003).
96. Takuwa, Y. Subtype-specific differential regulation of Rho family G proteins and cell migration by the Edg family sphingosine-1-phosphate receptors. *Biochim. Biophys. Acta - Mol. Cell Biol. Lipids* **1582**, 112–120 (2002).
97. Balthasar, S. *et al.* Sphingosine 1-phosphate receptor expression profile and regulation of migration in human thyroid cancer cells. *Biochem. J.* **398**, 547–556 (2006).
98. Akao, Y. *et al.* High expression of sphingosine kinase 1 and S1P receptors in chemotherapy-resistant prostate cancer PC3 cells and their camptothecin-induced up-regulation. *Biochem. Biophys. Res. Commun.* **342**, 1284–1290 (2006).
99. Yamashita, H. *et al.* Sphingosine 1-phosphate receptor expression profile in human gastric cancer cells: Differential regulation on the migration and proliferation. *J. Surg. Res.* **130**, 80–87 (2006).
100. Chambers, A. F., Groom, A. C. & MacDonald, I. C. Dissemination and growth of cancer cells in metastatic sites. *Nat. Rev. Cancer* **2**, 563–572 (2002).
101. Coughlin, S. R. Thrombin signalling and protease-activated receptors. *Nature* **407**, 258–264 (2000).
102. Morris, D. R. *et al.* Protease-activated receptor-2 is essential for factor VIIa and Xa-induced signaling, migration, and invasion of breast cancer cells. *Cancer Res.* **66**, 307–314 (2006).
103. Versteeg, H. H. *et al.* Inhibition of tissue factor signaling suppresses tumor growth. *Blood* **111**, 190–199 (2008).
104. Kato, M., Kitayama, J., Kazama, S. & Nagawa, H. Expression pattern of CXC chemokine receptor-4 is correlated with lymph node metastasis in human invasive ductal carcinoma. *Breast Cancer Res.* **5**, (2003).
105. Cardones, A. R., Murakami, T. & Hwang, S. T. CXCR4 Enhances Adhesion of B16 Tumor Cells to Endothelial Cells in Vitro and in Vivo via β1 Integrin. *Cancer Res.* **63**, 6751–6757 (2003).
106. Kleeff, J. *et al.* Detection and localization of MIP-3α/LARC/Exodus, a macrophage proinflammatory chemokine, and its CCR6 receptor in human pancreatic cancer. *Int. J. Cancer* **81**, 650–657 (1999).
107. Lee, Z. *et al.* Lysophosphatidic acid is a major regulator of growth-regulated oncogene α in ovarian cancer. *Cancer Res.* **66**, 2740–2748 (2006).
108. Slinger, E., Langemeijer, E., Siderius, M., Vischer, H. F. & Smit, M. J. Herpesvirus-encoded GPCRs rewire cellular signaling. *Mol. Cell. Endocrinol.* **331**, 179–184 (2011).
109. White, M. K., Gorrill, T. S. & Khalili, K. Reciprocal transactivation between HIV-1 and other human viruses. *Virology* **352**, 1–13 (2006).
110. Jenkins, F. J., Rowe, D. T. & Rinaldo, C. R. Herpesvirus infections in organ transplant recipients. *Clin. Diagn. Lab. Immunol.* **10**, 1–7 (2003).
111. Vischer, H. F., Siderius, M., Leurs, R. & Smit, M. J. Herpesvirus-encoded GPCRs: Neglected players in inflammatory and proliferative diseases? *Nat. Rev. Drug Discov.* **13**, 123–139 (2014).
112. Zhang, J., Feng, H., Xu, S. & Feng, P. Hijacking GPCRs by viral pathogens and tumor. *Biochem. Pharmacol.* **114**, 69–81 (2016).
113. Feng, H., Shuda, M., Chang, Y. & Moore, P. S. Clonal integration of a polyomavirus in human Merkel cell carcinoma. *Science.* **319**, 1096–1100 (2008).
114. Martin, D. & Gutkind, J. S. Human tumor-associated viruses and new insights into the molecular mechanisms of cancer. *Oncogene* **27**, S31–S42 (2008).
115. Montaner, S., Kufareva, I., Abagyan, R. & Gutkind, J. S. Molecular Mechanisms Deployed by Virally Encoded G Protein–Coupled Receptors in Human Diseases. *Annu. Rev. Pharmacol. Toxicol.* **53**, 331–354 (2013).
116. Arvanitakis, L., Geras-raakat, E., Varmat, A., Gershengornt, M. C. & Cesarman, E. Human herpesvirus KSHV active G-protein-coupled proliferation. *Nature* **385**, 347–350 (1997).
117. Sodhi, A., Montaner, S. & Gutkind, J. S. Viral hijacking of G-protein-coupled-receptor signalling networks. *Nat. Rev. Mol. Cell Biol.* **5**, 998–1012 (2004).
118. Mitra, D. *et al.* An ultraviolet-radiation-independent pathway to melanoma carcinogenesis in the red hair/fair skin background. *Nature* **491**, 449–53 (2012).
119. Velasco, G., Sánchez, C. & Guzmán, M. Towards the use of cannabinoids as antitumour agents. *Nat. Rev. Cancer* **12**, 436–444 (2012).
120. Green, J. A. *et al.* The sphingosine 1-phosphate receptor S1P2 maintains the homeostasis of germinal center B cells and promotes niche confinement. *Nat. Immunol.* **12**, 672–680 (2011).

121. Lee, J. H. *et al.* KiSS-1, a novel human malignant melanoma metastasis-suppressor gene. *J. Natl. Cancer Inst.* **88**, 1731–1737 (1996).
122. O'Hayre, M. *et al.* The emerging mutational landscape of G proteins and G-protein-coupled receptors in cancer. *Nat. Rev. Cancer* **13**, 412–24 (2013).
123. Kan, Z. *et al.* Diverse somatic mutation patterns and pathway alterations in human cancers. *Nature* **466**, 869–73 (2010).
124. *Broad Institute TCGA Genome Data Analysis Center (2016): Analysis-ready standardized TCGA data from Broad GDAC Firehose stddata_2015_08_21 run. Broad Institute of MIT and Harvard.* (2016). doi:10.7908/C18W3CNQ
125. Jensen, M. A., Ferretti, V., Grossman, R. L. & Staudt, L. M. The NCI Genomic Data Commons as an engine for precision medicine. *Blood* **130**, 453–459 (2017).
126. Finch, A. M., Sarramegna, V. & Graham, R. M. Ligand Binding, Activation, and Agonist Trafficking. in *The Adrenergic Receptors* 25–85 (Humana Press, 2006). doi:10.1385/1-59259-931-1:025
127. Salon, J. a, Lodowski, D. T. & Palczewski, K. The Significance of G Protein-Coupled Receptor. *Pharmacol. Rev.* **63**, 901–937 (2011).
128. Chang, S. D. & Bruchas, M. R. Functional selectivity at GPCRs: New opportunities in psychiatric drug discovery. *Neuropsychopharmacology* **39**, 248–249 (2014).
129. Leff, P. The two-state model of receptor activation. *Trends Pharmacol. Sci.* **16**, 89–97 (1995).
130. Seifert, R. & Wenzel-Seifert, K. Constitutive activity of G-protein-coupled receptors: cause of disease and common property of wild-type receptors. *Naunyn. Schmiedebergs. Arch. Pharmacol.* **366**, 381–416 (2002).
131. Peeters, M. C. *et al.* GPCR structure and activation: an essential role for the first extracellular loop in activating the adenosine A2B receptor. *FASEB J.* **25**, 632–43 (2011).
132. Parnot, C., Miserey-Lenkei, S., Bardin, S., Corvol, P. & Clauser, E. Lessons from constitutively active mutants of G protein-coupled receptors. *Trends in Endocrinology and Metabolism* **13**, 336–343 (2002).
133. Vassart, G., Pardo, L. & Costagliola, S. A molecular dissection of the glycoprotein hormone receptors. in *Insights into Receptor Function and New Drug Development Targets* (eds. Conn, M., Kordon, C. & Christen, Y.) 151–166 (Springer Berlin Heidelberg, 2006).
134. Lebon, G., Warne, T. & Tate, C. G. Agonist-bound structures of G protein-coupled receptors. *Curr. Opin. Struct. Biol.* **22**, 482–490 (2012).
135. Parma, J. *et al.* Somatic mutations in the thyrotropin receptor gene cause hyperfunctioning thyroid adenomas. *Nature* **365**, 649–651 (1993).
136. Tao, Y. X. & Segaloff, D. L. Functional analyses of melanocortin-4 receptor mutations identified from patients with binge eating disorder and nonobese or obese subjects. *J. Clin. Endocrinol. Metab.* **90**, 5632–5638 (2005).
137. Gromoll, J. *et al.* Functional and clinical consequences of mutations in the FSH receptor. *Mol. Cell. Endocrinol.* **125**, 177–182 (1996).
138. Laue, L. *et al.* Heterogeneity of activating mutations of the human luteinizing hormone receptor in male-limited precocious puberty. *Biochem. Mol. Med.* **58**, 192–198 (1996).
139. Rasmussen, S. G. F. *et al.* Structure of a nanobody-stabilized active state of the β_2 adrenoceptor. *Nature* **469**, 175–181 (2011).
140. Wonerow, P., Chey, S., Führer, D., Holzapfel, H. P. & Paschke, R. Functional characterization of five constitutively activating thyrotrophin receptor mutations. *Clin. Endocrinol. (Oxf).* **53**, 461–8 (2000).
141. Parma, J. *et al.* Diversity and Prevalence of Somatic Mutations in the Thyrotropin Receptor and Gs alpha Genes as a Cause of Toxic Thyroid Adenomas. *J. Clin. Endocrinol. Metab.* **82**, 2695–2701 (1997).
142. Stoy, H. & Gurevich, V. V. How genetic errors in GPCRs affect their function: Possible therapeutic strategies. *Genes Dis.* **2**, 108–132 (2015).
143. Tao, Y. X. Inactivating mutations of G protein-coupled receptors and diseases: Structure-function insights and therapeutic implications. *Pharmacol. Ther.* **111**, 949–973 (2006).
144. Ward, N. A., Hirst, S., Williams, J. & Findlay, J. B. C. Pharmacological chaperones increase the cell-surface expression of intracellularly retained mutants of the melanocortin 4 receptor with unique rescuing efficacy profiles. *Biochem. Soc. Trans.* **40**, 717–720 (2012).
145. Bichet, D. G. Chapter 2 V2R Mutations and Nephrogenic Diabetes Insipidus. *Progress in Molecular Biology and Translational Science* **89**, 15–29 (2009).
146. Venkatakrishnan, A. J. *et al.* Molecular signatures of G-protein-coupled receptors. *Nature* **494**, 185–194 (2013).
147. Ulloa-Aguirre, A., Dias, J. A., Bousfield, G., Huhtaniemi, I. & Reiter, E. Trafficking of the follitropin receptor. *Methods in Enzymology* **521**, 17-45 (2013).
148. Jespers, W. *et al.* Structural mapping of adenosine receptor mutations: ligand binding and signaling mechanisms. *Trends Pharmacol. Sci.* **39**, 75–89 (2017).
149. Rubin, L. L. & de Sauvage, F. J. Targeting the Hedgehog pathway in cancer. *Nat. Rev. Drug Discov.* **5**, 1026–1033 (2006).
150. Epstein, E. H. Basal cell carcinomas: attack of the hedgehog. *Nat. Rev. Cancer* **8**, 743–754 (2008).
151. Xie, J. *et al.* Mutations in Sporadic Basal-Cell Carcinoma. *Nature* **391**, 90–92 (1998).
152. Lum, L. & Beachy, P. A. The hedgehog response network: Sensors, switches, and routers. *Science.* **304**, 1755–1759 (2004).
153. Xie, J. *et al.* Activating Smoothened mutations in sporadic basal-cell carcinoma. *Nature* **391**, 90–92 (1998).
154. Clark, V. E. *et al.* Genomic Analysis of Non-NF2 Meningiomas Reveals Mutations in TRAF7, KLF4, AKT1, and SMO. *Science.* **339**, 1077–1081 (2013).
155. Brastianos, P. K. *et al.* Genomic sequencing of meningiomas identifies oncogenic SMO and AKT1 mutations. *Nat. Genet.* **45**, 285–289 (2013).
156. Scales, S. J. & de Sauvage, F. J. Mechanisms of Hedgehog pathway activation in cancer and implications for therapy. *Trends Pharmacol. Sci.* **30**, 303–312 (2009).
157. Prickett, T. D. *et al.* Exon capture analysis of G protein-coupled receptors identifies activating mutations in GRM3 in melanoma. *Nat. Genet.* **43**, 1119–1126 (2011).
158. Teh, J. L. F. & Chen, S. Glutamatergic signaling in cellular transformation. *Pigment Cell Melanoma Res.* **25**, 331–342 (2012).
159. Paavola, K. J. & Hall, R. A. Adhesion G protein-coupled receptors: Signaling, pharmacology, and mechanisms of activation. *Mol. Pharmacol.* **82**, 777–783 (2012).
160. Schuijers, J. & Clevers, H. Adult mammalian stem cells: The role of Wnt, Lgr5 and R-spondins. *EMBO J.* **31**, 2685–2696 (2012).
161. Gessi, S., Merighi, S., Sacchetto, V., Simioni, C. & Borea, P. A. Adenosine receptors and cancer. *Biochim. Biophys. Acta - Biomembr.* **1808**, 1400–1412 (2011).
162. Jockers, R. *et al.* Species difference in the G protein selectivity of the human and bovine A_1-adenosine receptor. *J. Biol. Chem.* **269**, 32077–32084 (1994).

163. Palmer, T. M., Gettys, T. W. & Stiles, G. L. Differential interaction with and regulation of multiple G-proteins by the rat A$_3$ adenosine receptor. *J. Biol. Chem.* **270**, 16895–16902 (1995).

164. Freund, S., Ungerer, M. & Lohse, M. J. A1 adenosine receptors expressed in CHO-cells couple to adenylyl cyclase and to phospholipase C. *Naunyn. Schmiedebergs. Arch. Pharmacol.* **350**, 49–56 (1994).

165. Zhou, Q.-Y. *et al.* Molecular cloning and characterization of an adenosine receptor: the A$_3$ adenosine receptor. *Proc. Natl. Acad. Sci.* **89**, 7432–7436 (1992).

166. Schulte, G. & Fredholm, B. B. The G$_s$-coupled adenosine A$_{2B}$ receptor recruits divergent pathways to regulate ERK1/2 and p38. *Exp. Cell Res.* **290**, 168–176 (2003).

167. Hirano, D. *et al.* Functional coupling of adenosine A$_{2a}$ receptor to inhibition of the mitogen-activated protein kinase cascade in Chinese hamster ovary cells. *Biochem. J.* **316**, 81–86 (1996).

168. Linden, J., Thai, T., Figler, H., Jin, X. & Robeva, A. S. Characterization of human A$_{2B}$ adenosine receptors: Radioligand binding, western blotting, and coupling to G$_q$ in human embryonic kidney 293 cells and HMC-1 mast cells. *Mol. Pharmacol.* **56**, 705–713 (1999).

169. Fredholm, B. B., Irenius, E., Kull, B. & Schulte, G. Comparison of the potency of adenosine as an agonist at human adenosine receptors expressed in Chinese hamster ovary cells. *Biochem. Pharmacol.* **61**, 443–8 (2001).

170. Yaar, R., Jones, M. R., Chen, J.-F. & Ravid, K. Animal models for the study of adenosine receptor function. *J. Cell. Physiol.* **202**, 9–20 (2005).

171. Palmer, T. M. & Stiles, G. L. Adenosine receptors. *Neuropharmacology* **34**, 683–694 (1995).

172. Fredholm, B. B., IJzerman, A. P., Jacobson, K. a, Klotz, K. N. & Linden, J. International Union of Pharmacology. XXV. Nomenclature and classification of adenosine receptors. *Pharmacol. Rev.* **53**, 527–52 (2001).

173. Glukhova, A. *et al.* Structure of the Adenosine A$_1$ Receptor Reveals the Basis for Subtype Selectivity. *Cell* **168**, 867-877.e13 (2017).

174. Nascimento, F. P. *et al.* Adenosine A$_1$ Receptor-Dependent Antinociception Induced by Inosine in Mice: Pharmacological, Genetic and Biochemical Aspects. *Mol. Neurobiol.* **51**, 1368–1378 (2015).

175. Porkka-Heiskanen, T. *et al.* Adenosine: A mediator of the sleep-inducing effects of prolonged wakefulness. *Science.* **276**, 1265–1267 (1997).

176. Elliott, K. J., Weber, E. T. & Rea, M. A. Adenosine A$_1$ receptors regulate the response of the hamster circadian clock to light. *Eur. J. Pharmacol.* **414**, 45–53 (2001).

177. De Mendonça, A. & Ribeiro, J. A. Influence of metabotropic glutamate receptor agonists on the inhibitory effects of adenosine A$_1$ receptor activation in the rat hippocampus. *Br. J. Pharmacol.* **121**, 1541–1548 (1997).

178. Jacobson, K. A. & Gao, Z.-G. Adenosine receptors as therapeutic targets. *Nat. Rev. Drug Discov.* **5**, 247–264 (2006).

179. Brown, R. M. & Short, J. L. Adenosine A$_{2A}$ receptors and their role in drug addiction. *J. Pharm. Pharmacol.* **60**, 1409–1430 (2008).

180. Poon, A. & Sawynok, J. Antinociceptive and anti-inflammatory properties of an adenosine kinase inhibitor and an adenosine deaminase inhibitor. *Eur. J. Pharmacol.* **384**, 123–138 (1999).

181. Gao, Y. & Phillis, J. W. CGS 15943, an adenosine A$_1$ receptor antagonist, reduces cerebral ischemic injury in the Mongolian gerbil. *Life Sci.* **55**, 61–65 (1994).

182. Mori, A. & Shindou, T. Modulation of GABAergic transmission in the striatopallidal system by adenosine A$_{2A}$ receptors. *Neurology* **61**, S44 LP-S48 (2003).

183. El Yacoubi, M., Costentin, J. & Vaugeois, J.-M. Adenosine A$_{2A}$ receptors and depression. *Neurology* **61**, S82 LP-S87 (2003).

184. Klotz, K. N. Adenosine receptors and their ligands. *Naunyn. Schmiedebergs. Arch. Pharmacol.* **362**, 382–391 (2000).

185. Franco, R. *et al.* Partners for adenosine A$_1$ receptors. *J. Mol. Neurosci.* **26**, 221–231 (2005).

186. Young, H. W. J. *et al.* A$_3$ Adenosine Receptor Signaling Contributes to Airway Inflammation and Mucus Production in Adenosine Deaminase-Deficient Mice. *J. Immunol.* **173**, 1380–1389 (2004).

187. Zhao, Z., Yaar, R., Ladd, D., Cataldo, L. M. & Ravid, K. Overexpression of A$_3$ adenosine receptors in smooth, cardiac, and skeletal muscle is lethal to embryos. *Microvasc. Res.* **63**, 61–69 (2002).

188. Lukashev, D., Ohta, A. & Sitkovsky, M. Targeting hypoxia-A$_{2A}$ adenosine receptor-mediated mechanisms of tissue protection. *Drug Discov. Today* **9**, 403–409 (2004).

189. Peyot, M., Gadeau, A., Dandré, F., Belloc, I. & Desgranges, C. Extracellular Adenosine Induces Apoptosis of Human Arterial Smooth Muscle Cells via A$_{2b}$ -Purinoceptor. *Circ. Res.* 76–85 (2000).

190. Rivkees, S. A., Thevananther, S. & Hao, H. Are A$_3$ adenosine receptors expressed in the brain? *Neuroreport* **11**, 1026-1030 (2000).

191. Gessi, S., Merighi, S., Sacchetto, V., Simioni, C. & Borea, P. A. Adenosine receptors and cancer. *Biochim. Biophys. Acta* **1808**, 1400–1412 (2011).

192. Zhou, Y. *et al.* The Adenosine A$_1$ Receptor Antagonist DPCPX Inhibits Tumor Progression via the ERK/JNK Pathway in Renal Cell Carcinoma. *Cell. Physiol. Biochem.* **43**, 733–742 (2017).

193. Mirza, A. *et al.* RNA interference targeting of A$_1$ receptor-overexpressing breast carcinoma cells leads to diminished rates of cell proliferation and induction of apoptosis. *Cancer Biol. Ther.* **4**, 1355–1360 (2005).

194. Dastjerdi, N. M., Valiani, A., Mardani, M. & Ra, M. Z. Adenosine A$_1$ receptor modifies P53 expression and apoptosis in breast cancer cell line MCF-7. *Bratislava Med. J.* **116**, 242–246 (2016).

195. Woodhouse, E. C. *et al.* Adenosine Receptor Mediates Motility in Human Melanoma Cells. *Biochem. Biophys. Res. Commun.* **246**, 888–894 (1998).

196. Sai, K. *et al.* A$_1$ adenosine receptor signal and AMPK involving caspase-9/-3 activation are responsible for adenosine-induced RCR-1 astrocytoma cell death. *Neurotoxicology* **27**, 458–67 (2006).

197. Saito, T. & Sadoshima, J. Molecular Mechanisms of Mitochondrial Autophagy/Mitophagy in the Heart. *Circ. Res.* **116**, 1477–1490 (2015).

198. D'Ancona, S. *et al.* Effect of dipyridamole, 5'-(N-ethyl)-carboxamidoadenosine and 1,3-dipropyl-8-(2-amino-4-chlorophenyl)-xanthine on LOVO cell growth and morphology. *Anticancer Res.* **14**, 93–7

199. Synowitz, M. *et al.* A1 Adenosine Receptors in Microglia Control Glioblastoma-Host Interaction. *Cancer Res.* **66**, 8550–8557 (2006).

200. Etique, N., Grillier-Vuissoz, I., Lecomte, J. & Flament, S. Crosstalk between adenosine receptor (A$_{2A}$ isoform) and ERα mediates ethanol action in MCF-7 breast cancer cells. *Oncol. Rep.* **21**, 977–981 (2009).

201. Gessi, S. *et al.* Adenosine receptor targeting in health and disease. *Expert Opin. Investig. Drugs* **20**, 1591–1609 (2011).

202. Sexl, V. *et al.* Stimulation of the mitogen-activated protein kinase via the A$_{2A}$-adenosine receptor in primary human endothelial cells. *J. Biol. Chem.* **272**, 5792–9 (1997).

203. Lutty, G. A. & McLeod, D. S. Retinal vascular development and oxygen-induced retinopathy: A role for adenosine. *Prog. Retin. Eye Res.* **22**, 95–111 (2003).

204. Raskovalova, T. *et al.* Gs Protein-Coupled Adenosine Receptor Signaling and Lytic Function of Activated NK Cells. *J. Immunol.* **175**, 4383–4391 (2005).
205. Merighi, S. *et al.* Adenosine Receptors as Mediators of Both Cell Proliferation and Cell Death of Cultured Human Melanoma Cells. *J. Invest. Dermatol.* **119**, 923–933 (2002).
206. Fisher, J. W. & Brookins, J. Adenosine A_{2A} and A_{2B} receptor activation of erythropoietin production. *Am. J. Physiol. Physiol.* **281**, F826–F832 (2001).
207. Nagashima, K. & Karasawa, A. Modulation of erythropoietin production by selective adenosine agonists and antagonists in normal and anemic rats. *Life Sci.* **59**, 761–771 (1996).
208. Yasuda, Y., Saito, M., Yamamura, T., Yaguchi, T. & Nishizaki, T. Extracellular adenosine induces apoptosis in Caco-2 human colonic cancer cells by activating caspase-9/-3 via A_{2a} adenosine receptors. *J. Gastroenterol.* **44**, 56–65 (2009).
209. Fredholm, B. B. Adenosine receptors as drug targets. *Exp. Cell Res.* **316**, 1284–1288 (2010).
210. Ciruela, F. *et al.* Adenosine receptors interacting proteins (ARIPs): Behind the biology of adenosine signaling. *Biochim. Biophys. Acta - Biomembr.* **1798**, 9–20 (2010).
211. Igor, F. *et al.* Differential Expression of Adenosine Receptors in Human Endothelial Cells. *Circ. Res.* **90**, 531–538 (2002).
212. Merighi, S. *et al.* Caffeine Inhibits Adenosine-Induced Accumulation of Hypoxia-Inducible Factor-1α, Vascular Endothelial Growth Factor, and Interleukin-8 Expression in Hypoxic Human Colon Cancer Cells. *Mol. Pharmacol.* **72**, 395–406 (2007).
213. Fernandez-Gallardo, M., González-Ramírez, R., Sandoval, A., Felix, R. & Monjaraz, E. Adenosine Stimulate Proliferation and Migration in Triple Negative Breast Cancer Cells. *PLoS One* **11**, e0167445 (2016).
214. Ryzhov, S. *et al.* Host A_{2B} receptors promote carcinoma growth. *Neoplasia* **10**, 987–995 (2008).
215. Mittal, D. *et al.* Adenosine 2B Receptor Expression on Cancer Cells Promotes Metastasis. *Cancer Res.* **76**, 4372–4382 (2016).
216. Beavis, P. A. *et al.* Adenosine receptor 2A blockade increases the efficacy of anti-PD-1 through enhanced antitumor T-cell responses. *Cancer Immunol. Res.* **3**, 506–517 (2015).
217. Cekic, C. *et al.* Adenosine A_{2B} Receptor Blockade Slows Growth of Bladder and Breast Tumors. *J. Immunol.* **188**, 198–205 (2012).
218. Dhillon, A. S., Hagan, S., Rath, O. & Kolch, W. MAP kinase signalling pathways in cancer. *Oncogene* **26**, 3279–3290 (2007).
219. D'Alimonte, I. *et al.* Potentiation of temozolomide antitumor effect by purine receptor ligands able to restrain the in vitro growth of human glioblastoma stem cells. *Purinergic Signal.* **11**, 331–346 (2015).
220. Aghaei, M., Panjehpour, M., Karami-Tehrani, F. & Salami, S. Molecular mechanisms of A_3 adenosine receptor-induced G1 cell cycle arrest and apoptosis in androgen-dependent and independent prostate cancer cell lines: Involvement of intrinsic pathway. *J. Cancer Res. Clin. Oncol.* **137**, 1511–1523 (2011).
221. Gessi, S. *et al.* Adenosine receptor targeting in health and disease. *Expert Opin. Investig. Drugs* **20**, 1591–609 (2011).
222. Jacobson, K. A. Adenosine A_3 receptors: Novel ligands and paradoxical effects. *Trends Pharmacol. Sci.* **19**, 184–191 (1998).
223. Feoktistov, I., Ryzhov, S., Goldstein, A. E. & Biaggioni, I. Mast cell-mediated stimulation of angiogenesis: Cooperative interaction between A_{2B} and A_3 adenosine receptors. *Circ. Res.* **92**, 485–492 (2003).
224. Merighi, S. *et al.* A_3 adenosine receptor activation inhibits cell proliferation via phosphatidylinositol 3-kinase/Akt-dependent inhibition of the extracellular signal-regulated kinase 1/2 phosphorylation in A375 human melanoma cells. *J. Biol. Chem.* **280**, 19516–19526 (2005).
225. Torres, A. *et al.* Adenosine A_3 receptor elicits chemoresistance mediated by multiple resistance-associated protein-1 in human glioblastoma stem-like cells. *Oncotarget* **7**, 67373–67386 (2016).
226. Fishman, P., Bar-Yehuda, S., Liang, B. T. & Jacobson, K. A. Pharmacological and therapeutic effects of A_3 adenosine receptor agonists. *Drug Discov. Today* **17**, 359–366 (2012).
227. Haskó, G., Antonioli, L. & Cronstein, B. N. Adenosine metabolism, immunity and joint health. *Biochem. Pharmacol.* **151**, 307–313 (2018).
228. Antonioli, L., Fornai, M., Blandizzi, C., Pacher, P. & Haskó, G. Adenosine signaling and the immune system: When a lot could be too much. *Immunol. Lett.* **205**, 9–15 (2019).
229. Palmer, T. M. & Trevethick, M. A. Suppression of inflammatory and immune responses by the A_{2A} adenosine receptor: an introduction. *Br. J. Pharmacol.* **153**, S27–S34 (2008).
230. Hatfield, S. M. *et al.* Immunological mechanisms of the antitumor effects of supplemental oxygenation. *Sci. Transl. Med.* **7**, 1–13 (2015).
231. Wang, Y. J., Fletcher, R., Yu, J. & Zhang, L. Immunogenic effects of chemotherapy-induced tumor cell death. *Genes Dis.* **5**, 194–203 (2018).
232. Di Virgilio, F., Sarti, A. C., Falzoni, S., De Marchi, E. & Adinolfi, E. Extracellular ATP and P2 purinergic signalling in the tumour microenvironment. *Nat. Rev. Cancer* **18**, 601–618 (2018).
233. Antonioli, L. *et al.* Adenosine and inflammation: what's new on the horizon? *Drug Discov. Today* **19**, 1051–1068 (2014).
234. Horenstein, A. L. *et al.* A CD38/CD203A/CD73 ectoenzymatic pathway independent of CD39 drives a novel adenosinergic loop in human T lymphocytes. *Oncoimmunology* **2**, 1–14 (2013).
235. Morandi, F. *et al.* A non-canonical adenosinergic pathway led by CD38 in human melanoma cells induces suppression of T cell activation. *Oncotarget* **6**, 25602–25618 (2015).
236. Ludwig, N. *et al.* Tumor-derived exosomes promote angiogenesis via adenosine A_{2B} receptor signaling. *Angiogenesis.* **23**, 599-610 (2020).
237. Sek, K. *et al.* Targeting Adenosine Receptor Signaling in Cancer Immunotherapy. *Int. J. Mol. Sci.* **19**, 3837 (2018).
238. Young, A., Mittal, D., Stagg, J. & Smyth, M. J. Targeting Cancer-Derived Adenosine: New Therapeutic Approaches. *Cancer Discov.* **4**, 879–888 (2014).
239. Liu, H. *et al.* ADORA1 Inhibition Promotes Tumor Immune Evasion by Regulating the ATF3-PD-L1 Axis. *Cancer Cell* **37**, 324-339.e8 (2020).
240. Boussiotis, V. A. Molecular and biochemical aspects of the PD-1 checkpoint pathway. *N. Engl. J. Med.* **375**, 1767–1778 (2016).
241. Zou, W., Wolchok, J. D. & Chen, L. PD-L1 (B7-H1) and PD-1 pathway blockade for cancer therapy: Mechanisms, response biomarkers, and combinations. *Sci. Transl. Med.* **8**, (2016).
242. Mandapathil, M. *et al.* Generation and accumulation of immunosuppressive adenosine by human $CD4^+CD25^{high}FOXP3^+$ regulatory T Cells. *J. Biol. Chem.* **285**, 7176–7186 (2010).
243. Deaglio, S. *et al.* Adenosine generation catalyzed by CD39 and CD73 expressed on regulatory T cells mediates immune suppression. *J. Exp. Med.* **204**, 1257–1265 (2007).

244. Koshiba, M., Kojima, H., Huang, S., Apasov, S. & Sitkovsky, M. V. Memory of extracellular adenosine A(2a) purinergic receptor-mediated signaling in murine T cells. *J. Biol. Chem.* **272**, 25881–25889 (1997).

245. Ohta, A. *et al.* In vitro induction of T cells that are resistant to A2 adenosine receptor-mediated immunosuppression. *Br. J. Pharmacol.* **156**, 297–306 (2009).

246. Csóka, B. *et al.* Adenosine promotes alternative macrophage activation via A_{2A} and A_{2B} receptors . *FASEB J.* **26**, 376–386 (2012).

247. Volpini, R., Costanzi, S., Vittori, S., Cristalli, G. & Klotz, K.-N. Medicinal chemistry and pharmacology of A_{2B} adenosine receptors. *Curr. Top. Med. Chem.* **3**, 427–43 (2003).

248. Vaupel, P., Kallinowski, F. & Okunieff, P. Blood Flow, Oxygen and Nutrient Supply, and Metabolic Microenvironment of Human Tumors: A Review. *Cancer Res.* **49**, 6449–6465 (1989).

249. Fozard, J. R., Pfannkuche, H. J. & Schuurman, H. J. Mast cell degranulation following adenosine A_3 receptor activation in rats. *Eur. J. Pharmacol.* **298**, 293–297 (1996).

250. Mediavilla-Varela, M. *et al.* A Novel Antagonist of the Immune Checkpoint Protein Adenosine A_{2a} Receptor Restores Tumor-Infiltrating Lymphocyte Activity in the Context of the Tumor Microenvironment. *Neoplasia (United States)* **19**, 530–536 (2017).

251. Willingham, S. B. *et al.* $A_{2A}R$ antagonism with CPI-444 induces antitumor responses and augments efficacy to anti-PD-(L)1 and anti-CTLA-4 in preclinical models. *Cancer Immunol. Res.* **6**, 1136–1149 (2018).

252. Kim, D. G. & Bynoe, M. S. A_{2A} adenosine receptor modulates drug efflux transporter P-glycoprotein at the blood-brain barrier. *J. Clin. Invest.* **126**, 1717–1733 (2016).

253. Jackson, S. *et al.* The effect of an adenosine A_{2A} agonist on intra-tumoral concentrations of temozolomide in patients with recurrent glioblastoma. *Fluids Barriers CNS* **15**, 1–9 (2018).

254. Hatfield, S. M. & Sitkovsky, M. A_{2A} adenosine receptor antagonists to weaken the hypoxia-HIF-1α driven immunosuppression and improve immunotherapies of cancer. *Curr. Opin. Pharmacol.* **29**, 90–96 (2016).

255. Wei, Q., Costanzi, S., Balasubramanian, R., Gao, Z. G. & Jacobson, K. A. A_{2B} adenosine receptor blockade inhibits growth of prostate cancer cells. *Purinergic Signal.* **9**, 271–280 (2013).

256. Iannone, R., Miele, L., Maiolino, P., Pinto, A. & Morello, S. Blockade of A_{2b} adenosine receptor reduces tumor growth and immune suppression mediated by myeloid-derived suppressor cells in a mouse model of melanoma. *Neoplasia (United States)* **15**, 1400–1409 (2013).

257. Ohta, A. *et al.* A_{2A} adenosine receptor protects tumors from antitumor T cells. *Proc. Natl. Acad. Sci. U. S. A.* **103**, 13132–13137 (2006).

258. Waickman, A. T. *et al.* Enhancement of tumor immunotherapy by deletion of the A_{2A} adenosine receptor. *Cancer Immunol. Immunother.* **61**, 917–926 (2012).

259. Iannone, R., Miele, L., Maiolino, P., Pinto, A. & Morello, S. Adenosine limits the therapeutic effectiveness of anti-CTLA4 mAb in a mouse melanoma model. *Am. J. Cancer Res.* **4**, 172–81 (2014).

260. Allard, B., Pommey, S., Smyth, M. J. & Stagg, J. Targeting CD73 enhances the antitumor activity of anti-PD-1 and anti-CTLA-4 mAbs. *Clin. Cancer Res.* **19**, 5626–5635 (2013).

261. Barbhaiya, H., McClain, R., IJzerman, A. P. & Rivkees, S. A. Site-directed mutagenesis of the human A_1 adenosine receptor: Influences of acidic and hydroxy residues in the first four transmembrane domains on ligand binding. *Mol. Pharmacol.* **50**, 1635–1642 (1996).

262. Kim, J., Wess, J., van Rhee, A. M., Schöneberg, T. & Jacobson, K. A. Site-directed mutagenesis identifies residues involved in ligand recognition in the human A_{2a} adenosine receptor. *J. Biol. Chem.* **270**, 13987–13997 (1995).

263. Jiang, Q. *et al.* Hydrophilic side chains in the third and seventh transmembrane helical domains of human A_{2A} adenosine receptors are required for ligand recognition. *Mol. Pharmacol.* **50**, 512–521 (1996).

264. Kim, J. Glutamate residues in the second extracellular loop of the human A_{2a} adenosine receptor are required for ligand recognition. *Mol. Pharmacol.* **49**, 683–691 (1996).

265. Beukers, M. W. *et al.* Random Mutagenesis of the Human Adenosine A_{2B} Receptor Followed by Growth Selection in Yeast. Identification of Constitutively Active and Gain of Function Mutations. *Mol. Pharmacol.* **65**, 702–710 (2004).

266. Thimm, D. *et al.* Ligand-Specific Binding and Activation of the Human Adenosine A_{2B} Receptor. *Biochemistry* **52**, 726–740 (2013).

267. IJzerman, A. P., Van Galen, P. J. & Jacobson, K. A. Molecular modeling of adenosine receptors. I. The ligand binding site on the A_1 receptor. *Drug Des. Discov.* **9**, 49–67 (1992).

268. Dudley, M. W. *et al.* Adenosine A_1 receptor and ligand molecular modeling. *Drug Dev. Res.* **28**, 237–243 (1993).

269. Gray, V. E., Hause, R. J. & Fowler, D. M. Analysis of Large-Scale Mutagenesis Data To Assess the Impact of Single Amino Acid Substitutions. *Genetics* **207**, 53–61 (2017).

270. Bromberg, Y. & Rost, B. Comprehensive in silico mutagenesis highlights functionally important residues in proteins. *Bioinformatics* **24**, i207-12 (2008).

271. Wang, X. *et al.* Characterization of cancer-related somatic mutations in the adenosine A_{2B} receptor. *Eur. J. Pharmacol.* **880**, 173126 (2020).

272. Kazemi, M. H. *et al.* Adenosine and adenosine receptors in the immunopathogenesis and treatment of cancer. *J. Cell. Physiol.* **233**, 2032–2057 (2018).

273. Home - ClinicalTrials.gov, https://clinicaltrials.gov/ct2/home, (accessed Aug 20, 2020).

274. Usman, S., Khawer, M., Rafique, S., Naz, Z. & Saleem, K. The current status of anti GPCR drugs against different cancers. *J. Pharm. Anal.* **10**, 517-521 (2020).

Chapter 4

Characterization of cancer-related somatic mutations in the adenosine A$_{2B}$ receptor.

Abstract

In cancer, G protein-coupled receptors (GPCRs) are involved in tumor progression and metastasis. In this study we particularly examined one GPCR, the adenosine A_{2B} receptor. This receptor is activated by high concentrations of its endogenous ligand adenosine, which suppresses the immune response to fight tumor progression. A series of adenosine A_{2B} receptor mutations were retrieved from the Cancer Genome Atlas harboring data from patient samples with different cancer types. The main goal of this work was to investigate the pharmacology of these mutant receptors using a 'single-GPCR-one-G protein' yeast assay technology. Concentration-growth curves were obtained with the full agonist NECA for the wild-type receptor and 15 mutants. Compared to wild-type receptor, the constitutive activity levels in mutant receptors $F141L^{4.61}$, $Y202C^{5.58}$ and $L310P^{8.63}$ were high, while the potency and efficacy of NECA and BAY 60-6583 on $Y202C^{5.58}$ was lower. A 33- and 26-fold higher constitutive activity on $F141L^{4.61}$ and $L310P^{8.63}$ was reduced to wild-type levels in response to the inverse agonist ZM241385. These constitutively active mutants may thus be tumor promoting. Mutant receptors $F259S^{6.60}$ and $Y113F^{34.53}$ showed a more than one log-unit decrease in potency. A complete loss of activation was observed in mutant receptors $C29R^{1.54}$, $W130C^{4.50}$ and $P249L^{6.50}$. All mutations were characterized at the structural level, generating hypotheses of their roles on modulating the receptor conformational equilibrium. Taken together, this study is the first to investigate the nature of adenosine A_{2B} receptor cancer mutations and may thus provide insights in mutant receptor function in cancer.

Keywords: G protein-coupled receptor, Cancer-related mutations, yeast system

Introduction

G protein-coupled receptors (GPCRs) are a family of membrane-bound proteins that have seven-transmembrane (7TM) domains, connected by three intracellular (IL) and three extracellular (EL) loops, an extracellular amino terminus, and an intracellular carboxyl terminus[1]. GPCRs are responsive to a diverse set of physiological endogenous ligands including hormones and neurotransmitters. In total approximately 800 GPCRs are present in the human genome which can be subdivided in five main families, namely glutamate, rhodopsin, adhesion, frizzled/taste, and secretin, according to the GRAFS classification system[2].

GPCRs have been relatively underappreciated in preclinical oncology, where primary focus over the last two decades has been on kinases due to their central role in the cell cycle. However, there is a growing body of evidence showing a more prominent role of GPCRs in all phases of cancer[3]. In addition, recent work has shown that the function of GPCRs present in patient isolates is altered due to mutation, and indeed GPCRs are mutated in an estimated 20% of all cancers[4,5].

One particular class of rhodopsin-like GPCRs are the adenosine receptors (ARs), which respond to adenosine as their natural ligand[6]. There are four adenosine receptor subtypes, namely A$_1$, A$_{2A}$, A$_{2B}$, and A$_3$. The adenosine A$_1$ and A$_3$ receptors couple to the G$_i$ protein and consequently inhibit adenylate cyclase and cAMP production. Conversely adenosine A$_{2A}$ and A$_{2B}$ receptors activate adenylate cyclase via coupling to the G$_s$ protein[6,7]. While the role of the immune system in cancer defense is vital, the underlying mechanisms are yet not very well understood[8]. However, studies in immune cells provide evidence for the involvement of adenosine and adenosine receptors in these mechanisms[9]. Additionally, increased concentrations of adenosine are present in the tumor microenvironment. Hence adenosine may activate all subtypes of the adenosine receptors in cancer, including the low-affinity adenosine A$_{2B}$ receptor[10].

Adenosine A$_{2B}$ receptors expressed in human microvascular cells are likely modulating expression of angiogenic factors like vascular endothelial growth factor, interleukin-8 and basic fibroblast growth factor[11,12]. In HT29 colon[13], U87MG glioblastoma[14] and A375 melanoma cancer cells[15], increased interleukin-8 levels were observed after stimulation of adenosine A$_{2B}$ receptor resulting in cell proliferation. Moreover, it has been suggested that adenosine A$_{2B}$ receptors also regulate immunosuppression in the tumor microenvironment[16,17]. Recently, constitutive activity of the adenosine A$_{2B}$ receptor has been determined and proven to be involved in the promotion of cell proliferation in prostate cancer[18]. Furthermore, the adenosine A$_{2B}$ receptor is frequently overexpressed in oral squamous cell carcinoma and triple negative breast cancer cell lines, and promotes cancer progression[19,20]. On the other hand, it was shown that this receptor inhibits ERK 1/2 phosphorylation, resulting in an anti-proliferative action in ER-negative MDA-MB-231 cells[21]. However, a more recent study provided evidence for enhanced MAPK signaling via activation of the A$_{2B}$

receptor, promoting tumor progression in bladder urothelial carcinoma[22]. Taken all evidences together, it appears that activation of the adenosine A_{2B} receptor promotes tumor progression[23,24].

From a mechanistic point of view, it has been shown that mutations in this receptor can result in altered constitutive and agonist-induced receptor activity[25–28]. Mutant receptors that show increased basal activity independent of an agonist, are referred to as constitutively active mutants (CAMs), while those with decreased basal activity are termed constitutively inactive mutants (CIMs)[26]. Based on the two-state-receptor model[29], the equilibrium between the inactive (R) and active (R*) receptor conformation is shifted in these CAMs and CIMs.

In the present study, we selected 15 mutations in adenosine A_{2B} receptor from all cancer types using a bioinformatics approach. Subsequently these mutations were screened in an *S.cerevisiae* strain to study the effect of these mutations on receptor activation using different reference ligands (Fig. 1). We found that these mutations resulted in 3 CAMs and 5 less active mutants. Moreover, we found 4 mutants that behaved similar to the wild-type receptor (i.e. no effect mutants) and 3 loss-of-function mutants. Taken together, this study is the first to characterize cancer mutations on adenosine A_{2B} receptor at the molecular level and may thus provide insights in mutant receptor function in cancer.

Methods

Data mining

Mutation data from The Cancer Genome Atlas (TCGA, version August 8th 2015) was downloaded using Firehose[30,31]. Subsequently the data was extracted, when available MutSig 2.0 data was used, in cases where this was not available MutSig 2CV was used (specifically Colon Adenocarcinoma, Acute Myeloid Leukemia, Ovarian Cerous Cystadenocarcinoma, Rectum Adenocarcinoma). Natural variance mutation data was downloaded from Uniprot in the form of 'Index of Protein Altering Variants' (version November 11th 2015)[32].Sequence data was filtered for missense somatic mutations and the protein of interest (human A_{2B} receptor, Uniprot accession P29275)[33]. The GPCRdb alignment tool was used to assign Ballesteros Weinstein numbers[34,35], indicated by superscripts after the corresponding residue number. Finally, 15 cancer-related mutations were identified of which one mutation (L310P) was a duplicate, i.e. present in samples from two separate patients both suffering from colon adenocarcinoma.

Materials

The MMY24 strain, the S. *cerevisiae* expression vectors, the pDT-PGK plasmid, and the wild-type human adenosine A_{2B} receptor in pDT-PGK plasmid were kindly provided by Dr. Simon Dowell from GSK (Stevenage, UK). The QuikChange II® Site-

Directed Mutagenesis Kit was purchased from Agilent Technologies, which includes XL10-Gold ultracompetent cells (Amstelveen, the Netherlands). The QIAprep mini plasmid purification kit was purchased from QIAGEN (Amsterdam, the Netherlands). NECA (Fig. 1), 3-amino-[1,2,4]-triazole (3-AT), bovine serum albumin (BSA) and 3, 3',5,5'-tetramethyl-benzidine (TMB) were purchased from Sigma-Aldrich (Zwijndrecht, the Netherlands). BAY 60-6583 (Fig. 1) was synthesized in house. ZM241385 was purchased from Ascent Scientific (Bristol, United Kingdom). PSB603 (Fig. 1) was purchased from TOCRIS Bioscience (Abingdon, United Kingdom). The Hybond-ECL membrane and the ECL Western blotting analysis system were purchased from GE Healthcare (Eindhoven, the Netherlands). The antibody directed against the C-terminal region of the human adenosine A$_{2B}$ receptor was kindly provided by Dr. I. Feoktistov (Vanderbilt University, Nashville, TN, USA), the antibody directed against the extracellular region of the human adenosine A$_{2B}$ receptor was purchased from Alpha Diagnostic International (San Antonio, USA) and goat anti-rabbit IgG was purchased from Jackson ImmunoResearch Laboratories (West Grove, PA, USA).
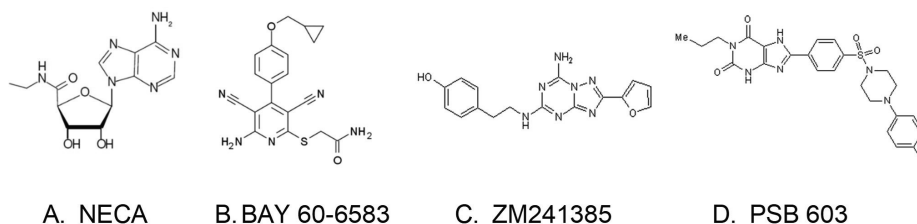

A. NECA   B. BAY 60-6583   C. ZM241385   D. PSB 603

Fig 1. Structures of four reference compounds for the adenosine A$_{2B}$ receptor: (A) agonist NECA, (B) non-ribose agonist BAY 60-6583, (C) inverse agonist ZM241385 and (D) neutral antagonist PSB603.

Generation of human adenosine A$_{2B}$ receptor mutations

The mutations were generated as described previously by Liu *et al*[25]. In short, DNA primers for the human adenosine A$_{2B}$ receptor (uniprot: P29275) mutations were designed by the QuikChange Primer Design Program of Agilent Technologies (Santa Clara, CA, USA). These primers contained a single substitution resulting in a codon change for the desired amino acid substitution. Primers and their complements were synthesized (Eurogentec, Maastricht, the Netherlands) and used to generate mutation plasmids according to the QuikChange method from Agilent Technologies. The mutagenic PCR was performed in the presence of 50 ng of template DNA, 10 µM concentration of each primer, 1 µl of dNTP mix, 2.5 µl of 10 x reaction buffer and 2.5 U *PfuUtra* HF DNA polymerase. The number of mutagenic PCR cycles was set to 22 (PCR cycling conditions: 95 °C for 30 s, 55 °C for 1 min, and 68 °C for 10 min). The methylated or hemimethylated non-mutated plasmid DNA was removed by 5 U *Dpn* I restriction enzyme incubating for 2 h at 37 °C. The mutated DNA plasmids were transformed into XL-1 Blue supercompetent cells according to the manual of the QuikChange II® Site-Directed Mutagenesis Kit. After plasmid isolation by using a QIAprep mini plasmid purification kit, the mutations were verified by double-strain

DNA sequencing (LGTC, Leiden University, the Netherlands).

Transformation in a MMY24 S. cerevisiae strain

The yeast strain was derived from the MMY11 strain and further adapted to communicate with mammalian GPCRs through a specific Gpa1p/$G_{\alpha i3}$ chimeric G protein. The genotype of the MMY24 is: **MATa** *his3 leu2 trp1 ura3 can1 gpa1_::G_i3 far1 ::ura3 sst2_::ura3 Fus1::FUS1-HIS3 LEU2::FUS1-lacZ ste2_::G418R* and the last five amino acid residues of C-terminus of Gpa1p/ $G_{\alpha i3}$ chimera were replaced by the same length sequence from mammalian $G_{\alpha i3}$ protein[36]. The pheromone pathway was coupled to HIS3 reporter gene via FUS1 promotor, so that the level of receptor activation can be measured directly by the yeast growth rate on histidine-deficient medium. The plasmids containing the mutant adenosine A_{2B} receptors were transformed into an S. *cerevisae* strain according to the Lithium-Acetate procedure [37].

Solid growth assay

To characterize the activation of various mutated receptors, concentration-growth curves were generated from a solid growth assay. This assay was performed with yeast cells from an overnight culture in selective YNB medium lacking uracil and leucine (YNB-UL) as this yeast strain can produce leucine and the plasmid also contains a gene encoding for uracil production. The yeast cells were diluted to 400,000 cells/ml ($OD_{600} \approx 0.02$) and droplets of 1.5 μl were spotted on selection agar plates, i.e. YNB agar medium lacking uracil, leucine and histidine (YNB-ULH). In addition, the agar on the plates contained 7mM 3-AT and the adenosine A_{2B} receptor full agonist NECA in a concentration range from 10^{-9} to 10^{-4} M, or the non-ribose adenosine A_{2B} receptor agonist BAY 60-6583[38] in a concentration range from 10^{-9} to 10^{-5} M, or the adenosine A_{2B} receptor inverse agonist ZM241385[39] in a concentration range from 10^{-9} to 10^{-5} M. After 50 h incubation at 30 °C, the plates were scanned and receptor activation-mediated yeast cell growth was quantified with ImageLab 5.2.1 software of a ChemiDoc MP Imaging System from Bio-Rad (Hercules, CA, USA). The level of yeast cell growth was calculated as the intensity of each spot after correction for local background on the plate.

Liquid growth assay and Schild-plot analysis

To characterize the mutant adenosine A_{2B} receptors further, similar concentration-growth curves were obtained using liquid YNB-ULH medium and 96-well plates. Yeast cells were inoculated in YNB-UL and diluted to $4 \cdot 10^6$ cells/ml ($OD_{600} \approx 0.2$). To each well, 150 μl YNB-ULH medium containing 7 mM 3-AT, 2 μl various concentrations of ligands and 50 μl yeast cells were added. The 96-well plate was then incubated at 30 °C for 35 h in a Genios plate reader, and was shaken every 10 min at 300 rpm for 1 min to keep the cells in suspension. The level of yeast cell growth was determined by the optical density at a wavelength of 595 nm. For the wild-type adenosine A_{2B} receptor, mutant receptor F141L[4.61], Y202C[5.58] and L310P[8.63], concentration-growth curves of

NECA were generated in the absence or presence of different concentrations of the selective adenosine A$_{2B}$ receptor antagonist PSB603.

Whole cell extracts and immunoblotting

In order to determine the expression level of the different mutant adenosine A$_{2B}$ receptors in the MMY24 yeast strain, an immunoblotting method was used as described previously[25]. In short, whole cell protein extracts were prepared using trichloroacetic acid (TCA) from an overnight culture (1.2·10^8 yeast cells). After two washing steps with 20% TCA, yeast cells were broken by thoroughly vortexing in the presence of glass beads. Then, a semi-automated electrophoresis technique (PhastSystem™, Amersham Pharmacia Biotech) was used to separate 4 μl (≈24 μg) of the yeast cell extract on a 12.5% SDS/PAGE gel. Subsequently the proteins were blotted on a Hybond-ECL membrane, where a rabbit anti-human adenosine A$_{2B}$ receptor primary antibody was used directed against the C-terminus of the human adenosine A$_{2B}$ receptor. The remaining unbound antibody was washed off the membranes repeatedly with TBST (0.05% Tween 20 in Tris-buffered saline), and the HRP-conjugated goat anti-rabbit IgG (Jackson ImmunoResearch Laboratories) was added. Via the ECL Western blotting analysis (GE Healthcare, the Netherlands), the specific human adenosine A$_{2B}$ receptor bands were found at 29 kDa and 48 kDa, whereas a nonspecific band was detected at approximately 45 kDa, which was used as loading control. Densitometric analysis was performed by the volume analysis tool in the ImageLab 5.2.1 software from Bio-Rad (Hercules, CA, USA). The ratio between the intensity of specific human adenosine A$_{2B}$ receptor protein bands and nonspecific protein band was determined, where the yeast strain carrying wild-type hA$_{2B}$R was set to 100% and the yeast strain carrying the empty vector pDT-PGK was set to 0%.

Yeast enzyme-linked immunosorbent assay (ELISA)

Yeast ELISA was adapted from a method reported previously[40]. About 2·10^7 yeast cells were collected from an overnight culture in YNB-UL medium. The cells were blocked with 2% BSA in Tris-buffered saline (TBS), followed by 1 hour incubation with polyclonal rabbit anti-human adenosine A$_{2B}$ receptor antibody (1:2000) in TBST containing 0.1% BSA at room temperature. After washing three times with TBST, HRP-conjugated goat anti-rabbit IgG (1:5000) was added and incubated for 1 h at room temperature. After removing the secondary antibody and washing the cells with TBS, TMB was added and incubated for 15 minutes in the dark. The reaction was stopped with 1 M H$_3$PO$_4$, and absorbance was read at 450 nm using a Wallac EnVision 2104 Multilabel reader (PerkinElmer).

Homology modelling

Homology models were generated using the GPCR-ModSim web-based pipeline for modeling GPCRs[41,42], available through http://open.gpcr-modsim.org/. Shortly, this webserver performs a multiple sequence alignment against a curated set of

crystalized GPCRs, divided in three categories: inactive, active-like and fully-active. The best templates are suggested based on the overall homology with the target sequence and the user can select between single-template or multi-template homology modeling. In this study, the adenosine A_{2A} receptor was the only template used to model the adenosine A_{2B} receptor, using the structures deposited with PDB codes 3EML for the inactive model, 2YDV for the active-like and 5G53 for the fully-active structure. After manual adjustment of the alignment of the extracellular loop 2 (ECL2) region, which is recommended due to the high variability within this loop region, homology models were created and sorted by the DOPHR scoring function by the server, using Modeller as a background engine[43]. The best model was finally selected among the top scored models based on visual inspection.

Data analysis

All experimental data were analyzed using GraphPad Prism 7.0 software (GraphPad Software Inc., San Diego, CA, USA). Solid and liquid growth assays were analyzed by non-linear regression using "log (agonist or inhibitor) vs. response (three parameters)" to obtain potency (EC_{50}), inhibitory potency (IC_{50}) and efficacy (E_{max}) values. For Schild-plot analysis, log[DR-1] was calculated by equation log[DR-1] = log[(A'/A)-1], where A' is the EC_{50} value obtained from the concentration-growth curves in the presence of antagonist, A is the EC_{50} value obtained from the concentration-growth curves in the absence of antagonist. pA_2 values were generated by using linear regression. Statistical evaluation was performed by a two-tailed unpaired Student's *t-test* between pEC_{50} or E_{max} values of mutant receptors and values of wild-type receptor obtained from the same experiments. All values obtained are means of at least three individual experiments performed in duplicate.

Results

Data mining and expression of mutants

In total 15 point mutations in the adenosine A_{2B} receptor were identified in cancer patient isolates by data mining the TCGA database on August 8th 2015. Three mutations were located at an extracellular loop (EL), two at an intracellular loop (IL), six in the 7-transmembrane domain and four at the C-terminus of the adenosine A_{2B} receptor. Of note, three mutations were found for position L310[8.63,] i.e. L310F, L310I and L310P, of which the latter was present in two separate patient isolates. In the natural variance set 16 point mutations were identified, namely A35V[1.60], T37S[12.49], C72Y[23.51], A82T[3.29], I126T[4.46], L129I[4.49], G135R[4.55], C171S[45.50], L172P[45.51], R223W[6.24], R228W[6.29], K267E[EL3], R293W[7.56], R295Q[8.48], D296G[8.49] and R298H[8.51]. However, none of these were found to match any of the residue positions of the cancer-related mutations. All 15 cancer-related mutants were constructed and transformed into the MMY24 yeast strain, and showed overall receptor expression, as determined by Western blot analysis of whole cell lysates (Fig. 2A and Table S1). Besides, all

mutant receptors also showed cell surface expression, as determined by ELISA performed on intact yeast cells (Fig. 2B and Table S1).

Characterization of mutant adenosine A$_{2B}$ receptors on receptor activation

To characterize the effects of the cancer-related mutations on receptor activation,
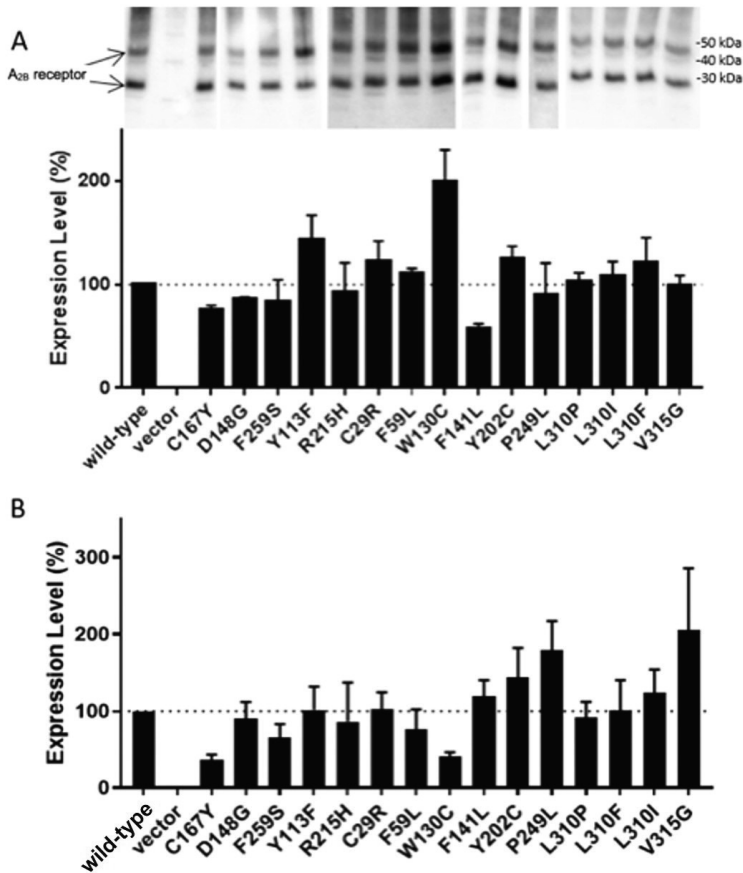
4

Fig 2. Expression levels of wild-type and mutant adenosine A$_{2B}$ receptors. A) Western blot analysis of yeast transfected with vector in absence (vector) or presence of wild-type or 15 mutant adenosine A$_{2B}$ receptors. The upper panel shows one representative blot, where the arrows indicate the specific human adenosine A$_{2B}$ receptor bands at 29 kDa and 48 kDa. The lower panel shows the bar graph obtained from the densitometric analysis. Expression levels were determined between the density of specific bands and the density of the non-specific band that is present in all lanes. Wild-type receptor was set at 100% and the empty vector pDT-PGK was set at 0%. The combined bar graph is shown in mean ± SEM from at least three individual experiments. B) Representative experiment of cell surface expression levels of wild-type and mutant adenosine A$_{2B}$ receptors, determined in an enzyme-linked immunosorbent assay. Wild-type receptor was set at 100% and the empty vector pDT-PGK was set at 0%. The bar graph is shown in mean ± SD of two individual experiment performed in duplicate. Table S1 has the full data set for two independent experiments.
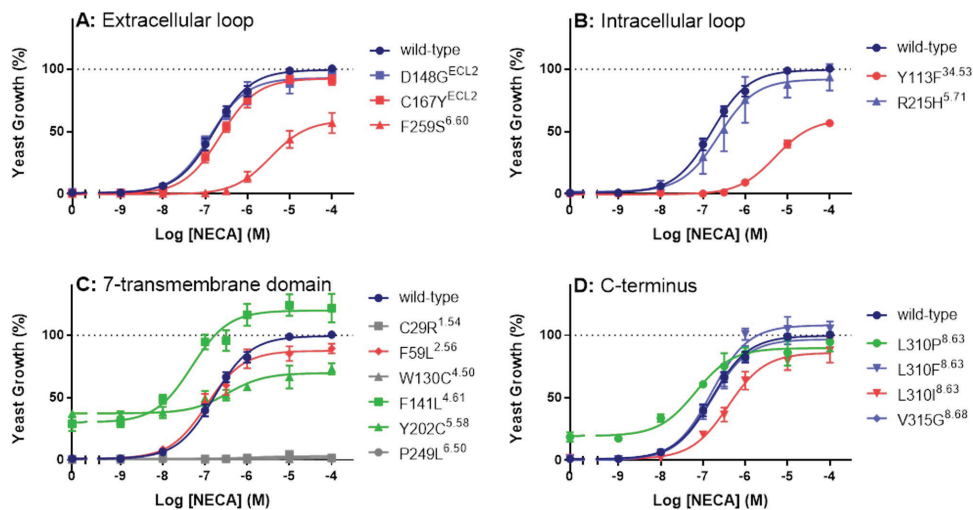
Fig 3. Concentration-response curves for NECA at the wildtype and 15 mutant adenosine A_{2B} receptors. Data is separated for mutations located on (A) extracellular loop, (B) intracellular loop, (C) 7-transmembrane domain and (D) C-terminus. The maximum activation level of wild-type adenosine A_{2B} receptor was set at 100%, while the background of the selection plate was set at 0%. Combined graphs are shown as mean ± SEM from at least three individual experiments, each performed in triplicate.

the pharmacology of these 15 mutant receptors was investigated by yeast-growth assays. Concentration-growth curves and results of the mutant receptors in response to the full agonist NECA are shown in Fig. 3 and Table 1.

In this system, the wild-type receptor showed a pEC_{50} value of 6.79±0.09 for NECA and a low level of basal activity, if any. Overall half of the mutant receptors showed similar constitutive activity, potency and efficacy as the wild-type receptors (Table 1). In the ECL and ICL, two mutants behaved significantly different from wild-type adenosine A_{2B} receptor in response to NECA, i.e. mutant receptor F259S$^{6.60}$ (Fig. 3A) and mutant receptor Y113F$^{34.53}$ (Fig. 3B) displayed a more than 1 log-unit decreased potency. The maximum receptor activation (E_{max}) of these two mutant receptors was also decreased to 57% for both (Table 1). At the 7-transmembrane domain of the adenosine A_{2B} receptor, mutants C29R$^{1.54}$, W130C$^{4.50}$ and P249L$^{6.50}$ showed a complete loss of function (Fig. 3C). In contrast, increased constitutive activities were observed for mutant receptors F141L$^{4.61}$ and Y202C$^{5.58}$, which were 34- and 48- fold higher than the wild-type receptor, respectively (Fig. 3C and Table 1). In response to NECA, mutant receptor F141L$^{4.61}$ showed a significantly increased potency with a pEC_{50} value of 7.31±0.03 and an increased E_{max} value of 122%, while mutant receptor Y202C$^{5.58}$ showed a significantly reduced pEC_{50} value of 6.30±0.09 and reduced E_{max} value of 73% in comparison to the wild-type receptor (Fig. 3C and Table 1). At the C-terminus, mutant receptor L310P$^{8.63}$ showed a relatively high level of constitutive activity, i.e. 26-fold higher than wild-type receptor, as well as an increased potency for NECA. Mutant receptor L310I$^{8.63}$ showed a significantly decreased pEC_{50} value

4

of 6.40±0.01 compared to wild-type receptor (Fig. 3D and Table 1), while the E$_{max}$ value did not decrease significantly. Mutant receptor V315G$^{8.68}$ showed similar pEC$_{50}$ and E$_{max}$ values to wild-type receptor (Fig. 3D and Table 1), although the cell surface expression level was much higher than wild-type receptor (Fig. 2B). Additional yeast ELISA experiments were performed on yeast colonies carrying either wild-type or mutant receptor V315G$^{8.68}$, and colonies with similar expression levels were selected in yeast liquid growth assay to further investigate receptor activation in response to NECA. Interestingly, similar pEC$_{50}$ and E$_{max}$ values were still obtained for mutant receptor V315G$^{8.68}$ and wild-type adenosine A$_{2B}$ receptor (Table S2).

The mutant receptors F259S$^{6.60}$, Y113F$^{34.53}$, C29R$^{1.54}$, W130C$^{4.50}$, P249L$^{6.50}$, F141L$^{4.61}$, Y202C$^{5.58}$ and L310P$^{8.63}$ which all showed the more altered pharmacological response to NECA were also studied with BAY 60-6583, a non-ribose adenosine A$_{2B}$ receptor agonist (Fig. 1). On the wild-type receptor, BAY 60-6583 showed a pEC$_{50}$ value of 7.49±0.33. As for NECA, decreased potencies and E$_{max}$ values were also observed for BAY 60-6583 at F259S$^{6.60}$ and Y113F$^{34.53}$ in comparison to the wild-type receptor (Table 1). Mutant receptors C29R$^{1.54}$, W130C$^{4.50}$ and P249L$^{6.50}$, which did not show any activity in the presence of NECA, were not activated by BAY 60-6583 either (Table 1). As opposed to NECA, the effects of BAY 60-6583 on mutant receptors F141L$^{4.61}$, Y202C$^{5.58}$ and L310P$^{8.63}$ were similar when compared to the wild-type receptor (Table 1).

Taken together, based on the different pharmacological effects we characterized mutant receptors F141L$^{4.61}$, Y202C$^{5.58}$ and L310P$^{8.63}$ as CAMs, mutant receptors C29R$^{1.54}$, W130C$^{4.50}$ and P249L$^{6.50}$ as loss of function mutants (LFMs), mutant receptors C167Y^{ECL2}, F259S$^{6.60}$, Y113F$^{34.53}$, F59L$^{2.56}$ and L310I$^{8.63}$ as less active mutants (LAMs) and mutant receptors D148S^{ECL2}, R215H$^{5.71}$, L310F$^{8.63}$ and V315G$^{8.68}$ as no effect mutants (NEMs).

Inverse agonism of the CAMs

To study whether receptors bearing CAMs (F141L$^{4.61}$, Y202C$^{5.58}$ and L310P$^{8.63}$) could still be inhibited, an inverse agonist of the A$_{2B}$ receptor, ZM241385, was used in the yeast solid growth assay, and compared to the wild-type receptor. The concentration-growth inhibition curves are shown in Fig. 4. The wild-type adenosine A$_{2B}$ receptor had low basal activity in this system, and ZM241385 did not further reduce this. All CAMs displayed a decreased activity upon increasing concentrations of ZM241385. The level of constitutive activity of F141L$^{4.61}$ and L310P$^{8.63}$ was fully suppressed, with pIC$_{50}$ values of 7.43±0.17 and 7.49±0.27 for ZM241385, respectively (Fig. 4 and Table 1). For the mutant receptor with the highest constitutive activity Y202C$^{5.58}$, ZM241385 caused a partial reduction to a residual activity of 19% and with a lower pIC$_{50}$ of 6.62±0.23 than for the less active CAMs, i.e. F141L$^{4.61}$ and L310P$^{8.63}$ (Fig. 4).

Table 1. Characterization of adenosine A_{2B} receptor mutations identified in cancer patient samples in yeast solid growth assays. Mutations are shown in the numbering of the adenosine A_{2B} receptor amino acid sequence as well as according to the Ballesteros and Weinstein GPCR numbering system.

Mutation	Fold CA	NECA		BAY 60-6583		Type
		pEC_{50}	E_{max} (%)	pEC_{50}	E_{max} (%)	
wild-type	1.0	6.79±0.23	100±4	7.49±0.57	100±3	-
C167Y^{ECL2}	1.0	6.65±0.19	91±7*	-	-	LAM
D148G^{ECL2}	2.5	6.87±0.11	98±5	-	-	NEM
F259S$^{6.60}$	0.6	5.44±0.23****	57±14***	6.71±0.41	20±9###	LAM
Y113F$^{34.53}$	0.6	5.28±0.12****	57±4****	6.51±0.45#	15±1####	LAM
R215H$^{5.71}$	2.8	6.57±0.48	94±18	-	-	NEM
C29R$^{1.54}$	1.1	ND	ND	ND	ND	LFM
F59L$^{2.56}$	1.0	6.94±0.23	89±7*	-	-	LAM
W130C$^{4.50}$	0.4	ND	ND	ND	ND	LFM
F141L$^{4.61}$	33	7.31±0.06**	122±19*	7.64±0.27	108±9	CAM
Y202C$^{5.58}$	48	6.30±0.15*	73±8***	7.21±0.18	74±18#	CAM
P249L$^{6.50}$	0.4	ND	ND	ND	ND	LFM
L310P$^{8.63}$	26	7.21±0.14*	95±13	7.16±0.23	80±8#	CAM
L310F$^{8.63}$	2.0	6.80±0.12	105±10	-	-	NEM
L310I$^{8.63}$	3.6	6.40±0.02*	88±17	-	-	LAM
V315G$^{8.68}$	1.4	6.89±0.19	94±4	-	-	NEM

pEC_{50} and E_{max} values are shown as mean ± SD from at least three individual experiments, each performed in triplicate. The percentage maximum effect (% E_{max}) and the fold constitutive activity values were calculated by the mean values generated from the concentration-growth curves, compared to the wild-type receptor. Dose-growth curves of BAY 60-6583 were only generated for mutants that responded significantly different to NECA in comparison to the wild-type receptor.

* $P < 0.05$, ** $P < 0.01$, *** $P < 0.001$, **** $P < 0.0001$ compared to the wild-type receptor in response to NECA; # $P < 0.05$, ### $P < 0.001$, #### $P < 0.0001$ compared to the wild-type receptor in response to BAY 60-6583, determined by a two-tailed unpaired Student's t-test.

ND: not detectable, -: not measured, CA: constitutive activity; CAM: constitutively active mutant, LAM: less active mutant, LFM: loss of function mutant, NEM: no effect mutant

Characterization of CAMs on ligand binding

To investigate whether the affinity of an antagonist had changed on the CAM receptors F141L$^{4.61}$, Y202C$^{5.58}$ and L310P$^{8.63}$, a Schild-plot analysis was performed (Fig. 5). Concentration-growth curves were generated of the agonist NECA in the absence or presence of increasing concentrations of the competitive adenosine A_{2B} receptor antagonist PSB603 (Fig. 1). For the wild-type and mutant receptors F141L$^{4.61}$ and L310P$^{8.63}$, a rightward shift of the concentration-growth curves was observed with increasing concentrations of PSB603 (Fig. 5A-C). This resulted in decreased apparent pEC_{50} values for NECA, while the maximal growth levels for

these mutant receptors were still reached. The pA$_2$ values, as determined from the Schild-plot, were 8.47 for wild-type, 8.07 for F141L[4.61] and 8.27 for L310P[8.63], showing that the antagonist affinity for these two mutants was not significantly influenced by the mutations (p = 0.0776 and p = 0.3097, respectively). Of note, a Schild-plot could not be generated for mutant receptor Y202C[5.58], as the presence of PSB603 (at the selected concentrations) did not cause a shift in agonist potency (Fig. 5D).

Structural mapping and analysis of mutations

The mutations investigated in this study were mapped on a homology model of the adenosine A$_{2B}$ receptor to provide structural hypotheses for the observed pharmacological effect (NEM, LFM, CAM and LAM) of the different mutations. As illustrated in Figure 6A, the studied mutations are distributed over the whole receptor. The NEMs are positioned in the ECL, ICLs and C-terminus regions, while all three LFMs are exclusively located in the transmembrane region. These mutations are either part of highly conserved areas of the receptor (W130C[4.50] and P249L[6.50], Fig. 6C) and/or introduce a drastic change in the properties of the amino acid (C29R[1.54], W130C[4.50]). The two LAMs are located in either the ECL (F259S[6.60], Fig. 6C) or ICL (Y113F[34.53], Fig. 6D) region, where F259[6.60] is located on the top of the helix 6, while Y113[34.53] is part of the TDY triad (see Discussion). Finally, the three CAMs are located in the transmembrane region or in helix 8. Mutant receptor L310P[8.63] has been identified in two individual patients. Additionally, mutations of this residue to Phe (F) and Ile (I) were found, where mutation to F did not alter receptor functionality. The F141L[4.61] mutation is positioned at the membrane-helix interface on the top of TM4 and at the start of ECL2. Noteworthy are the opposing pharmacological effects observed between F259S[6.60] and F141L[4.61] (i.e. LAM and CAM, respectively), although they are both situated at a structurally similar location. Y202[5.58] is part of an activation switch with Y290[7.53] in the NPxxY motif, moving outward into the membrane in the agonist-bound receptor as observed in the adenosine A$_{2A}$ receptor crystal structures (Fig. 6B).

Discussion

Numerous GPCR mutations are known to alter the pharmacological function of the receptor by affecting constitutive activity, ligand binding, GPCR-G protein interaction, and / or cell surface expression, resulting in a wide range of disease phenotypes[44]. Moreover, a variety of mutations within GPCRs have been linked to different types of cancer[45–47], but the pharmacological effects of these cancer-related mutations are not yet fully understood. Previously, several studies performed on the adenosine A$_{2B}$ receptor demonstrated some residues to be essential in receptor activation[25–28,35,48]. Hence, in this study 15 single-site point mutations of adenosine A$_{2B}$ receptor identified from The Cancer Genome Atlas (TCGA)[31] were examined in the *S.cerevisiae* system to improve our understanding of the mechanism of receptor

activation in relation to cancer progression. As none of these mutations were found in the natural variance mutation dataset[32], they could be cancer specific, yet follow up research is warranted.
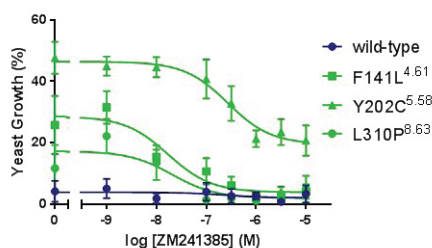

Fig 4. Concentration-inhibition curves of the adenosine A_{2B} receptor inverse agonist ZM241385 at the wild-type adenosine A_{2B} receptor and CAMs, F141L[4.61], Y202C[5.58] and L310P[8.63]. The maximum activation level of wild-type adenosine A_{2B} receptor was set at 100%, the background of the selection plate was set at 0%. Combined graphs are shown from at least three individual experiments, each performed in triplicate.
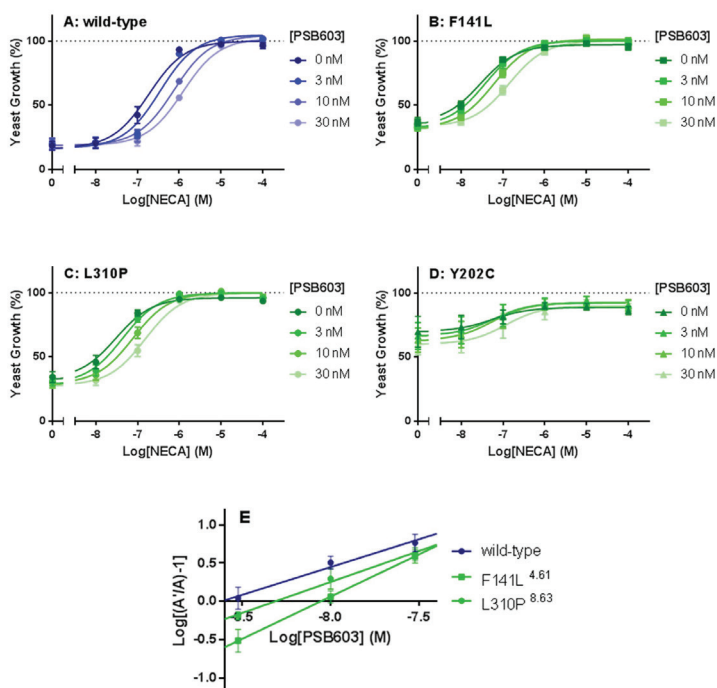
Fig 5. Schild analysis of adenosine A_{2B} receptor antagonist PSB603 binding to wild-type receptor and CAMs. Concentration-growth curves of NECA for (A) wild-type adenosine A_{2B} receptor, (B) F141L[4.61] Y202C[5.58], (C) L310P[8.63] and (D) Y202C[5.58] were obtained in the absence or presence of increasing concentrations of PSB603. (E) A Schild-plot to obtain pA_2 values of PSB603 on the wild-type and mutant receptors F141L[4.61] and L310P[8.63]. Data are shown as mean ± SEM from at least three individual experiments, each performed in duplicate.

Less active mutants

Mutant receptors F259S[6.60] and Y113F[34.53] were identified from colon adenocarcinoma and lung adenocarcinoma located at opposite sides of the receptor, ECL3 and ICL2. However, both showed decreased potency and efficacy in the case of ribose and non-ribose agonists (Fig. 1 and Table 1, LAMs). These data are consistent with a previous study on the CC-chemokine receptor 5 (CCR5) receptor, showing that mutation from phenylalanine to alanine at position 6.60 resulted in a decreased affinity of the agonist gp120[49].

Residue Y113[34.53] is completely conserved among adenosine receptors and several other class A GPCRs. Structures of the adenosine A$_1$ and A$_{2A}$ receptor show that this residue is part of a conserved triad (T[2.39]–D[3.49]–Y[34.53]). We and others previously hypothesized a regulatory role of this motif in receptor activation [35] by mediating the strength of the D102-R103 ionic lock[50,51], preventing an outward movement of R[3.50] necessary for G protein binding (Fig. 6D). The Y113F[34.53] mutation increases the electrostatic attraction between D102[3.49] and R103[3.50], reducing the mobility of this residue. Notably, at the same position in the β$_1$-adrenergic receptor, mutation Y149A[34.53] leads to a large decrease in thermal stability of the antagonist bound state of the receptor[52].

Loss of function mutants

Mutant receptors C29R[1.54], W130C[4.50] and P249L[6.50], identified from stomach adenocarcinoma, liver hepatocellular carcinoma, and colon adenocarcinoma, respectively, showed a complete loss of activation (Fig. 3C and Table 1). Importantly, none of these mutant receptors showed severely reduced expression levels compared to the wild-type receptor (Fig. 2A and B, Table S1), indicating that the loss of activation is not due to the loss of expression in our model system. At residue C1.54, a drastic change from cysteine to arginine resulted in a LFM in our study. At the same position (1.54) in CCR2 and CCR5, the conservative mutation CCR2-V62I[1.54] did not affect receptor expression or ligand binding[53], yet the inverse mutation on CCR5-I52V[1.54] showed a decreased affinity for CCL5[54].

The tryptophan at position 130[4.50] and proline at position 249[6.50] are highly conserved among all class A GPCRs with a presence of 96% and 100%[55]. Mutant W4.50Cinvestigated on CXCR4 and melanocortin-4 receptor (MC4R) showed abolished ligand binding and cAMP response[56,57], indicating that the introduction of a drastic change in the amino acid properties at highly conserved positions can dramatically change receptor functionality. A rigid body motion of TM6 related to TM3 is known to be facilitated through the presence of the conserved proline in TM6 (6.50)[58]. Pro[6.50] is also known as a rotamer toggle switch, playing a role in the structural rearrangement of class A GPCRs on transition from the inactive to the active state (Fig. 6C)[59]. Hence the observed loss of function for the mutations at positions 130[4.50] and 249[6.50] has some precedent.
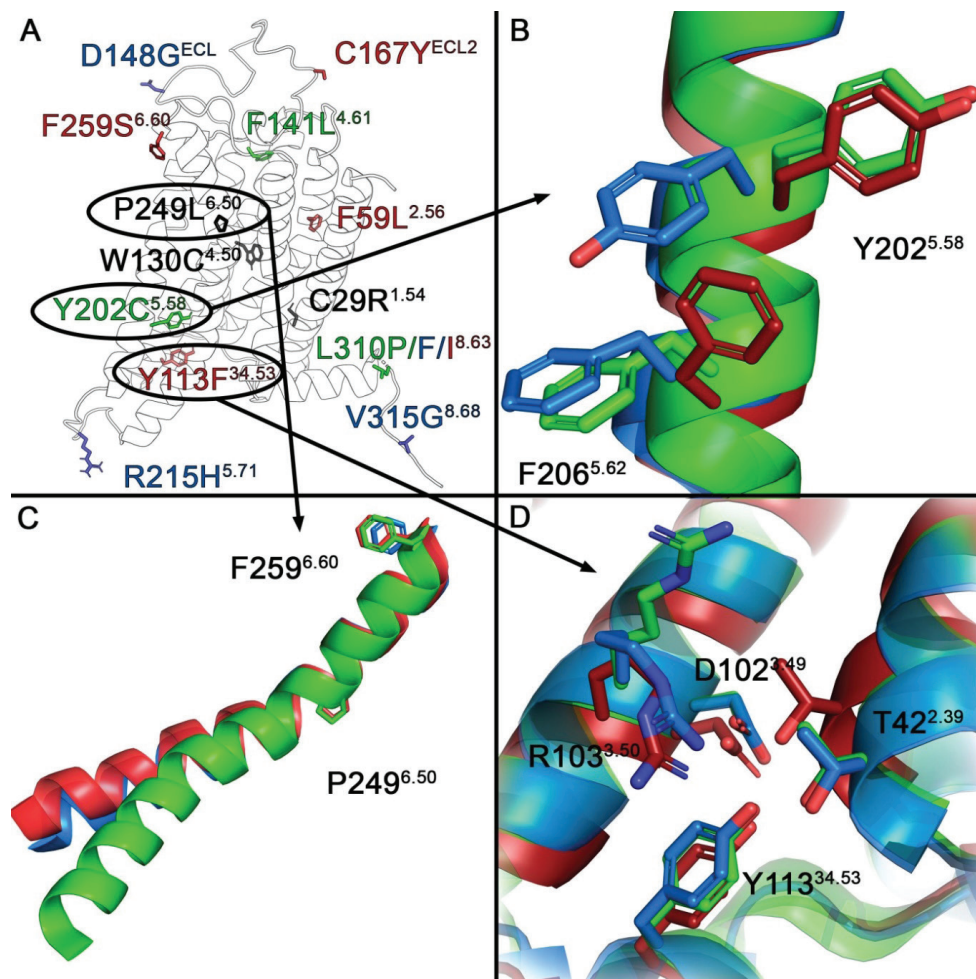
Fig 6. (A) Homology model of the adenosine A_{2B} receptor, showing the mutated residues subject of analysis. Color code is green for constitutively active mutants; black for loss-of-function mutants; red for less active mutants; and blue for no-effect-mutants. Panels (B, C and D) zoom in on selected residues mapped on the respective conformational models (inactive: orange, generated with 3eml; active-like: blue, generated with 2ydv; active: green, generated with 5g53). (B) The CAM $Y202C^{5.58}$ is located on part of an activation switch, which moves outwards to the membrane in the active-like structure and again inwards in the active structure, simultaneously $F206^{5.62}$ moves out in the active-like structure but remains in this position in the active structure. (C) The loss-of-function mutant $P249L^{6.50}$ disturbs a hinge region in the outward movement of TM6 observed upon receptor activation. (D) The less active mutant $Y113F^{34.53}$ is proposed to prevent the outward movement of $R103^{3.50}$ observed upon receptor activation.

Constitutively active mutants

Mutant receptors $F141L^{4.61}$, $Y202C^{5.58}$ and $L310P^{8.63}$, identified from skin cutaneous melanoma, liver hepatocellular carcinoma, and colon adenocarcinoma, respectively, showed increased constitutive activities compared to the wild-type receptor (Fig. 3 and Table 1). These CAMs are located at TM4, TM5, and helix 8. It is known that

TM4, TM5, ECL2, and helix 8 of the receptor are involved in receptor activation[25,60]. Upon activation, a coupling between movements of ECL2 and TM5 has been observed as well as a rearrangement in the H-bond networks connecting ECL2 with the extracellular ends of TM4, TM5 and TM6[61]. Among the CAMs in this study, constitutive activities of F141L[4.61] and L310P[8.63] were reduced to wild-type level by inverse agonist ZM241385 with pIC$_{50}$ values of 7.43 and 7.49 (Fig. 4). These values are comparable to reference pK$_i$ values for wild-type adenosine A$_{2B}$ receptor in the cAMP assay[62,63]. However, ZM241385 reduced the high constitutive activity of Y202C[5.58] roughly by half (Fig. 4), demonstrating that adenosine A$_{2B}$ receptor is locked in an active conformation by mutation Y202C[5.58], but not by F141L[4.61] or L310P[8.63]. Concordantly, PSB603 did not significantly inhibit the Y202C[5.58] mutant in a Schild-plot analysis at concentrations that inhibited the other two mutants (Fig. 5). Such "locked-in" receptor mutants have been described before, e.g. for the adenosine A$_1$ receptor[64]. An altered potency value of NECA was observed on these CAMs compared to wild-type, while this difference was absent with BAY 60-6583 (Table 3). Similar results have been reported on adenosine A$_{2A}$ receptor[65]. The difference in receptor activation among wild-type and mutant receptors in response to CGS21680 (a ribose agonist) was not seen upon the activation mediated by LUF5834 (a non-ribose agonist).

F141L[4.61], located at the membrane-helix interface on the top of TM4 and at the start of ECL2 (Figure 6A), has been reported to increase affinity and potency for NECA and BAY 60-6583 in a random mutagenesis study[28]. Similar results were observed here (Fig. 3C and Table 1), while no significant changes on affinity of PSB603 were observed (Fig. 5E). As residue F141[4.61] is not located at the binding pocket of either NECA or BAY 60-6583[66] but still able to affect agonist activation, it is therefore likely that this mutation plays a role in the stabilization of ECL2[28] and also participates in the entry conformation of the agonist binding pocket. Interestingly, opposite pharmacological effects were observed between F259S[6.60] and F141L[4.61], both situated at a structurally similar position (Figure 3A, 3C, 6A and Table 1).

Three mutations were identified at "hotspot" L310[8.63]. L310P showed increased constitutive activity and potency on NECA, while L310F and L310I did not dramatically alter receptor functionality. Interestingly, the introduction of a proline mutation has a high impact as it may introduce a kink in helix 8, and thus potentially affect G protein coupling.

Residue Y5.58 is completely conserved among adenosine receptors and 88% conserved among class A GPCRs. Mutant receptor Y202C[5.58] showed the highest constitutive activity and reduced potency and efficacy of NECA compared to the wild-type receptor (Figure 3C and Table 1), indicating that maximal G protein coupling and signaling were decreased but consistently present. The residues Y[7.53] (part of NPxxY motif) and Y[5.58] were previously proposed as a possible activation switch for adenosine receptors, based on conformational changes observed in the agonist bound crystal structure[67] and their high conservation in class A GPCRs[51]. Comparing

the inactive and active structures of adenosine A_{2A} receptor (PDB: 3EML, 2YDV and 5G53), we noticed the side chain of Y197[5.58] stretched into the membrane in the active structures[67–69]. As a consequence, TM5 and TM6 moved closer together enabling access of the G protein (Figure 6B). Upon G protein binding, Y197[5.58] moves back into the receptor interior, filling up a space previously occupied by L235[6.37] and I238[6.40]. Additionally, the constitutive activities of the mutated receptors Y202C and Y202S[28] are high, but not higher than the maximum observed effect of agonist bound receptors, further providing evidence that this residue is key for controlled modulation of the receptor.

Conclusion

In conclusion, 15 cancer-related somatic mutations on the adenosine A_{2B} receptor were retrieved from TCGA and characterized in a robust yeast system. We identified mutations that dramatically change receptor activation and function. Mutations in the adenosine A_{2B} receptor showing altered function in the yeast system may also be associated with cell proliferation and migration in cancer cell lines, and involved in cancer progression. Further studies in mammalian and/or cancer cell lines are warranted starting from the results in the present study to investigate mutation-mediated receptor activation and inactivation in a pathological setting. Since adenosine is an anti-inflammatory stimulus in the tumor microenvironment[10], both wild-type and mutant adenosine receptors may play an important, yet largely undefined role in cancer progression, which eventually may be modulated with medicinal products.

References

1. Vassilatis, D. K. *et al.* The G protein-coupled receptor repertoires of human and mouse. *Proc. Natl. Acad. Sci.* **100**, 4903–4908 (2003).
2. Fredriksson, R., Lagerström, M. C., Lundin, L.-G. & Schiöth, H. B. The G-protein-coupled receptors in the human genome form five main families. Phylogenetic analysis, paralogon groups, and fingerprints. *Mol. Pharmacol.* **63**, 1256–72 (2003).
3. Lappano, R. & Maggiolini, M. GPCRs and cancer. *Acta Pharmacol. Sin.* **33**, 351–362 (2012).
4. Watson, I. R., Takahashi, K., Futreal, P. A. & Chin, L. Emerging patterns of somatic mutations in cancer. *Nat. Rev. Genet.* **14**, 703–18 (2013).
5. Kan, Z. *et al.* Diverse somatic mutation patterns and pathway alterations in human cancers. *Nature* **466**, 869–73 (2010).
6. Fredholm, B. B. Adenosine receptors as drug targets. *Exp. Cell Res.* **316**, 1284–1288 (2010).
7. Fredholm, B. B., Irenius, E., Kull, B. & Schulte, G. Comparison of the potency of adenosine as an agonist at human adenosine receptors expressed in Chinese hamster ovary cells. *Biochem. Pharmacol.* **61**, 443–8 (2001).
8. M. Candeias, S. & S. Gaipl, U. The Immune System in Cancer Prevention, Development and Therapy. *Anticancer. Agents Med. Chem.* **16**, 101–107 (2015).
9. Antonioli, L. *et al.* Adenosine and inflammation: what's new on the horizon? *Drug Discov. Today* **19**, 1051–1068 (2014).
10. Gessi, S., Merighi, S., Sacchetto, V., Simioni, C. & Borea, P. A. Adenosine receptors and cancer. *Biochim. Biophys. Acta* **1808**, 1400–1412 (2011).
11. Fredholm, B. B., IJzerman, A. P., Jacobson, K. a, Klotz, K. N. & Linden, J. International Union of Pharmacology. XXV. Nomenclature and classification of adenosine receptors. *Pharmacol. Rev.* **53**, 527–52 (2001).
12. Feoktistov, I. *et al.* Differential expression of adenosine receptors in human endothelial cells: role of A_{2B} receptors in angiogenic factor regulation. *Circ. Res.* **90**, 531–8 (2002).
13. Merighi, S. *et al.* Caffeine Inhibits Adenosine-Induced Accumulation of Hypoxia-Inducible Factor-1α, Vascular Endothelial Growth Factor, and Interleukin-8 Expression in Hypoxic Human Colon Cancer Cells. *Mol. Pharmacol.* **72**, 395–406 (2007).
14. Zeng, D. *et al.* Expression and function of A_{2B} adenosine receptors in the U87MG tumor cells. *Drug Dev. Res.* **58**,

405–411 (2003).

15. Merighi, S. *et al.* Pharmacological and biochemical characterization of adenosine receptors in the human malignant melanoma A375 cell line. *Br. J. Pharmacol.* **134**, 1215–1226 (2001).

16. Ryzhov, S. *et al.* Host A$_{2B}$ receptors promote carcinoma growth. *Neoplasia* **10**, 987–995 (2008).

17. Sorrentino, C., Miele, L., Porta, A., Pinto, A. & Morello, S. Myeloid-derived suppressor cells contribute to A$_{2B}$ adenosine receptor-induced VEGF production and angiogenesis in a mouse melanoma model. *Oncotarget* **6**, 27478–27489 (2015).

18. Vecchio, E. a. *et al.* Ligand-Independent Adenosine A$_{2B}$ Receptor Constitutive Activity as a Promoter of Prostate Cancer Cell Proliferation. *J. Pharmacol. Exp. Ther.* **357**, 36–44 (2016).

19. Kasama, H. *et al.* Adenosine A$_{2b}$ receptor promotes progression of human oral cancer. *BMC Cancer* **15**, 563-575 (2015).

20. Mittal, D. *et al.* Adenosine 2B Receptor Expression on Cancer Cells Promotes Metastasis. *Cancer Res.* **76**, 4372–4382 (2016).

21. Bieber, D., Lorenz, K., Yadav, R. & Klotz, K.-N. A$_{2B}$ adenosine receptors mediate an inhibition of ERK1/2 phosphorylation in the breast cancer cell line MDA-MB-231. *Naunyn-Schmiedebergs Arch Pharmacol* **377**, 1–98 (2008).

22. Zhou, Y. *et al.* The adenosine A$_{2b}$ receptor promotes tumor progression of bladder urothelial carcinoma by enhancing MAPK signaling pathway. *Oncotarget* **8**, 48755–48768 (2017).

23. Sepúlveda, C., Palomo, I. & Fuentes, E. Role of adenosine A$_{2b}$ receptor overexpression in tumor progression. *Life Sci.* **166**, 92–99 (2016).

24. Allard, B., Beavis, P. A., Darcy, P. K. & Stagg, J. Immunosuppressive activities of adenosine in cancer. *Curr. Opin. Pharmacol.* **29**, 7–16 (2016).

25. Liu, R., Nahon, D., le Roy, B., Lenselink, E. B. & IJzerman, A. P. Scanning mutagenesis in a yeast system delineates the role of the NPxxY(x)5,6F motif and helix 8 of the adenosine A$_{2B}$ receptor in G protein coupling. *Biochem. Pharmacol.* **95**, 290–300 (2015).

26. Peeters, M. C. *et al.* GPCR structure and activation: an essential role for the first extracellular loop in activating the adenosine A$_{2B}$ receptor. *FASEB J.* **25**, 632–43 (2011).

27. Peeters, M. C. *et al.* Domains for activation and inactivation in G protein-coupled receptors--a mutational analysis of constitutive activity of the adenosine A$_{2B}$ receptor. *Biochem. Pharmacol.* **92**, 348–57 (2014).

28. Peeters, M. C., Li, Q., van Westen, G. J. P. & IJzerman, A. P. Three 'hotspots' important for adenosine A$_{2B}$ receptor activation: a mutational analysis of transmembrane domains 4 and 5 and the second extracellular loop. *Purinergic Signal.* **8**, 23–38 (2012).

29. Leff, P. The two-state model of receptor activation. *Trends Pharmacol. Sci.* **16**, 89–97 (1995).

30. Weinstein, J. N. *et al.* The Cancer Genome Atlas Pan-Cancer analysis project. *Nat. Genet.* **45**, 1113–1120 (2013).

31. *Broad Institute TCGA Genome Data Analysis Center (2016): Analysis-ready standardized TCGA data from Broad GDAC Firehose stddata_2015_08_21 run. Broad Institute of MIT and Harvard.* (2016). doi:10.7908/C18W3CNQ

32. The 1000 Genomes Project Consortium. A global reference for human genetic variation. *Nature* **526**, 68–74 (2015).

33. UniProt: the universal protein knowledgebase. *Nucleic Acids Res.* **45**, D158–D169 (2017).

34. Ballesteros, J. A. & Weinstein, H. Integrated methods for the construction of three-dimensional models and computational probing of structure-function relations in G protein-coupled receptors. in *Methods in Neurosciences* **25**, 366–428 (1995).

35. Isberg, V. *et al.* GPCRdb: an information system for G protein-coupled receptors. *Nucleic Acids Res.* **44**, D356–D364 (2016).

36. Dowell, S. J. & Brown, A. J. Yeast Assays for G Protein-Coupled Receptors. *Methods in molecular biology (Clifton, N.J.)* (ed. Filizola, M.) **552**, 213–229 (Springer New York, 2009).

37. Gietz, R. D. & Schiestl, R. H. Quick and easy yeast transformation using the LiAc/SS carrier DNA/PEG method. *Nat. Protoc.* **2**, 35–37 (2007).

38. Eckle, T. *et al.* Cardioprotection by Ecto-5′-Nucleotidase (CD73) and A$_{2B}$ Adenosine Receptors. *Circulation* **115**, 1581–1590 (2007).

39. Li, Q. *et al.* ZM241385, DPCPX, MRS1706 Are Inverse Agonists with Different Relative Intrinsic Efficacies on Constitutively Active Mutants of the Human Adenosine A$_{2B}$ Receptor. *J. Pharmacol. Exp. Ther.* **320**, 637–645 (2007).

40. Guo, Y., Cheng, D., Lee, T. Y., Wang, J. & Hsing, I. New Immunoassay Platform Utilizing Yeast Surface Display and Direct Cell Counting. *Anal. Chem.* **82**, 9601–9605 (2010).

41. Rodríguez, D., Bello, X. & Gutiérrez-De-Terán, H. Molecular modelling of G protein-coupled receptors through the web. *Mol. Inform.* **31**, 334–341 (2012).

42. Esguerra, M., Siretskiy, A., Bello, X., Sallander, J. & Gutiérrez-de-Terán, H. GPCR-ModSim: A comprehensive web based solution for modeling G-protein coupled receptors. *Nucleic Acids Res.* **44**, W455–W462 (2016).

43. Webb, B. & Sali, A. Comparative Protein Structure Modeling Using MODELLER. *Curr. Protoc. Bioinforma.* **47**, 5.6.1-5.6.32 (2014).

44. Stoy, H. & Gurevich, V. V. How genetic errors in GPCRs affect their function: Possible therapeutic strategies. *Genes Dis.* **2**, 108–132 (2015).

45. Sodhi, A., Montaner, S. & Gutkind, J. S. Viral hijacking of G-protein-coupled-receptor signalling networks. *Nat. Rev. Mol. Cell Biol.* **5**, 998–1012 (2004).

46. Bar-Shavit, R. *et al.* G Protein-Coupled Receptors in Cancer. *Int. J. Mol. Sci.* **17**, 1320 (2016).

47. O'Hayre, M. *et al.* The emerging mutational landscape of G proteins and G-protein-coupled receptors in cancer. *Nat. Rev. Cancer* **13**, 412–24 (2013).

48. Beukers, M. W. *et al.* Random Mutagenesis of the Human Adenosine A$_{2B}$ Receptor Followed by Growth Selection in Yeast. Identification of Constitutively Active and Gain of Function Mutations. *Mol. Pharmacol.* **65**, 702–710 (2004).

49. Garcia-Perez, J. *et al.* Allosteric Model of Maraviroc Binding to CC Chemokine Receptor 5 (CCR5). *J. Biol. Chem.* **286**, 33409–33421 (2011).

50. Rodríguez, D., Piñeiro, A. & Gutiérrez-de-Terán, H. Molecular Dynamics Simulations Reveal Insights into Key Structural Elements of Adenosine Receptors. *Biochemistry* **50**, 4194–4208 (2011).

51. Jespers, W. *et al.* Structural mapping of adenosine receptor mutations: ligand binding and signaling mechanisms. *Trends Pharmacol. Sci.* **39**, 75–89 (2017).

52. Warne, T. *et al.* Structure of a β$_1$-adrenergic G-protein-coupled receptor. *Nature* **454**, 486–491 (2008).

53. Mariani, R. *et al.* CCR2-64I polymorphism is not associated with altered CCR5 expression or coreceptor function. *J. Virol.* **73**, 2450–9 (1999).

54. Saita, Y. *et al.* Structural Basis for the Interaction of CCR5 with a Small Molecule, Functionally Selective CCR5 Agonist. *J. Immunol.* **177**, 3116–3122 (2006).

55. Deupi, X. *et al.* Structural Models of Class A G Protein-Coupled Receptors as a Tool for Drug Design: Insights on Transmembrane Bundle Plasticity. *Curr. Top. Med. Chem.* **7**, 991–998 (2007).

4

56. Boulais, P. E., Escher, E. & Leduc, R. Analysis by substituted cysteine scanning mutagenesis of the fourth transmembrane domain of the CXCR4 receptor in its inactive and active state. *Biochem. Pharmacol.* **85**, 541–550 (2013).

57. Fan, Z.-C. & Tao, Y.-X. Functional characterization and pharmacological rescue of melanocortin-4 receptor mutations identified from obese patients. *J. Cell. Mol. Med.* **13**, 3268–3282 (2009).

58. Palczewski, K. *et al.* Crystal Structure of Rhodopsin : A G Protein – Coupled Receptor. *Science.* **289**, 739–745 (2000).

59. Visiers, I., Ballesteros, J. A. & Weinstein, H. Three-dimensional representations of G protein-coupled receptor structures and mechanisms. in *Methods in Enzymology* **343**, 329–371 (2002).

60. Peeters, M. C., van Westen, G. J. P., Li, Q. & IJzerman, A. P. Importance of the extracellular loops in G protein-coupled receptors for ligand recognition and receptor activation. *Trends Pharmacol. Sci.* **32**, 35–42 (2011).

61. Ahuja, S. *et al.* Helix movement is coupled to displacement of the second extracellular loop in rhodopsin activation. *Nat. Struct. Mol. Biol.* **16**, 168–175 (2009).

62. Ongini, E., Dionisotti, S., Gessi, S., Irenius, E. & Fredholm, B. B. Comparison of CGS 15943, ZM 241385 and SCH 58261 as antagonists at human adenosine receptors. *Naunyn. Schmiedebergs. Arch. Pharmacol.* **359**, 7–10 (1999).

63. de Zwart, M. *et al.* Potent antagonists for the human adenosine A_{2B} receptor. Derivatives of the triazolotriazine adenosine receptor antagonist ZM241385 with high affinity. *Drug Dev. Res.* **48**, 95–103 (1999).

64. de Ligt, R. A. F., Rivkees, S. A., Lorenzen, A., Leurs, R. & IJzerman, A. P. A "locked-on," constitutively active mutant of the adenosine A_1 receptor. *Eur. J. Pharmacol.* **510**, 1–8 (2005).

65. Lane, J. R. *et al.* A novel nonribose agonist, LUF5834, engages residues that are distinct from those of adenosine-like ligands to activate the adenosine A_{2B} receptor. *Mol. Pharmacol.* **81**, 475–487 (2012).

66. Sherbiny, F. F., Schiedel, A. C., Maass, A. & Müller, C. E. Homology modelling of the human adenosine A_{2B} receptor based on X-ray structures of bovine rhodopsin, the beta2-adrenergic receptor and the human adenosine A_{2A} receptor. *J Comput Aided Mol Des* **23**, 807–828 (2009).

67. Xu, F. *et al.* Structure of an Agonist-Bound Human A_{2A} Adenosine Receptor. *Science.* **332**, 322–327 (2011).

68. Lebon, G., Edwards, P. C., Leslie, A. G. W. & Tate, C. G. Molecular Determinants of CGS21680 Binding to the Human Adenosine A_{2A} Receptor. *Mol. Pharmacol.* **87**, 907–915 (2015).

69. Liu, W. *et al.* Structural basis for allosteric regulation of GPCRs by sodium ions. *Science.* **337**, 232–236 (2012).

Supplementary Information

Table S1. Expression levels of wild-type and mutant human adenosine A$_{2B}$ receptors. Values are shown as mean ± SD from at least three individual experiments.

Mutation	Expression level (%)	
	Western Blot	Yeast ELISA
Wild-type	100	100
vector	-	-
C167Y^{ECL2}	76 ± 7	36 ± 11
D148G^{ECL2}	86 ± 1	90 ± 36
F259S$^{6.60}$	83 ± 37	66 ± 30
Y113F$^{34.53}$	143 ± 40	101 ± 52
R215H$^{5.71}$	92 ± 49	86 ± 51
C29R$^{1.54}$	123 ± 34	102 ± 22
F59L$^{2.56}$	111 ± 8	76 ± 26
W130C$^{4.50}$	200 ± 53	40 ± 6
F141L$^{4.61}$	58 ± 9	119 ± 20
Y202C$^{5.58}$	126 ± 20	144 ± 38
P249L$^{6.50}$	91 ± 43	179 ± 38
L310P$^{8.63}$	103 ± 14	92 ± 20
L310F$^{8.63}$	109 ± 24	101 ± 39
L310I$^{8.63}$	121 ± 42	124 ± 30
V315G$^{8.68}$	100 ± 16	205 ± 81

Table S2. Additional characterization of wild-type adenosine A$_{2B}$ receptor and mutant receptor V315G$^{8.68}$ in yeast liquid growth assay and ELISA. pEC$_{50}$ and E$_{max}$ values are shown as mean ± SD from three individual experiments, each performed in duplicate. Yeast ELISA values are shown as mean ± SD from four individual experiments.

Mutations	pEC$_{50}$	E$_{max}$	Yeast ELISA
Wild-type	6.84 ± 0.05	100 ± 3	100
V315G$^{8.68}$	7.01 ± 0.05	101 ± 2	102 ± 23
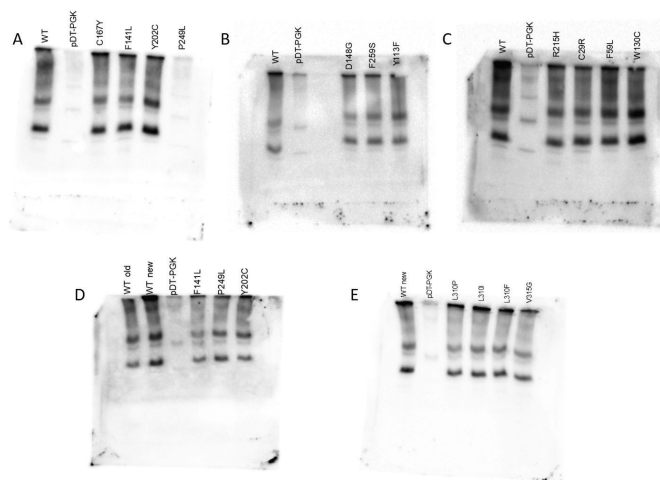
Supplemental Fig. Representative Western blots used in **Fig. 2** for (A) wild-type (WT), vector (pDT-PGK), C167Y, F141L and Y202C, (B) D148G, F259S and Y113F, (C) R215H, C29R, F59L and W130C, (D) P249L and (E) L310P, L310I, L310F and V315G.

Chapter 5

Cancer-related somatic mutations alter adenosine A₁ receptor pharmacology.
- a focus on mutations in the loops and C-terminus.

Abstract

G protein-coupled receptors (GPCRs) are known to be involved in tumor progression and metastasis. The adenosine A_1 receptor (A_1AR) has been detected to be over-expressed in various cancer cell lines. However, the role of A_1AR in tumor development is not yet well characterized. A series of A_1AR mutations were identified in the Cancer Genome Atlas from cancer patient samples. In this study, we have investigated the pharmacology of mutations located outside of the 7-transmembrane domain by using a 'single-GPCR-one-G protein' yeast system. Concentration-growth curves were obtained with the full agonist CPA for 12 mutant receptors and compared to the wild-type hA_1AR. Most mutations located at the extracellular loops (EL) reduced the levels of constitutive activity of the receptor and agonist potency. For mutants at the intracellular loops (IL) of the receptor, an increased constitutive activity was found for mutant receptor L211R[5.69], while a decreased constitutive activity and agonist response were found for mutant receptor L113F[34.51]. Lastly, mutations identified on the C-terminus did not significantly influence the pharmacological function of the receptor. A selection of mutations was also investigated in a mammalian system. Overall, similar effects on receptor activation compared to the yeast system were found with mutations located at the EL, but some contradictory effects were observed for mutations located at the IL. Taken together, this study will enrich the insight of A_1AR receptor structure and function, enlightening the consequences of these mutations in cancer. Ultimately, this may provide potential precision medicine in cancer treatment.

Keywords: G protein-coupled receptors, adenosine A_1 receptor, cancer, mutations, yeast system

Introduction

G protein-coupled receptors (GPCRs) are the largest family of membrane-bound proteins in the human genome with approximately 800 subtypes[1]. They share a common structure of seven-transmembrane helices (TMs) linked by three extracellular loops (ELs) and three intracellular loops (ILs) together with an extracellular N-terminus and an intracellular C-terminus[2]. GPCRs regulate various cellular and physiological effects via responding to a diverse set of endogenous ligands[3]. However, their aberrant activity and expression also contribute to some of the most prevalent human diseases[4].

In preclinical oncology, kinases have been studied as primary focus due to their central roles in the cell cycle[5]. GPCRs, on the other hand, have been relatively under-investigated over the last two decades. Yet, an increasing amount of evidence shows that GPCRs are also prominently involved in all phases of cancer[6]. Additionally, the normal physiological function of GPCRs is often hijacked by malignant cells to survive as well as to invade surrounding tissue and evade the immune system[7]. Moreover, a systematic analysis of somatic mutations in cancer genomes has led to the discovery that GPCRs are mutated in an estimated 20% of all cancers[5]. Combined, these observations warrant a close investigation of the role of GPCRs in cancer.

Adenosine is a ubiquitous purine nucleoside that mediates its physiological effects via the adenosine receptors (ARs); the A$_1$, the A$_{2A}$, the A$_{2B}$, and the A$_3$ receptor. The A$_1$AR and A$_3$AR mainly recruit a G$_i$ protein and inhibit adenylate cyclase, while the A$_{2A}$AR and A$_{2B}$AR stimulate adenylate cyclase through coupling to a G$_s$ protein[8]. It is known that the immune system plays a fundamental and essential role in the defense against cancer, yet the mechanisms have not been fully characterized. Adenosine and ARs have been reported to be involved in the immune response in cancer[9]. Additionally, ARs are expressed diversely in various tumor types[10]. Compared to healthy tissue, adenosine concentrations are increased by more than 50 fold in the hypoxic tumor environment[11]. Therefore, all four subtypes of ARs may be activated in cancer and may play a role in cancer progression.

A$_1$AR has mainly been under investigation as a drug target for pathologies in brain, heart, kidney and fat cells, due to its high expression in these cells/organs[12,13]. Growing evidence suggests that the A$_1$AR is also involved in cancer progression, although its role is not well understood and sometimes observations are inconsistent[13,14]. An increased expression level of the A$_1$AR has been observed in diverse cancer cells[15–17]. In MCF7 breast cancer cells, activation of the A$_1$AR leads to decreased apoptosis and thereby induces tumor growth[17]. In renal cell carcinoma, cell proliferation and migration is inhibited by an A$_1$AR antagonist through the ERK/JNK signaling pathway[15]. Conversely, the stimulation of A$_1$AR significantly decreases tumor cell proliferation in CW2 colonic cell tumor and glioblastomas[18,19]. An RNA interference study on breast cancer cells indicates that depletion of A$_1$AR results in more apoptosis[16]. Taken together, it appears that A$_1$AR activation induces both

anti- and pro-tumoral effects in cancer development[11]. Various mutations have been identified on A_1AR from patient samples with different cancer types[20]. Mutations in A_1AR are known to alter the receptor-ligand interaction, receptor constitutive activity and agonist-mediated receptor activation[21]. Notably, these function-altering mutations can be located all over the protein, including the TMs, ELs and ILs[22]. Based on the altered constitutive activity independent of an agonist, mutant receptors with increased level of activation are referred to as constitutively active mutants (CAMs), while those with lowered level are named constitutively inactive mutants (CIMs)[23].

In the present study, 12 mutations, which were located in ELs, ILs, and C-terminus of the A_1AR, were selected from cancer patients using a bioinformatics approach. These mutant receptors were tested in an *S. cerevisiae* strain to study the effect of them on receptor activation. Subsequently, some mutant receptors were further investigated for their effect on ligand binding and receptor activation in a mammalian system. Based on the pharmacological effects of these mutant receptors, we identified 1 CAM and 7 CIMs. In addition, we found 1 loss-of-function mutant (LFM) and 3 mutant receptors, which were functionally indistinguishable from the wild-type hA_1AR (no effect mutants, NEMs).

Materials and methods

Data mining

Data was downloaded from The Cancer Genome Atlas (TCGA, version August 8th 2015) via the Firehose tool[24]. MutSig 2.0 data was extracted, but MutSig 2CV was used when the former was not available (the case for colon adenocarcinoma, acute myeloid leukemia, ovarian serous cystadenocarcinoma, rectum adenocarcinoma). In parallel natural variance data was downloaded from Uniprot (Index of Protein Altering Variants, version November 11th 2015)[25]. Somatic mutations were selected from the sequence data and filters were applied to only select data for the A_1AR (Uniprot identifier P30542). The GPCRdb alignment tool was used to assign Ballesteros-Weinstein numbers[26,27] to the positions through which a selection could be made for non-TM domain positions.

Materials

The MMY24 strain and the *S. cerevisiae* expression vectors, the pDT-PGK plasmid and the pDT-PGK_hA_1AR plasmid (i.e. expressing by coding for the wild-type hA_1AR) were kindly provided by Dr. Simon Dowell from GSK (Stevenage, UK). The QuikChange II® Site-Directed Mutagenesis Kit was purchased from Agilent Technologies, which includes XL10-Gold ultracompetent cells (Amstelveen, the Netherlands). The QIAprep mini plasmid purification kit and QIAGEN® plasmid midi kit were purchased from QIAGEN (Amsterdam, the Netherlands). Adenosine deaminase (ADA), 1,4-dithiothreitol (DTT), 8-cyclopentyl-1,3-dipropylxanthine

(DPCPX) and 3-amino-[1,2,4]-triazole (3-AT) were purchased from Sigma-Aldrich (Zwijndrecht, the Netherlands). N[6]-cyclopentyladenosine (CPA) was purchased from Santa Cruz Biotechnology (Heidelberg, Germany). Radioligand 1,3-[^{3}H]-dipropyl-8-cyclopentylxanthine ([^{3}H]DPCPX, specific activity of 120 Ci × mmol^{-1}) was purchased from ARC Inc. (St. Louis, MO). Bicinchoninic acid (BCA) and BCA protein assay reagent were obtained from Pierce Chemical Company (Rockford, IL, USA). [^{35}S]-Guanosine 5'-(γ-thio)triphosphate ([^{35}S]GTPγS, specific activity 1250 Ci × mmol^{-1}) was purchased from PerkinElmer, Inc. (Waltham, MA, USA). Rabbit anti-HA antibody (71-5500) was purchased from Thermo Fisher Scientific (Waltham, MA, USA). Goat anti-rabbit IgG Fc (Alexa Fluor® 647) was purchased from Abcam (Cambridge, UK).

Generation of hA$_1$AR mutations

Mutant hA$_1$ARs were generated by polymerase chain reaction (PCR) mutagenesis as previously described[28]. pDT-PGK_hA$_1$AR or pcDNA3.1(+)_hA$_1$AR with N-terminal HA tag was used as the template[21,29]. Primers for mutant receptors were designed by the QuikChange Primer Design Program of Agilent Technologies (Santa Clara, CA, USA) and primers were obtained from Eurogentec (Maastricht, The Netherlands). All DNA sequences were verified by Sanger sequencing at LGTC (Leiden, The Netherlands).

Transformation in MMY24 S. cerevisiae strain

The plasmids, pDT-PGK_hA$_1$AR, containing either wild-type or mutant hA$_1$AR were transformed into a MMY24 *S. cerevisiae* strain using the Lithium-Acetate procedure[30].

Liquid growth assay

To characterize the mutant hA$_1$ARs, concentration-growth curves were obtained from a liquid growth assay in 96-well plates as previously described[21]. Briefly, selective medium lacking uracil and leucine (YNB-UL, 1ml) was inoculated with yeast cells expressing wild-type or mutant hA$_1$AR. After overnight incubation at 30 °C, the cultures were diluted to 40,000 cells/ml (OD$_{600}$ ≈ 0.02) in selective medium without histidine (YNB-ULH).Various concentrations of ligands (2 *μL*), yeast cells (50 *μL*) and YNB-ULH medium containing 7 mM 3-AT and 0.8 IU/ml ADA (150 *μL*) were added to each well. Then, the 96-well plate was incubated at 30 °C for 35 h in a Genios plate reader while shaking for 1 min at 300 rpm every 10 min.

Cell culture, transient transfection and membrane preparation

Chinese hamster ovary (CHO) cells were cultured in Dulbecco's modified Eagle's medium/Ham's F12 (1:1, DMEM/F12) containing 10% bovine calf serum, streptomycin (50 μg/mL) and penicillin (50 IU/mL) at 37 °C in 5% CO$_2$. The cells were subcultured twice weekly at a ratio of 1:30. 24 h before transfection, cells were seeded in 10-cm culture dishes containing 10 mL culture medium to achieve 50-60% confluency. Cells were then transfected with plasmid DNA (10 μg/dish) by the PEI method with a PEI:DNA ratio of 3:1[31]. 24 h after transfection, the medium was refreshed by 10

mL fresh culture medium. After an additional 24 h incubation at 37 °C in 5% CO_2, cells were collected and membranes were prepared as described previously[32]. Membranes were then aliquoted in 250 or 100 µL and stored at -80 °C till further use. Membrane protein concentrations were measured by the BCA method[33].

Western blot analysis

Membranes containing 8.5 µg protein were denatured in 1x Laemmli sample buffer before loading. Samples were separated on a 12.5% SDS/PAGE gel and then electro-blotted onto polyvinylidene fluoride (PVDF) membranes via Bio-Rad Trans-blot® Turbo™ transfer system. After blocking with 5% BSA in TBST (0.05% Tween 20 in Tris-buffered saline), the membranes were incubated with rabbit anti-HA tag primary antibody (1:2000, Thermo Fisher Scientific) in TBST containing 1% BSA at 4 °C for overnight. The membranes were then washed three times in TBST and incubated with goat anti-rabbit IgG Fc (1:7500, Alexa Fluor® 647) in TBST containing 1% BSA for 1 hour at room temperature, followed by washing twice in TBST and once in TBS. Images of the blots were taken with a ChemiDoc MP imaging system (Hercules, CA, USA) using a Cy5 filter.

Radioligand displacement assay

The displacement assays were performed as described previously[34]. Briefly, experiments were performed in a total volume of 100 µL, consisting of 25 µL cell membranes (10 – 25 µg protein to achieve an assay window of approximately 1500 DPM), 25 µL of radioligand [³H]DPCPX with a final concentration of ~1.6 nM, 25 µL of assay buffer (50 mM Tris-HCl, pH 7.4) and 25 µL of DPCPX or CPA in 6 or 10 increasing concentrations (final concentrations of 10^{-11} to 10^{-6} M and 10^{-10} to 10^{-5} M, respectively) in assay buffer, and incubated for 1h at 25 °C. Nonspecific binding was determined in the presence of 100 µM CPA and represented less than 10% of the total binding. For homologous competition assays, radioligand displacement experiments were done in the presence of three concentrations of [³H]DPCPX (final concentrations of ~1.6 nM, 4.5 nM and 10 nM) and 6 increasing concentrations of DPCPX (final concentration of 10^{-11} to 10^{-6} M). After incubation, reactions were terminated by rapid vacuum filtration through GF/B filter plates (PerkinElmer, Groningen, Netherlands) using a Perkin Elmer Filtermate-harvester. Filter plates were subsequently washed ten times with ice-cold buffer (50 mM Tris-HCl, pH 7.4). After drying the filter plates at 55 °C for 30 min, the filter-bound radioactivity was determined by scintillation spectrometry using a Microbeta2® 2450 microplate counter (PerkinElmer).

[³⁵S]GTPγS binding assay

[³⁵S]GTPγS binding assays were adapted from a previously reported method[34]. Experiments were performed in a total volume of 80 µL assay buffer (50 mM Tris-HCl buffer, 5 mM $MgCl_2$, 1 mM EDTA, 100 mM NaCl, 0.05% BSA and 1 mM DTT pH 7.4 supplemented with 10 **µM** GDP, 10 µg saponin), consisting of 20 µL membranes (15 µg protein), 20 µL of CPA in 9 increasing concentrations (final concentrations

of 10^{-11} to 10^{-6} M) or 20 µL of DPCPX (final concentrations of 10^{-11} to 10^{-6} M) in 9 increasing concentrations combined with a fixed concentration (EC$_{80}$ for wild-type or mutant hA$_1$ARs) of CPA, and incubated for 30 min at 4 °C. Then 20 µL of [^{35}S]GTPγS (final concentration of 0.3 nM) was added and followed by 90 min incubation at 25 °C. Incubation was terminated and filter-bound activity was determined as described above.

Modelling

Figures were created based on the experimentally determined structures for the A$_1$AR crystal structures, with PDB codes 5UEN[35] for the inactive and 6D9H[36] for the fully active structure. DPCPX and CPA were manually docked based on high similarity with the co-crystallized ligands in the respective structures, and figures were generated using the PyMOL Molecular Graphics System version 2.0 (Schrödinger, LLC., USA).

Data analysis

All experimental data were analyzed by GraphPad Prism 7.0 software (GraphPad Software Inc., San Diego, CA, USA). Liquid growth assays and [^{35}S]GTPγS binding assay were analyzed by non-linear regression using a "log (agonist or inhibitor) vs. response (three parameters)" model to obtain potency (EC$_{50}$), inhibitory potency (IC$_{50}$) and efficacy (E$_{max}$) values. Homologous competition assays were analyzed by non-linear regression using a "one-site homologous" model to obtain pK$_D$ and B$_{max}$ values. Radioligand displacement curves were analyzed by non-linear regression using a "one site - IC50" or "two site – IC50" model to obtain pIC$_{50}$ values. pK$_i$ values were calculated from pIC$_{50}$ values using the Cheng-Prusoff equation[37].

Results

Data mining

Mutation data from cancer patient isolates of a selection of cancer types, i.e. breast invasive carcinoma, colon adenocarcinoma, lung adenocarcinoma, lung squamous cell carcinoma, lymphoid neoplasm diffuse large B-cell lymphoma and rectum adenocarcinoma, were obtained by data mining the TCGA database on August 8th 2015. This resulted in a selection of 27 somatic point mutations for the hA$_1$AR out of a total of 48 cancer-related mutations of hA$_1$AR. After assigning Ballesteros Weinstein numbers to the positions by using the GPCRdb alignment tool, 12 mutations located outside the 7-TM domains were selected for this study (Table 1). Five mutations were located at the second EL, four at the IL and three at the C-terminus of hA$_1$AR, which are shown in the snake-plot in Figure 1A.

Table 1. List of cancer-related somatic mutations identified from different cancer types.

Mutations	Cancer types
N148S^{EL2}	Lung adenocarcinoma
A151V ^{EL2}	Lymphoid neoplasm diffuse large B-cell lymphoma
V152L ^{EL2}	Lung adenocarcinoma
E170G$^{45.51}$	Colon adenocarcinoma
M177V$^{5.37}$	Lung adenocarcinoma
L113F$^{34.51}$	Lung squamous cell carcinoma
L211R$^{5.69}$	Lung adenocarcinoma
V215L^{IL3}	Lung adenocarcinoma
D221N^{IL3}	Lung squamous cell carcinoma
H306N$^{8.61}$	Colon adenocarcinoma
R308H$^{8.63}$	Lung adenocarcinoma
I315V^{C-term}	Lung squamous cell carcinoma

Constitutive activity of mutant hA$_1$ARs

To characterize the effect of the cancer-related mutations on the constitutive activity of the receptor, yeast growth assays were performed in the absence of an agonist. Results are shown in Figure 1B and 1C. In response to increasing concentrations of 3-AT yeast cell growth was dose-dependently decreased for yeast cells both in the presence and absence of wild-type hA$_1$AR (Figure 1B). The presence of hA$_1$AR resulted in a lower apparent potency of 3-AT. At a concentration of 4 mM 3-AT, the two curves showed the largest difference in growth as yeast cells with hA$_1$AR were still able to grow, while yeast cells transformed with empty vector hardly grew. Importantly, in this system mutant receptors with increased constitutive activity, i.e. CAMs, would show a larger response than wild-type hA$_1$AR, while mutant receptor with decreased constitutive activity, i.e. CIMs, would show a response in between wild-type hA$_1$AR and empty vector at this concentration of 3-AT (Figure 1B).

Cancer-related mutations had various effects on the constitutive activities of the hA$_1$AR (Figure 1C). All 5 mutants within the EL showed decreased constitutive activity compared to the wild-type hA$_1$AR. Interestingly, the 4 mutations located at the IL of the receptor showed a large variance in their constitutive activities. Specifically, mutant receptor L113F$^{34.51}$, located at IL2, showed a significantly decreased constitutive activity. In contrast, increased constitutive activity was observed for mutant receptor L211R$^{5.69}$ and V215L^{IL3}, where the increase on V215L^{IL3} was not significant. Mutant receptors D221N^{IL3} and R308H$^{8.63}$, located at IL3 and the C-terminus respectively, did not behave significantly different from wild-type hA$_1$AR. Two other mutations located at the C-terminus hA$_1$AR, H306N$^{8.61}$ and I315V^{C-term}, were constitutively inactive.
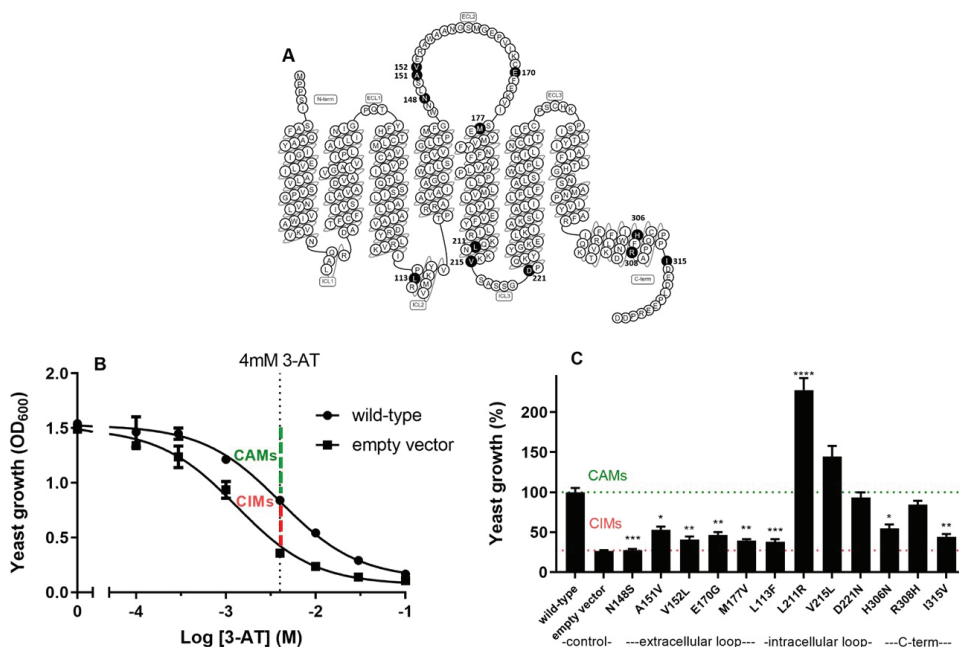
Figure 1. (A) Snake-plot of the wild-type hA$_1$AR. Mutated residues are marked in black. (B) Concentration-growth curves of yeast in the absence (empty vector) or presence of wild-type hA$_1$AR. A concentration of 4 mM 3-AT (dotted line) resulted in the largest assay window to detect either CAMs or CIMs. Specifically, mutant receptors with increased constitutive activity (CAMs) would show a higher growth level than wild-type hA$_1$AR (assay window depicted as green dotted line), while those with decreased constitutive activity (CIMs) would show a growth level lower than wild-type hA$_1$AR but higher than empty vector (assay window depicted as red dotted line). Combined graph is shown as mean ± SEM from three individual experiments performed in duplicate. (C) Constitutive activity of wild-type and 12 mutant hA$_1$ARs in presence of 4 mM 3-AT. Yeast growth in presence of wild-type hA$_1$AR was set to 100% (green dotted line) and the background of the selection medium was set to 0%. The yeast growth of empty vector is 26% (red dotted line). The bar graph is the combined result of three independent experiments performed in quadruplicate.
* $p < 0.05$; ** $p < 0.01$; *** $p < 0.001$; **** $p < 0.0001$ compared to wild-type hA$_1$AR, determined by using one-way ANOVA with Dunnett's post-test.

Characterization of receptor activation of mutant hA$_1$ARs

To further characterize the effects of cancer-related mutations on receptor activation concentration-growth curves were obtained for all 12 mutants hA$_1$ARs in response to the selective hA$_1$AR full agonist CPA (Figure 2 and Table 2). In this yeast system, wild-type hA$_1$AR showed a pEC$_{50}$ value of 9.29 ± 0.07 and a maximum effect (E$_{max}$) of 5.37 ± 0.53 for CPA, and a constitutive activation level of 1.00 ± 0.04. Over half of the mutant receptors showed a decreased constitutive activity, but similar potency and efficacy values for CPA as at the wild-type hA$_1$AR (Figure 2 – dark blue curves and Table 2).

Within the mutant receptors of the EL, the largest change in receptor function was observed for mutant receptor E170G[45.51], which showed no response to CPA

(Figure 2A). Other mutations in the EL did not lead to such severe changes in the pharmacological behavior of the receptor, i.e. these mutant receptors could all be activated by CPA to reach a similar E_{max} as at wild-type hA_1AR with up to 10-fold decreased potency values. Among them, mutant receptors N148S^{EL2}, V152L^{EL2} and M177V$^{5.37}$ showed significantly reduced pEC_{50} values of 8.54 ± 0.08, 8.80 ± 0.06 and 8.32 ± 0.06 (Table 2).

Mutant receptors located at the IL showed a more divergent behavior, unlike mutant receptors located at the EL (Figure 2B and Table 2). Mutant receptor L113F$^{34.51}$ showed a reduced basal activity and activation in response to CPA with both a decreased pEC_{50} value of 8.43 ± 0.13 and E_{max} value of 2.45 ± 0.30. Mutant receptors V215L^{IL3} and D221N^{IL3} did not show altered receptor function with similar dose – growth curves for CPA as on wild-type hA_1AR. The mutant receptor with increased constitutive activity, L211R$^{5.69}$ showed a similar potency value of 9.48 ± 0.14 and similar efficacy value of 5.33 ± 0.66 compared to wild-type hA_1AR. Of note, its high constitutive activity could be reduced by the inverse agonist, DPCPX with a pIC_{50} of 8.80 ± 0.15 to a similar level as on the wild-type hA_1AR (Figure 3).

Mutations located at the C-terminus had the least effect on receptor activation of the hA_1AR (Figure 2C and Table 2). All three mutant receptors could be activated to similar E_{max} values with similar pEC_{50} values of CPA (9.47 ± 0.07 on H306N$^{8.61}$, 9.48 ± 0.06 on R308H$^{8.63}$ and 9.14 ± 0.14 on I315V^{C-term}) as wild-type hA_1AR. As found in the screening of constitutive activity (Figure 1C), H306N$^{8.61}$ and I315V^{C-term} had lower basal activity levels than wild-type hA_1AR.

Taken together, based on the different pharmacological effects of these mutant receptors, we characterized mutant receptor L211R$^{5.69}$ as CAM, mutant receptor E170G as a loss of function mutant (LFM), mutant receptors N148S^{EL2}, A151V^{EL2}, V152L^{EL2}, M177V$^{5.37}$, L113F$^{34.51}$, H306N$^{8.61}$ and I315V^{C-term} as CIMs and mutant receptors V215L^{IL3}, D221N^{IL3} and R308H$^{8.63}$ as no effect mutants (NEMs).

Ligand binding on wild-type and mutated hA_1AR

To further investigate mutant receptor function in a mammalian system, the 9 mutant receptors located at the ELs and ILs were selected. Mutations at these domains were expected to regulate the receptor-ligand interaction or receptor-G protein interaction. Therefore, wild-type and mutant receptors were transiently transfected into CHO cells. Cell membranes were collected and used in radioligand displacement assays (Figure 4 and Table 3). Receptor expression levels were measured by Western blot analysis where a band of the hA_1AR appeared around 37 kDa, and a non-specific band was seen at 15 kDa. As shown in Figure 4A, decreased expression levels for mutant receptors L113F$^{34.51}$, N148S^{EL2}, V152L^{EL2}, E170G$^{45.51}$, M177V$^{5.37}$, L211R$^{5.69}$ and V215L^{IL3} were observed compared to wild-type hA_1AR (Figure 4A), while only mutant receptor N148S^{EL2} showed significancy.
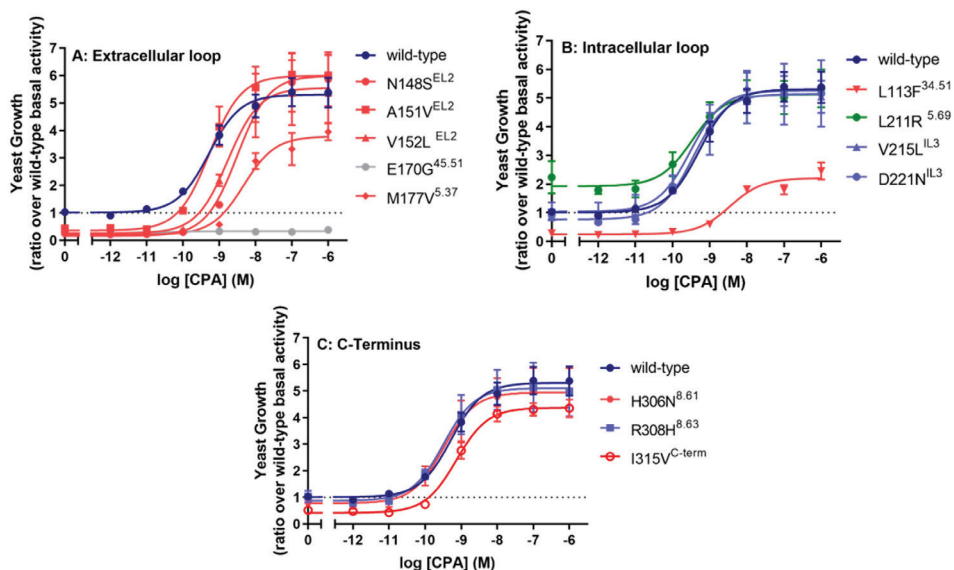
Figure 2. Concentration-response curves of the hA$_1$AR full agonist CPA at wild-type and mutated hA$_1$ARs. Data is separated for mutations located at (A) the extracellular loop, (B) the intracellular loop and (C) the C-terminus. Data were normalized as ratio over basal activity of wild-type hA$_1$AR (dotted line). Combined graphs are shown as mean ± SEM from at least three individual experiments performed in duplicate. CIMs are shown in red, CAMs in green, LFMs in grey and NEMs in blue.
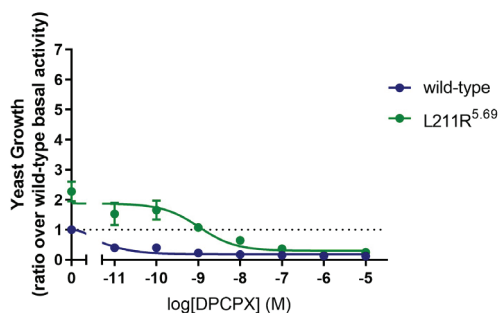

Figure 3. Concentration-inhibition curves of the hA$_1$AR inverse agonist DPCPX at the wild-type A$_1$AR and the CAM, L211R$^{5.69}$ Data were normalized as ratio over basal activity of wild-type hA$_1$AR (dotted line). Combined graphs are shown as mean ± SEM from at least three individual experiments performed in duplicate.

Homologous displacement experiments with [^{3}H]DPCPX and DPCPX resulted in a pK$_D$ value of 8.42 ± 0.01 for the wild-type hA$_1$AR, which was not different from the values for mutant receptors L113F$^{34.51}$ and L211R$^{5.69}$ (8.48 ± 0.02 and 8.52 ± 0.05, Table 3). Mutant receptors N148S^{EL2}, A151V^{EL2}, V152L^{EL2} and D221N^{IL3} had decreased pK$_D$ values of 8.15 ± 0.04, 8.22 ± 0.06, 8.19 ± 0.05 and 8.12 ± 0.05 (Table 3). Increased pK$_D$ values were obtained on mutant receptors E170G$^{45.51}$ and V215L^{IL3} (8.81 ± 0.04 and 8.65 ± 0.04, Table 3). All mutant receptors showed lower B$_{max}$ values than the wild-type hA$_1$AR (2.92 ± 0.17 pmol/mg, Table 3), where mutant V152L^{EL2} had the lowest expression level of 0.72 ± 0.05 pmol/mg. Notably, no specific binding

Table 2. *In vitro* pharmacological characterization of A_1AR mutants identified from cancer patient samples in yeast liquid growth assays, yielding information on level of constitutive activity, agonist potency and efficacy at these receptors.

Mutation	Basal[†]	pEC$_{50}$	E$_{max}$[†]	Type[‡]
Wild-type	1.00 ± 0.04	9.29 ± 0.07	5.37 ± 0.53	-
N148S^{EL2}	0.25 ± 0.05[***]	8.54 ± 0.08[**]	5.87 ± 0.98	CIM
A151V^{EL2}	0.43 ± 0.02[****]	9.26 ± 0.13	6.00 ± 0.74	CIM
V152L^{EL2}	0.33 ± 0.04[***]	8.80 ± 0.06[*]	5.52 ± 1.24	CIM
E170G$^{45.51}$	0.26 ± 0.04[***]	ND	ND	LFM
M177V$^{5.37}$	0.26 ± 0.02[**]	8.32 ± 0.06[**]	3.95 ± 0.31	CIM
L113F$^{34.51}$	0.28 ± 0.05[**]	8.43 ± 0.1[3**]	2.45 ± 0.30[***]	CIM
L211R$^{5.69}$	2.24 ± 0.56[*]	9.48 ± 0.14	5.33 ± 0.66	CAM
V215L^{IL3}	1.07 ± 0.29	9.58 ± 0.08	5.04 ± 0.56	NEM
D221N^{IL3}	0.92 ± 0.19	9.48 ± 0.25	5.16 ± 1.16	NEM
H306N$^{8.61}$	0.80 ± 0.12	9.47 ± 0.07	4.94 ± 0.93	CIM
R308H$^{8.63}$	1.03 ± 0.22	9.48 ± 0.06	4.99 ± 0.93	NEM
I315V^{C-term}	0.52 ± 0.09[*]	9.14 ± 0.14	4.35 ± 0.33	CIM

Mutations are shown in the numbering of the hA$_1$AR amino acid sequence as well as according to the Ballesteros-Weinstein GPCR numbering system. Potency (pEC$_{50}$) and efficacy (E$_{max}$) values are shown as mean ± SEM obtained from at least three individual experiments performed in duplicate.
[†] values were calculated as ratio over basal activity of wild-type hA$_1$AR.
[‡] types of mutants were depending on both screening of constitutive activity and receptor activation.
[*] $p < 0.05$; [**] $p < 0.01$; [***] $p < 0.001$ compared to wild-type hA$_1$AR, determined by a two-tailed unpaired Student's t-test.
ND: not detectable, CAM: constitutively active mutant, CIM: constitutively inactive mutant, LFM: loss of function mutant, NEM: no effect mutant

could be detected for mutant receptor M177V$^{5.37}$ in the presence of 1.6 nM [^{3}H] DPCPX (data not shown).

Next, heterologous displacement experiments were performed on wild-type and mutant hA$_1$ARs with the agonist CPA. Interestingly, for the wild-type hA$_1$AR the data was best fitted by a two-site model whereas the data was preferable fitted by a one-site model when DPCPX was used as a displacer (Figure 4B and 4C). With regard to CPA binding to mutant hA$_1$ARs, the two-site model was also preferred for mutant receptors L113F$^{34.51}$, N148S^{EL2}, V152L^{EL2}, E170G$^{45.51}$ and L211R$^{5.69}$. Conversely, for mutant receptors A151V^{EL2}, V215L^{IL3} and D221N^{IL3} a one-site binding model was preferred (Figure 4D and 4E). After fitting wild-type hA$_1$AR data to the two-site binding model, pK$_i$ values of 8.89 ± 0.19 at the high affinity state and 6.65 ± 0.03 at the low affinity state were obtained with a fraction of 0.23 ± 0.02 for the high affinity state (Table 3). An altered pK$_i$ value at the high affinity state was only obtained on mutant receptor V152L^{EL2} (7.49 ± 0.31) compared to wild-type hA$_1$AR. Interestingly, more diverse effects of mutant receptors on CPA binding were observed at the low affinity state. Mutant receptor L211R$^{5.69}$ showed an increased pK$_i$(low) value of 7.11 ± 0.06 compared to wild-type hA$_1$AR, while mutant receptors N148S^{EL2} and V152L^{EL2} had reduced values of 6.10 ± 0.09 and 6.02 ± 0.10 (Figure 4D, 4E and Table 3).

Table 3. B$_{max}$ and pK$_D$ values of [^{3}H]DPCPX and binding affinity of CPA on wild-type and mutant hA$_1$ARs.

	[^{3}H]DPCPX		CPA			
	B$_{max}$ (pmol/mg) [†]	pK$_D$ [†]	pK$_i$ (high) [‡]	pK$_i$ (low) [‡]	Fraction (high) [‡]	pK$_i$ [§]
Wild-type	2.92 ± 0.17	8.42 ± 0.01	8.89 ± 0.19	6.65 ± 0.03	0.23 ± 0.02	n.a.
L113F[34.51]	1.22 ± 0.08[****]	8.48 ± 0.02	9.08 ± 0.20	6.81 ± 0.02	0.26 ± 0.02	n.a.
N148S[EL2]	0.75 ± 0.07[****]	8.15 ± 0.04[**]	8.02 ± 0.10	6.10 ± 0.0[9*]	0.22 ± 0.02	n.a.
A151V[EL2]	0.89 ± 0.22[****]	8.22 ± 0.06[*]	n.a.	n.a.	n.a.	6.40 ± 0.05[**]
V152L[EL2]	0.72 ± 0.08[****]	8.19 ± 0.05[**]	7.49 ± 0.31[**]	6.02 ± 0.10[**]	0.40 ± 0.08	n.a.
E170G[45.51]	1.52 ± 0.04[****]	8.81 ± 0.04[****]	8.33 ± 0.36	6.77 ± 0.14	0.39 ± 0.09	n.a.
M177V[5.37]	ND	ND	ND	ND	ND	ND
L211R[5.69]	1.20 ± 0.10[****]	8.52 ± 0.03	8.35 ± 0.16	7.11 ± 0.06[*]	0.20 ± 0.07	n.a.
V215L[IL3]	1.00 ± 0.06[****]	8.65 ± 0.04[**]	n.a.	n.a.	n.a.	6.87 ± 0.08
D221N[IL3]	1.56 ± 0.11[****]	8.12 ± 0.05[***]	n.a.	n.a.	n.a.	6.40 ± 0.06[**]

B$_{max}$, pK$_D$, pK$_i$ and fraction values are shown as mean ± SEM obtained from three individual experiments performed in duplicate.
[*] $p < 0.05$; [**] $p < 0.01$; [***] $p < 0.001$; [****] $p < 0.0001$ compared to wild-type hA$_1$AR, as determined by one-way ANOVA with Dunnett's post-test.
[†] Values obtained from homologous displacement of ~1.6, 4.5 and 10 nM [^{3}H]DPCPX from transiently transfected wild-type and mutant CHO-hA$_1$AR membranes at 25°C.
[‡] In cases where the CPA displacement curve fitted best to a two-site model pK$_i$ (high), pK$_i$ (low) and Fraction (high) values were determined by fitting data to a two-site model.
[§] In cases where the CPA displacement curve fitted best to a one-site model pK$_i$ values are provided. For comparison, the pK$_i$ value of wild-type hA$_1$AR (6.85 ± 0.06) was used determined by fitting data to a one-site model.
ND: not detectable
n.a.: not applicable, as this was not statistically preferred

To be able to compare to some "one-site" mutants, a pKi value of 6.85 ± 0.06 was determined for wild-type hA$_1$AR by fitting the data to the one-site model (Table 3). Compared to wild-type hA$_1$AR, mutant receptors A151V[EL2] and D221N[IL3] showed decreased affinity values (pK$_i$) of 6.40 ± 0.05 and 6.40 ± 0.06 for CPA.

[^{35}S]GTPγS functional assay

CHO cell membranes transiently transfected with wild-type hA$_1$AR and 9 mutant receptors were further evaluated in a [^{35}S]GTPγS-binding assay. In this system, the wild-type A$_1$AR had a potency value of 8.80 ± 0.09 for CPA and an E$_{max}$ value of 1.67 ± 0.07. In the mammalian system, all mutant receptors could be activated by CPA with some differences in efficacy or potency values compared to wild-type hA$_1$AR, similar to the yeast system with one exception being mutant receptor E170G[45.51] This receptor was characterized as a LFM in the yeast system, while in the [^{35}S]GTPγS-binding assay it behaved similar to wild-type hA$_1$AR (Figure 5A, 5B and Table 4). Mutant receptors N148S[EL2], V152L[EL2] and M177V[5.37] showed a reduced potency for CPA in the yeast system, and also showed decreased potency values in the [^{35}S]GTPγS-binding assay, although this decrease was not significant for V152L[EL2]

(Figure 5A and Table 4). Mutant receptor M177V$^{5.37}$ behaved similarly in the yeast and mammalian assay, i.e. the potency of CPA decreased more than one log-unit and the efficacy remained unchanged (Figure 5A).

While data on mutant receptors in EL were very similar in the yeast and mammalian system, mutant receptors in IL showed more divergence in receptor pharmacology between systems (Figure 5B and Table 4). Mutant receptor L113F$^{34.51}$, was characterized as a CIM with decreased potency and efficacy in the yeast system, while it did not behave differently from the wild-type hA$_1$AR in the [^{35}S]GTPγS-binding assay (Figure 5B and Table 4). Mutant receptor L211R$^{5.69}$, characterized as a CAM in
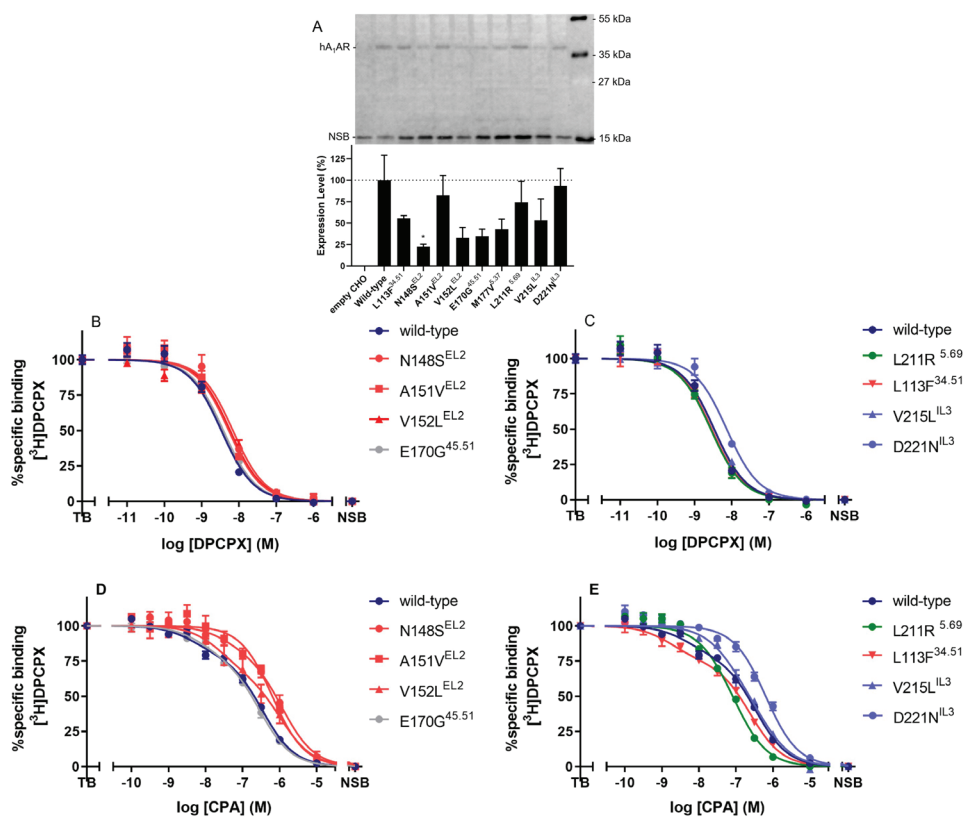
Figure 4. (A) Western blot analysis of CHO cell membranes transiently transfected with wild-type and mutant hA$_1$ARs. The specific hA$_1$AR band was found around 37 kDa, whereas a non-specific band (NSB) was found around 15 kDa. Expression level of wild-type hA$_1$AR relative to NSB was set to 100%, while expression level of mock transfected CHO cell membrane (empty CHO) relative to NSB was set to 0%. * $p < 0.05$ compared to wild-type hA$_1$AR, determined by using one-way ANOVA with Dunnett's post-test. (B-E) Displacement of specific [^{3}H]DPCPX binding to the transiently transfected wild-type hA$_1$AR, as well as 9 mutant receptors located at the extracellular loops (EL) (B and D) and intracellular loops (IL) (C and E), on CHO cell membranes by DPCPX and CPA. Combined graphs are shown as mean ± SEM from three individual experiments, each performed in duplicate. CIMs are shown in red, CAMs in green, LFMs in grey and NEMs in blue.

the yeast system, did not show altered constitutive activity in the mammalian system. Lastly, V215L^{IL3} and D221N^{IL3} were characterized as NEMs in the yeast system, but showed distinct pharmacological behavior in mammalian cells. Specifically, compared to the wild-type hA$_1$AR, both mutant receptors showed similar constitutive activity and potency values, but significantly decreased efficacy values (1.38 ± 0.04 on V215L^{IL3} and 1.35 ± 0.04 D221N^{IL3}) in response to CPA in the [^{35}S]GTPγS-binding assay (Figure 5B and Table 4).

For wild-type and all mutant hA$_1$AR receptors, the CPA-mediated activation was inhibited by the inverse agonist DPCPX (Figure 5C, 5D and Table 4). The activation level of mutant receptors L113F$^{34.51}$, N148S^{EL2}, V152L^{EL2} and L211R$^{5.69}$ was decreased to wild-type hA$_1$AR level with similar pIC$_{50}$ values for DPCPX as for the wild-type hA$_1$AR (8.00 ± 0.11 for wild-type, 7.88 ± 0.06 for L113F$^{34.51}$, 7.64 ± 0.05 for N148S^{EL2}, 7.58 ± 0.07 for V152L^{EL2} and 7.82 ± 0.26 for L211R$^{5.69}$). Decreased potency values of 7.50 ± 0.16 and 7.54 ± 0.05 for DPCPX were observed on mutant receptor A151V^{EL2} and D221N^{IL3} respectively, while the activation levels of these two mutant receptors could be reduced to wild-type hA$_1$AR level. For mutant receptors E170G$^{45.51}$ and V215L^{IL3}, the agonist-mediated receptor activation levels were decreased to a significantly lower level than wild-type hA$_1$AR (0.92 ± 0.01 for wild-type hA$_1$AR, 0.78
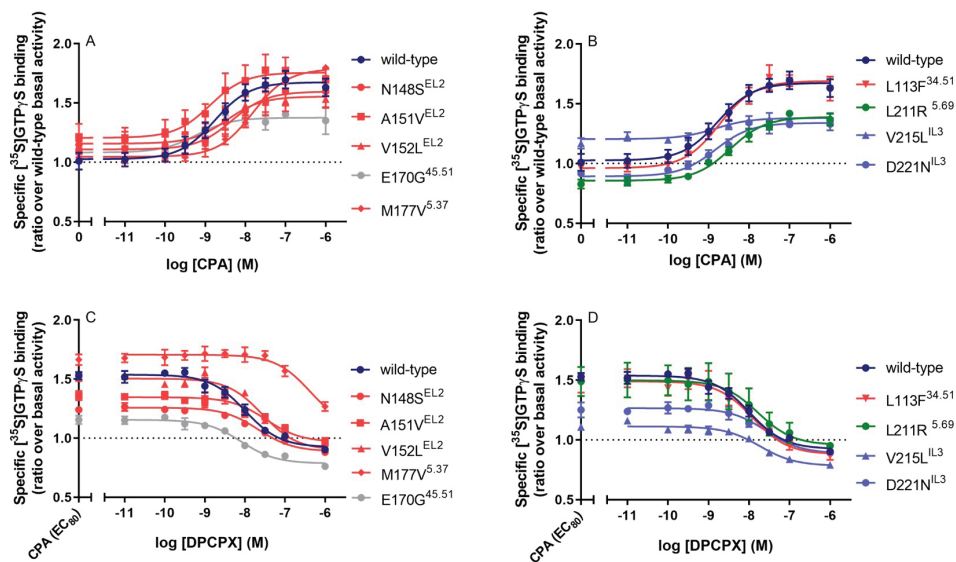

Figure 5. CPA-stimulated [^{35}S]GTPγS binding to transiently transfected wild-type hA$_1$AR and 9 mutant receptors located at the extracellular loops (EL) (A and C) and intracellular loops (IL) (B and D) on CHO cell membranes. (A and B) Receptor activation of wild-type and mutant receptors in response to CPA. Data were normalized as ratio over basal activity of wild-type hA$_1$AR. (C and D) Concentration-inhibition curves of DPCPX with the presence of CPA at the concentration of EC$_{80}$ for wild-type and mutant hA$_1$AR. Data were normalized as ratio over basal activity of wild-type or mutant hA$_1$AR. Combined graphs were shown as mean ± SEM obtained from three different experiments each performed in duplicate. CIMs are shown in red, CAMs in green, LFMs in grey and NEMs in blue.

± 0.01 for E170G$^{45.51}$ and 0.78 ± 0.02 for V215L^{IL3}), though the potency values of DPCPX remained unchanged. Of note, the inhibitory potency of DPCPX on mutant receptor M177V$^{5.37}$ was decreased the most with a pIC$_{50}$ of 6.31 ± 0.08, where basal wild-type hA$_1$AR activation levels could still not be reached in presence of 1 µM DPCPX (Figure 5C and Table 4). This significantly lower potency value of DPCPX on the mutant receptor M177V$^{5.37}$ is in line with the observation that no binding of [³H] DPCPX was detected at this mutant receptor (data not shown).

Table 4. Potency and efficacy of CPA and DPCPX in [³⁵S]GTPγS binding assays on wild-type and mutant hA$_1$ARs.

	CPA			DPCPX	
	Basal†	**pEC$_{50}$**	**E$_{max}$ †**	**pIC$_{50}$**	**I$_{max}$ ‡**
Wild-type	1.00 ± 0.06	8.80 ± 0.09	1.67 ± 0.07	8.00 ± 0.11	0.92 ± 0.01
L113F$^{34.51}$	0.96 ± 0.02	8.75 ± 0.07	1.69 ± 0.09	7.88 ± 0.06	0.88 ± 0.03
N148S^{EL2}	1.12 ± 0.09	8.29 ± 0.11*	1.60 ± 0.12	7.64 ± 0.05	0.89 ± 0.01
A151V^{EL2}	1.20 ± 0.10	8.88 ± 0.13	1.76 ± 0.12	7.50 ± 0.16*	0.97 ± 0.04
V152L^{EL2}	1.14 ± 0.05	8.49 ± 0.07	1.55 ± 0.08	7.58 ± 0.07	0.90 ± 0.01
E170G$^{45.51}$	1.09 ± 0.08	9.17 ± 0.11	1.38 ± 0.07	8.08 ± 0.10	0.78 ± 0.01**
M177V$^{5.37}$	1.04 ± 0.03	7.81 ± 0.06****	1.79 ± 0.02	6.31 ± 0.08****	1.27 ± 0.04****
L211R$^{5.69}$	0.85 ± 0.02	8.48 ± 0.09	1.39 ± 0.04	7.82 ± 0.15	0.95 ± 0.03
V215L^{IL3}	1.19 ± 0.04	8.93 ± 0.07	1.38 ± 0.04*	7.76 ± 0.14	0.78 ± 0.02**
D221N^{IL3}	0.90 ± 0.03	8.79 ± 0.21	1.35 ± 0.04*	7.54 ± 0.05*	0.88 ± 0.02

Basal, potency (pEC$_{50}$ or pIC$_{50}$) and efficacy (E$_{max}$ or I$_{max}$) values are shown as mean ± SEM obtained from at least three individual experiments performed in duplicate.
† values were calculated as ratio over basal activity of wild-type hA$_1$AR.
‡ values were calculated as ratio over basal activity of wild-type or mutant hA$_1$AR.
* $p < 0.05$; ** $p < 0.01$; *** $p < 0.001$; **** $p < 0.0001$ compared to wild-type hA$_1$AR, as determined by one-way ANOVA with Dunnett's post-test.

Structural mapping and bioinformatics analysis of mutations

The mutations investigated in this study were mapped on the inactive A$_1$AR structure (5UEN) to provide structural hypotheses for the observed pharmacological effect (i.e. NEM, LFM, CAM and CIM) of the different mutations. Two residues in the intracellular region (V215L^{IL3} (NEM) and I315V^{C-term} (CIM)) were not mapped, because this part of the receptor is unresolved in both active and inactive structures.

Mutations in the ELs are located close to one another, both sequentially and structurally (Figure 6A). Most mutations in the EL region cause relatively mild structural changes, as mutants residues mostly retain the properties of the wild-type hA$_1$AR residues, except the LFM E170G$^{45.51}$ (Figure 6B). This mutation dramatically interrupted receptor activation and is located next to the conserved residue C169$^{45.50}$ and F171$^{45.52}$, of which the latter is part of the orthosteric binding site. The M177V$^{5.35}$ mutation had a large effect on receptor-ligand recognition (both agonist and antagonist) and this mutation is found in direct contact with the cyclopentyl moieties
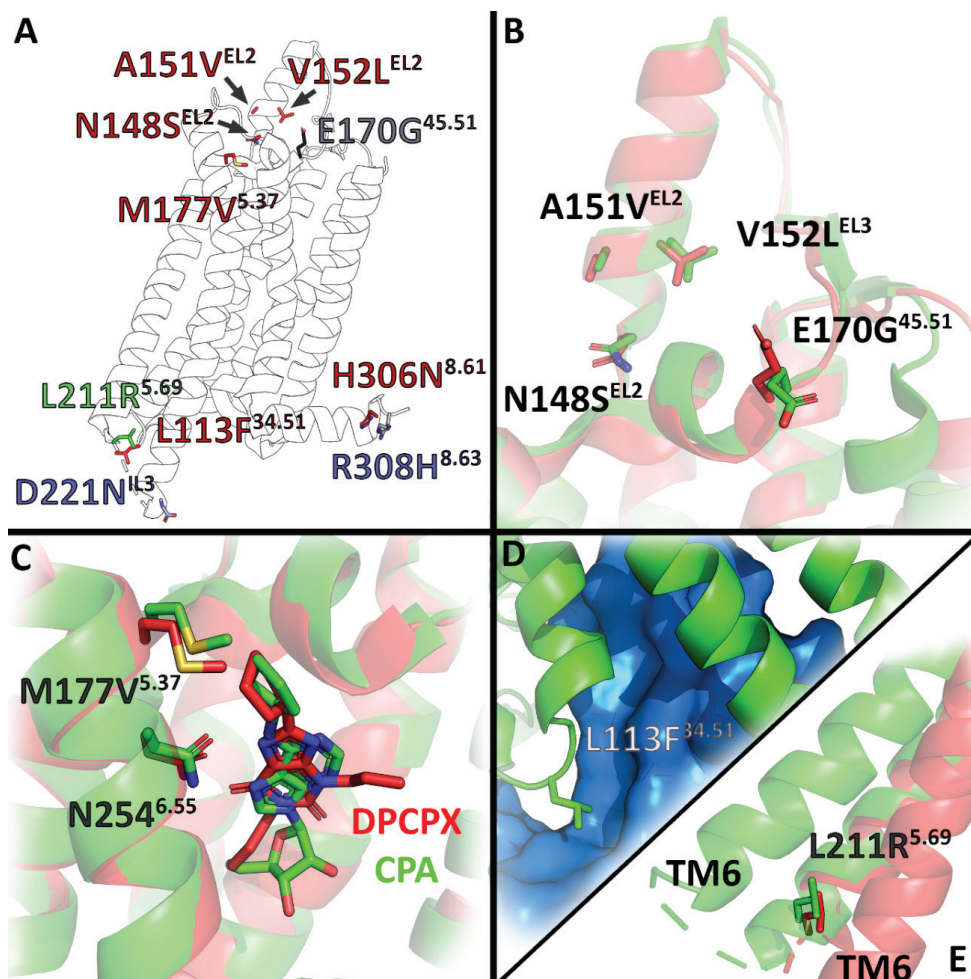
Figure 6. (A) Mutations from this study are mapped on the inactive A$_1$AR structure (5UEN). CIMs are shown in red, CAMs in green, LFMs in grey and NEMs in blue. (B-E) A close up is shown for the residues that showed the largest impact on receptor function upon mutation. The active structure (6D9H) is shown in green and the inactive in red (5UEN). Unresolved parts of the structure are shown as dashed cartoon representation. (B) Close up of the N148^{EL2}, A151^{EL2}, V152^{EL2}, E170$^{45.51}$ mutations located in the ELs. (C) Close up of the M177V$^{5.35}$ mutation in the orthosteric binding site. The reference ligands CPA (green) and DPCPX (red) used in this study are shown as sticks. (D) Close up of the L113F$^{34.51}$ mutation, which is found in the A$_1$AR-G protein interface. The G protein is shown in blue with surface representation. (E) Close-up of the L211R$^{5.69}$ mutation located at the bottom of TM5.

of both reference ligands used in this study (Figure 6C).

For the IL mutations, most constitute small changes in structural properties, with an exception for the two mutations L113F$^{34.51}$ (Figure 6D) and L211R$^{5.69}$ (Figure 6E), which are positioned close to the A$_1$AR – G protein interface. Moreover, L211$^{5.69}$ is situated in TM6, which undergoes a large conformational change upon receptor

activation. Notably, mutations on these residues exerted a large effect on receptor activation in yeast cells, but were found not to significantly alter receptor function in mammalian cells (compare Table 2 and 4).

Discussion

GPCR mutations are known to make alterations to receptor pharmacology by altering cell surface expression, GPCR-ligand interaction, basal activity and / or GPCR-G protein interaction, which can result in various disease phenotypes [38]. Additionally, it has been shown that various GPCR mutations are involved in cancer progression in different types of cancer [10,39], yet the role of these mutations in cancer is not fully characterized. Previous structural studies on hA$_1$AR indicated that some residues are crucial to ligand binding and receptor activation [21,35,36,40]. Moreover, crystal structures of hA$_1$AR have been published, which provided us with more structural information in the inactive receptor state [35,41] and in G protein-coupling [36]. Therefore, in this study we investigated 12 single-site point mutations located at the ELs, ILs and C-term of A$_1$AR that were obtained from The Cancer Genome Atlas (TCGA) [20]. These mutations were subsequently examined in the *S. cerevisiae* system and mammalian system to enrich our insight of the receptor activation mechanism in respect of cancer progression.

Mutations in the extracellular loops

All of the mutant receptors in the extracellular loops were located at EL2. EL2 of wild-type hA$_1$AR is known to be a positive regulator of receptor activation, as alanine mutations in this loop have been found to have negative regulatory effects[21]. Similarly, most of the EL2 mutant receptors in this study (i.e. N148S[EL2], A151V[EL2], V152L[EL2] and M177V[5.37]) led to a decrease in constitutive activity (Figure 1B), while the maximal activation levels were not influenced in response to CPA (Figure 2A and Table 2). According to the two-state-receptor model[42], in CIMs the equilibrium is shifted from the active (R*) to the inactive (R) receptor conformation. Supporting, these mutant receptors N148S[EL2] and V152L[EL2] showed lower potency and affinity of CPA compared to the wild-type hA$_1$AR. Moreover, mutant receptor A151V[EL2] preferred a one-site CPA binding model, which showed that the equilibrium was shifted to one certain receptor conformation[43]. Interestingly, mutant receptors N148S[EL2], A151V[EL2], V152L[EL] showed a significantly lower affinity of DPCPX. It has been reported that these residues modulate ligand residence time of both agonist and antagonist of A$_1$AR[44]. Therefore, it is possible that these mutations indirectly affect CPA's and DPCPX's dissociation kinetics from the hA$_1$AR binding pocket. Notably, decreased potency of CPA was observed on mutant receptor M177V[5.35] in both the yeast and mammalian system (Figure 2A, 5A and Table 2, 4). Mutant receptor M177V[5.35] also showed a decreased potency for DPCPX (Figure 5C), which was corroborated by the loss of a [³H]DPCPX window in the displacement experiments (Table 4). A similar

result has been reported by Nguyen *et al.* that introduced an alanine mutation at residue M177[5.35], resulting in a decreased affinity of DPCPX and full agonist NECA, indicating this residue is essential for ligand recognition[40]. Specifically, residue M177[5.35], together with residues L253[6.54] and T257[6.57], has been shown to form a hydrophobic pocket that engages the xanthine moiety of DPCPX[35]. Of note, the methionine at residue 5.35 is conserved among all adenosine receptors[45], which also indicates its essential role in the orthosteric binding site.

A complete loss of activation was observed for mutant receptor E170G[45.51] in the yeast system. However, it could be activated by CPA to a lower level with similar potency at the wild-type hA$_1$AR in the mammalian system. This CPA-mediated receptor activation could be reduced by DPCPX to a significantly lower level than wild-type hA$_1$AR (Figure 5C), indicating that mutant receptor E170G[45.51] might be constitutively active in the mammalian system. Residue E170[45.51] is situated between residues F171[45.52] and C169[EL2], where F171[45.52] is in the orthosteric binding pocket and residue C169[EL2] forms the highly conserved Class A GPCR disulfide bond with C80[3.25][35,36]. Due to the lack of a side chain in glycine, replacing glutamic acid with glycine at residue 170 makes it prone to flexibility, which often leads to disruptions in protein structure[46]. The introduced flexibility might open up space around F171[45.52] and possibly even lead to W247[6.48] ('toggle switch') bending away from the binding pocket, resulting in disruption of the 'ligand-binding cradle'[47]. In turn, this might lead to an incomplete functionality of the receptor.

Mutations in the intracellular loops

Compared to mutant receptors from other locations in hA$_1$AR, mutant receptors in intracellular loops showed diverse effects on receptor pharmacology. Mutant receptors V215L[IL3] and D221N[IL3] were characterized as NEMs in the yeast system, while mutant receptor L211R[5.69] and L113F[34.51] behaved as CAM and CIM, respectively (Table 2). However, these mutational effects on receptor activation were not as clearly observed in the mammalian system.

The CIM L113F[34.51], located in the middle of IL2, showed not only low constitutive activity, but also a prominently decreased potency and efficacy of CPA in the yeast system (Figure 1B, 2B and Table 2). However, on the CHO cell membranes, the affinity, potency and efficacy of neither DPCPX or CPA were influenced by the phenylalanine mutation at residue L113[34.51]. It has been shown that residue L113[34.51] in hA$_1$AR forms a Van der Waals interaction with the residue I344 (GH5.15) in Gα_{i2}[36]. This receptor-G protein interaction is also seen at other GPCRs, such as the muscarinic acetylcholine receptor M$_1$ (M$_1$R), where mutant receptor L131F[34.51] has also been shown not to influence G protein coupling[48]. Additionally, bulky hydrophobic amino acids at residue 34.51 commonly occur among GPCRs, indicating that the introduction of phenylalanine at residue L113[34.51] in hA$_1$AR should not significantly alter receptor - G protein coupling[45]. Therefore, the altered receptor pharmacology on mutant receptor L113F[34.51] in the yeast system might be specific for the receptor-

yeast G protein interaction.

CAM L211R[5.69], located at the end of TM5 and the beginning of IL3, showed a high activation level in the absence of an agonist in the yeast strain MMY24, but not in the mammalian system. The increased constitutive activity was reduced to wild-type hA$_1$AR level by the inverse agonist DPCPX (Figure 3), indicating that hA$_1$AR is not locked in an active conformation by mutation L211R[5.69]. Based on the two-state receptor model[42], elevated constitutive activity is a result of the mutant receptor being more in the active state than the wild-type hA$_1$AR[49]. While the increased constitutive activity was not observed on CHO cell membranes transiently transfected by mutant receptor L211R[5.69], the affinity of CPA was increased on the mutant receptor L211R[5.69] (Figure 4C and Table 3). This indicated that the receptor might be in a more activated state that agonists prefer to bind to. Although L5.69 is completely conserved among all adenosine receptors, structural studies on residue 5.69 are limited, due to the high flexibility and minor effects in receptor function of IL3[50]. It has been shown that L211[5.69] interacts with K346 (GH5.19) and F355 (GH5.26) in Gα$_{i2}$ by Van der Waals interactions[36,51]. Therefore, the divergent mutational effects observed between the yeast and mammalian system are likely due to the positions of these mutations close to the A$_1$AR – G protein interface, which is arguably different between mammalian and yeast cells even though the yeast system uses a partially humanized G protein[52].

Mutations in the C-terminus

In the C-terminus, CIMs H306N[8.61] and I315V[C-term] showed decreased constitutive activity, while the potency and efficacy of an agonist remained the same as for the wild-type hA$_1$AR. Moreover, mutant receptor R308H[8.63] was characterized as NEM (Figure 2C and Table 2). From a crystal structure of hA$_1$AR-G$_i$ complex, it has been concluded that the C-terminus of the Gα$_i$ subunit mainly interacts with the cytoplasmic end of TM2, TM3, TM5, TM6 and TM7, as well as the beginning of helix 8[36]. However, since mutant receptors H306N[8.61], R308H[8.63] and I315V[C-term] are located at the end part of helix 8, the receptor-G protein interaction is probably not affected much. Hence, the constitutive activity and receptor activation were not dramatically altered by these cancer-related mutations.

Potential role for hA$_1$AR mutations in cancer

ARs have been found to be involved in cancer biology[9,10]. In particular, multiple antagonistic antibodies and small molecule inhibitors against adenosine A$_{2A}$ and A$_{2B}$ receptors have been developed and display therapeutic efficacy in clinical trials against different solid tumors[10]. Anti-proliferative effects of hA$_1$AR activation have been identified in colon cancer, breast cancer, glioblastoma and leukemia[11,18,53]. The LFM E170G[45.51], identified from colon cancer, might therefore play a pro-proliferative role in cancer development. Interestingly in melanoma cells, deletion or blockade of hA$_1$AR suppressed cell proliferation but induced PD-L1 upregulation, resulting in compromised anti-tumor immunity[54]. Moreover, preclinical observations showed

that hA$_1$AR blockade by DPCPX inhibits cancer cell proliferation and promotes cell apoptosis[15,55,56]. Mutant receptors with altered receptor-ligand interaction, for example N148S[EL2], V152L[EL2] and M177V[5.35] in this study, may thus result in mis-dosing while using these small molecules as therapeutic approaches. Studies on GPCR heteromers provided evidence for the presence of hA$_1$AR[57]. A mutation with a mild impact on hA$_1$AR functionality was shown to play a pathogenic role in Parkinson's disease via a heteromeric complex with the dopamine D$_1$ receptor[58]. Analogously, mutant hA$_1$ARs may alter cancer biology through heteromers or oligomers, but further studies are warranted focusing on the role of hA$_1$AR heteromers in cancer progression. Although some of the cancer-related mutations in hA$_1$AR have a dramatic impact on receptor functionality, these effects are unlikely to be cancer-driving due to their lower frequency in cancer patients compared to known driver mutations e.g., RET proto-oncogene mutant M918T of which occurs in 50% of sporadic medullary thyroid carcinoma[20,59].

In conclusion, 12 cancer-related somatic mutations located at the extracellular, intracellular loops and C-terminus of the adenosine A$_1$ receptor were retrieved from TCGA and characterized in a robust yeast system, with follow-up in a mammalian system. The present study taught us that the yeast system is suitable for initial receptor pharmacology screening on mutations located outside the receptor-G protein interaction interface, and enabled us to identify mutations with dramatic effect on ligand binding and receptor activation. These mutations in the A$_1$AR may also regulate cell proliferation and migration in cancer cell lines, and thus might be further involved in cancer progression. Further studies are needed to investigate mutation-mediated receptor activation in a disease-relevant system. Together with the results from this study and the increasing evidence supporting the involvement of A$_1$AR in cancer[9,10,15,16,54], this will shed further light on the role of the A$_1$AR in cancer progression, which eventually may result in improved cancer therapy.

References

1. Fredriksson, R., Lagerström, M. C., Lundin, L.-G. & Schiöth, H. B. The G-protein-coupled receptors in the human genome form five main families. Phylogenetic analysis, paralogon groups, and fingerprints. *Mol. Pharmacol.* **63**, 1256–72 (2003).
2. Vassilatis, D. K. *et al.* The G protein-coupled receptor repertoires of human and mouse. *Proc. Natl. Acad. Sci.* **100**, 4903–4908 (2003).
3. Lagerström, M. C. & Schiöth, H. B. Structural diversity of G protein-coupled receptors and significance for drug discovery. *Nat. Rev. Drug Discov.* **7**, 339–57 (2008).
4. Pierce, K. L., Premont, R. T. & Lefkowitz, R. J. Seven-transmembrane receptors. *Nat. Rev. Mol. Cell Biol.* **3**, 639–650 (2002).
5. Kan, Z. *et al.* Diverse somatic mutation patterns and pathway alterations in human cancers. *Nature* **466**, 869–73 (2010).
6. Lappano, R. & Maggiolini, M. GPCRs and cancer. *Acta Pharmacol. Sin.* **33**, 351–362 (2012).
7. Dorsam, R. T. & Gutkind, J. S. G-protein-coupled receptors and cancer. *Nat. Rev. Cancer* **7**, 79–94 (2007).
8. Fredholm, B. B., IJzerman, A. P., Jacobson, K. a, Klotz, K. N. & Linden, J. International Union of Pharmacology. XXV. Nomenclature and classification of adenosine receptors. *Pharmacol. Rev.* **53**, 527–52 (2001).
9. Merighi, S. *et al.* A glance at adenosine receptors: novel target for antitumor therapy. *Pharmacol. Ther.* **100**, 31–48 (2003).
10. Sek, K. *et al.* Targeting Adenosine Receptor Signaling in Cancer Immunotherapy. *Int. J. Mol. Sci.* **19**, 3837 (2018).
11. Gessi, S., Merighi, S., Sacchetto, V., Simioni, C. & Borea, P. A. Adenosine receptors and cancer. *Biochim. Biophys. Acta* **1808**, 1400–1412 (2011).
12. Johnston, J. B. *et al.* Diminished adenosine A$_1$ receptor expression on macrophages in brain and blood of patients with multiple sclerosis. *Ann. Neurol.* **49**, 650–658 (2001).

13. Borea, P. A., Gessi, S., Merighi, S., Vincenzi, F. & Varani, K. Pharmacology of Adenosine Receptors: The State of the Art. *Physiol. Rev.* **98**, 1591–1625 (2018).
14. Merighi, S. *et al.* Pharmacological and biochemical characterization of adenosine receptors in the human malignant melanoma A375 cell line. *Br. J. Pharmacol.* **134**, 1215–1226 (2001).
15. Zhou, Y. *et al.* The Adenosine A₃ Receptor Antagonist DPCPX Inhibits Tumor Progression via the ERK/JNK Pathway in Renal Cell Carcinoma. *Cell. Physiol. Biochem.* **43**, 733–742 (2017).
16. Mirza, A. *et al.* RNA interference targeting of A₁ receptor-overexpressing breast carcinoma cells leads to diminished rates of cell proliferation and induction of apoptosis. *Cancer Biol. Ther.* **4**, 1355–1360 (2005).
17. Dastjerdi, M. N., Rarani, M. Z., Valiani, A. & Mahmoudieh, M. The effect of adenosine A₁ receptor agonist and antagonist on p53 and caspase 3, 8, and 9 expression and apoptosis rate in MCF-7 breast cancer cell line. *Res. Pharm. Sci.* **11**, 303–310 (2016).
18. Saito, M., Yaguchi, T., Yasuda, Y., Nakano, T. & Nishizaki, T. Adenosine suppresses CW2 human colonic cancer growth by inducing apoptosis via A₁ adenosine receptors. *Cancer Lett.* **290**, 211–215 (2010).
19. Synowitz, M. *et al.* A₁ Adenosine Receptors in Microglia Control Glioblastoma-Host Interaction. *Cancer Res.* **66**, 8550–8557 (2006).
20. *Broad Institute TCGA Genome Data Analysis Center (2016): Analysis-ready standardized TCGA data from Broad GDAC Firehose stddata_2015_08_21 run. Broad Institute of MIT and Harvard.* (2016). doi:10.7908/C18W3CNQ
21. Peeters, M. C. *et al.* The role of the second and third extracellular loops of the adenosine A₁ receptor in activation and allosteric modulation. *Biochem. Pharmacol.* **84**, 76–87 (2012).
22. Peeters, M. C., van Westen, G. J. P., Li, Q. & IJzerman, A. P. Importance of the extracellular loops in G protein-coupled receptors for ligand recognition and receptor activation. *Trends Pharmacol. Sci.* **32**, 35–42 (2011).
23. Peeters, M. C. *et al.* GPCR structure and activation: an essential role for the first extracellular loop in activating the adenosine A₂B receptor. *FASEB J.* **25**, 632–43 (2011).
24. Weinstein, J. N. *et al.* The Cancer Genome Atlas Pan-Cancer analysis project. *Nat. Genet.* **45**, 1113–1120 (2013).
25. UniProt: the universal protein knowledgebase. *Nucleic Acids Res.* **45**, D158–D169 (2017).
26. Ballesteros, J. A. & Weinstein, H. Integrated methods for the construction of three-dimensional models and computational probing of structure-function relations in G protein-coupled receptors. in *Methods in Neurosciences* **25**, 366–428 (1995).
27. Isberg, V. *et al.* Generic GPCR residue numbers – aligning topology maps while minding the gaps. *Trends Pharmacol. Sci.* **36**, 22–31 (2015).
28. Liu, R., Nahon, D., le Roy, B., Lenselink, E. B. & IJzerman, A. P. Scanning mutagenesis in a yeast system delineates the role of the NPxxY(x)5,6F motif and helix 8 of the adenosine A₂B receptor in G protein coupling. *Biochem. Pharmacol.* **95**, 290–300 (2015).
29. Yang, X. *et al.* Design and pharmacological profile of a novel covalent partial agonist for the adenosine A₁ receptor. *Biochem. Pharmacol.* **180**, 114144 (2020).
30. Dowell, S. J. & Brown, A. J. Yeast Assays for G Protein-Coupled Receptors. in *Methods in molecular biology (Clifton, N.J.)* (ed. Filizola, M.) **552**, 213–229 (Springer New York, 2009).
31. Longo, P. A., Kavran, J. M., Kim, M. S. & Leahy, D. J. Transient mammalian cell transfection with polyethylenimine (PEI). *Methods Enzymol.* **529**, 227–240 (2013).
32. Heitman, L. H. *et al.* A Series of 2,4-Disubstituted Quinolines as a New Class of Allosteric Enhancers of the Adenosine A₃ Receptor. *J. Med. Chem.* **52**, 926–931 (2009).
33. Smith, P. K. *et al.* Measurement of protein using bicinchoninic acid. *Anal. Biochem.* **150**, 76–85 (1985).
34. de Ligt, R. A. F., Rivkees, S. A., Lorenzen, A., Leurs, R. & IJzerman, A. P. A "locked-on," constitutively active mutant of the adenosine A₁ receptor. *Eur. J. Pharmacol.* **510**, 1–8 (2005).
35. Glukhova, A. *et al.* Structure of the Adenosine A₁ Receptor Reveals the Basis for Subtype Selectivity. *Cell* **168**, 867-877.e13 (2017).
36. Draper-Joyce, C. J. *et al.* Structure of the adenosine-bound human adenosine A₁ receptor–Gi complex. *Nature* **558**, 559–563 (2018).
37. Cheng, Y.-C. & Prusoff, W. H. Relationship between the inhibition constant (KI) and the concentration of inhibitor which causes 50 per cent inhibition (I50) of an enzymatic reaction. *Biochem. Pharmacol.* **22**, 3099–3108 (1973).
38. Stoy, H. & Gurevich, V. V. How genetic errors in GPCRs affect their function: Possible therapeutic strategies. *Genes Dis.* **2**, 108–132 (2015).
39. O'Hayre, M. *et al.* The emerging mutational landscape of G proteins and G-protein-coupled receptors in cancer. *Nat. Rev. Cancer* **13**, 412–24 (2013).
40. Nguyen, A. T. N. *et al.* Extracellular Loop 2 of the Adenosine A₁ Receptor Has a Key Role in Orthosteric Ligand Affinity and Agonist Efficacy. *Mol. Pharmacol.* **90**, 703–714 (2016).
41. Cheng, R. K. Y. *et al.* Structures of Human A₁ and A₂A Adenosine Receptors with Xanthines Reveal Determinants of Selectivity. *Structure* **25**, 1275-1285.e4 (2017).
42. Leff, P. The two-state model of receptor activation. *Trends Pharmacol. Sci.* **16**, 89–97 (1995).
43. Guo, D. *et al.* A two-state model for the kinetics of competitive radioligand binding. *Br. J. Pharmacol.* **175**, 1719–1730 (2018).
44. Nguyen, A. T. N. *et al.* Role of the Second Extracellular Loop of the Adenosine A₁ Receptor on Allosteric Modulator Binding, Signaling, and Cooperativity. *Mol. Pharmacol.* **90**, 715–725 (2016).
45. Isberg, V. *et al.* GPCRdb: an information system for G protein-coupled receptors. *Nucleic Acids Res.* **44**, D356–D364 (2016).
46. Yohannan, S., Faham, S., Yang, D., Whitelegge, J. P. & Bowie, J. U. The evolution of transmembrane helix kinks and the structural diversity of G protein-coupled receptors. *Proc. Natl. Acad. Sci.* **101**, 959–963 (2004).
47. Venkatakrishnan, A. J. *et al.* Molecular signatures of G-protein-coupled receptors. *Nature* **494**, 185–194 (2013).
48. Moro, O., Lameh, J., Högger, P. & Sadée, W. Hydrophobic amino acid in the i2 loop plays a key role in receptor-G protein coupling. *J. Biol. Chem.* **268**, 22273–6 (1993).
49. Kobilka, B. K. G protein coupled receptor structure and activation. *Biochim. Biophys. Acta - Biomembr.* **1768**, 794–807 (2007).
50. Dror, R. O. *et al.* Structural basis for nucleotide exchange in heterotrimeric G proteins. *Science.* **348**, 1361–1365 (2015).
51. Wang, J. & Miao, Y. Mechanistic Insights into Specific G Protein Interactions with Adenosine Receptors. *J. Phys. Chem. B* **123** 6462–6473 (2019).
52. Brown, A. J. *et al.* Functional coupling of mammalian receptors to the yeast mating pathway using novel yeast/mammalian G protein α-subunit chimeras. *Yeast* **16**, 11–22 (2000).
53. Borea, P. A., Gessi, S., Merighi, S., Vincenzi, F. & Varani, K. Pathological overproduction: the bad side of adenosine. *Br. J. Pharmacol.* **174**, 1945–1960 (2017).
54. Liu, H. *et al.* ADORA1 Inhibition Promotes Tumor Immune Evasion by Regulating the ATF3-PD-L1 Axis. *Cancer Cell*

37, 324-339.e8 (2020).

55. Ma, H. *et al.* Dual Inhibition of Ornithine Decarboxylase and A$_1$ Adenosine Receptor Efficiently Suppresses Breast Tumor Cells. *Front. Oncol.* **11**, 1–10 (2021).

56. Zamani Rarani, M. *et al.* Adenosine A$_1$ Receptor Antagonist Up-regulates Casp3 and Stimulates Apoptosis Rate in Breast Cancer Cell Line T47D. *Int. Electron. J. Med.* **9**, 14–20 (2020).

57. Navarro, G. *et al.* Quaternary structure of a G-protein-coupled receptor heterotetramer in complex with Gi and Gs. *BMC Biol.* **14**, 1–12 (2016).

58. Nasrollahi-Shirazi, S. *et al.* Functional impact of the G279S substitution in the adenosine A$_1$-receptor (A$_1$R-G279S[7.44]), a mutation associated with Parkinson's disease. *Mol. Pharmacol.* **98**, 250-266 (2020).

59. Gimm, O. *et al.* Over-representation of a germline RET sequence variant in patients with sporadic medullary thyroid carcinoma and somatic RET codon 918 mutation. *Oncogene* **18**, 1369–1373 (1999).

5

Chapter 6

Cancer-related somatic mutations in transmembrane helices alter adenosine A$_1$ receptor pharmacology.

Abstract

Over-expression of the adenosine A_1 receptor (A_1AR) has been detected in various cancer cell lines. However, the role of A_1AR in tumor development is still unclear. Thirteen A_1AR mutations were identified in the Cancer Genome Atlas from cancer patient samples. We have investigated the pharmacology of the mutations located at the 7-transmembrane domain using a yeast system. Concentration-growth curves were obtained with the full agonist CPA and compared to the wild-type hA_1AR. H78L[3.23] and S246T[6.47] showed increased constitutive activity, while only the constitutive activity of S246T[6.47] could be reduced to wild-type levels by the inverse agonist DPCPX. Decreased constitutive activity was observed on 5 mutant receptors, among which A52V[2.47] and W188C[5.46] showed a diminished potency for CPA. Lastly, a complete loss of activation was observed in 5 mutant receptors. A selection of mutations was also investigated in a mammalian system, showing comparable effects on receptor activation as in the yeast system, except for residues pointing towards the membrane. Taken together, this study will enrich the view of receptor structure and function on A_1AR, enlightening the consequences of these mutations in cancer. Ultimately, this may provide an opportunity of precision medicine for cancer patients with pathological phenotypes involving these mutations.

Keywords: G protein-coupled receptors, adenosine A_1 receptor, cancer, mutation, yeast system

Introduction

G protein-coupled receptors (GPCRs) are the largest protein superfamily in the human genome with approximately 800 subtypes[1]. They share a characteristic structure of seven-transmembrane helices (TMs) connected by an extracellular N-terminus, three extracellular loops (ELs), three intracellular loops (ILs) and an intracellular C-terminus[2]. GPCRs are widely distributed throughout the human body and regulate various crucial cellular and physiological functions by responding to a diverse set of endogenous ligands[3]. However, their aberrant activity and expression also substantially contributes to human pathophysiology[4].

Kinases, due to their central roles in the cell cycle, have been studied as primary focus in preclinical oncology over the last two decades[5]. GPCRs, however, have been relatively under-investigated in this context, while an increasing amount of evidence shows that GPCRs act as regulators of tumor initiation and progression as well[6]. Malignant cells often hijack the normal physiological function of GPCRs to survive, invade surrounding tissue and evade the immune system[7]. Moreover, somatic mutations of GPCRs have been identified in approximately 20% of all cancers by a systematic analysis of cancer genomes[5].

The immune system plays a fundamental and essential role in the defense against cancer[8]. Adenosine, a nucleoside and derivative of ATP, has emerged as a major immune-metabolomic checkpoint in tumors[9]. Compared to healthy tissue, adenosine is accumulated over 50-fold in the hypoxic tumor environment, leading to a reduced anti-tumoral immune response[10]. Adenosine regulates various physiological effects and immune responses in cancer via adenosine receptors (ARs): the A$_1$, the A$_{2A}$, the A$_{2B}$, and the A$_3$ receptor[11]. Additionally, all ARs have been detected in different human tumor tissues[12]. Therefore, all four subtypes of ARs may regulate cancer progression in one way or another.

Growing evidence addresses the involvement of A$_1$AR in cancer progression, although its precise role is not well understood[13,14]. An increased expression level of the A$_1$AR has been detected in diverse cancer cells[15,16], where it appears to behave as both an anti- and pro-tumoral regulator in the development of different cancer types[10]. Interestingly, various single-site point mutations on A$_1$AR have been isolated from patients with different cancer types and collected by the TCGA Research Network (https://www.cancer.gov/tcga). Previous site-directed mutagenesis and docking studies on A$_1$AR have identified residues all over the protein involved in ligand recognition and/or functional activity[17,18]. Furthermore, several GPCR-conserved residues and motifs, for instance the D2.50 residue, the ionic lock, the NPxxY motif and the DRY motif, are located at 7-TM domains mediating ligand binding and signaling [19].

In this study, 13 mutations located at the 7-TM domains of the A$_1$AR have been selected from cancer patients using a bioinformatics approach. The effects of these

mutant receptors on constitutive receptor activity and agonist-induced activation were tested in a 'single-GPCR-one-G protein' *S. cerevisiae* strain, which has been reported to be predictive of the mammalian situation[20,21]. A selection of mutant receptors were further investigated for their effect on ligand binding and receptor activation in a mammalian system. Subsequently, we identified 2 CAMs, 5 CIMs and 6 loss-of-function mutants (LFMs) based on the pharmacological effects of these mutant receptors. Thus, cancer-related mutations within the 7-TM domain may alter the role of A_1AR in cancer progression and the efficacy of drugs targeting A_1AR as a cancer therapeutic approach.

Materials and methods

Data mining

Mutation data was downloaded from The Cancer Genome Atlas (TCGA, version August 8th 2015) by using the Firehose tool[22]. MutSig 2.0 data was extracted when available, MutSig 2CV was used in cases where the former was not available (specifically for Colon Adenocarcinoma, Acute Myeloid Leukemia, Ovarian Cerous Cystadenocarcinoma, Rectum Adenocarcinoma). Natural variance data was downloaded from Uniprot (Index of Protein Altering Variants, version November 11th 2015)[23]. Sequence data was filtered for missense somatic mutations and the A_1AR (Uniprot identifier P30542). The GPCRdb alignment tool was used to assign Ballesteros Weinstein numbers[24,25] to the positions through which a selection could be made for transmembrane domain positions.

Materials

The MMY24 strain and the *S. cerevisiae* expression vectors, the pDT-PGK plasmid and the pDT-PGK_hA$_1$AR plasmid (i.e. expressing the wild-type receptor) were kindly provided by Dr. Simon Dowell from GSK (Stevenage, UK). The pcDNA3.1(+) plasmid cloned with N-terminal 3xHA-tagged hA$_1$AR was ordered from cDNA Resource Center (Bloomsburg, USA). The QuikChange II® Site-Directed Mutagenesis Kit containing XL10-Gold ultracompetent cells was purchased from Agilent Technologies (Amstelveen, the Netherlands). The QIAprep mini plasmid purification kit and QIAGEN® plasmid midi kit were purchased from QIAGEN (Amsterdam, the Netherlands). Adenosine deaminase (ADA), 1,4-dithiothreitol (DTT), 8-cyclopentyl-1,3-dipropylxanthine (DPCPX) and 3-amino-[1,2,4]-triazole (3-AT) were purchased from Sigma-Aldrich (Zwijndrecht, the Netherlands). N^6-cyclopentyladenosine (CPA) was purchased from Santa Cruz Biotechnology (Heidelberg, Germany). Bicinchoninic acid (BCA) and BCA protein assay reagent were obtained from Pierce Chemical Company (Rockford, IL, USA). Radioligands 1,3-[^{3}H]-dipropyl-8-cyclopentylxanthine ([^{3}H]DPCPX, specific activity of 137 Ci × mmol^{-1}) and [^{35}S]-Guanosine 5'-(γ-thio) triphosphate ([^{35}S]GTPγS, a specific activity 1250 Ci × mmol^{-1}) were purchased from PerkinElmer, Inc. (Waltham, MA, USA). Rabbit anti-HA antibody (71-5500)

was purchased from Thermo Fisher Scientific (Waltham, MA, USA), while goat anti-rabbit IgG HRP was purchased from Jackson ImmunoResearch Laboratories (West Grove, PA, USA).

Generation of hA$_1$AR mutations

The plasmids carrying hA$_1$AR mutations were constructed by polymerase chain reaction (PCR) mutagenesis as previously described, using pDT-PGK_hA$_1$AR or pcDNA3.1_hA$_1$AR with N-terminal 3xHA tag as the template[17]. The QuikChange Primer Design Program of Agilent Technologies (Santa Clara, CA, USA) was used to design primers for mutant receptors and primers were purchased from Eurogentec (Maastricht, The Netherlands). All DNA sequences were verified by Sanger sequencing at LGTC (Leiden, The Netherlands).

Transformation in MMY24 S. cerevisiae strain

The plasmids, pDT-PGK_hA$_1$AR, containing either wild-type or mutated hA$_1$AR were transformed into a MMY24 *S. cerevisiae* strain following the Lithium-Acetate procedure[26].

Liquid growth assay

In order to characterize the mutant hA$_1$ARs, liquid growth assays in 96-well plates were performed to obtain concentration-growth curves as previously described[17]. Briefly, yeast cells expressing wild-type or mutant hA$_1$AR were inoculated to 1 mL selective YNB medium lacking uracil and leucine (YNB-UL) and incubated overnight at 30 °C. The overnight cultures were then diluted to 40,000 cells/ml (OD$_{600}$ ≈ 0.02) in selective medium without uracil, leucine and histidine (YNB-ULH). For the determination of constitutive activity, 50 µL yeast cells and 150 µL YNB-ULH medium containing different concentrations of 3-AT and 0.8 IU/ml ADA were then added to each well. To obtain concentration-growth curves, 2 µL various concentrations of ligands, 50 µL yeast cells and 150 µL YNB-ULH medium containing 7 mM 3-AT and 0.8 IU/ml ADA were then added to each well. After incubation at 30 °C for 35 h in a Genios plate reader (TECAN, Switzerland) with shaking 1 min at 300 rpm every 10 min, the optical density was measured at a wavelength of 595 nm, which represented the level of yeast cell growth.

Cell culture, transient transfection and membrane preparation

Chinese hamster ovary (CHO) cells were cultured at 37 °C in 5% CO$_2$ in a Dulbecco's modified Eagle's medium/Ham's F12 (1 : 1, DMEM/F12) containing 10% bovine calf serum, streptomycin (50 µg/mL) and penicillin (50 IU/mL). Cells were grown until 80-90% confluency and subcultured twice weekly.

Transient transfection of CHO cells with wild-type or mutated hA$_1$AR plasmid constructs was performed using a polyethylenimine (PEI) method[27]. Cells were seeded in 10-cm culture dishes to achieve 50-60% confluency 24 h prior to

6

transfection. On the day of transfection, cells were transfected with a PEI : DNA ratio of 3 : 1 and plasmid DNA amount of 10 μg/dish. 24 h post-transfection, the medium was refreshed, and 48 h after transfection, cells were collected and membranes were prepared as previously described[28]. Membranes were aliquoted in 250 or 100 μL and stored at -80 °C. Membrane protein concentrations were determined using the BCA method[29].

Enzyme-linked Immunosorbent assay

The ELISA experiments were performed with some modifications of a previously published procedure[30]. 24 h after transfection, cells were seeded in a 96-well plate with a density of 10^6 cells per well. 48 h post-transfection, the cells were fixed with 4% formaldehyde and blocked with 2% bovine serum albumin (BSA) (Sigma-Aldrich Chemie N.V., Zwijndrecht, The Netherlands) in Tris-buffered saline (TBS) for 1 h. Then, the cells were incubated with rabbit anti-HA tag primary antibody (1:2500) in TBST (0.05% Tween 20 in TBS) overnight at 4 °C. The cells were washed 3 times in TBST and incubated with the goat anti-rabbit IgG HRP secondary antibody (1:6000) for 1 hour at RT. After removing the secondary antibody and washing the cells with TBS, 3, 3',5,5'-tetramethyl-benzidine (TMB) was added and incubated for 10 minutes in the dark. The reaction was stopped with 1 M H_3PO4, and absorbance was read at 450 nm using a Wallac EnVision 2104 Multilabel reader (PerkinElmer).

Radioligand displacement assay

The displacement assays were performed as described previously[31]. Briefly, to each well the following was added: 25 μL cell membrane suspension, 25 μL of 1.6 nM radioligand [^{3}H]DPCPX, 25 μL of assay buffer (50 mM Tris-HCl, pH 7.4) and 25 μL of six increasing concentrations of DPCPX (10^{-11} to 10^{-6} M) or CPA (10^{-10} to 10^{-5} M) , all dissolved in assay buffer. Note, the quantity of cell membranes (10-25 μg) was adjusted to obtain approximately 1500 DPM assay window for each mutant. Nonspecific binding was determined in the presence of 10^{-4} M CPA and represented less than 10% of the total binding. For homologous competition assays, radioligand displacement experiments were performed in the presence of 3 different concentrations of [^{3}H]DPCPX (1.6 nM, 4.5 nM and 10 nM) as well as 6 increasing concentrations of DPCPX (10^{-11} to 10^{-6} M). Incubations were terminated after 1 h at 25 °C by rapid vacuum filtration through GF/B filter plates (PerkinElmer, Groningen, Netherlands) using a Perkin Elmer Filtermate-harvester. Afterwards, filter plates were washed ten times with ice-cold buffer (50 mM Tris-HCl, pH 7.4) and dried at 55 °C for 30 min. After addition of 25 μl per well of Microscint scintillation cocktail (PerkinElmer, Groningen, the Netherlands), the filter-bound radioactivity was measured by scintillation spectrometry in a Microbeta2® 2450 microplate counter (PerkinElmer).

[^{35}S]GTPγS binding assay

[^{35}S]GTPγS binding assays were adapted from a previously published method[31].

Membrane aliquots containing 15 µg protein were incubated with a total volume of 80 µL assay buffer (50 mM Tris-HCl buffer, 5 mM MgCl$_2$, 1 mM EDTA, 100 mM NaCl, 0.05% BSA and 1 mM DTT pH 7.4 supplemented with 10 **µ**M GDP and 10 µg saponin) and 9 increasing concentrations of CPA (10^{-11} to 10^{-6} M) or 9 increasing concentrations of DPCPX (10^{-11} to 10^{-6} M) in the presence of a fixed concentration (EC$_{80}$ for wild-type or mutant hA$_1$ARs) of CPA for 30 min at 4 °C. Then 20 µL of [^{35}S] GTP**γ**S (final concentration of 0.3 nM) was added to each well and followed by 90 min incubation at 25 °C. Incubations were terminated and filter-bound radioactivity was measured as described above.

Modelling

Structures of the A$_1$AR in the inactive (PDB: 5UEN)[32] and active (PDB: 6D9H) state[33], and the inactive state of the A$_{2A}$AR (PDB: 4EIY)[34] were retrieved from the PDB. Missing side chains and loop regions were added using the GPCR-ModSim webserver[35]. All structures were aligned to the inactive A$_1$AR, and figures were generated using the PyMOL Molecular Graphics System version 2.0 (Schrödinger, LLC., USA).

Data analysis

All experimental data were analyzed by GraphPad Prism 7.0 or 8.0 (GraphPad Software Inc., San Diego, CA, USA). Data from yeast liquid growth and [^{35}S]GTPγS binding assays were analyzed by non-linear regression using "log (agonist) vs. response (three parameters)" or "log (inhibitor) vs. response (three parameters)" to obtain potency (EC$_{50}$), inhibitory potency (IC$_{50}$) and efficacy (E$_{max}$ or I$_{max}$) values. The radioligand displacement curves were obtained from a statistically preferred one-site or two-site binding model. pK$_i$ values were calculated from pIC$_{50}$ values using the Cheng-Prusoff equation, where K$_D$ values were obtained from the homologous competition assays from this study and calculated by non-linear regression using "one site – homologous"[36].

Results

Data mining

Mutation data from cancer patient isolates were obtained by data mining the TCGA database on August 8th 2015. 27 point somatic mutations were selected from in total 48 cancer-related point mutations of hA$_1$ARs based on selected cancer types, i.e. breast invasive carcinoma, colon adenocarcinoma, lung adenocarcinoma, lung squamous cell carcinoma, lymphoid neoplasm diffuse large B-cell lymphoma and rectum adenocarcinoma. After assigning Ballesteros Weinstein numbers to the positions by using the GPCRdb alignment tool, 13 mutations located at the 7-TM domains were selected for this study (Table 1). One mutation was located at the first, two at the second, two at the third, one at the fourth, one at the fifth, two at the sixth and two at the seventh TM (Figure 1A).

Table 1. List of cancer-related somatic mutations identified from different cancer types.

Mutations	Cancer types
A20T$^{1.43}$	Colon adenocarcinoma
A52V$^{2.47}$	Breast invasive carcinoma
D55V$^{2.50}$	Breast invasive carcinoma
D55G$^{2.50}$	Colon adenocarcinoma
H78L$^{3.23}$	Lung adenocarcinoma
P86L$^{3.31}$	Rectum adenocarcinoma
R122Q$^{4.40}$	Colon adenocarcinoma
L134F$^{4.52}$	Lung squamous cell carcinoma
W188C$^{5.46}$	Colon adenocarcinoma
S246T$^{6.47}$	Breast invasive carcinoma
T257P$^{6.58}$	Lung adenocarcinoma
S267I$^{7.32}$	Colon adenocarcinoma
G279S$^{7.44}$	Colon adenocarcinoma

Constitutive activity of mutant hA$_1$ARs

To first characterize the effect of the cancer-related mutations on the constitutive activity of the receptor, i.e. activity independent from an agonist, yeast growth assays were performed in the absence of agonist. First, the optimal concentration of the histidine biosynthesis inhibitor (3-amino-1,2,4-triazole, 3-AT) for constitutive activity screening was determined in response to increasing concentrations of 3-AT (Figure 1B). Upon increasing concentrations of 3-AT, cell growth of both yeast cells transformed with plasmid with or without wild-type hA$_1$AR were decreased (Figure 1B). At a concentration of 4 mM 3-AT, the two curves showed the largest difference in yeast growth, and at this point, mutant receptors with increased constitutive activity (CAM) would show a higher growth level than wild-type hA$_1$AR, while mutant receptors with decreased constitutive activity (CIM) would show a growth level in between wild-type hA$_1$AR and empty vector. Thus, using this concentration of 3-AT provided the best window to screen for both CAMs and CIMs.

Cancer-related mutations showed various effects on the constitutive activity of the hA$_1$AR (Figure 1C). Eleven out of the thirteen mutant receptors had a decreased constitutive activity compared to the wild-type hA$_1$AR. Among them, mutant receptors A52V$^{2.47}$, D55V$^{2.50}$, R122Q$^{4.40}$, L134F$^{4.52}$, W188C$^{5.46}$ and T257P$^{6.58}$ even showed similar activities as yeast cells transformed by empty vector. In contrast, increased constitutive activity was observed on two mutant receptors, i.e. H78L$^{3.23}$ and S246T$^{6.47}$.
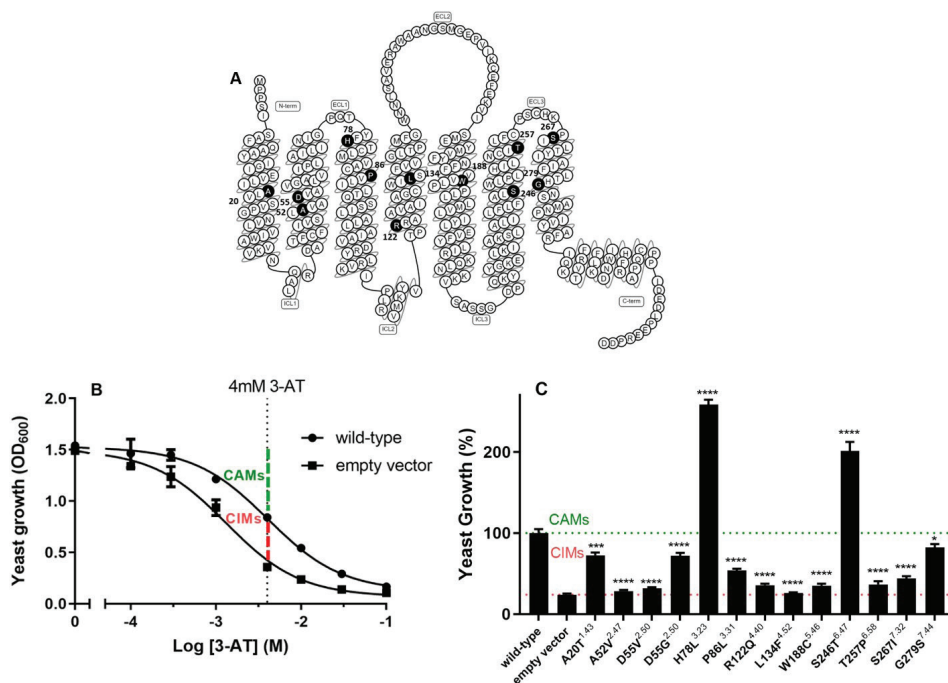
Figure 1. (A) Snake-plot of wild-type hA$_1$AR. Mutated residues are marked in black. (B) Concentration-growth curves of yeast strain in the presence or absence of wild-type hA$_1$AR. Combined graph is shown as mean ± SEM from three individual experiments performed in duplicate. (C) Constitutive activity of wild-type and 13 mutant hA$_1$ARs in the presence of 4 mM 3-AT. The yeast growth with wild-type hA$_1$AR was set to 100% and the background of the selection medium was set to 0%. The bar graph is the combined result of three independent experiments performed in quadruplicate.
[*] $p < 0.05$; [***] $p < 0.001$; [****] $p < 0.0001$ compared to wild-type hA$_1$AR, determined by using one-way ANOVA with Dunnett's post-test.
CAM: constitutively active mutant, CIM: constitutively inactive mutant

Agonist-induced receptor activation of mutant hA$_1$ARs

To further characterize the activation profiles of these mutations, concentration-growth curves were determined in the presence of increasing concentrations of the selective hA$_1$AR full agonist, CPA (Figure 2 and Table 2). Wild-type hA$_1$AR showed a potency/pEC$_{50}$ value of 9.30 ± 0.08 and a maximum effect/E$_{max}$ value (ratio over wild-type basal activity) of 4.83 ± 0.30 in the yeast system (Table 2).

Almost half of the mutant receptors with decreased constitutive activity could not be activated by CPA anymore, namely D55V$^{2.50}$, D55G$^{2.50}$, P86L$^{3.31}$, L134F$^{4.52}$, T257P$^{6.58}$ and S246I$^{7.32}$, which resulted in typing them as loss of function mutants (Figure 2 and Table 2). Other mutant receptors with decreased constitutive activity could still be activated by CPA with equal or lower potency and efficacy values. Specifically, in response to CPA, mutant receptors A20T$^{1.43}$, R122Q$^{4.40}$ and G279S$^{7.44}$ were activated to a similar activation level as wild-type hA$_1$AR with pEC$_{50}$ values of 9.24 ± 0.08, 9.04

± 0.14 and 9.27 ± 0.09, which were also not significantly different from the pEC_{50} value of the wild-type receptor. Mutant receptor $A52V^{2.47}$ had a much lower efficacy (1.86 ± 0.14) in the presence of 1 µM of CPA than wild-type hA_1AR, and also showed a more than 400-fold decreased potency. The activation level of mutant receptor $W188C^{5.46}$ was similar to wild-type hA_1AR (4.35 ± 0.10), while the potency of CPA was decreased by 10-fold.

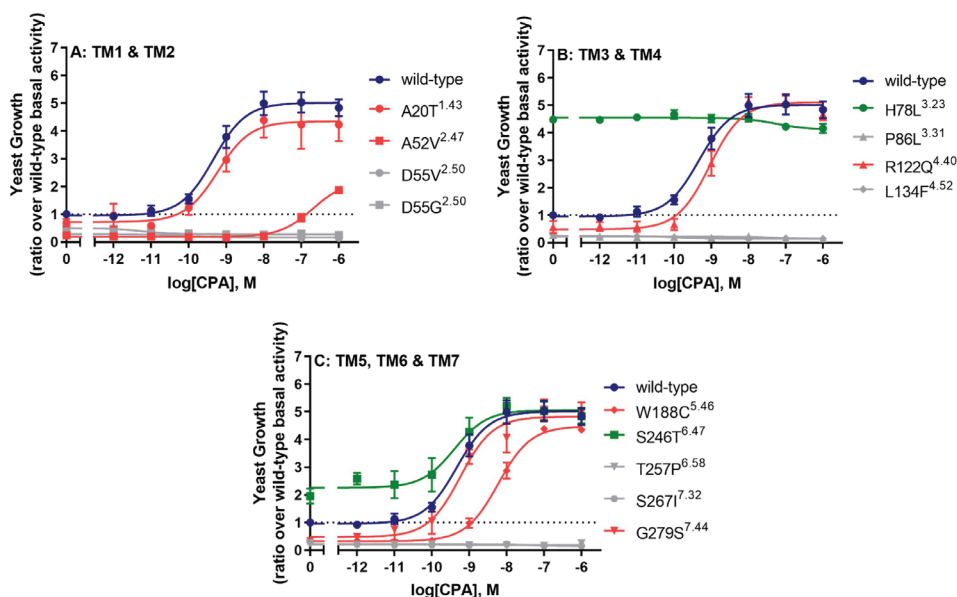The two mutant receptors with increased constitutive activity, namely $H78L^{3.23}$

Figure 2. Concentration-response curves of wild-type and mutated hA_1ARs. Data is separated for mutations located on (A) 1st and 2nd transmembrane helix, (B) 3rd and 4th transmembrane helix and (C) 5th, 6th and 7th transmembrane helix. Data were normalized as ratio over basal activity of wild-type hA_1AR (dotted line). Combined graphs are shown as mean ± SEM from at least three individual experiments performed in duplicate. Data for wild-type is shown in dark blue, for CIMs in red, for CAMs in green and for LFMs in grey.
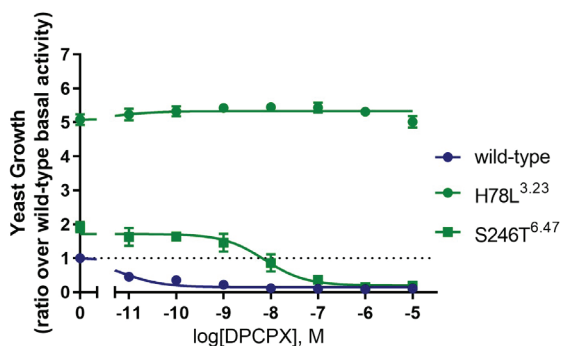

Figure 3. Concentration-inhibition curves of the hA_1AR inverse agonist DPCPX at the wild-type A_1AR and the CAMs, $H78L^{3.23}$ and $S246T^{6.47}$. Data were normalized as ratio over basal activity of wild-type hA_1AR (dotted line). Combined graphs are shown as mean ± SEM from at least three individual experiments performed in duplicate. Data for wild-type is shown in dark blue and for CAMs in green.

and S246T$^{6.47}$, also showed increased constitutive activity in concentration-growth curves. In response to CPA, mutant receptor S246T$^{6.47}$ was activated to a similar E$_{max}$ level (4.81 ± 0.26) with a similar pEC$_{50}$ value for CPA (9.42 ± 0.33) as at the wild-type hA$_1$AR (Figure 2C and Table 2). Interestingly, mutant receptor H78L$^{3.23}$ showed a 4.5-fold increase in constitutive activity compared to wild-type, where further activation could not be obtained anymore by addition of CPA (Figure 2B and Table 2).

Next, we investigated whether the increased constitutive activity of these two mutants could be decreased using an inverse agonist, DPCPX (Figure 3). For mutant receptor S246T$^{6.47}$, DPCPX reduced the constitutive activity to wild-type hA$_1$AR levels with a pIC$_{50}$ value of 8.55 ± 0.25. However, the high constitutive activity of mutant receptor H78L$^{3.23}$ was not reduced by DPCPX.

Evaluating the diverse pharmacological effects of these mutant receptors, we characterized mutant receptors H78L$^{3.23}$ and S246T$^{6.47}$ as CAMs, mutant receptors A20T$^{1.43}$, A52V$^{2.47}$, R122Q$^{4.40}$, W188C$^{5.46}$ and G279S$^{7.44}$ as CIMs and mutant receptors D55V$^{2.50}$, D55G$^{2.50}$, P86L$^{3.31}$, L134F$^{4.52}$, T257P$^{6.58}$ and S267I$^{7.32}$ as loss of function

6

Table 2. Agonist (CPA)-induced receptor activation of wild-type and mutant hA$_1$ARs in yeast liquid growth assays.

Mutation	Basal[a]	pEC$_{50}$ (-log M)	E$_{max}$[a]	Type[b]
Wild-type	1.00 ± 0.08	9.30 ± 0.08	4.83 ± 0.30	-
A20T$^{1.43}$	0.68 ± 0.14	9.24 ± 0.08	4.23 ± 0.60	CIM
A52V$^{2.47}$	0.24 ± 0.02[***]	6.68 ± 0.09[****]	1.86 ± 0.14[**]	CIM
D55V$^{2.50}$	0.24 ± 0.04[***]	ND	ND	LFM
D55G$^{2.50}$	0.50 ± 0.06[**]	ND	ND	LFM
H78L$^{3.23}$	4.48 ± 0.12[****]	ND	4.15 ± 0.17	CAM
P86L$^{3.31}$	0.28 ± 0.03[**]	ND	ND	LFM
R122Q$^{4.40}$	0.57 ± 0.22	9.04 ± 0.14	4.67 ± 0.22	CIM
L134F$^{4.52}$	0.29 ± 0.04[**]	ND	ND	LFM
W188C$^{5.46}$	0.32 ± 0.02[**]	8.21 ± 0.10[**]	4.35 ± 0.10	CIM
S246T$^{6.47}$	1.95 ± 0.27[*]	9.42 ± 0.33	4.81 ± 0.26	CAM
T257P$^{6.58}$	0.24 ± 0.01[*]	ND	ND	LFM
S267I$^{7.32}$	0.28 ± 0.01[*]	ND	ND	LFM
G279S$^{7.44}$	0.33 ± 0.12[*]	9.27 ± 0.09	4.96 ± 0.38	CIM

Mutations are indicated using the numbering of the hA$_1$AR amino acid sequence as well according to the Ballesteros and Weinstein GPCR numbering system[24]. All values are shown as mean ± SEM obtained from at least three individual experiments performed in duplicate.
[a] Values were calculated as ratio over basal activity of wild-type hA$_1$AR.
[b] Typing of the mutants was done according to their constitutive (in)activity and agonist-induced receptor activation.
[**] $p < 0.01$; [***] $p < 0.001$; [****] $p < 0.0001$ compared to wild-type hA$_1$AR, determined by a two-tailed unpaired Student's t-test.
ND: not detectable, CAM: constitutively active mutant, CIM: constitutively inactive mutant, LFM: loss of function mutant

mutants (LFMs) (Table 2).

Ligand binding on wild-type and mutant hA$_1$ARs

Selected mutants with diverse effects on receptor activation, i.e. H78L[3.23], L134F[4.52], W188C[5.46], S246T[6.47] and G279S[7.44], were further investigated on ligand binding in a mammalian expression system. Wild-type and mutant receptors were transiently transfected into Chinese Hamster Ovary (CHO) cells, and receptor expression levels were measured by ELISA. All mutant receptors were expressed on the cell surface with similar levels to the wild-type hA$_1$AR (Figure 4A).

Affinity values of the radioligand [^{3}H]DPCPX and B$_{max}$ values of wild-type and mutant hA$_1$ARs were determined by homologous competition displacement assays on transiently transfected membranes (Figure 4 and Table 3). [^{3}H]DPCPX had a pK$_D$ value of 8.36 ± 0.03 at the wild-type hA$_1$AR, which was significantly higher than the value on LFM L134F[4.52] (8.06 ± 0.08), but lower than the value on CIM G279S[7.44] (8.62 ± 0.06, Table 3). Mutant receptors H78L[3.23], W188C[5.46] and S246T[6.47] showed similar pK$_D$ values of [^{3}H]DPCPX compared to the wild-type hA$_1$AR. Diverse B$_{max}$ values were obtained on mutant receptors in comparison to wild-type hA$_1$AR (1.18 ± 0.14 pmol/mg). A significantly increased expression level of 3.74 ± 0.65 pmol/mg was observed on LFM L134F[4.52], while expression levels of CAMs H78L[3.23] and S246T[6.47] were decreased (0.17 ± 0.01 pmol/mg and 0.11 ± 0.01 pmol/mg). Note that these values did not correlate with the cell surface expression data obtained from ELISA.

Heterologous displacement by CPA of [^{3}H]DPCPX radioligand binding on all mutant receptors as well as wild-type hA$_1$AR, was best fitted to a two-site model (Figure 4C and Table 3). Wild-type hA$_1$AR had a pK$_i$ value of 9.24 ± 0.26 for the high affinity state, 6.76 ± 0.05 for the low affinity state with a fraction value of 0.15 ± 0.03 for the high affinity state. Decreased pK$_i$ values were observed on CIM W188C[5.46] for both high and low affinity states (8.02 ± 0.16 at high affinity state and 6.15 ± 0.01 at low affinity state). LFM L134F[4.52] also showed a decreased affinity value of 6.26 ± 0.11 at the low affinity state compared to wild-type receptor, while the high affinity state was unchanged. Lastly, CAM S246T[6.47] had an increased affinity value of 7.19 ± 0.08 at the low affinity state with an unaffected affinity on the high affinity state.

[^{35}S]GTPγS functional assay on wild-type and mutant hA$_1$ARs

CHO cell membranes transiently transfected with wild-type and mutant hA$_1$AR were further tested in a functional assay, i.e. GTPγS binding (Figure 5 and Table 4). All selected mutant receptors showed a similar basal activity to wild-type hA$_1$AR. In response to CPA wild-type hA$_1$AR showed a potency/pEC$_{50}$ value of 8.98 ± 0.08 and an E$_{max}$ value (ratio over wild-type basal activity) of 1.48 ± 0.13. Only CIM W188C[5.46] showed altered receptor pharmacology upon activation by CPA with a decreased potency value of 8.28 ± 0.10, while the efficacy was not significantly affected. While
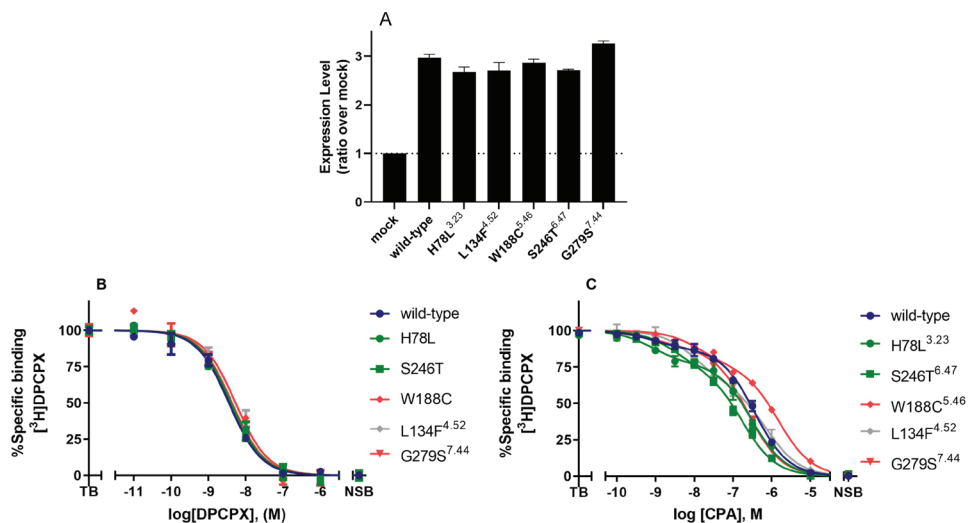
Figure 4. (A) Cell surface expression levels of wild-type and mutant hA$_1$AR transiently transfected on CHO cell membranes, as determined by ELISA. Data were normalized as ratio over mock transfected CHO cells (mock, dotted line) and shown as mean ± SEM obtained from three individual experiments performed in pentaplicate. (B and C) Displacement of specific [^{3}H]DPCPX binding to the transiently transfected wild-type hA$_1$AR, LFM L134F$^{4.52}$, CIMs W188C$^{5.46}$ and G279S$^{7.44}$, and CAMs H78L$^{3.23}$ and S246T$^{6.47}$ on CHO cell membranes by DPCPX and CPA, respectively. Combined graphs are shown as mean ± SEM from three individual experiments, each performed in duplicate. Data for wild-type is shown in dark blue, for CIMs shown in red, for CAMs in green and for LFMs in grey.
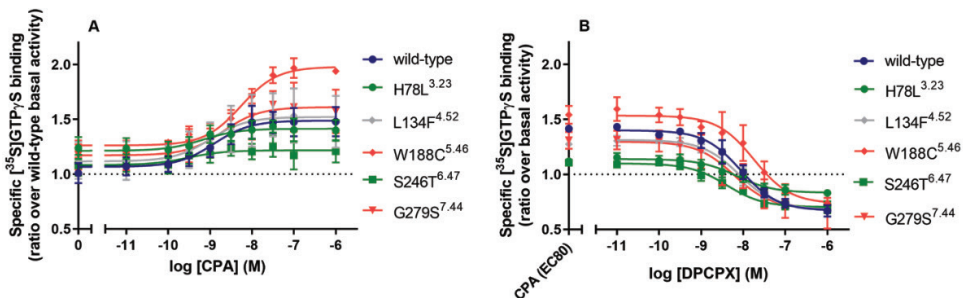

Figure 5. [^{35}S]GTPγS binding to the transiently transfected wild-type hA$_1$AR, LFM L134F$^{4.52}$, CIMs W188C$^{5.46}$ and G279S$^{7.44}$, and CAMs H78L$^{3.23}$ and S246T$^{6.47}$ on CHO cell membranes. (A) Receptor activation of wild-type and mutant hA$_1$ARs stimulated by CPA. Data were normalized as ratio over basal activity of wild-type hA$_1$AR. (B) Concentration-inhibition curves of DPCPX with the presence of CPA at the concentration of EC$_{80}$ for wild-type and mutant hA$_1$AR. Data were normalized as ratio over basal activity of wild-type or mutant hA$_1$AR. Data were obtained from three different experiments each performed in duplicate. Data for CIMs are shown in red, for CAMs in green and for LFMs in grey.

LFM L134F$^{4.52}$ did not show any activation in the yeast system, it could be activated in the mammalian system with similar potency and efficacy values for CPA compared to wild-type. CAM S246T$^{6.47}$ showed an altered receptor pharmacology upon CPA-

mediated activation with a higher pEC_{50} value of 9.44 ± 0.22 and slightly lower efficacy value of 1.21 ± 0.10 than wild-type hA_1AR, albeit not significantly different. CIM $G279S^{7.44}$ did not show a significantly different receptor pharmacology to wild-type hA_1AR in the mammalian system. Next, we investigated whether the agonist-mediated activation could be inhibited by the antagonist, DPCPX, on wild-type and mutant receptors (Figure 5B). For the wild-type receptor, the activation level was reduced to 0.67 ± 0.05 with a pIC_{50} value of 8.09 ± 0.16 for DPCPX. In the mammalian system, the CPA-mediated activation for all mutant receptors was reduced to wild-type levels with similar pIC_{50} values (Table 4).

Table 3. Affinity and B_{max} values of [^{3}H]DPCPX and binding affinity of CPA on wild-type and mutant hA_1ARs.

	[^{3}H]DPCPX[a]		CPA		
	pK_D	B_{max} (pmol/mg)	pK_i (high)	pK_i (low)	Fraction (high)
Wild-type	8.36 ± 0.03	1.81 ± 0.14	9.24 ± 0.26	6.76 ± 0.05	0.15 ± 0.03
H78L[3.23]	8.46 ± 0.03	0.17 ± 0.01**	8.97 ± 0.35	6.83 ± 0.09	0.33 ± 0.04
L134F[4.52]	8.06 ± 0.08**	3.74 ± 0.65**	8.38 ± 0.29	6.26 ± 0.11**	0.34 ± 0.03
W188C[5.46]	8.42 ± 0.03	1.87 ± 0.12	8.02 ± 0.16*	6.15 ± 0.01***	0.29 ± 0.01
S246T[6.47]	8.44 ± 0.05	0.11 ± 0.01**	8.98 ± 0.16	7.19 ± 0.08**	0.26 ± 0.03
G279S[7.44]	8.62 ± 0.06*	2.11 ± 0.07	8.74 ± 0.48	6.78 ± 0.06	0.17 ± 0.04

All values are shown as mean ± SEM obtained from at least three individual experiments performed in duplicate.
[a] Values obtained from homologous displacement of ~1.6, 4.5 and 10 nM [^{3}H]DPCPX from transiently transfected wild-type and mutant CHO-hA_1AR membranes at 25°C.
* $p < 0.05$; ** $p < 0.01$; *** $p < 0.001$ compared to wild-type hA_1AR, determined by one-way ANOVA with Dunnett's post-test.

Table 4. Potency and efficacy values of CPA and DPCPX in [^{35}S]GTPγS binding assays on wild-type and mutant hA_1ARs.

	CPA			DPCPX	
	Basal[a]	pEC_{50}	E_{max}[a]	pIC_{50}	I_{max}[b]
Wild-type	1.00 ± 0.09	8.98 ± 0.08	1.48 ± 0.13	8.09 ± 0.16	0.67 ± 0.05
H78L[3.23]	1.24 ± 0.10	9.09 ± 0.12	1.40 ± 0.10	8.19 ± 0.25	0.83 ± 0.03
L134F[4.52]	1.12 ± 0.17	9.08 ± 0.16	1.48 ± 0.24	8.14 ± 0.23	0.68 ± 0.01
W188C[5.46]	1.21 ± 0.06	8.28 ± 0.10*	1.94 ± 0.02	7.87 ± 0.25	0.74 ± 0.03
S246T[6.47]	1.08 ± 0.10	9.44 ± 0.22	1.21 ± 0.10	8.44 ± 0.10	0.70 ± 0.05
G279S[7.44]	1.17 ± 0.13	8.69 ± 0.10	1.57 ± 0.20	8.23 ± 0.06	0.65 ± 0.08

All values are shown as mean ± SEM obtained from at least three individual experiments performed in duplicate.
[a] Values were calculated as ratio over basal activity of wild-type hA_1AR.
[b] Values were calculated as ratio over basal activity of wild-type or mutant hA_1AR.
* $p < 0.05$ compared to wild-type hA_1AR, determined by one-way ANOVA with Dunnett's post-test.

Structural mapping and bioinformatics analysis of mutations

The mutations investigated in this study were mapped on the inactive (5UEN) and active (6D9H) hA$_1$AR structure to provide structural hypotheses for the observed pharmacological effects (i.e. CIM, CAM and LFM) of the different mutations, and explain differences between yeast and mammalian data. Mutations were found scattered over the receptor structure, with LFMs indicated in black, CIMs in red, and CAMs in green (Figure 6A). Whilst some LFMs can be considered drastic changes (for instance T257P$^{6.58}$ and P86L$^{3.31}$), others are relatively mild from a structural perspective (e.g. S267I$^{7.32}$). LFMs D55V/G$^{2.50}$ sit in the sodium ion binding pocket in direct contact with the sodium ion (Figure 6B). The CAM S246T$^{6.47}$ is found near the middle of helix 6, which undergoes a large conformational change upon receptor activation (Figure 6C). Finally, W188C$^{5.46}$ and L134F$^{4.52}$ are positioned closely to one another and point towards the membrane.

6

Discussion

Although the role of hA$_1$AR in cancer progression still remains unclear, a growing amount of studies suggest that hA$_1$AR is involved in cancer development[13,14]. Previous structural studies and crystal structures of hA$_1$AR provided us with information on crucial residues for ligand binding and receptor activation, as well as essential interactions in the inactive receptor state and in G protein coupling[17,32,33,37]. Therefore, in this study we studied 13 single-site point mutations located at the 7-TM domains of A$_1$AR obtained from The Cancer Genome Atlas (TCGA). All mutations were examined in the *S. cerevisiae* system and a selection of mutations were further investigated in the mammalian system to improve our understanding of the mechanism of receptor activation with respect to cancer development and progression.

Mutations located at the top part of receptor

Mutant receptors H78L$^{3.23}$, P86L$^{3.31}$, T257P$^{6.58}$ and S267I$^{7.32}$, located at the top, extracellular part of the receptor, all showed dramatic changes upon receptor activation in the yeast system. Mutant receptor H78L$^{3.23}$ showed an extremely high constitutive activity, which could not be further induced by CPA or reduced by DPCPX (Figure 2C, 3 and Table 2). Although this could not be confirmed in the mammalian system (probably due to its low expression level), it indicates that H78L$^{3.23}$-hA$_1$AR is locked in an active conformation, which has been described previously on mutant receptor G14T$^{1.37}$ in hA$_1$AR[31]. Similar expression levels were not observed in between ELISA and homologous competition assays (Figure 4A and Table 3) due to different experimental setups that whole cell expression of functioning receptors were determined in homologous competition assays[38]. Crystallographic structural evidence of the inactive-state A$_1$AR reveals that H78$^{3.23}$ forms a salt bridge with E164, which is important for the stabilization of a β-sheet between EL1 and EL2[32].
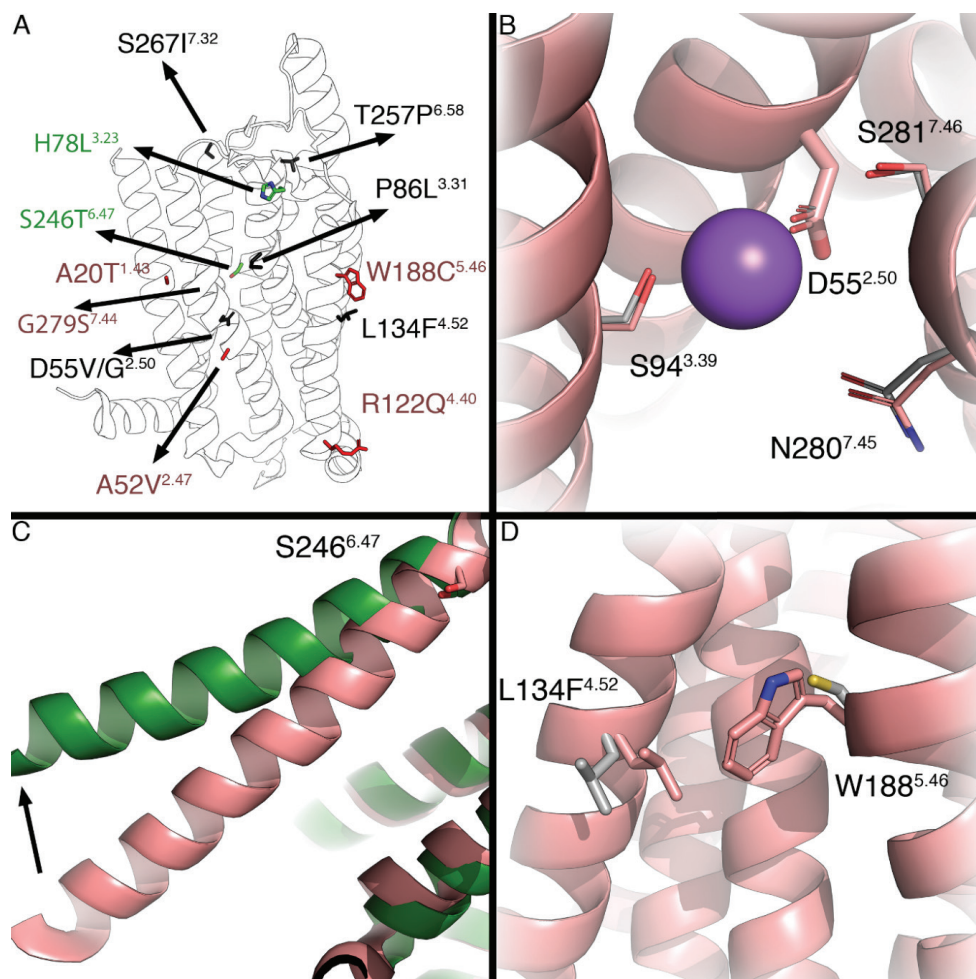
Figure 6. A) Overview of all mutations mapped on the X-ray structure of the hA$_1$AR, inactive (5UEN) in red and active (6D9H) in green. Residues are colored by their observed effect, CAMs in green, CIMs in red and LFMs in black. B) Close up of residue D55$^{2.50}$. In grey, residues that are found in the A$_{2A}$AR binding site, with the sodium ion from that structure (PDB: 4EIY) in purple. C) Residue S246$^{6.47}$ is found near the hinging region of TM6, the outward motion of which is associated with receptor activation (shown with arrow). D) Residues L134$^{4.52}$ and W188$^{5.46}$ form a cluster and are pointing toward the membrane.

It is known that ELs are essential in ligand binding and the receptor activation mechanism in class A GPCR[18]. Therefore, we hypothesize that the loss of the anionic charge hinders the salt bridge formation and stabilizes the receptor conformation in its active state.

Mutant receptors P86L$^{3.31}$, T257P$^{6.58}$ and S267I$^{7.32}$ were characterized as LFMs with complete loss of activation. Although this could be due to loss of expression (expression levels could not be determined in yeast), it had been shown in a previous study on A$_1$AR that mutant receptor P86F$^{3.31}$ resulted in abolished CPA binding. This indicates

that the proline at residue 86 indirectly affects ligand binding by re-orienting the TM1 conformation to favor N^6 substituents[39]. Both P86L[3.31] and P86F[3.31] are mutations in which the small size and rigid residue proline was exchanged by larger amino acids with hydrophobic side chains. Introduction of these larger side chains is potentially the causal factor for the loss of receptor activation. The residue T257[6.58], located at the top part of the helix 6, forms a hydrophobic pocket along with M177[5.35], L253[6.54] and T270[7.35] which has been shown to accommodate the antagonist DU172 in the A$_1$AR[32]. In A$_{2A}$AR, an alanine mutation at residue T256[6.58] has been shown to result in decreased affinity of reference antagonist ZM241385[40]. It is known that proline introduces kinks in α-helices due to the absence of an H-bond donor in addition to steric hindrance disrupting amide backbone hydrogen bond formation[41]. Therefore, in A$_1$AR, the proline mutation at T257[6.58] likely altered the receptor conformation, and resulted in loss of receptor activation. Mutant receptor S267I[7.32], located at the top of helix 7 and end of ECL3, showed a complete loss of activation in response to CPA, indicating that residue S267 may indirectly affect ligand binding.

Mutations located on conserved residues

Conserved residues and motifs of GPCRs are known to mediate ligand binding and receptor functionality[19]. Thus, mutations located at these residues may cause prominent alterations of receptor pharmacology. Alanine at residue 2.47 is highly conserved among class A GPCRs (72 %)[42]. Mutant receptor A52V[2.47] showed a dramatic decrease in both potency and efficacy of CPA (Figure 2A and Table 2), which could not be confirmed in mammalian cells due to a lack of expression. Interestingly, this same mutation occurs in CCR5, where this seemingly small change in the side chain, has been reported to greatly affect binding of CCL5[43], indicating the essential role of residue A2.47 in receptor-ligand interaction.

Two LFMs, D55G[2.50] and D55V[2.50], are found at residue D[2.50], which is the most highly conserved residue among class A GPCRs (92 %)[44]. D[2.50] together with S[3.39] regulates Na$^+$-binding[45]. Mutations at residue D[2.50] are known to alter ligand binding and/or G protein signaling[34,46]. Abolished G protein signaling has also been reported on mutant receptor D52N[2.50] in A$_{2A}$AR, in which it was shown that inter-helical packing was impacted by the change from aspartic acid to asparagine[46]. Therefore, our results implicate that the loss of the negatively charged side chain in D[2.50] impedes electrostatic interactions with Na$^+$-ions and thereby leads to decreased receptor activation.

S246[6.47] belongs to the conserved CWxP motif in helix 6, which is classified as the microswitch region and associated with receptor activation[47]. In the CWxP motif, cysteine at residue 6.47 is conserved by 71 % among class A GPCR and serine is 10 %[44]. In both yeast and mammalian systems, mutant receptor S246T[6.47] showed slightly increased potency values of CPA (Figure 2C, 5A, Table 2 and 4). The increase in potency value could be caused by the increase in ligand binding of CPA (Figure 4C). Additionally, hA$_1$AR was not locked in the active conformation by mutation

S246T[6.47], as DPCPX could still deactivate the receptor (Figure 3). Similarly, in the ß$_2$-adrenergic receptor, the mutation C285T[6.47] has been characterized as a CAM, while C285S[6.47] had similar properties to the wild-type receptor[47]. As it is known that residue 6.47 is crucial for the rotamer toggle switch[47], a threonine mutation on 6.47 may alter the side chain modulation of the rotamer toggle switch, therefore, further impacting the movement of TM6 during receptor activation.

Mutations located on residues pointing towards the membrane

In mammalian cell membranes, cholesterol has been reported to have a modulatory role in GPCR function via interaction with residues in the lipid-protein interface[48]. Moreover, compared to the membranes of mammalian cells, the yeast cell membrane contains less cholesterol and more ergosterol, which may result in a different receptor conformation, and thus functionality of human GPCRs between expression systems[48,49]. Moreover, the conflicting results obtained from different expression systems could be caused by differences in receptor expression levels.

Mutant receptor G279S[7.44] has been characterized as a CIM with retained potency and efficacy of CPA in the yeast system, while decreased constitutive activity could not be observed in the mammalian system, possibly due to the slightly higher expression level than wild-type hA$_1$AR. Interestingly, G279S[7.44] has also been identified as a Parkinson's disease-associated mutation, which did not alter receptor expression or ligand binding but influenced the heteromerization with the dopamine D$_1$ receptor[50].

Mutant receptor W188C[5.46] showed a 10-fold decrease in the potency value of CPA in both yeast and mammalian systems (Figure 2C, Figure 5A,Table 4 and Table 2). This decrease in potency was caused by the decrease in affinity of CPA (Figure 4C and Table 3). Despite the maintenance of hydrophobicity of the side chain, the substitution of tryptophan to cysteine introduced a dramatic reduction of side chain size. Reducing the amino acid side chain size at position W188[5.46] may affect the receptor-ligand interaction of CPA on hA$_1$AR. Moreover, it has been shown that W188[5.46] together with residues V137[4.55], F144[4.62], W146, Y182[5.40], F183[5.41] and V187[5.45] are part of a hydrophobic core, which along with residues S150 and R154 forms contacts with the EL2 of two A$_1$AR homodimers in mammalian cells[32]. It has been hypothesized that EL2 exerts a crucial role in the transition between G protein-coupled and -uncoupled states[51]. While it was previously suggested that A$_1$AR homodimerizes, leading to cooperative orthosteric ligand binding in mammalian cells[52], the homodimerization of A$_1$AR in yeast cells remains undetermined.

Residue L134[4.52] forms a cluster with W188[5.46] pointing towards the membrane (Figure 6D). Mutant receptor L134F[4.52] has been characterized as LFM in the yeast system. However, it behaved quite similar to wild-type A$_1$AR in the mammalian system (Figure 5 and Table 4). L134[4.52] is conserved amongst all ARs and located close to the highly conserved residue in TM4, W[4.50]. The latter is known to be involved in ligand binding and interaction with the cell membrane via cholesterol,

where complete loss of ligand binding has been observed previously by mutating tryptophan to other amino acids[48,53,54]. Phenylalanine mutation at L134[4.52] might thus indirectly change the interaction among residues W132[4.50], L99[3.44], A100[3.45], L193[5.51] and Y200[5.58] [53], by the dramatic size change of the side chain, and this might be different when using a different cell membrane background.

Potential role for hA$_1$AR mutations in cancer

Activation of hA$_1$AR has been identified with anti-proliferative effects in colon cancer, glioblastoma and leukemia[10,55,56]. Mutations with inhibitory effects on receptor activation identified from colon cancer, such as the LFM D55G[2.50] and CIM W188C[5.46], might then behave as pro-proliferative regulators in cancer progression. In contrast, deletion or blockade of hA$_1$AR resulted in inhibited cell proliferation but induced PD-L1 upregulation in melanoma cells, which led to compromised anti-tumor immunity[57]. Additionally, the hA$_1$AR antagonist DPCPX shows inhibitory effects on tumor cell proliferation, migration, while promoting apoptosis[12,15]. Mutant receptors with altered binding affinity of DPCPX, namely L134F[4.52] and W188C[5.46] in this study, may thus impact the efficacy of DPCPX treatments. Of note, due to the low frequency in comparison to known driver mutations in cancer patients, these cancer-related mutations in hA$_1$AR are unlikely to be cancer-drivers[58]. However, passenger mutations should not be ruled out for in the consideration of cancer personalized therapy[59].

In conclusion, 13 cancer-induced somatic mutations located at the 7-transmembrane domain of the adenosine A$_1$ receptor were retrieved from TCGA and characterized in a robust yeast system. 2 CAMs (H78L[3.23] and S246T[6.47]), 1 LFM (L134F[4.52]) and 2 CIMs (W188C[5.46] and G279S[7.44]) were also investigated in mammalian cells. The yeast system is a suitable, rapid and accurate method for initial mutation screening that enables us to identify mutations with dramatic effect on receptor activation. However, the current study shows that this system is best used for receptor mutations on the extracellular side, ligand binding pocket or pointing inwards from the membrane. Based on the results of this study, follow-up studies in a disease-relevant system are warranted to further investigate the effect of these hA$_1$AR mutations in cell proliferation and migration, and eventually in cancer progression. Taken together, this study will enrich our understanding of the largely undefined role of hA$_1$AR in cancer progression, which may eventually improve cancer therapies.

References

1. Fredriksson, R., Lagerström, M. C., Lundin, L.-G. & Schiöth, H. B. The G-protein-coupled receptors in the human genome form five main families. Phylogenetic analysis, paralogon groups, and fingerprints. *Mol. Pharmacol.* **63**, 1256–72 (2003).
2. Vassilatis, D. K. *et al*. The G protein-coupled receptor repertoires of human and mouse. *Proc. Natl. Acad. Sci.* **100**, 4903–4908 (2003).
3. Lagerström, M. C. & Schiöth, H. B. Structural diversity of G protein-coupled receptors and significance for drug discovery. *Nat. Rev. Drug Discov.* **7**, 339–57 (2008).
4. Pierce, K. L., Premont, R. T. & Lefkowitz, R. J. Seven-transmembrane receptors. *Nat. Rev. Mol. Cell Biol.* **3**, 639–650 (2002).

5. Kan, Z. *et al.* Diverse somatic mutation patterns and pathway alterations in human cancers. *Nature* **466**, 869–73 (2010).
6. Lappano, R. & Maggiolini, M. GPCRs and cancer. *Acta Pharmacol. Sin.* **33**, 351–362 (2012).
7. Dorsam, R. T. & Gutkind, J. S. G-protein-coupled receptors and cancer. *Nat. Rev. Cancer* **7**, 79–94 (2007).
8. Gonzalez, H., Hagerling, C. & Werb, Z. Roles of the immune system in cancer: From tumor initiation to metastatic progression. *Genes Dev.* **32**, 1267–1284 (2018).
9. Vijayan, D., Young, A., Teng, M. W. L. & Smyth, M. J. Targeting immunosuppressive adenosine in cancer. *Nat. Rev. Cancer* **17**, 709–724 (2017).
10. Gessi, S., Merighi, S., Sacchetto, V., Simioni, C. & Borea, P. A. Adenosine receptors and cancer. *Biochim. Biophys. Acta* **1808**, 1400–1412 (2011).
11. Merighi, S. *et al.* A glance at adenosine receptors: novel target for antitumor therapy. *Pharmacol. Ther.* **100**, 31–48 (2003).
12. Sek, K. *et al.* Targeting Adenosine Receptor Signaling in Cancer Immunotherapy. *Int. J. Mol. Sci.* **19**, 3837 (2018).
13. Merighi, S. *et al.* Pharmacological and biochemical characterization of adenosine receptors in the human malignant melanoma A375 cell line. *Br. J. Pharmacol.* **134**, 1215–1226 (2001).
14. Borea, P. A., Gessi, S., Merighi, S., Vincenzi, F. & Varani, K. Pharmacology of Adenosine Receptors: The State of the Art. *Physiol. Rev.* **98**, 1591–1625 (2018).
15. Zhou, Y. *et al.* The Adenosine A₁ Receptor Antagonist DPCPX Inhibits Tumor Progression via the ERK/JNK Pathway in Renal Cell Carcinoma. *Cell. Physiol. Biochem.* **43**, 733–742 (2017).
16. Mirza, A. *et al.* RNA interference targeting of A₁ receptor-overexpressing breast carcinoma cells leads to diminished rates of cell proliferation and induction of apoptosis. *Cancer Biol. Ther.* **4**, 1355–1360 (2005).
17. Peeters, M. C. *et al.* The role of the second and third extracellular loops of the adenosine A₁ receptor in activation and allosteric modulation. *Biochem. Pharmacol.* **84**, 76–87 (2012).
18. Peeters, M. C., van Westen, G. J. P., Li, Q. & IJzerman, A. P. Importance of the extracellular loops in G protein-coupled receptors for ligand recognition and receptor activation. *Trends Pharmacol. Sci.* **32**, 35–42 (2011).
19. Jespers, W. *et al.* Structural mapping of adenosine receptor mutations: ligand binding and signaling mechanisms. *Trends Pharmacol. Sci.* **39**, 75–89 (2017).
20. Beukers, M. W. *et al.* Random Mutagenesis of the Human Adenosine A₂ᵦ Receptor Followed by Growth Selection in Yeast. Identification of Constitutively Active and Gain of Function Mutations. *Mol. Pharmacol.* **65**, 702–710 (2004).
21. Stewart, G. D. *et al.* Determination of adenosine A₁ receptor agonist and antagonist pharmacology using *Saccharomyces cerevisiae*: Implications for ligand screening and functional selectivity. *J. Pharmacol. Exp. Ther.* **331**, 277–286 (2009).
22. Weinstein, J. N. *et al.* The Cancer Genome Atlas Pan-Cancer analysis project. *Nat. Genet.* **45**, 1113–1120 (2013).
23. UniProt: the universal protein knowledgebase. *Nucleic Acids Res.* **45**, D158–D169 (2017).
24. Ballesteros, J. A. & Weinstein, H. Integrated methods for the construction of three-dimensional models and computational probing of structure-function relations in G protein-coupled receptors. in *Methods in Neurosciences* **25**, 366–428 (1995).
25. Isberg, V. *et al.* Generic GPCR residue numbers – aligning topology maps while minding the gaps. *Trends Pharmacol. Sci.* **36**, 22–31 (2015).
26. Dowell, S. J. & Brown, A. J. Yeast Assays for G Protein-Coupled Receptors. in *Methods in molecular biology (Clifton, N.J.)* **552**, 213–229 (Springer New York, 2009).
27. Longo, P. A., Kavran, J. M., Kim, M. S. & Leahy, D. J. Transient mammalian cell transfection with polyethylenimine (PEI). *Methods Enzymol.* **529**, 227–240 (2013).
28. Heitman, L. H. *et al.* A Series of 2,4-Disubstituted Quinolines as a New Class of Allosteric Enhancers of the Adenosine A₃ Receptor. *J. Med. Chem.* **52**, 926–931 (2009).
29. Smith, P. K. *et al.* Measurement of protein using bicinchoninic acid. *Anal. Biochem.* **150**, 76–85 (1985).
30. Schöneberg, T., Liu, J. & Wess, J. Plasma Membrane Localization and Functional Rescue of Truncated Forms of a G Protein-coupled Receptor. *J. Biol. Chem.* **270**, 18000–18006 (1995).
31. de Ligt, R. A. F., Rivkees, S. A., Lorenzen, A., Leurs, R. & IJzerman, A. P. A "locked-on," constitutively active mutant of the adenosine A₁ receptor. *Eur. J. Pharmacol.* **510**, 1–8 (2005).
32. Glukhova, A. *et al.* Structure of the Adenosine A₁ Receptor Reveals the Basis for Subtype Selectivity. *Cell* **168**, 867-877.e13 (2017).
33. Draper-Joyce, C. J. *et al.* Structure of the adenosine-bound human adenosine A₁ receptor–Gᵢ complex. *Nature* **558**, 559–563 (2018).
34. Liu, W. *et al.* Structural basis for allosteric regulation of GPCRs by sodium ions. *Science.* **337**, 232–236 (2012).
35. Esguerra, M., Siretskiy, A., Bello, X., Sallander, J. & Gutiérrez-de-Terán, H. GPCR-ModSim: A comprehensive web based solution for modeling G-protein coupled receptors. *Nucleic Acids Res.* **44**, W455–W462 (2016).
36. Cheng, Y.-C. & Prusoff, W. H. Relationship between the inhibition constant (KI) and the concentration of inhibitor which causes 50 per cent inhibition (I50) of an enzymatic reaction. *Biochem. Pharmacol.* **22**, 3099–3108 (1973).
37. Nguyen, A. T. N. *et al.* Extracellular Loop 2 of the Adenosine A₁ Receptor Has a Key Role in Orthosteric Ligand Affinity and Agonist Efficacy. *Mol. Pharmacol.* **90**, 703–714 (2016).
38. Motulsky, H. J. & Neubig, R. R. Analyzing Binding Data. *Current Protocols in Neuroscience* **52**, 7.5.1-7.5.65 (2010).
39. Rivkees, S. A., Barbhaiya, H. & IJzerman, A. P. Identification of the adenine binding site of the human A₁ adenosine receptor. *J Biol Chem* **274**, 3617–3621 (1999).
40. Guo, D. *et al.* Molecular basis of ligand dissociation from the adenosine A₂ₐ receptor. *Mol. Pharmacol.* **89**, 485–491 (2016).
41. Chou, P. Y. & Fasman, G. D. Secondary structural prediction of proteins from their amino acid sequence. *Trends in Biochemical Sciences.* **2**, 128-131 (1977).
42. Isberg, V. *et al.* GPCRdb: an information system for G protein-coupled receptors. *Nucleic Acids Res.* **44**, D356–D364 (2016).
43. Howard, O. M. Z. *et al.* Naturally occurring CCR5 extracellular and transmembrane domain variants affect HIV-1 co-receptor and ligand binding function. *J. Biol. Chem.* **274**, 16228–16234 (1999).
44. Katritch, V. *et al.* Allosteric sodium in class A GPCR signaling. *Trends Biochem Sci* **39**, 233–244 (2014).
45. Barbhaiya, H., McClain, R., IJzerman, A. & Rivkees, S. A. Site-directed mutagenesis of the human A₁ adenosine receptor: influences of acidic and hydroxy residues in the first four transmembrane domains on ligand binding. *Mol. Pharmacol.* **50**, 1635–42 (1996).
46. White, K. L. *et al.* Structural Connection between Activation Microswitch and Allosteric Sodium Site in GPCR Signaling. *Structure* **26**, 259-269.e5 (2018).
47. Shi, L. *et al.* β₂ adrenergic receptor activation: Modulation of the proline kink in transmembrane 6 by a rotamer toggle switch. *J. Biol. Chem.* **277**, 40989–40996 (2002).
48. Paila, Y. D., Tiwari, S. & Chattopadhyay, A. Are specific nonannular cholesterol binding sites present in G-protein

coupled receptors? *Biochim. Biophys. Acta - Biomembr.* **1788**, 295–302 (2009).

49. Elkins, M. R., Sergeyev, I. V. & Hong, M. Determining Cholesterol Binding to Membrane Proteins by Cholesterol 13C Labeling in Yeast and Dynamic Nuclear Polarization NMR. *J. Am. Chem. Soc.* **140**, 15437–15449 (2018).

50. Nasrollahi-Shirazi, S. *et al.* Functional impact of the G279S substitution in the adenosine A$_1$-receptor (A$_1$R-G279S[7.44]), a mutation associated with Parkinson's disease. *Mol. Pharmacol.* **98**, 250-266 (2020).

51. Bokoch, M. P. *et al.* Ligand-specific regulation of the extracellular surface of a G-protein-coupled receptor. *Nature* **463**, 108–112 (2010).

52. Gracia, E. *et al.* Homodimerization of adenosine A$_1$ receptors in brain cortex explains the biphasic effects of caffeine. *Neuropharmacology* **71**, 56–69 (2013).

53. Suzuki, T. *et al.* A highly conserved tryptophan residue in the fourth transmembrane domain of the A$_1$ adenosine receptor is essential for ligand binding but not receptor homodimerization. *J. Neurochem.* **110**, 1352–1362 (2009).

54. Rhee, M. H., Nevo, I., Bayewitch, M. L., Zagoory, O. & Vogel, Z. Functional role of tryptophan residues in the fourth transmembrane domain of the CB2 cannabinoid receptor. *J. Neurochem.* **75**, 2485–2491 (2000).

55. Saito, M., Yaguchi, T., Yasuda, Y., Nakano, T. & Nishizaki, T. Adenosine suppresses CW2 human colonic cancer growth by inducing apoptosis via A$_1$ adenosine receptors. *Cancer Lett.* **290**, 211–215 (2010).

56. Lan, B. *et al.* Metformin suppresses CRC growth by inducing apoptosis via ADORA1. *Front. Biosci. - Landmark* **22**, 248–257 (2017).

57. Liu, H. *et al.* ADORA1 Inhibition Promotes Tumor Immune Evasion by Regulating the ATF3-PD-L1 Axis. *Cancer Cell* **37**, 324-339.e8 (2020).

58. Gimm, O. *et al.* Over-representation of a germline RET sequence variant in patients with sporadic medullary thyroid carcinoma and somatic RET codon 918 mutation. *Oncogene* **18**, 1369–1373 (1999).

59. Monticelli, M. *et al.* Passenger mutations as a target for the personalized therapy of cancer. *PeerJ* **Preprints**, (2018).

6

Chapter 7

Identification of V6.51L as a selectivity hotspot in stereoselective A$_{2B}$ adenosine receptor antagonist recognition.

Abstract

The four adenosine receptors (ARs) A_1AR, $A_{2A}AR$, $A_{2B}AR$, and A_3AR are G protein-coupled receptors (GPCRs) for which an exceptional amount of experimental and structural data is available. Still, limited success has been achieved in getting new chemical modulators on the market. As such, there is a clear interest in the design of novel selective chemical entities for this family of receptors. In this work, we investigate the selective recognition of ISAM-140, a recently reported $A_{2B}AR$ reference antagonist. A combination of semipreparative chiral HPLC, circular dichroism and X-ray crystallography was used to separate and unequivocally assign the configuration of each enantiomer. Subsequently affinity evaluation for both A_{2A} and A_{2B} receptors demonstrate the stereospecific and selective recognition of (*S*)-ISAM140 to the $A_{2B}AR$. The molecular modeling suggested that the structural determinants of this selectivity profile would be residue $V250^{6.51}$ in $A_{2B}AR$, which is a leucine in all other ARs including the closely related $A_{2A}AR$. This was herein confirmed by radioligand binding assays and rigorous free energy perturbation (FEP) calculations performed on the $L249^{6.51}V$ mutant $A_{2A}AR$ receptor. Taken together, this study provides further insights in the binding mode of these $A_{2B}AR$ antagonists, paving the way for future ligand optimization.

Introduction

Adenosine receptors (ARs) are a family of G protein-coupled receptors (GPCR) for which an exceptional amount of structural and experimental data is available[1,2]. Still, the number of therapeutic agents on the market that specifically target this family of receptors remains relatively low[3]. On the other hand, selectively targeting any of the four adenosine receptor subtypes (A$_1$, A$_{2A}$, A$_{2B}$ and A$_3$) provides an interesting avenue to address not only unmet therapeutic needs[4] and limited off-target effects[5], but also to help elucidating the (patho)physiological role of the different receptors within the family. One topic that is receiving increasing interest is the molecular mechanisms by which the two A$_2$AR subtypes regulate the immune response to tumor growth and metastasis[6].

Over the last years, different AR ligands have been developed with optimized selectivity profiles[7–9]. Within these AR ligand design programs, the generation of potent and selective antagonists has allowed the identification of powerful chemical tools to characterize each of the members of this receptor family. Examples include the A$_{2A}$AR selective antagonist ZM241385, and the A$_{2B}$AR selective antagonist ISAM-140, the latter originating from our in-house optimization program (Figure 1)[7,9–11]. The development of ISAM-140 was done following careful structure-affinity relationship (SAR) modeling, based on a computational binding mode of this chemotype, which suggested an important role of the stereogenic center in the heterocyclic scaffold in its high binding affinity (Figure 1)[7,11]. The prediction of the active stereoisomer for this chemotype was later confirmed indirectly by experimental characterization of the active stereoisomers for representative compounds of a series of cyanopyrimidines[10], fluorinated tricyclic derivatives[12] and aza-bioisosteres of the pentagonal heterocycle[13]. This binding model proposed that the stereospecific complementarity to the A$_{2B}$AR cavity was due to the optimal accommodation of the thiophene/furan ring around the chiral center of the core scaffold (Figure 1), with the A$_{2B}$AR specific residue V250$^{6.51}$ (Ballesteros Weinstein numbering in superscripts)[14]. Indeed, this valine is replaced by a leucine in all other AR subtypes, which could explain the highly selective profile of these series of non-planar antagonists towards the A$_{2B}$AR.
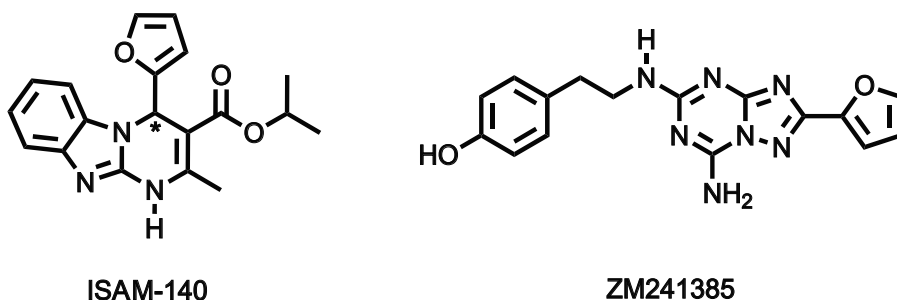

ISAM-140   **ZM241385**

Figure 1: 2D representation of the chemical structures of the AR ligands used in this work, i.e. ZM241385, (±) ISAM-140, (R)-ISAM-140 and (S)-ISAM-140. The chiral center in ISAM-140 is indicated with an asterisk.

In this work, we report the chiral separation of ISAM140 and confirm its stereospecific binding mode to the $A_{2B}AR$. An $A_{2A}AR$ construct was designed to include the corresponding $A_{2B}AR$ valine sidechain (L249V[6.51] $A_{2A}AR$ mutant), which in line with the starting hypothesis partially recovered the affinity for ISAM-140. Interestingly, this effect was observed for both stereoisomers of the antagonist, and is herein explained on the basis of structure-energetic modeling via rigorous free energy perturbation (FEP) calculations. These results validate the proposed role of V250[6.51] in the $A_{2B}AR$ subtype selectivity of these stereospecific chemotype, and paves the road for further design of selective antagonists as well as dual A_2AR ligands.

Methods

HPLC separation and characterization of ISAM-140 enantiomers

The chiral resolution was performed using a Water Breeze™ 2 (binary pump 1525, detector UV/Visible 2489, 7725i Manual Injector Kit 1500 Series). Compound ISAM-140 enantiomers were separated using a 250 mm x 20 mm Chiralpak® 5μm IE-3 (DAICEL) All the separations were performed at 25 ºC with hexane/isopropanol 7:3 as mobile phase. The enantiomers [(*R*)-ISAM-140 (3 mg, t_R = 17.90 min), (*S*)-ISAM-140 (3.1 mg, t_R = 20.31 min)] were isolated, their stereochemical purity analyzed by chiral HPLC (ee: 97-99% for each enantiomer) and then characterized by NMR.

Circular dichroism

Circular dichroism spectra were recorded on a Jasco-815 system equipped with a Peltier-type thermostatic accessory (CDF-426S, Jasco). Measurements were carried out at 20 °C using a 1 mm quartz cell in a volume of 600 μL. Compounds (0.5 mg) were dissolved in MeOH (1.0 mL) and then diluted 10-fld in MeOH. The instrument settings were bandwidth, 1.0 nm; data pitch, 1.0 nm; speed, 500 nm/min; accumulation, 10; wavelengths, 400−190 nm.

X-ray crystallography of ISAM-140 enantiomers

Crystals of (*S*)-ISAM-140 and (*R*)-ISAM-140 were grown by slow evaporation from ethanol solutions. For the crystal structure determination, the data were collected by applying the omega and phi scans method on a Bruker D8 VENTURE PHOTON III-14 diffractometer using Incoatec multilayer mirror monochromated with Cu-Kα radiation (λ = 1.54178 Å) from a microfocus sealed tube source at 100 K with detector resolution of 7.3910 pixels mm-1. Computing data and reduction were made with the APEX3 v2018.7-2 (BRUKER AXS, 2005). The structure was solved using SHELXT2018/22 and finally refined by full-matrix least-squares based on F2 by SHELXL2018/3.3 An empirical absorption correction was applied using the SADABS2016/2 program. Software used to molecular graphics: ORTEP for Windows. Software used to prepare material for publication: WinGX2018.3 publication routines4 and Mercury.

The obtained structures were refined as follows: All non-hydrogen atoms were refined anisotropically and the hydrogen atom positions were included in the model on the basis of Fourier difference electron density maps. All aromatic CH hydrogen (C-H = 0.95 Å), methine hydrogen (C-H = 1.0 Å) and methylene hydrogen (C-H=0.99 Å) atoms were refined using a riding model with Uiso(H) = 1.2 Ueq(C). The methyl hydrogen (C-H = 0.98 Å) atoms were refined as a rigid group with torsional freedom [Uiso(H) = 1.5 Ueq(C)] and the hydrogens atom of NH groups (HiN) as a free atom with Uiso(H) = 1.2 Ueq(C).

Site-directed mutagenesis

Site-directed mutants of the A$_{2A}$AR were generated by polymerase chain reaction (PCR) mutagenesis as described previously[15]. pcDNA3.1(+)-hA$_{2A}$AR with N-terminal HA and FLAG tags and a C-terminal His tag was used as the template. Primers for mutants L249V[6.51] and L249A[6.51] were designed by the QuikChange Primer Design Program of Agilent Technologies (Santa Clara, CA, USA) and primers were obtained from Eurogentec (Maastricht, The Netherlands). All DNA sequences were verified by Sanger sequencing at LGTC (Leiden, The Netherlands).

Cell culture and transient transfection

CHO cells stably expressing the human A$_{2B}$AR (CHO-spap-hA$_{2B}$AR) were cultured in Dulbecco's modified Eagle's medium: Nutrient Mixture F-12 (DMEM/F12) supplemented with 10% newborn calf serum, 50 µg/mL streptomycin, and 50 IU/mL penicillin at 37°C and 5% CO$_2$ atmosphere. Cells were subcultured twice a week at a confluency of 80 - 90%. For transient transfections, human embryonic kidney (HEK) 293 cells were cultured as monolayers in DMEM supplemented with stable glutamine, 10% newborn calf serum, 50 µg/mL streptomycin, and 50 IU/mL penicillin at 37°C and 7% CO$_2$ atmosphere as reported previously[15,16]. The cells were seeded on 10 cm ø plates and transfected with 10 µg plasmid DNA of wild-type (WT) or mutant hA$_{2A}$AR using the calcium phosphate precipitation method[17], followed by a 48-hour incubation.

Membrane preparation

HEK293 cells transiently expressing WT or mutant human A$_{2A}$AR (HEK293-hA$_{2A}$AR) were detached from the plates 48 h post-transfection by scraping into phosphate-buffered saline (PBS) and collected by centrifugation at 1,000 × g for 5 minutes. The pellets from 10 plates were pooled and resuspended in ice-cold Tris-HCl buffer (50 mM, pH 7.4) and then homogenized with an UltraTurrax homogenizer (Heidolph Instruments, Schwabach, Germany). The cell membrane suspensions were centrifuged at 100,000 × g at 4°C for 20 minutes in a Beckman Optima LE-80K ultracentrifuge. The pellet was resuspended in ice-cold Tris-HCl buffer, and the homogenization and centrifugation steps were repeated one more time. After this, Tris-HCl buffer was used to resuspend the pellet of HEK293 cell membranes. Membrane preparation for CHO-spap-hA$_{2B}$AR cells followed a similar procedure after

they were grown to 90% confluence in 15 cm plates, and membranes pellets were finally resuspended in Tris-HCL buffer containing 10 % (w/v) CHAPS. In both cases, 0.8 IU/ml adenosine deaminase was added to break down endogenous adenosine and membranes were aliquoted into 250 μL and stored at -80°C until further use. Membrane protein concentrations were determined using the BCA method[18].

Radioligand binding assays

Radioligand binding experiments on CHO-spap-hA$_{2B}$AR membranes were adjusted from previously reported data[19]. Membrane aliquots containing 30 μg of protein were incubated in a total volume of 100 μL of assay buffer. Nonspecific binding was determined with 10 μM ZM241385. Then 25 μL cell membrane suspension, 25 μL of 1.5 nM radioligand [^{3}H]PSB-603, 25 μL of assay buffer [50 mM Tris-HCl, 0.1 % (w/v) CHAPS, pH 7.4 at 25°C] and 25 μL of the indicated compounds in increasing concentrations in the same assay buffer were added to each well and followed by a 120 min incubation at 25 °C. Radioligand displacement experiments with transient HEK293-hA$_{2A}$AR cell membranes were performed as described previously[20]. Briefly, membrane aliquots containing 5-7.5 μg of protein were incubated in a total volume of 100 μL of assay buffer to adjust the assay window to approximately 2000 DPM. Nonspecific binding was determined in the presence of 100 μM NECA and represented less than 10% of the total binding. Then 25 μL membrane suspension (5-7.5 μg of protein), 25 μL of 5.0 nM radioligand [^{3}H]ZM241385, 25 μL of assay buffer [50 mM Tris-HCl, pH 7.4] and 25 μL of the indicated compounds at different concentrations in the same assay buffer were added to each well, with final assay concentration of radioligand of 5 nM. For homologous displacement experiments, radioligand displacement experiments were performed with the presence of three concentrations of [^{3}H]ZM241385 (1.7 nM, 5.0 nM and 9.5 nM) and increasing concentrations of unlabeled ZM241385. After 120 minutes at 25°C, incubations were terminated by rapid vacuum filtration through GF/B filter plates (PerkinElmer, Groningen, Netherlands) using a Perkin Elmer Filtermate-harvester. Filterplates were subsequently washed ten times with ice-cold assay buffer. Filter-bound radioactivity was determined by scintillation spectrometry using a Microbeta^2® 2450 microplate counter (PerkinElmer).

Data analysis

Data analyses were performed using GraphPad Prism 7.0 software (GraphPad Software Inc., San Diego, CA). pK_D values and B_{max} were obtained by non-linear regression analysis using "one-site homologous" model. pIC_{50} values were determined by fitting the data using non-linear regression to a sigmoidal concentration-response curve equation. pK_i values were calculated from pIC_{50} values using the Cheng-Prusoff equation[21].

Computational Modeling

The high resolution crystal structure of the A$_{2A}$AR (PDB code 4EIY[22]) was used as

a starting point for the calculations. The protein was prepared for MD simulations as follows: (i) removing co-factors and fused proteins employed for crystallization, (ii) reverting the crystal construct to the wild-type (WT) A$_{2A}$AR receptor, (iii) the assignment of protonation states of ionizable residues. (iv) mutation of the WT Leu249[6.51] to Val as in the corresponding A$_{2B}$AR and (v) membrane insertion using PyMemDyn[23]. The latter stage involves embedding of the protein in a pre-equilibrated POPC membrane, soaking of the system with bulk water and a short (5 ns) equilibration period with GROMACS 4.6.[24] using the OPLS-AA force field[25] and Berger parameters for the lipids[26]. Thereafter, ligands were manually docked to the equilibrated receptor using as a reference the putative binding mode of SYAF014[7] to the A$_{2B}$AR previously described. In the case of ZM241385, the coordinates of the crystal structure ligand were retained during the equilibration process. Subsequently, each equilibrated L249[6.51]V-A$_{2A}$AR-ligand complex was transferred to the MD software Q[27] for free energy perturbation (FEP) calculations under spherical boundary conditions using QligFEP[28]. A 25Å sphere centered on the center of geometry of the ligand was constructed for these MD simulations. Solvent atoms were subject to polarization and radial restraints using the surface-constrained all-atom solvent (SCAAS)[29] model to mimic the properties of bulk water at the sphere surface. Atoms lying outside the simulation sphere were tightly constrained (200 kcal/mol/Å^2 force constant) and excluded from the calculation of non-bonded interactions. Long range electrostatic interactions beyond a 10 Å cut off were treated with the local reaction field method[30], except for the atoms undergoing the FEP transformation, where no cutoff was applied. Solvent bond and angles were constrained using the SHAKE algorithm[31]. All titratable residues outside the sphere were neutralized as reported elsewhere[28]. Residue parameters were translated from the OPLS-AA/M force field[32] and the parameters for the ligand and lipids were inherited from the previous MD stage. The simulation sphere was warmed up from 0.1 to 298 K, during a first equilibration period of 0.61 nanoseconds, where an initial restraint of 25 kcal/mol/Å^2 imposed on all heavy atoms was slowly released for all complexes. Thereafter the system was subject to 10 parallel replica MD simulations, in which the FEP protocol was applied for each residue transformation. Each of these MD replicates started with a 0.25 nanosecond unbiased equilibration period, with different initial velocities. The FEP protocol for the L $\rightarrow$ V mutation was generated by combing the QresFEP[33] protocol for residue mutations with a dual topology approach inspired from QligFEP[28], where the effective topology along the transformation is a linear combination of the two original sidechain topologies. Each FEP transformation consisted of 51 evenly distributed λ-windows with 10 ps MD sampling each. In order to fulfill a thermodynamic cycle and calculate relative binding free energies, parallel FEP transformations were run for the apo-structure, i.e. the protein structure without ligand. In these simulations the same parameters were applied (i.e., sphere size, simulation time, etc.), and a total of 10 replicates x 2 (apo/holo) states x 2 (WT and mut) annihilations x 51 λ-windows x 10 ps = 20.4 ns sampling was performed for each mutation simulation. The relative binding free energy shift between WT and mutant receptors for each ligand was estimated by solving the thermodynamic

cycle utilizing the Bennett acceptance ratio (BAR)[34]. All 3D images were produced in PyMOL[44].

Results

Generating $A_{2A}AR$-ligand models

The binding mode of (*S*)-ISAM-140 was obtained by superposition of the previously published complex of this molecule with our $A_{2B}AR$ homology-based model[11] onto a modeled L249[6.51]V $A_{2A}AR$ mutant, i.e. introducing the $A_{2B}AR$ sidechain in this position. Such a construct was built and equilibrated on the basis of the high-resolution crystal structure of the ZM241385 — $A_{2A}AR$ complex (see *Methods*)[22]. The binding mode obtained included the two key interactions typical of ARs antagonists: (i) hydrogen bond(s) with N253[6.55] and (ii) π–π stacking with F168[EL2], both residues completely conserved among ARs[1]. The high-affinity $A_{2A}AR$ antagonist ZM241385 showed an optimal shape complementarity with the $A_{2A}AR$ WT residue L249[6.51] (Figure 2A), whereas the corresponding L249V[6.51] mutant is expected to minimally disrupt this shape complementarity due to a reduced volume (Figure 2B). On the other hand, the obtained binding modes for (*S*)-ISAM-140 on the WT $A_{2A}AR$ (also obtained assuming the same binding mode as in the $A_{2B}AR$ homology-based model[11]) showed a non-optimal fit, in accordance with the lack of affinity exhibited for the $A_{2A}AR$ receptor by this derivative and other compounds within the series[8–11]. In particular, the presence of the native L249[6.51] in the $A_{2A}AR$ appeared to introduce a steric clash with either the 2-furyl or 3-thienyl substituents of the ligands, which we hypothesized would reduce binding affinities (Figure 2C). Conversely, introducing the $A_{2B}AR$ sidechain on the modeled L249V[6.51] $A_{2A}AR$ mutant provided a better shape complementarity (Figure 2D), allowing us to hypothesize that the binding affinity of these antagonists might be recovered to some extent.

Chiral separation of ISAM-140

The racemic mixture of ISAM-140, obtained as previously described,[11] was resolved into its enantiopure forms. A combination of chiral HPLC, circular dichroism (CD) spectroscopy and X-ray crystallography was employed to separate and unequivocally assign the configuration of the heterocyclic stereocenter in each stereoisomer. Semipreparative HPLC separation of (±) ISAM-140 on a chiral stationary phase (see *Experimental information*) provided the expected enantiomers (Figure 3) with excellent stereochemical purity (> 97%). As described previously for 3,4-dihydropyrimidin-2-ones[35–37], the characteristic CD activity of the enamide chromophore (300–350 nm) allowed the unambiguous assignment of the absolute configuration of each enantiomer (Figure 3) by comparison with the reported CD data for enantiopure 3,4-dihydropyrimidin-2(1*H*)-ones of known configuration. In the structures shown in Figure 3, enantiomers that show a negative Cotton effect (red line) contain the furan ring pointing backwards, which corresponds to (*S*)-ISAM-140.

In contrast, the stereoisomers giving a positive Cotton effect (blue line) contain the pentagonal heterocycle pointing forward, which corresponds to (*R*)-ISAM-140. Single crystals suitable for X-ray analysis were grown by slow evaporation of each enantiomer in ethanol. The structures were solved and the data extracted form X-ray crystallography of both monocrystals presented in the Supporting Information (Supplementary Table S1)[12]. The crystal structures of (*S*)-ISAM-140 and (*R*)-ISAM-140 (monoclinic, Figure 3) confirmed the configuration assignment established by circular dichroism. The benzimidazole moiety is essentially planar in both enantiomers, while the dihydropyrimidine core adopt a pseudo envelope conformation, with the C$_4$ atom being lightly displaced by 0.26Å.
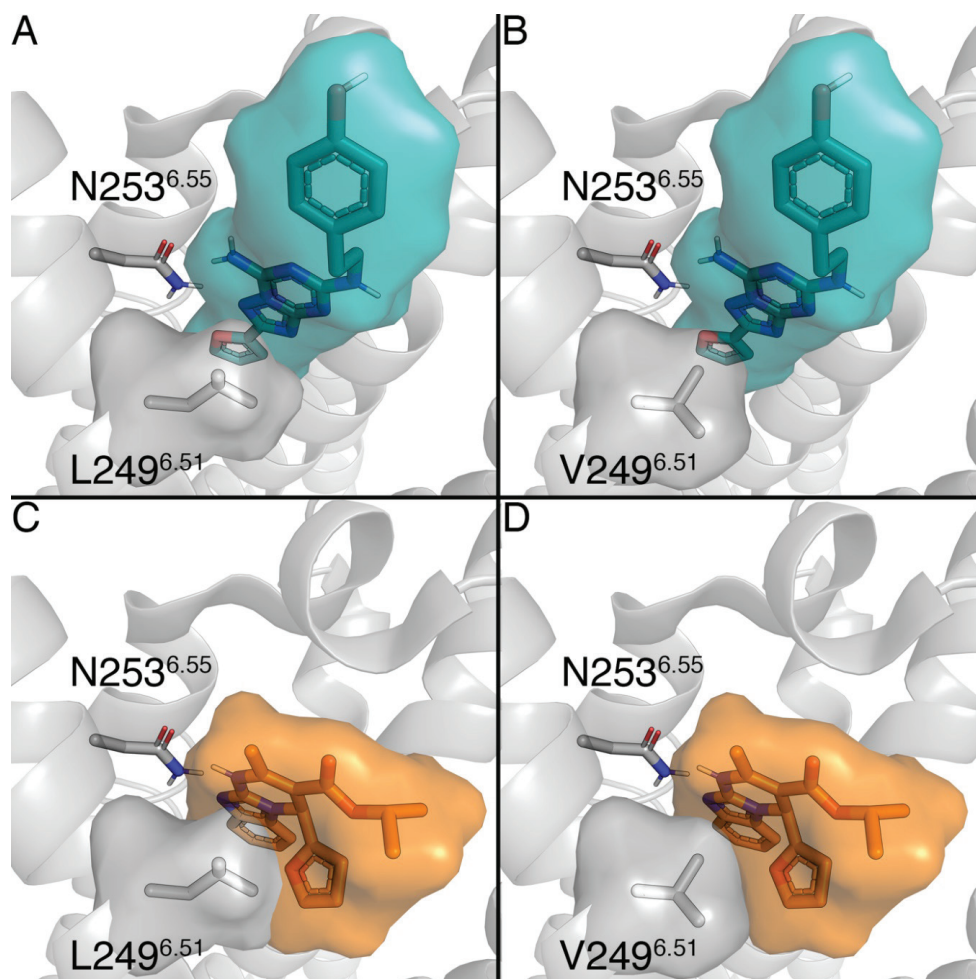

Figure 2: Binding mode of two ligands, ZM241385 (in blue, panels A and B) and (*S*)-ISAM-140 (orange, panels C and D), to the WT (panels A and C) and the L249V[6.51] mutant (panels B and D) A$_{2A}$AR. Volumetric occupancies are shown as surface. Figure created with Pymol v2.0.
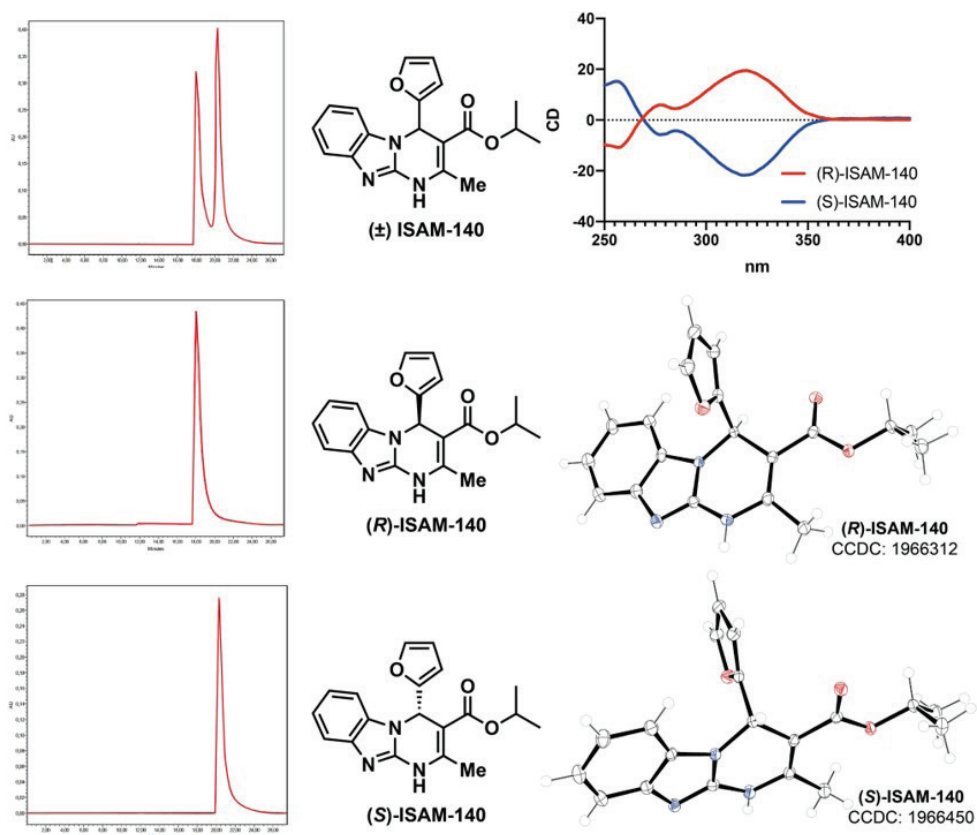
7

Figure 3. Chiral HPLC separation, circular dichroism spectra and crystal X-ray structure of compounds *(R)*-ISAM-140 and *(S)*-ISAM-140.

Determination of ligand binding affinities

To further confirm the role of position 6.51 as a receptor selectivity hotspot, we attempted to express L249V/A$^{6.51}$ A$_{2A}$AR and V250L/A$^{6.51}$ A$_{2B}$AR mutant receptors. Whilst both A$_{2A}$AR mutant receptors were successfully expressed (Supplementary Fig. S1), none of the A$_{2B}$AR mutants could be expressed using standard (non-viral) transfection methods, and consequently the A$_{2B}$AR mutants designed had to be excluded from further experimentation. Thereafter, we determined the binding affinity of ISAM-140, both as a racemate and pure enantiomers, together with the prototypical antagonist ZM241385 at both WT and mutant A$_{2A}$ARs, as well as at the WT A$_{2B}$AR (Figure 4 and Table 1). The affinities determined for ZM241385 and racemic ISAM-140 on WT A$_{2B}$AR (pKi of 6.78 and 7.86, respectively, see Table 1) were in line with previous reports[10]. As expected from the modeling, the corresponding data for the enantiopure forms of ISAM-140 showed that the affinity of the racemic mixture was due to *(S)*-ISAM-140, with even a gain in binding affinity as compared to the racemic mixture (ΔpK$_i$ = 0.19), which was dramatically reduced for the low-affinity

(R)-ISAM-140 (ΔpK$_i$ = 1.31 between both enantiomers, Figure 4A and Table 1).

For the A$_{2A}$AR, we first established whether the L249V/A$^{6.51}$ mutants still sufficiently bound ZM241385, to validate the viability of using it as a radioligand in the homologous displacement assays. Of note, the resulting K$_D$ values could then be used to obtain K$_i$ values from the IC$_{50}$ values (see *Methods*), which enabled us to compare affinity values for WT and mutant A$_{2A}$ARs. Moreover, the resulting B$_{max}$ values showed that the A$_{2A}$AR L249V$^{6.51}$ mutant had a lower expression level than compare affinity values for WT and mutant A$_{2A}$ARs. Moreover, the resulting B$_{max}$ values showed that the A$_{2A}$AR L249V$^{6.51}$ mutant had a lower expression level than the WT A$_{2A}$AR. A slight reduction in affinity of both [^{3}H]ZM241385 and ZM241385 was observed on this mutant (Table 1), which was in line with our hypothesis that the shape complementarity between ZM241385 and L249 is mostly preserved with
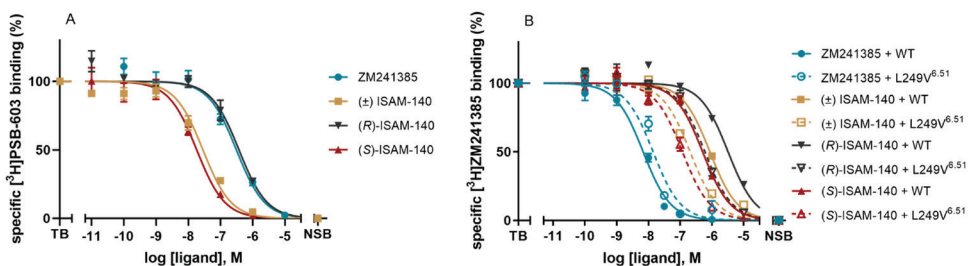

Figure 4: Displacement of (A) specific [^{3}H]PSB-603 binding from A$_{2B}$AR and (B) specific [^{3}H]ZM241385 binding from the WT and the L249V$^{6.51}$ mutant A$_{2A}$AR at 25 °C by ZM241385 (blue), ($\pm$) ISAM-140 (yellow), (R)-ISAM-140 (black) and (S)-ISAM-140 (red). Combined graphs are from three individual experiments performed in duplicate.
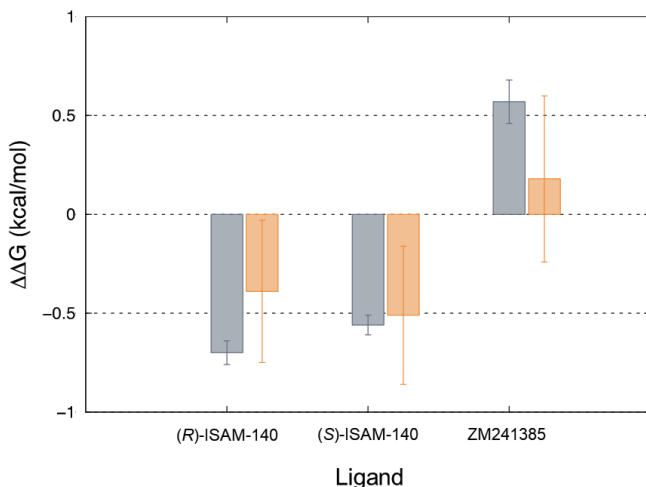

Figure 5: Experimental (grey) and calculated (orange) relative changes in binding free energies to the L249V$^{6.51}$ mutant A$_{2A}$AR for the two enantiomers of ISAM-140 and ZM241385.

Table 1: B_{max} and pK_D values of [³H]ZM241385 and binding affinities of ZM241385, (±) ISAM-140, (R)-ISAM-140 and (S)-ISAM-140 on WT $A_{2B}AR$, WT and L249V[6.51] mutant $A_{2A}ARs$.

Receptor	B_{max} (pmol/mg) [a]	pK_D [a]	pK_i [b]			
	[³H]ZM241385	ZM241385	ZM241385	(±) ISAM-140	(R)-ISAM-140	(S)-ISAM-140
$A_{2B}AR$ (WT)	-	-	6.78 ± 0.06	7.86 ± 0.09	6.74 ± 0.09	8.05 ± 0.06
$A_{2A}AR$ (WT)	3.92 ± 0.23	8.59 ± 0.09	8.62 ± 0.04	6.53 ± 0.03	5.96 ± 0.02	6.76 ± 0.04
$A_{2A}AR$ (L249V)	1.15 ± 0.15	8.17 ± 0.06	8.09 ± 0.03	6.92 ± 0.03	6.47 ± 0.07	7.17 ± 0.09

Data is presented as mean ± SEM of three individual experiments, each performed in duplicate.
[a] B_{max} and pK_D values obtained from homologous competition displacement assays on transiently transfected HEK293-$A_{2A}AR$ membranes at 25 °C.
[b] pK_i values obtained from displacement assays of specific [³H]PSB-603 binding from CHO-spap-h$A_{2B}AR$ membrane or specific [³H]ZM241385 binding from transiently transfected WT and mutant HEK293-$A_{2A}AR$ membranes at 25 °C.

a smaller Val. However, a substantial hydrophobic side chain was important for the binding of this antagonist to the $A_{2A}Rs$, since its affinity to the $A_{2A}AR$ L249A[6.51] mutant was completely lost (Supplementary Figure. S2), in line with previous reports[38]. The results of the displacement assays for ISAM-140 (racemate and both stereoisomers) are illustrated in Figure 4B and Table 1. Although one data point for (±) ISAM-140 at the concentration of 10⁻⁵ M was excluded from the curve of WT $A_{2A}AR$, due to low water solubility, in all cases the binding affinity for the WT $A_{2A}AR$ was very low (within micromolar range). Notably, it followed the same trend as observed on WT $A_{2B}AR$, i.e. the highest affinity for (S)-ISAM-140 and the lowest for (R)-ISAM-140. The selectivity ratio between A_{2B} and A_{2A} ARs was substantial for (±) ISAM-140, (ΔpK_i = 1.33), in line with the previous reports for this ligand[11]. This difference that was maintained for the active eutomer (S)-ISAM-140 (ΔpK_i = 1.29) and, to a lower extent, even for (R)-ISAM-140 (ΔpK_i = 0.79), which is expected due to its already low affinity for $A_{2B}AR$. Notably, the affinity values were significantly recovered at the $A_{2A}AR$ L249A[6.51] mutant, i.e. when the receptor was more "$A_{2B}AR$-like", thus supporting the initial modeling hypothesis. The moderate affinity gains observed for the $A_{2A}AR$ L249A[6.51] mutant as compared to the $A_{2A}AR$ WT (0.39, 0.41 and 0.51 log unit for (±) ISAM-140, (S)-ISAM-140, and (R)-ISAM-140, respectively, see Table 1) did not restore the affinity values as in the WT $A_{2B}AR$.

Computational characterization of binding free energies.

Finally, we investigated the observed shifts in binding affinities for (S)-ISAM-140, (R)-ISAM-140 and ZM241385 in the context of the structural binding model of these molecules to the $A_{2A}AR$. The approach was to compare the WT and L249[6.51]V mutant (A_{2B} equivalent) versions of $A_{2A}AR$ using the Q-FEP protocols[28,33]. This strategy consists on the simulation of the mutation (Leu to Val) both in the presence and absence of each of the docked ligands. While the structure of the ZM241385 — $A_{2A}AR$ complex is experimentally known[22], the binding mode of each enantiomer

of ISAM140 was inferred from our previous work on this chemotype[7]. Figure 5 summarizes the calculated shift in the free energy of binding due to the L249$^{6.51}$V mutation for each enantiomer of ISAM-140 and for ZM241385. It can be observed a very good agreement between the calculations and the experimental affinity data here reported in Figure 4B, with a very low mean average error (MAE=0.25 kcal/mol, numerical data provided in Supplementary Table S2). Thus, the simulation of this mutation resulted in a predicted increase in affinity (negative $\Delta\Delta G_{bind\ (mut\ –\ WT)}$ values in Figure 5) for both enantiomers of ISAM-140, with values proportional to those extracted from the experimental data. Conversely, the experimental affinity of ZM241385 is decreased for the L249$^{6.51}$V mutant A$_{2A}$AR, which is also captured by our modeling as a mild positive value for the calculated $\Delta\Delta G_{bind\ (mut\ –\ WT)}$.

Discussion

In this work, we investigated the role of position 6.51 in determining the specificity for A$_{2B}$AR binding of a series of chiral antagonists recently developed for this receptor. The modeling hypothesis behind the design of the potent antagonist ISAM-140 placed the *S*-stereoisomer in perfect shape complementarity with Val250$^{6.51}$ in the A$_{2B}$AR, while analogous docking in the high resolution A$_{2A}$AR bearing a bulkier Leu in the same position showed initial steric clashes. This allowed us to propose this sidechain as a landmark for A$_{2B}$AR selectivity for this ligand class, and the (*S*)-ISAM-140 as the active stereoisomer. To experimentally validate this hypothesis, the ISAM-140 enantiomers were separated and their absolute configuration unequivocally assigned. Besides this goal, the enantiomeric separation and pharmacological characterization of this reference A$_{2B}$AR antagonist allowed to confirm the expected higher affinity of the *S* enantiomer, in line with the original modeling hypothesis[11] and recent similar results obtained with derivatives of this scaffold[10,12,13].

Site-directed mutagenesis of position 6.51 was performed on the A$_{2A}$AR to replace the WT Leu by the Val specific of A$_{2B}$AR, as the reverse mutation of the A$_{2B}$AR appeared unfeasible in our hands, somehow in contrast to previous report of Müller and co-workers who managed to express the corresponding Ala mutant (V250A$^{6.51}$) in the A$_{2B}$AR[39]. It is worth noting that, while there had been reports of the Alanine scan of position 6.51 in both A$_{2A}$[38] and A$_{2B}$ARs[39], this is the first time that the introduction of the A$_{2B}$AR characteristic Val sidechain on the A$_{2A}$AR is evaluated.

The L249$^{6.51}$V A$_{2A}$AR mutant partially recovered the affinity of ISAM-140 lost for this receptor, supporting the initial modeling hypothesis. This partial recovery in affinity, consistently observed for all three forms of this molecule (i.e., racemic mixture and both eutomers) is in line with recent reports on 'selectivity hotspots' between A$_1$AR and A$_{2A}$AR, where a single-point mutation clearly affecting the experimental binding mode could only partially explain the observed selectivity profile of the A$_1$AR selective xanthines under investigation[40]. On the other hand, the opposed effect was observed
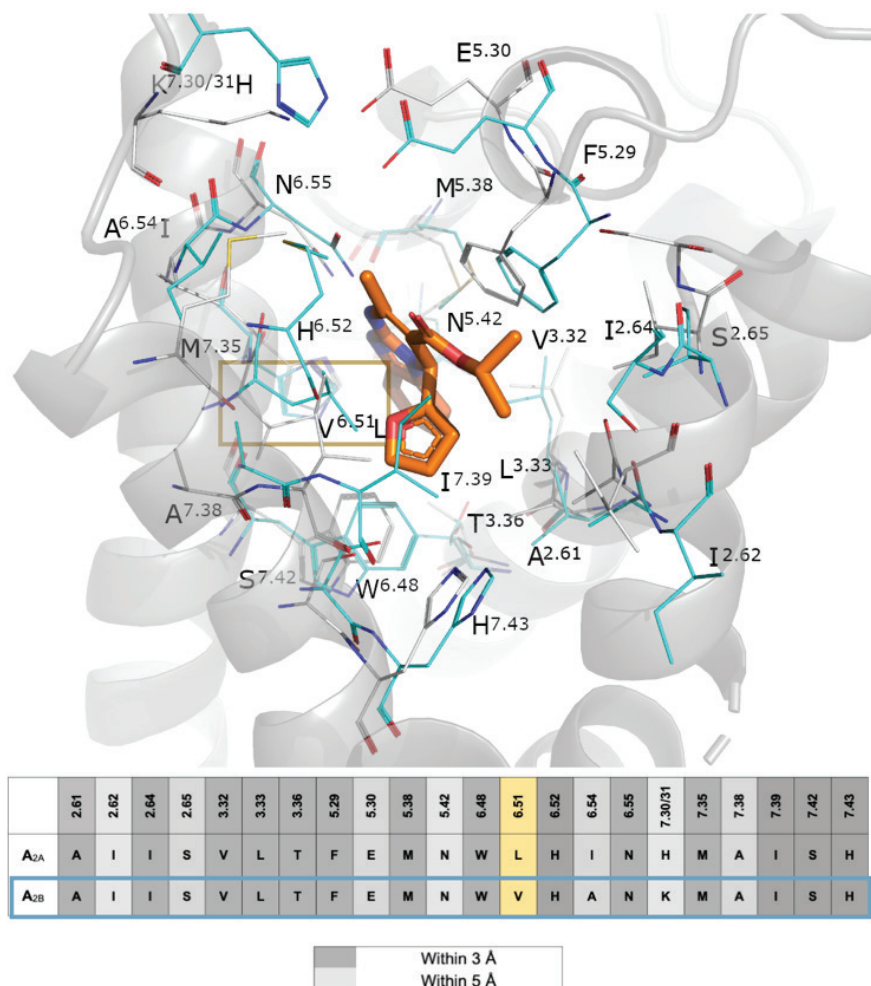
7

Figure 6: Pseudo-sequence alignment of the residues within 5 Å of any atom of *(S)*-ISAM140, as predicted by docking on the A$_{2B}$AR, between this receptor and the A$_{2A}$AR. The location of each sidechain is shown in the 3D superposition of the *(S)*-ISAM140-A$_{2B}$AR (gray sidechains and cartoon, ligand in orange sticks) with the A$_{2A}$AR crystal structure (cyan sidechains). Position 6.51 is highlighted on a yellow box. Figure created with Pymol v2.0.

for ZM241385 (i.e. decrease in affinity for the L249$^{6.51}$V A$_{2A}$AR mutant) in line with the well-described preference of this ligand for the A$_{2A}$AR.

To further assess the amino acid conservation between the A$_{2A}$ and A$_{2B}$ARs binding sites, a pseudo-sequence alignment is presented in Figure 6. One can observe that, in addition to position 6.51 here studied, only two sidechains vary within the 5Å cut-off distance with the ligand: Ala253$^{6.54}$ in A$_{2B}$AR, situated one helix turn below position 6.51, is an Ile in A$_{2A}$AR. This residue, however, is not in contact with the ligand and instead involved in the TM packing as shown in the Fig. 6. In the EL3 region, His264$^{7.31}$ in A$_{2A}$AR is making a salt bridge interaction with Glu169$^{5.30}$ in EL2,

a role that in our A$_{2B}$AR model is undertaken by Lys267[7.31] (Figure. 6). While this residue has been shown to be involved in ligand binding kinetics[1], we should not rule out an additional role of the more variable EL regions in the selectivity profile of this antagonist. This analysis also allows to explore potential indirect effects of the V6.51L mutation on neighbouring residues conserved in the ARs, like His[6.52] that has been shown to be involved in both agonist and antagonist binding[1]. As it can be seen in Fig 6., this residue is not predicted to change conformation between A$_{2A}$ and A$_{2B}$ARs, which is supported by the water-mediated interaction with Asn[5.42] previously characterized by MD simulations of this pair of receptors[23].

In the lack of a crystal structure of the A$_{2B}$AR, the observed effects were rationalized back in the modeled structures, by means of first-principle FEP simulations of this mutation. The QresFEP protocol has been broadly applied to investigate the A$_{2A}$AR mutational landscape[41–43], showing exceptional sensitivity to capture the correct affinity shifts for different chemotypes. The binding model of *(S)*-ISAM-140 to the WT and L249[6.51]V mutant versions of A$_{2A}$AR was here assumed to be the same as our docking model of this compound to the WT A$_{2B}$AR[12]. That model suggested that the high A$_{2B}$AR affinity of (±) ISAM-140 was due to the stereoselective optimal fitting of the *(S)* isomer to the A$_{2B}$AR binding site, facilitated by the Val sidechain in position 6.51 of this receptor[12]. The calculated recovery of the binding affinity of *(S)*-ISAM-140 upon the L249[6.51]V mutation in the A$_{2A}$AR, which is in line with the experimental design of this A$_{2B}$-like mutation on the A$_{2A}$AR, further confirms the validity of the binding model for this chemotype on the A$_{2B}$AR.

Overall, both experimental and computational results of this study clearly support the binding mode used to design this study, providing useful structural insights in the selective recognition of these A$_{2B}$AR antagonists that should aid in future structure-based optimization.

7

References

1. Jespers, W. *et al.* Structural mapping of adenosine receptor mutations: ligand binding and signaling mechanisms. *Trends Pharmacol. Sci.* **39**, 75–89 (2017).
2. Jazayeri, A., Andrews, S. P. & Marshall, F. H. Structurally enabled discovery of adenosine A$_{2A}$ receptor antagonists. *Chem. Rev.* **117**, 21–37 (2017).
3. Gessi, S., Merighi, S. & Varani, K. Adenosine receptors: the status of the art. in *The Adenosine Receptors* **34**, 1–11 (2018).
4. Jacobson, K. A. & Gao, Z.-G. Adenosine receptors as therapeutic targets. *Nat. Rev. Drug Discov.* **5**, 247–264 (2006).
5. Chen, J.-F., Eltzschig, H. K. & Fredholm, B. B. Adenosine receptors as drug targets — what are the challenges? *Nat. Rev. Drug Discov.* **12**, 265–286 (2013).
6. Pardoll, D. M. The blockade of immune checkpoints in cancer immunotherapy. *Nature Reviews Cancer* **12**, 252–264 (2012).
7. Crespo, A. *et al.* Discovery of 3,4-dihydropyrimidin-2(1H)-ones as a novel class of potent and selective A$_{2B}$ adenosine receptor antagonists. *ACS Med. Chem. Lett.* **4**, 1031–1036 (2013).
8. Yaziji, V. *et al.* Pyrimidine derivatives as potent and selective A$_3$ adenosine receptor antagonists. *J. Med. Chem.* **54**, 457–471 (2011).
9. Jespers, W. *et al.* Structure-based design of potent and selective ligands at the four adenosine receptors. *Molecules* **22**, 1945 (2017).
10. Carbajales, C. *et al.* Enantiospecific recognition at the A$_{2B}$ adenosine receptor by alkyl 2-cyanoimino-4-substituted-6-methyl-1,2,3,4-tetrahydropyrimidine-5-carboxylates. *J. Med. Chem.* **60**, 3372–3382 (2017).
11. El Maatougui, A. *et al.* Discovery of potent and highly selective A$_{2B}$ adenosine receptor antagonist chemotypes. *J. Med. Chem.* **59**, 1967–1983 (2016).
12. Mallo-Abreu, A. *et al.* Trifluorinated pyrimidine-based A$_{2B}$ antagonists: optimization and evidence of stereospecific

recognition. *J. Med. Chem.* **62**, 9315–9330 (2019).

13. Mallo-Abreu, A. *et al.* Nitrogen-Walk Approach to Explore Bioisosteric Replacements in a Series of Potent A$_{2B}$ Adenosine Receptor Antagonists. *J. Med. Chem.* **63**, 7721–7739 (2020).

14. Ballesteros, J. A. & Weinstein, H. Integrated methods for the construction of three-dimensional models and computational probing of structure-function relations in G protein-coupled receptors. in *Methods in Neurosciences* **25**, 366–428 (1995).

15. Guo, D. *et al.* Molecular basis of ligand dissociation from the adenosine A$_{2A}$ receptor. *Mol. Pharmacol.* **89**, 485–491 (2016).

16. Guo, D., Mulder-Krieger, T., IJzerman, A. P. & Heitman, L. H. Functional efficacy of adenosine A$_{2A}$ receptor agonists is positively correlated to their receptor residence time. *Br. J. Pharmacol.* **166**, 1846–1859 (2012).

17. Dasgupta, S. *et al.* Adenosine A$_{2A}$ receptors modulate the binding characteristics of dopamine D$_2$ receptors in stably cotransfected fibroblast cells. *Eur. J. Pharmacol.* **316**, 325–331 (1996).

18. Smith, P. K. *et al.* Measurement of protein using bicinchoninic acid. *Anal. Biochem.* **150**, 76–85 (1985).

19. Schiedel, A. C. *et al.* The four cysteine residues in the second extracellular loop of the human adenosine A$_{2B}$ receptor: role in ligand binding and receptor function. *Biochem. Pharmacol.* **82**, 389–99 (2011).

20. Yang, X. *et al.* A covalent antagonist for the human adenosine A$_{2A}$ receptor. *Purinergic Signal.* **13**, 191–201 (2017).

21. Cheng, Y.-C. & Prusoff, W. H. Relationship between the inhibition constant (KI) and the concentration of inhibitor which causes 50 per cent inhibition (I50) of an enzymatic reaction. *Biochem. Pharmacol.* **22**, 3099–3108 (1973).

22. Liu, W. *et al.* Structural basis for allosteric regulation of GPCRs by sodium ions. *Science.* **337**, 232–236 (2012).

23. Rodríguez, D., Piñeiro, Á. & Gutiérrez-de-Terán, H. Molecular dynamics simulations reveal insights into key structural elements of adenosine receptors. *Biochemistry* **50**, 4194–208 (2011).

24. Hess, B., Kutzner, C., van der Spoel, D. & Lindahl, E. GROMACS 4: algorithms for highly efficient, load-balanced, and scalable molecular simulation. *J. Chem. Theory Comput.* **4**, 435–447 (2008).

25. Kaminski, G. A., Friesner, R. A., Tirado-Rives, J. & Jorgensen, W. L. Evaluation and reparametrization of the OPLS-AA force field for proteins via comparison with accurate quantum chemical calculations on peptides. *J. Phys. Chem. B* **105**, 6474–6487 (2001).

26. Berger, O., Edholm, O. & Jähnig, F. Molecular dynamics simulations of a fluid bilayer of dipalmitoylphosphatidylcholine at full hydration, constant pressure, and constant temperature. *Biophys. J.* **72**, 2002–2013 (1997).

27. Marelius, J., Kolmodin, K., Feierberg, I., Åqvist, J. & Aqvist, J. Q: a molecular dynamics program for free energy calculations and empirical valence bond simulations in biomolecular systems. *J. Mol. Graph. Model.* **16**, 213–225 (1998).

28. Jespers, W., Esguerra, M., Åqvist, J. & Gutiérrez-de-Terán, H. QligFEP: an automated workflow for small molecule free energy calculations in Q. *J. Cheminform.* **11**, 26 (2019).

29. King, G. & Warshel, A. A surface constrained all-atom solvent model for effective simulations of polar solutions. *J. Chem. Phys.* **91**, 3647–3661 (1989).

30. Lee, F. S. & Warshel, A. A local reaction field method for fast evaluation of long-range electrostatic interactions in molecular simulations. *J. Chem. Phys.* **97**, 3100–3107 (1992).

31. Ryckaert, J.-P., Ciccotti, G. & Berendsen, H. J. . Numerical integration of the cartesian equations of motion of a system with constraints: molecular dynamics of n-alkanes. *J. Comput. Phys.* **23**, 327–341 (1977).

32. Robertson, M. J., Tirado-Rives, J. & Jorgensen, W. L. Improved peptide and protein torsional energetics with the OPLS-AA force field. *J. Chem. Theory Comput.* **11**, 3499–3509 (2015).

33. Jespers, W. *et al.* QresFEP: an automated protocol for free energy calculations of protein mutations in Q. *J. Chem. Theory Comput.* **15**, 5461–5473 (2019).

34. Bennett, C. H. Efficient estimation of free energy differences from Monte Carlo data. *J. Comput. Phys.* **22**, 245–268 (1976).

35. Lacotte, P., Buisson, D. A. & Ambroise, Y. Synthesis, evaluation and absolute configuration assignment of novel dihydropyrimidin-2-ones as picomolar sodium iodide symporter inhibitors. *Eur. J. Med. Chem.* **62**, 722–727 (2013).

36. Krenn, W., Verdino, P., Uray, G., Faber, K. & Kappe, C. O. Determination of absolute configuration in 4-aryl-3, 4-dihydro-2(1H)-pyrimidones by high performance liquid chromatography and CD spectroscopy. *Chirality* **11**, 659–662 (1999).

37. Uray, G., Verdino, P., Belaj, F., Kappe, C. O. & Fabian, W. M. F. Absolute configuration in 4-alkyl- and 4-aryl-3,4-dihydro-2(1H)-pyrimidones: a combined theoretical and experimental investigation. *J. Org. Chem.* **66**, 6685–6694 (2001).

38. Jaakola, V. P. *et al.* Ligand binding and subtype selectivity of the human A$_{2A}$ adenosine receptor: identification and characterization of essential amino acid residues. *J. Biol. Chem.* **285**, 13032–13044 (2010).

39. Thimm, D. *et al.* Ligand-Specific Binding and Activation of the Human Adenosine A$_{2B}$ Receptor. *Biochemistry* **52**, 726–740 (2013).

40. Cheng, R. K. Y. *et al.* Structures of Human A$_1$ and A$_{2A}$ Adenosine Receptors with Xanthines Reveal Determinants of Selectivity. *Structure* **25**, 1275-1285.e4 (2017).

41. Jespers, W. *et al.* X-Ray Crystallography and Free Energy Calculations Reveal the Binding Mechanism of A$_{2A}$ Adenosine Receptor Antagonists. *Angew. Chemie Int. Ed.* **59**, 16536–16543 (2020).

42. Keränen, H., Gutiérrez-de-Terán, H. & Åqvist, J. Structural and energetic effects of A$_{2A}$ adenosine receptor mutations on agonist and antagonist binding. *PLoS One* **9**, e108492 (2014).

43. Keränen, H., Åqvist, J. & Gutiérrez-De-Terán, H. Free energy calculations of A$_{2A}$ adenosine receptor mutation effects on agonist binding. *Chem. Commun.* **51**, 3522–3525 (2015).

44. *The PyMOL Molecular Graphics System, Version 2.0.* Schrödinger, LLC.

Supplementary Information
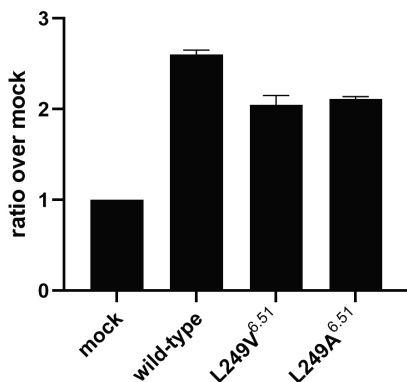
Supplementary Figure S1. Expression level of the transiently transfected WT A$_{2A}$AR, and L249V[6.51] and L249A[6.51] mutant A$_{2A}$AR at the surface of HEK293 cells. Data are shown as the mean ± SEM of three individual experiments performed in sextuplicate.
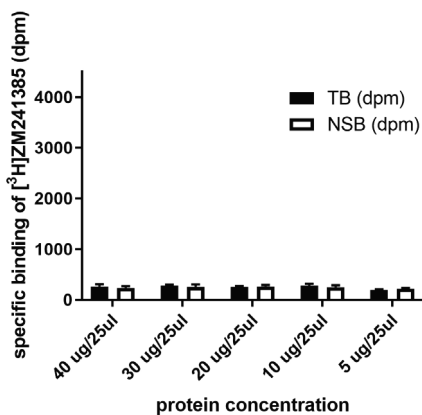
Supplementary Figure S2. Window check of HEK293 cell membrane transiently transfected by the L249[6.51]A mutant A$_{2A}$AR in the presence of 1.7 nM [^{3}H] ZM241385 in the absence (total binding; TB) and presence (non-specific binding; NSB) of NECA (100 μM). Data is shown as the mean ± SEM of three individual experiments performed in duplicate.

7

Supplementary Table S1. X-ray diffractometry experimental details of crystallographic (*R*)-ISAM-140 and (*S*)-ISAM-140.

Crystal data		(*R*)-ISAM140		(*S*)-ISAM140		
CCDC		1966312		1966450		
Chemical formula		$C_{19}H_{19}N_3O_3$		$C_{19}H_{19}N_3O_3$		
M_r		337.37		337.37		
Crystal system		Monoclinic		Monoclinic		
Space group		C2		C2		
Temperature (K)		100		100		
a (Å)		16,4552	(9)	16.4553	(4)	
B (Å)		8.0613	(4)	8.0605	(2)	
c (Å)		13.5259	(7)	13.5260	(3)	
α (°)		90		90		
β (°)		112.684	(3)	112.678	(1)	
γ (°)		90		90		
V (Å³)		1655.42	(16)	1655.35	(7)	
Z		4		4		
Radiation type		Cu-Kα		Cu-Kα		
μ (mm⁻¹)		0.76		0.76		
Crystal size (mm)		0.12 × 0.11 × 0.10		0.11 ×	0.01 ×	0.03
Tmin, Tmax		0.852, 0.929		-		
(sin θ/λ) max (Å⁻¹)		0.633		0.625		
Measured/Independent/ observed [I>2σ(I)] reflection		20568/3488/3266		17353/3370/3346		
Rint		0.068		0.076		
$R[F^2>2\sigma(F^2)]$, wR(F2), S		0.043, 0.102,	1.10	0.025, 0.069,	1.01	
Δρmax/Δρmin (eÅ⁻³)		0.19, −0.25		0.16, -0.20		
Absolute structure (Flack)		-0.1(2)		-0.02	(4)	

Supplementary Table S2. Experimental and FEP calculated energies for the L6.51V mutation, with the value for each FEP leg in the thermodynamic cycle included. The DDG values values are plotted on Fig 5 on the main text.

	ΔΔGexp	error	ΔΔGcalc	sem	ΔGholo	sem	ΔGapo	sem
ISAM-140(R)	-0.70	0.06	-0.39	0.36	-4.52	0.24	-4.91	0.27
ISAM-140(S)	-0.56	0.05	-0.50	0.35	-4.41	0.22	-4.91	0.28
ZM241385	0.57	0.11	0.20	0.42	-5.11	0.31	-4.91	0.29

(D)DG values and expressed in Kcal·mol⁻¹. Standard erorr of the mean (sem) calculated from 10 replica simulations (FEP) or from the experimental data (see main text). $DDGexp = -RT\ln(K_i^{wt}/K_i^{mut})$

Spectroscopic and analytical data for racemates and enantiomers isolated through chiral HPLC

(±) Isopropyl 4-(furan-2-yl)-2-methyl-1,4-dihydrobenzo[4,5]imidazo[1,2-*a*]pyrimidine-3-carboxylate [(±) ISAM-140][1]. ^{1}H NMR (300 MHz, DMSO-*d₆*), δ (ppm): 10.78 (brs, 1H), 7.67−7.23 (m, 3H), 7.19−6.84 (m, 2H), 6.52 (s, 1H), 6.44 (d, *J* = 3.3 Hz, 1H), 6.37−6.23 (m, 1H), 4.86 (h, *J* = 6.3 Hz, 1H), 2.44 (s, 3H), 1.21 (d, *J* = 6.2 Hz, 3H), 1.05 (d, *J* = 6.1 Hz, 3H). ^{13}C NMR (75 MHz, DMSO-*d₆*), δ (ppm): 165.0, 153.3, 148.0,

146.0, 143.0, 142.6, 132.0, 122.3, 120.7, 117.2, 110.8, 110.2, 108.2, 94.9, 67.0, 49.7, 22.3, 22.0, 19.1. HRMS (ESI) m/z: calcd for C$_{19}$H$_{20}$N$_3$O$_3$ [M + H]$^+$: 338.1488; found: 338.7927.

Isopropyl (R)-4-(furan-2-yl)-2-methyl-1,4-dihydrobenzo[4,5]imidazo[1,2-a]pyrimidine-3-carboxylate [(R)-ISAM-140]. ^{1}H NMR (300 MHz, DMSO-d_6), δ (ppm): 10.76 (s, 1H), 7.41 (d, J = 11.0 Hz, 2H), 7.34 (d, J = 7.7 Hz, 1H), 7.04 (dt, J = 18.2, 7.0 Hz, 2H), 6.52 (s, 1H), 6.44 (d, J = 3.3 Hz, 1H), 6.35 − 6.27 (m, 1H), 4.87 (p, J = 6.3 Hz, 1H), 2.44 (s, 3H), 1.21 (d, J = 6.3 Hz, 3H), 1.05 (d, J = 6.4 Hz, 3H). ^{13}C NMR (75 MHz, DMSO-d_6), δ (ppm): 165.0, 153.3, 148.0, 146.0, 143.1, 142.6, 132.0, 122.3, 121.0, 117.2, 110.8, 110.2, 108.7, 95.0, 67.0, 49.7, 22.3, 22.1, 19.1. HRMS (APCI) *m/z* calcd for C$_{19}$H$_{19}$N$_3$O$_3$ [M+H]$^+$: 338.1499; found: 338.1501.

Isopropyl (R)-4-(furan-2-yl)-2-methyl-1,4-dihydrobenzo[4,5]imidazo[1,2-a]pyrimidine-3-carboxylate [(S)-ISAM-140]. ^{1}H NMR (300 MHz, DMSO-d_6), δ (ppm): 10.78 (s, 1H), 7.42 (d, J = 10.9 Hz, 2H), 7.35 (d, J = 7.8 Hz, 1H), 7.04 (dt, J = 18.2, 7.0 Hz, 2H), 6.54 (s, 1H), 6.44 (d, J = 3.3 Hz, 1H), 6.40 − 6.29 (m, 1H), 4.87 (p, J = 6.3 Hz, 1H), 2.44 (s, 3H), 1.21 (d, J = 6.3 Hz, 3H), 1.05 (d, J = 6.4 Hz, 3H). ^{13}C NMR (75 MHz, DMSO-d_6), δ (ppm): 165.0, 153.3, 148.0, 146.0, 143.0, 142.6, 132.0, 122.3, 120.7, 117.5, 110.8, 110.3, 108.4, 94.9, 67.0, 49.7, 22.3, 22.2, 19.0. HRMS (APCI) *m/z* calcd for C$_{19}$H$_{19}$N$_3$O$_3$ [M+H]$^+$: 338.1499; found: 338.1501.

Enzyme-linked Immunosorbent assay (ELISA)

The experiment was performed as described previously[2]. Briefly, 24 hours after transfection, cells were split into a 96-well poly-D- lysine-coated plates at a density of 10^6 cells per well. After an additional 24 h, the cells were fixed with 4% formaldehyde and blocked with 2% bovine serum albumin (BSA) (Sigma-Aldrich Chemie N.V., Zwijndrecht, The Netherlands) in Tris-buffered saline (TBS). Then, the cells were incubated with monoclonal M1-anti-FLAG antibody (1:2250) (Sigma-Aldrich Chemie N.V. Zwijndrecht, The Netherlands) in Tris-buffered saline (TBS)/1 mM CaCl$_2$ for 2 hours at room temperature (RT). Next, the antibody was removed and the cells were washed with TBS/1 mM CaCl$_2$ before adding the secondary antibody, monoclonal anti-Mouse-HRP (1:5000) (Jackson ImmunoResearch Europe Ltd., Cambridgeshire, UK) and incubating for 1 hour at RT. After removing the secondary antibody and washing the cells with TBS/1 mM CaCl$_2$, 3, 3',5,5'-tetramethyl-benzidine (TMB) was added and incubated for 5 minutes in the dark. The reaction was stopped with 1 M H$_3$PO$_4$, and absorbance was read at 450 nm using a Wallac EnVision 2104 Multilabel reader (PerkinElmer).

References

1. El Maatougui, A. *et al.* Discovery of potent and highly selective A$_{2B}$ adenosine receptor antagonist chemotypes. *J. Med. Chem.* **59**, 1967–1983 (2016).
2. Lane, J. R. *et al.* A novel nonribose agonist, LUF5834, engages residues that are distinct from those of adenosine-like ligands to activate the adenosine A$_{2a}$ receptor. *Mol. Pharmacol.* **81**, 475–487 (2012).

Chapter 8

Conclusion and future perspectives.

Conclusions

### *Yeast system is suitable for GPCR studies*

Engineered yeast systems *Saccharomyces cerevisiae* (*S. cerevisiae*) and *Pichia pastoris* (*P. pastoris*) have been used during the past three decades as a synthetic "null" background for human GPCRs studies. They serve various purposes, including receptor purification, characterization of novel ligands and GPCR mutations, as a biosensor, and for receptor deorphanization[1]. These yeast systems are cheap, stable and versatile for GPCR expression and characterization. As reviewed in **Chapter 2**, we summarized the strategies of linking human GPCRs' expression and functionality to these yeast systems and highlighted the studies on adenosine receptors heterologously expressed in yeast. The *P. pastoris* system with high similarity to advanced eukaryotic expression systems is commonly used for GPCR expression with the purpose of receptor purification[2], while the *S. cerevisiae* system is often used for GPCR signaling research due to the similarity between the yeast mating pathway and human GPCR signaling[3]. Moreover, multiple modifications have been generated on the yeast pheromone signaling pathway in order to enhance human GPCR expression, to couple to the yeast signaling pathway, and obtain quantifiable read-outs[1].

The yeast strain used in this thesis (**Chapter 4, 5** and **6**), namely MMY24, contains one chimeric G protein subtype and the HIS3 reporter gene (Figure 1). In this yeast strain, the last five C-terminal amino acids of the yeast G_α protein were transplanted by the corresponding sequence of the mammalian $G_{\alpha i}$ protein. With the HIS3 reporter gene present, yeast cell growth on histidine-deficient medium can be used as a measurement of human receptor activation. We concluded that this yeast system was suitable for functional characterization of cancer-related mutations on the $A_{2B}AR$ (**Chapter 4**) and for initial functional screening of cancer-related mutations on the A_1AR (**Chapter 5** and **6**).

Cancer-related mutations alter receptor pharmacology

GPCRs are the largest membrane protein family, and regulate divergent physiological and pathological activities throughout the human body[4]. They are targeted by around 30% of current therapeutic drugs for the treatment of various types of diseases. However, only a few members of this superfamily are currently being explored as oncological drug targets[5]. In **Chapter 3**, we discussed the role of GPCRs, their signaling pathways and their mutations in cancer, with a focus on adenosine receptors. In that chapter we summarized current existing evidence for the involvement of GPCRs in tumor biology, as well as the effect of mutations in receptor pharmacology, including receptor expression, receptor-ligand interaction and GPCR-G protein coupling. Moreover, we discussed the potential impact of GPCR mutations occurring in all stages of cancer development and progression. The accumulation of adenosine has been reported in the hypoxic tumor micro-

environment and regulates cancer hallmarks via its corresponding GPCRs, the adenosine receptors[6]. Therefore, adenosine receptors have attracted much attention as therapeutic targets for cancer treatment, although their exact roles in cancer progression still remain unclear[7]. Cancer-associated mutations in adenosine receptors have been identified from cancer patient isolates, their data stored in the Cancer Genome Atlas[8] and used by us.
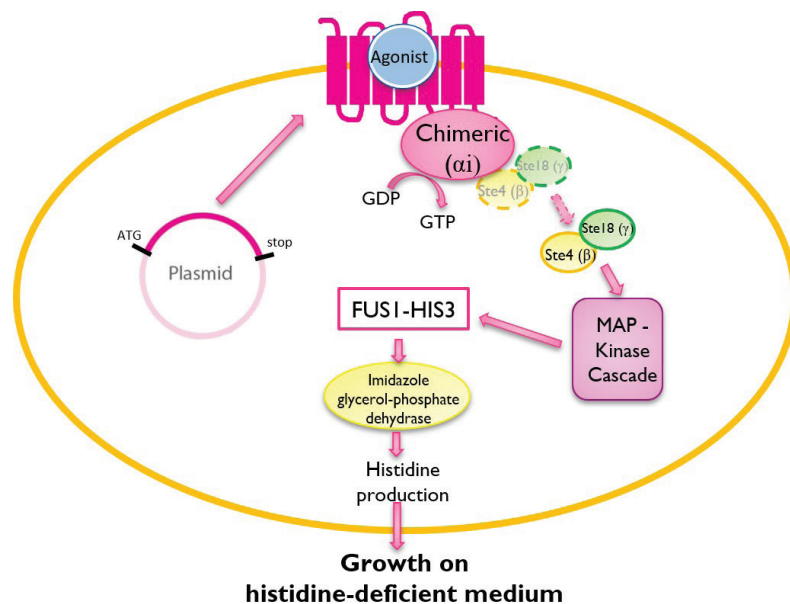
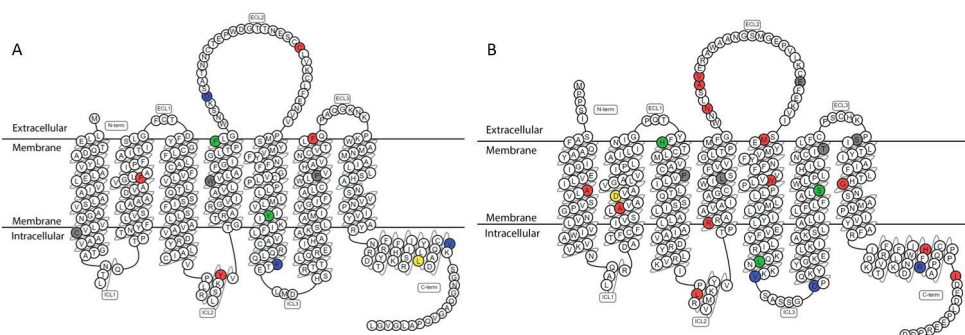**Figure 1.** Schematic picture of human GPCR expression and activation in genetically modified yeast strain MMY24.

Figure 2. Snake plot of (A) $A_{2B}AR$ and (B) A_1AR. Residues where cancer-related mutations were found are marked in colors. Yellow residues were found with more than 1 mutation. Residues identified with CAMs are colored in green, LAMs/CIMs in red, NEMs in blue and LFMs in grey. Most of the LFMs are located at the 7-TM domains. Half of mutant receptors with reduced agonist affinity or potency are at the extracellular region. Mutations positioned in the intracellular region lead to diverse effects in receptor activation.

In this thesis, we further investigated the effects of these mutations on receptor activation and ligand binding. The 15 cancer-related mutations on $A_{2B}AR$ have been identified as cancer-specific, as they do not overlap with any point mutations from the natural variance (Figure 2A). The effects of these mutations on receptor activation have been reported in **Chapter 4**. We found that these mutations resulted in 3 constitutively active mutants (CAMs), 5 less active mutants (LAMs), 4 no effect mutants (NEMs) and 3 loss of function mutants (LFMs) by using the yeast system. Among the CAMs, mutant receptor Y202C[5.58], located on a GPCR activation switch, locked the receptor in an active conformation. All 3 LFMs are located on/near the most conserved residues of the transmembrane helices, indicating the important roles of these residues in receptor functionality of $A_{2B}AR$.

In **Chapter 5 and 6**, we selected 27 point somatic mutations out of 48 total cancer-related mutations of A_1AR based on cancer types of interest (Figure 2B). In **Chapter 5**, we focused on the mutations located outside the 7-TM domains. By using the yeast system, we characterized 1 CAM, 7 constitutively inactive mutants (CIMs), 1 LFM and 3 NEMs. Mutant receptors found in ELs all showed decreased constitutive activity and/or potency of reference agonist CPA, as well as decreased affinity of DPCPX, a prototypic antagonist. However, the findings of mutational effects on receptor activation when we used the mammalian system diverged from the yeast system, especially for mutations located at ILs namely L113F[34.51] and L211R[5.69]. **Chapter 6** presents 13 cancer-related somatic mutations positioned within the 7-TM domains of A_1AR, resulting in 2 CAMs, 5 CIMs and 6 LFMs. Similar to $A_{2B}AR$, mutations located on or near conserved residues in GPCRs showed abolished receptor activation. The CAM H78L[3.23] locked the receptor in an active conformation with an extremely high constitutive activity. In summary, most of these cancer-related mutations in both $A_{2B}AR$ and A_1AR influence receptor activation, and they might eventually alter cancer hallmarks where adenosine receptors play a key role.

Residue V6.51 is a selectivity hotspot in A_2 receptors

In **Chapter 7**, we investigated the stereospecific and selective recognition of a selective $A_{2B}AR$ antagonist ISAM-140. Molecular modeling suggested that the structural determinants of this selectivity profile would be residue V250[6.51] on $A_{2B}AR$ and (*S*)-ISAM-140 as the active stereoisomer. The enantiomers of ISAM-140 were separated and their absolute configurations were unequivocally assigned via a combination of semipreparative chiral HPLC, circular dichroism spectroscopy and X-ray crystallography. The stereospecific binding mode was then confirmed by radioligand binding assays. Higher affinity of (*S*)-ISAM-140 was obtained on $A_{2B}AR$, and partially recovered affinity for both stereoisomers was observed on the L249V[6.51] $A_{2A}AR$ mutant (the $A_{2B}AR$-like mutation). This effect was explained on the basis of structure-energy modeling via rigorous free energy perturbation (FEP) calculations. In summary, this study provides useful structural insights in the stereospecific binding mode of these novel $A_{2B}AR$ antagonists, paving the way for future structure-based ligand design and optimization of selective antagonists as well as dual $A_{2A}AR/A_{2B}AR$

ligands.

Taken together, this thesis contributes to a better understanding of cancer-related mutations in GPCR pharmacology and eventually will provide potential novel approaches of modulating their activities with medicinal products. Combinatorial strategies of computational and experimental techniques could provide further insight for structure-based ligand optimization.

Future perspectives

What's more with the yeast system?

Adenosine receptors are widely distributed throughout the human body and regulate various physiological and pathological processes including neurological, cardiovascular and inflammatory diseases, and cancer[9]. In this thesis, we successfully expressed human adenosine receptors in an engineered yeast system and performed functional characterization on the cancer-related mutations of these receptors (**Chapter 4-6**). Especially for $A_{2B}AR$, as mutant receptors cannot be expressed in mammalian cells using non-viral transfection methods as mentioned in **Chapter 7**, the yeast cells in this case are the alternative expressing system with a low cost of cultivation (**Chapter 4**). Apart from mutations identified from cancer patients, adenosine receptors are known to be mutated in neurological diseases[10–13]. These mutations have been reported to associate with disease development, some are even identified to be disease-causing[11]. In this case, the yeast system can also be used for rapid functional screening of mutant receptors, as well as high-throughput screening of novel ligands targeting these disease-causing mutations in adenosine receptors.

Up till 2020, nearly 100 of human GPCRs have been expressed in *P. pastoris*[14] and more than 50 have been functionally coupled to the pheromone pathway of *S. cerevisiae*[1]. Despite the many successes in human GPCR studies with the engineered yeast cells (**Chapter 2**), drawbacks of this system are still remaining. Firstly, compared to the membranes of mammalian cells, the yeast cell membrane contains less cholesterol and higher levels of ergosterol, which may dramatically change the conformation and thus functionality of human GPCRs with specific cholesterol binding sites[15]. As discussed in **Chapter 6**, some of the mutations located on the residues pointing towards the cell membrane showed diverged effects on receptor activation in between the yeast and mammalian expressing system. Humanized yeast strains with engineered cholesterol synthesis have already been applied to better express membrane proteins[16,17]. The same approach might also help in enhancing heterologous expression of functional human GPCRs in yeast. Secondly, in order to couple a human GPCR to the yeast signaling pathway, several different types of chimeric G_α protein have been investigated resulting in chimeric G_α proteins[18]. However, as discussed in **Chapter 5**, the yeast system used in this thesis

8

might not be suitable for the investigation of mutations located in the receptor-G protein interaction interface, due to the lack of similarity to the human G_α protein. Key interactions between GPCRs and G_α proteins involve residues 12–20 of the G protein's α5-helix, although the strongest interactions are provided by the last 5 amino acids of the C-terminus[19]. Therefore, replacing only the last 5 amino acids from the yeast G_α protein might not be enough to precisely mimic human GPCR-G protein interactions. In this regard, heavily genome-modified yeast systems have been generated via the CRISPR/Cas9 technique with rational tuning of cell sensing, transcriptional regulations and various reporters[20–22]. The CRISPR technique may also be useful in generating a more humanized yeast expressing system for human GPCR studies.

How will the cancer-related mutations on GPCRs affect cancer hallmarks?

To obtain a better understanding of the complexity of cancer, "Hallmarks of Cancer" have been introduced as a useful conceptual framework to capture the complex biology of cancer in a few basic principles. The current framework consists of 10 hallmarks (Figure 3), including sustaining proliferative signaling, evading growth suppressors, activating invasion and metastasis, enabling replicative immortality, inducing angiogenesis and resisting cell death, with the addition of two emerging hallmarks (i.e. deregulating cellular energetics and avoiding immune destruction) and two enabling characteristics (i.e. genome instability and mutation, and tumor-promoting inflammation)[23]. Kinases have been investigated as prominent therapeutic targets in preclinical oncology due to their critical involvement in protein phosphorylation[24], of which abnormal function has been linked to a driver or direct outcome of the disease[23,25]. Kinase signaling pathways have been proven to be the driver in many hallmarks of cancer indeed, such as cell proliferation, angiogenesis and evasion of antitumor immune response[23]. Receptor tyrosine kinases (RTKs) in particular have been intensively investigated as promising drug targets in different types of cancer during the last two decades[26]. Up till 2019, 43 inhibitors targeting RTKs have been approved by the FDA for cancer indications[27], however, drug resistance or adverse effects appear to limit the efficacy of these RTK inhibitors (RTKIs). The most common mechanism of drug resistance is the association of mutations occurring within RTKs, which diminish the binding of RTKIs[28]. Mutations of RTKs have been identified in around 46% of all cancers[29]. Moreover, notable cancer driver hotspots, such as mutants D1228H/N/V and M1250T of hepatocyte growth factor receptor kinases, have been identified in RTKs leading to abnormal cell proliferation and tumorigenesis, and possibly the rise of drug resistance upon treatment[30]. To overcome drug resistance caused by on-target mutations, various therapeutic strategies have been designed, including combinatorial treatments targeting single or parallel kinase pathways, other therapies addressing a hallmark phenotype[31], as well as third generation RTKIs (e.g. osimertinib) with higher selectivity towards mutant RTKs[32]. Similar approaches might also benefit drug design targeting GPCRs in cancer treatment, as the many findings in RTK aberrations seem to have

a correlate in GPCRs. Also, intervening with GPCR function may help to overcome resistance in RTK-based therapy.
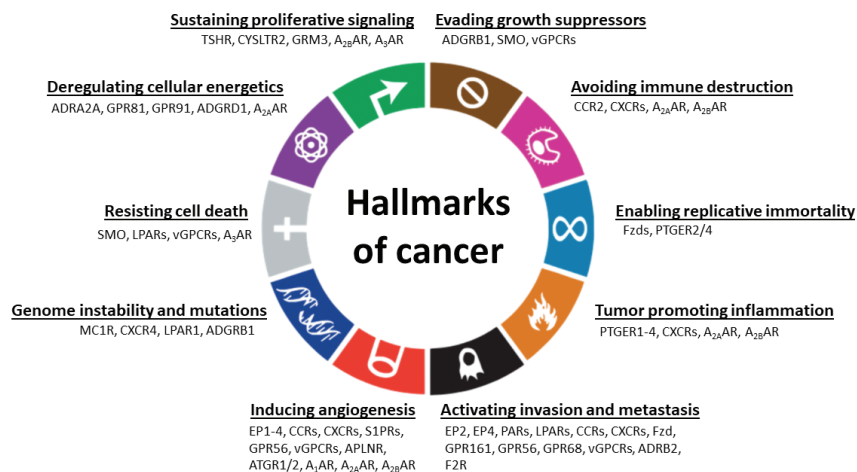

Figure 3. Examples of GPCRs in the hallmarks of cancer. Figure adapted from Arang and Gutkind[34] and Hanahan and Weinberg[23].

As summarized in **Chapter 3**, GPCRs, due to their remarkable centrality in various cellular and physiological processes, have also been identified as key participants in facilitating the hallmarks of cancer (Figure 3). Moreover, mutated GPCRs have been revealed in approximately 20% of all cancers covering various tumor types[33], which is comparable with the mutation frequency of RTKs[29]. However, for many of the GPCR mutations, their biological effects in cancer are largely unknown due to the complexity in the prediction of cancer-driving mutations[34]. Luckily, structure-function analysis of cancer-associated GPCR mutations has been developed to provide a better understanding of the functional effects of these mutations from a structural point of view[34]. An accumulation of cancer-related mutations has been observed in several highly conserved receptor sequence motifs (e.g. "DRY" and "NPxxY") as well as the highly conserved positions of TM domains (3.50, 4.50 and 7.50 according to BW numbering[35]) in comparison to other residues[36]. These conserved motifs and residues are known as key regulators in ligand binding, G protein-coupling and/ or receptor stability[37]. Mutations in these locations may lead to disabled receptor function, which has been shown in **Chapter 4** where mutant $A_{2B}AR$ W130C[4.50] resulted in a complete loss of receptor activation.

In this thesis altogether, we have characterized 40 cancer-related mutations in $A_{2B}AR$ and A_1AR (**chapter 4**, **5** and **6**) with the aim to contribute to a biological understanding from a molecular pharmacological point of view. These mutations are located all over the receptor structure (Figure 2), while interestingly enough their effects are in line with the role of receptor structure in receptor functionality. For

159

instance, the 7-TM domains including conserved motifs and residues are known to maintain receptor conformation upon activation[38]. Most of the LFMs in this thesis have been identified within this region; of note, all mutants located at the conserved residues are LFMs. Half of the mutant receptors with decreased agonist potency or affinity are positioned in the extracellular region, which regulates ligand binding[37,39]. Moreover, diverse mutational effects in receptor activation have been observed for mutations within the intracellular regions of which the conformational change influences G protein coupling[38]. Unfortunately, the effect of these cancer-related mutations on allosteric modulation still remains unclear, awaiting complete characterization of these mutations in receptor functionality. As a side note, among 40 mutations involved in this thesis, 7 of them are leucine mutations, which might be due to the higher amount of codons encoding leucine.

Although the roles of some GPCRs in cancer progression have been published, more research on their mutations and signaling pathways is warranted to fully understand their involvement in cancer hallmarks. Further studies in combination with structure-function analysis may benefit the identification of cancer driver hotspots within GPCRs. Of note, specific inhibitors targeting protein products of some passenger mutations could enhance the metabolic deleteriousness in cancer cells[40]. Taken together, addressing both driver and passenger mutations may provide strategies for the design of personalized therapeutics.

What can we improve in ligand optimization for drug discovery in oncology (and beyond)?

The first crystallographic structure of a GPCR was elucidated in 2000 for bovine rhodopsin[41]. In 2007, the first crystallographic structure of a human GPCR was published, i.e. the β_2-adrenergic receptor bound to an inverse agonist[42]. Thereafter, more high-resolution crystal structures of human GPCRs have been deciphered, paving the way for a more detailed structural insight of receptor-ligand interactions in GPCRs. Knowing the architecture of the ligand binding site is very helpful for structure-based drug design[43]. Unfortunately, huge numbers of GPCR structures still remain unresolved due to difficulties in pure protein isolation, crystal diffraction and many other technical problems. Homology/comparative modeling in this case could be used in structure-based studies when 3D structures are not available for the GPCR of interest[44].

A homology model predicts the 3D structure of an unknown protein based on known 3D structures of proteins with homologous sequence [45,46]. It has been shown that the usage of multiple templates provides better homology models when templates share low sequence identity with the target protein[47–49]. A homology model of $A_{2B}AR$, developed using crystal structures of $hA_{2A}AR$ as templates, has been used in this thesis to provide a structural explanation of the impact the cancer-related mutations may have in receptor activation (**Chapter 4**). Docking is a computational method used to predict ligand-protein interactions and relative measures of affinity for series

of ligands binding to a protein of interest[50]. Having an $A_{2B}AR$ homology model, we were able to predict the selectivity hotspot for stereoselective antagonist recognition in $A_{2B}AR$, which was confirmed by site-directed mutagenesis experiments (**Chapter 7**). Additionally, receptor ensemble docking studies have shown promising results supporting the application of a homology model in virtual screening for the discovery of novel GPCR ligands[51]. Moreover, key residues in A_3AR and $A_{2A}AR$ for covalent interaction between ligand and receptor were predicted via assigning the docking mode towards a specific amino acid residue, and the hypothesis was further confirmed by mutagenesis study[52,53]. An increasing number of crystal structures of human GPCRs are expected to be resolved in the near future, and be used for *in silico* drug discovery studies and homology model development. More recently, a novel neural network AlphaFold has been published with atomic accuracy in predicting protein structures based on sequence combined with machine learning, providing a complementary approach to homology modeling[54]. With the help of various computer-aided techniques, more accurate homology modeling for other GPCRs will be developed in order to increase the chance of novel ligand identification, as well as ligand design and optimization for GPCRs in general.

8

Final notes

All in all, this thesis is focused on characterizing cancer-related somatic mutations in adenosine receptors with respect to receptor activation and ligand binding. We also confirmed that the yeast system is well suitable for the rapid and initial functional screening of these mutations on $A_{2B}AR$ and A_1AR. The results obtained in the thesis contribute to a better understanding of receptor functionality at the structural level, as well as at the pathologically relevant level. Additionally, with the combination of computational and experimental approaches, we expanded the insight of structure-based selective ligand design and optimization. Finally, we hope that the findings from this thesis can provide potential strategies in cancer therapeutics and further drug development.

References

1. Lengger, B. & Jensen, M. K. Engineering G protein-coupled receptor signalling in yeast for biotechnological and medical purposes. *FEMS Yeast Res.* **20**, 1–13 (2020).
2. Karbalaei, M., Rezaee, S. A. & Farsiani, H. Pichia pastoris: A highly successful expression system for optimal synthesis of heterologous proteins. *J. Cell. Physiol.* **235**, 5867–5881 (2020).
3. Nakayama, N., Miyajima, A. & Arai, K. Nucleotide sequences of STE2 and STE3 , cell type-specific sterile genes from Saccharomyces cerevisiae . *EMBO J.* **4**, 2643–2648 (1985).
4. Hauser, A. S., Attwood, M. M., Rask-Andersen, M., Schiöth, H. B. & Gloriam, D. E. Trends in GPCR drug discovery: New agents, targets and indications. *Nat. Rev. Drug Discov.* **16**, 829–842 (2017).
5. Lagerström, M. C. & Schiöth, H. B. Structural diversity of G protein-coupled receptors and significance for drug discovery. *Nat. Rev. Drug Discov.* **7**, 339–57 (2008).
6. Antonioli, L. *et al.* Adenosine and inflammation: what's new on the horizon? *Drug Discov. Today* **19**, 1051–1068 (2014).
7. Borea, P. A., Gessi, S., Merighi, S., Vincenzi, F. & Varani, K. Pathological overproduction: the bad side of adenosine. *Br. J. Pharmacol.* **174**, 1945–1960 (2017).
8. *Broad Institute TCGA Genome Data Analysis Center (2016): Analysis-ready standardized TCGA data from Broad GDAC Firehose stddata_2015_08_21 run. Broad Institute of MIT and Harvard.* (2016). doi:10.7908/C18W3CNQ

9. Trincavelli, M. L., Daniele, S. & Martini, C. Adenosine Receptors: What We Know and What We are Learning. *Curr. Top. Med. Chem.* **10**, 860–877 (2010).
10. Nasrollahi-Shirazi, S. *et al.* Functional impact of the G279S substitution in the adenosine A$_1$-receptor (A$_1$R-G279S[7.44]), a mutation associated with Parkinson's disease. *Mol. Pharmacol.* **98**, 250-266 (2020).
11. Jaberi, E. *et al.* Mutation in ADORA1 identified as likely cause of early-onset parkinsonism and cognitive dysfunction. *Mov. Disord.* **31**, 1004–1011 (2016).
12. Huin, V. *et al.* Neurogenetics of the Human Adenosine Receptor Genes: Genetic Structures and Involvement in Brain Diseases. *J. Caffeine Adenosine Res.* **9**, 73–88 (2019).
13. Luu, S. U. *et al.* Mutation analysis of adenosine A$_{2a}$ receptor gene and interaction study with dopamine D$_2$ receptor gene in schizophrenia. *Psychiatr. Genet.* **18**, 43 (2008).
14. Lundstrom, K. *et al.* Structural genomics on membrane proteins: Comparison of more than 100 GPCRs in 3 expression systems. *J. Struct. Funct. Genomics* **7**, 77–91 (2006).
15. Paila, Y. D., Tiwari, S. & Chattopadhyay, A. Are specific nonannular cholesterol binding sites present in G-protein coupled receptors? *Biochim. Biophys. Acta - Biomembr.* **1788**, 295–302 (2009).
16. Elkins, M. R., Sergeyev, I. V. & Hong, M. Determining Cholesterol Binding to Membrane Proteins by Cholesterol 13C Labeling in Yeast and Dynamic Nuclear Polarization NMR. *J. Am. Chem. Soc.* **140**, 15437–15449 (2018).
17. Hirz, M., Richter, G., Leitner, E., Wriessnegger, T. & Pichler, H. A novel cholesterol-producing *Pichia pastoris* strain is an ideal host for functional expression of human Na,K-ATPase α3β1 isoform. *Appl. Microbiol. Biotechnol.* **97**, 9465–9478 (2013).
18. Brown, A. J. *et al.* Functional coupling of mammalian receptors to the yeast mating pathway using novel yeast/mammalian G protein α-subunit chimeras. *Yeast* **16**, 11–22 (2000).
19. Draper-Joyce, C. J. *et al.* Structure of the adenosine-bound human adenosine A$_1$ receptor–G$_i$ complex. *Nature* **558**, 559–563 (2018).
20. Shaw, W. M. *et al.* Engineering a Model Cell for Rational Tuning of GPCR Signaling. *Cell* **177**, 782-796.e27 (2019).
21. Rowe, J. B., Taghon, G. J., Kapolka, N. J., Morgan, W. M. & Isom, D. G. CRISPR-addressable yeast strains with applications in human G protein– coupled receptor profiling and synthetic biology. *J. Biol. Chem.* **295**, 8262–8271 (2020).
22. Meng, J., Qiu, Y. & Shi, S. CRISPR/Cas9 Systems for the Development of *Saccharomyces cerevisiae* Cell Factories. *Front. Bioeng. Biotechnol.* **8**, 1–8 (2020).
23. Hanahan, D. & Weinberg, R. A. Hallmarks of cancer: The next generation. *Cell* **144**, 646–674 (2011).
24. Kan, Z. *et al.* Diverse somatic mutation patterns and pathway alterations in human cancers. *Nature* **466**, 869–73 (2010).
25. Cohen, P. Protein kinases — the major drug targets of the twenty-first century? *Nat. Rev. Drug Discov.* **1**, 309–315 (2002).
26. Pottier, C. *et al.* Tyrosine kinase inhibitors in cancer: Breakthrough and challenges of targeted therapy. *Cancers (Basel).* **12**, (2020).
27. Roskoski, R. Properties of FDA-approved small molecule protein kinase inhibitors: A 2020 update. *Pharmacol. Res.* **152**, 104609 (2020).
28. Fabbro, D., Cowan-Jacob, S. W. & Moebitz, H. Ten things you should know about protein kinases: IUPHAR Review 14. *Br. J. Pharmacol.* **172**, 2675–2700 (2015).
29. Sanchez-Vega, F. *et al.* Oncogenic Signaling Pathways in The Cancer Genome Atlas. *Cell* **173**, 321-337.e10 (2018).
30. Torkamani, A., Verkhivker, G. & Schork, N. J. Cancer driver mutations in protein kinase genes. *Cancer Lett.* **281**, 117–127 (2009).
31. Gross, S., Rahal, R., Stransky, N., Lengauer, C. & Hoeflich, K. P. Targeting cancer with kinase inhibitors Find the latest version : Targeting cancer with kinase inhibitors. *J. Clin. Invest.* **125**, 1780–1789 (2015).
32. Song, Q., Sun, X., Guo, H. & Yu, Q. Concomitant inhibition of receptor tyrosine kinases and downstream AKT synergistically inhibited growth of KRAS/BRAF mutant colorectal cancer cells. *Oncotarget* **8**, 5003–5015 (2017).
33. O'Hayre, M. *et al.* The emerging mutational landscape of G proteins and G-protein-coupled receptors in cancer. *Nat. Rev. Cancer* **13**, 412–24 (2013).
34. Arang, N. & Gutkind, J. S. G Protein-Coupled receptors and heterotrimeric G proteins as cancer drivers. *FEBS Lett.* **594**, 4201–4232 (2020).
35. Ballesteros, J. A. & Weinstein, H. Integrated methods for the construction of three-dimensional models and computational probing of structure-function relations in G protein-coupled receptors. in *Methods in Neurosciences* **25**, 366–428 (1995).
36. Bongers, B. J. *et al.* Pan-cancer in silico analysis of somatic mutations in G-protein coupled receptors: The effect of evolutionary conservation and natural variance. *bioRxiv Prepr.* (2021). doi:doi.org/10.1101/2021.10.25.465693
37. Jespers, W. *et al.* Structural mapping of adenosine receptor mutations: ligand binding and signaling mechanisms. *Trends Pharmacol. Sci.* **39**, 75–89 (2017).
38. Yang, D. *et al.* G protein-coupled receptors: structure- and function-based drug discovery. *Signal Transduct. Target. Ther.* **6**, (2021).
39. Peeters, M. C., van Westen, G. J. P., Li, Q. & IJzerman, A. P. Importance of the extracellular loops in G protein-coupled receptors for ligand recognition and receptor activation. *Trends Pharmacol. Sci.* **32**, 35–42 (2011).
40. Monticelli, M. *et al.* Passenger mutations as a target for the personalized therapy of cancer. *PeerJ* **Preprints**, (2018).
41. Palczewski, K. *et al.* Crystal structure of rhodopsin: A G protein-coupled receptor. *Science* **289**, 739–745 (2000).
42. Lemoine, D. *et al.* Ligand-Gated Ion Channels: New Insights into Neurological Disorders and Ligand Recognition. *Chem. Rev.* **112**, 6285–6318 (2012).
43. Henry, C. Structure-based drug design. *Chem. Eng. News* **79**, 69–78 (2001).
44. Payghan, P. V, Bera, I., Bhattacharyya, D. & Ghoshal, N. Computational Studies for Structure-Based Drug Designing Against Transmembrane Receptors: pLGICs and Class A GPCRs. *Front. Phys.* **6**, 1–23 (2018).
45. Blundell, T. L., Sibanda, B. L., Sternberg, M. J. & Thornton, J. M. Knowledge-based prediction of protein structures and the design of novel molecules. *Nature* **326**, 347–352 (1987).
46. Martí-Renom, M. A. *et al.* Comparative protein structure modeling of genes and genomes. *Annu. Rev. Biophys. Biomol. Struct.* **29**, 291–325 (2000).
47. Kneissl, B., Leonhardt, B., Hildebrandt, A. & Tautermann, C. S. Revisiting automated G-protein coupled receptor modeling: the benefit of additional template structures for a neurokinin-1 receptor model. *J. Med. Chem.* **52**, 3166–3173 (2009).
48. Mobarec, J. C., Sanchez, R. & Filizola, M. Modern Homology Modeling of G-Protein Coupled Receptors: Which Structural Template to Use? *J. Med. Chem.* **52**, 5207–5216 (2009).
49. de Graaf, C. & Rognan, D. Customizing G Protein-coupled receptor models for structure-based virtual screening. *Curr. Pharm. Des.* **15**, 4026–4048 (2009).
50. Dias, R. & de Azevedo, W. F. J. Molecular docking algorithms. *Curr. Drug Targets* **9**, 1040–1047 (2008).

51. Vilar, S. *et al.* Docking-based virtual screening for ligands of G protein-coupled receptors: Not only crystal structures but also in silico models. *J. Mol. Graph. Model.* **29**, 614–623 (2011).

52. Yang, X. *et al.* Development of Covalent Ligands for G Protein-Coupled Receptors: A Case for the Human Adenosine A_3 Receptor. *J. Med. Chem.* **62**, 3539–3552 (2019).

53. Yang, X. *et al.* A covalent antagonist for the human adenosine A_{2A} receptor. *Purinergic Signal.* **13**, 191–201 (2017).

54. Jumper, J. *et al.* Highly accurate protein structure prediction with AlphaFold. *Nature* **596**, 583–589 (2021).

8

Summary

G protein-coupled receptors (GPCRs), one of the largest families of membrane proteins, are responsive to a diverse set of physiological endogenous ligands including hormones and neurotransmitters. Due to the various GPCR ligand binding domains present on GPCRs and their sensitivities to a diverse array of ligands, these proteins have shown to be very 'druggable' as they are the main target for an estimated 30% of approved drugs. A growing body of evidence shows a prominent role of GPCRs in all phases of cancer with a mutation frequency of approximately 20% in all cancers. Mutations occurring in GPCRs can severely alter their normal function and may ultimately convert their physiological and pathological roles. One particular class of rhodopsin-like GPCRs included in this thesis are the adenosine receptors (ARs). Due to the accumulation of adenosine in the tumor microenvironment, all four subtypes of ARs might be targets for the development of novel approaches for the treatment of cancer. For each of the four subtypes, a number of somatic mutations have been identified in patient isolates. In this thesis, we examined them on receptor activation and ligand binding using reference adenosine receptor ligands, and determined the impact mutations have on these pharmacological readouts.

Chapter 1 serves as an introduction covering the main concepts in this thesis. **Chapter 2** continues with the strategies of using yeast systems in human GPCR studies with a focus on adenosine receptors. The chapter starts with general features of budding yeast with multiple modifications in the yeast pheromone signaling pathway to be used for human GPCR studies. Subsequently, highlighted studies on ARs expression and functionality in yeast expressing systems are described. **Chapter 3** provides an overview of current existing evidence for the involvements of GPCRs and their signaling pathways in tumor biology, as well as the effect of mutations in receptor pharmacology and their potential impacts in cancer development and progression. Furthermore, evidence for ARs in cancer development is discussed in detail.

As mutations of ARs have been identified from cancer patient isolates, **Chapter 4-6** provide information on the impact of these mutations in receptor functionality. **Chapter 4** focuses on receptor expression and activation of cancer-related mutations on adenosine A_{2B} receptors ($A_{2B}AR$) using an engineered yeast system, MMY24. The 15 cancer-related mutations included in this chapter have been identified as cancer-specific. These mutations resulted in 3 constitutively active mutants (CAMs), 5 less active mutants (LAMs), 4 no effect mutants (NEMs) and 3 loss of function mutants (LFMs). Among the CAMs, mutant receptor $Y202C^{5.58}$, located on a GPCR activation switch, locked the receptor in an active conformation. All 3 LFMs are located on/near the most conserved residues of the transmembrane helices, indicating the important roles of these residues in receptor functionality of $A_{2B}AR$.

The effects of cancer-related mutations on adenosine A_1 receptors (A_1AR) on receptor activation and ligand binding are described in **Chapters 5** and **6**. **Chapter 5** describes twelve mutations located at the loop regions. By using the same yeast system, we characterized 1 CAM, 7 constitutively inactive mutants (CIMs), 1 LFM and 3 NEMs. All mutant receptors found in extracellular loops (ELs) showed decreased constitutive activity and/or potency of reference agonist CPA, as well as decreased affinity of DPCPX, a prototypic antagonist. However, the findings of mutational effects on receptor activation when we used a mammalian system diverged from the yeast system, especially for mutations located at intracellular loops (ILs), namely L113F[34.51] and L211R[5.69]. The yeast system used in this thesis might therefore not be suitable for the investigation of mutations located in the receptor-G protein interaction interface, due to the lack of similarity to the human G_α protein. **Chapter 6** focuses on 13 mutations positioned in the 7-transmembrane (7-TM) domains, resulting in 2 CAMs, 5 CIMs and 6 LFMs. Similar to A_{2B}AR, mutations located on or near conserved residues in GPCRs showed abolished receptor activation. The CAM H78L[3.23] locked the receptor in an active conformation with an extremely high constitutive activity. Some of the mutations located on the residues pointing towards the cell membrane showed divergent effects on receptor activation between the yeast and mammalian expression system. Most of the investigated cancer-related mutations in both A_{2B}AR and A_1AR influence receptor activation, and they might eventually alter cancer hallmarks where adenosine and adenosine receptors play a key role.

Chapter 7 reports the approach for the identification of a stereoselectivity hotspot in A_{2B}AR antagonist recognition from both computational and experimental aspects. Having an A_{2B}AR homology model, we were able to predict the selectivity hotspot for stereoselective antagonist recognition. Molecular modeling suggested that the structural determinants of this selectivity profile would be residue V250[6.51] on A_{2B}AR and the (*S*)-stereoisomer of the ligand ISAM-140. The enantiomers of ISAM-140 were separated and their absolute configurations were unequivocally assigned via a combination of semipreparative chiral HPLC, circular dichroism spectroscopy and X-ray crystallography. The stereospecific binding mode was then confirmed by site-directed mutagenesis experiments and radioligand binding assays. Higher affinity of (*S*)-ISAM-140 was obtained on A_{2B}AR, and a partially recovered affinity for both stereoisomers was observed on the L249V[6.51] A_{2A}AR mutant (the A_{2B}AR-like mutation). This effect was explained on the basis of structure-energy modeling via rigorous free energy perturbation (FEP) calculations.

The overall conclusion from the results of the individual experimental chapters are discussed in detail in **Chapter 8**. This chapter also provides future prospects and challenges that emerge from the research presented in this thesis.

Samenvatting

G-proteïnegekoppelde receptoren (GPCRs), één van de grootste families van membraaneiwitten, reageren op een diverse reeks fysiologische endogene liganden, waaronder hormonen en neurotransmitters. Door hun verschillende ligand-bindende domeinen en hun gevoeligheden voor een diverse reeks liganden is aangetoond dat deze eiwitten zeer 'druggable' zijn. Ze vormen het belangrijkste doelwit voor naar schatting 30% van de goedgekeurde geneesmiddelen. Een groeiend aantal bewijzen toont een prominente rol aan voor GPCRs in alle fasen van kanker, met een mutatiefrequentie van ongeveer 20% in alle kankers. Mutaties die optreden in GPCRs kunnen hun normale functie ernstig veranderen, zelfs zodanig dat hun fysiologische in een pathologische rol verandert. Een bepaalde klasse van rodopsine-achtige GPCRs die in dit proefschrift zijn opgenomen, is die van de adenosinereceptoren (ARs). Vanwege de accumulatie van adenosine in de tumor micro-omgeving kunnen alle vier de subtypes van ARs aangrijpingspunten zijn voor de ontwikkeling van nieuwe geneesmiddelen voor de behandeling van kanker. Voor elk van de vier subtypes is een aantal somatische mutaties geïdentificeerd in monsters van kankerpatiënten. In dit proefschrift hebben we de impact bepaald van deze mutaties op receptoractivering en ligandbinding met behulp van referentie-adenosinereceptorliganden, en op deze farmacologische eindpunten.

Hoofdstuk 1 dient als inleiding en behandelt de belangrijkste concepten in dit proefschrift. **Hoofdstuk 2** gaat verder met de strategieën van het gebruik van gistsystemen in menselijke GPCR-onderzoeken met een focus op adenosinereceptoren. Het hoofdstuk begint met algemene kenmerken van gistcellen met meerdere modificaties in de gistferomoon signaleringsroute voor menselijke GPCR-onderzoeken. Vervolgens worden studies over de expressie en functionaliteit van ARs in gistsystemen die ARs tot expressie brengen, beschreven. **Hoofdstuk 3** geeft een overzicht van het huidige bewijs voor de betrokkenheid van GPCRs en hun signaalroutes in de tumorbiologie, evenals het effect van mutaties in de receptorfarmacologie en hun mogelijke effecten op de ontwikkeling en progressie van kanker. Bovendien wordt het bewijs voor ARs bij de ontwikkeling van kanker in detail besproken.

Aangezien mutaties van de adenosinereceptoren zijn geïdentificeerd in monsters van kankerpatiënten, wordt in **Hoofdstuk 4-6** informatie gegeven over de impact van deze mutaties op de receptorfunctionaliteit. **Hoofdstuk 4** richt zich op receptorexpressie en activering van kanker-gerelateerde mutaties op adenosine A_{2B} receptoren ($A_{2B}AR$) met behulp van het bovengenoemde gemanipuleerde gistsysteem, gecodeerd als MMY24. De 15 kanker-gerelateerde mutaties die in dit hoofdstuk zijn opgenomen, zijn geïdentificeerd als kankerspecifiek. Deze mutaties resulteerden in 3 constitutief actieve mutanten (CAM), 5 minder actieve mutanten (LAM), 4 geen effect-mutanten (NEM) en 3 functieverliesmutanten (LFM). Van de CAM's zette de ge-

muteerde receptor Y202C[5.58], die zich op een GPCR-activeringsschakelaar bevindt, de receptor vast in een actieve conformatie. Alle drie LFM's bevinden zich op/bij de meest geconserveerde residuen van de transmembraanhelices, wat de belangrijke rol van deze residuen in de receptorfunctionaliteit van $A_{2B}AR$ aangeeft.

De effecten van kanker-gerelateerde mutaties in adenosine A_1 receptoren (A_1AR) op receptoractivering en ligandbinding worden beschreven in **Hoofdstuk 5** en **6**. **Hoofdstuk 5** beschrijft twaalf mutaties die zich in de loopregio's bevinden. Door hetzelfde gistsysteem te gebruiken, hebben we 1 CAM, 7 constitutief inactieve mutanten (CIM), 1 LFM en 3 NEM's gekarakteriseerd. Alle gemuteerde receptoren die in de extracellulaire loops (EL's) werden gevonden, vertoonden verminderde constitutieve activiteit en/of potentie van referentie-agonist CPA, evenals verminderde affiniteit van DPCPX, een prototypische antagonist. In een aan zoogdieren gerelateerd testsysteem weken de effecten van mutaties op receptoractivering af van het gistsysteem, vooral voor mutaties L113F[34.51] en L211R[5.69]die zich op intracellulaire loops (IL's) bevinden. Het gistsysteem dat in dit proefschrift wordt gebruikt is mogelijk niet geschikt voor het onderzoeken van mutaties in de receptor-G-eiwitinteractie-interface, vanwege het gebrek aan gelijkenis met het menselijke G_α-eiwit. **Hoofdstuk 6** richt zich op 13 mutaties gepositioneerd in de 7-transmembraan (7-TM) domeinen, resulterend in 2 CAMs, 5 CIMs en 6 LFMs. Net als bij $A_{2B}AR$ vertoonden mutaties op of nabij geconserveerde residuen in GPCRs een verminderde receptoractivering. De CAM H78L[3.23] zette de receptor vast in een actieve conformatie met een extreem hoge constitutieve activiteit. Sommige van de mutaties op de residuen die naar het celmembraan wijzen vertoonden uiteenlopende effecten op de receptoractivering tussen het gist- en zoogdierexpressiesysteem. De meeste van deze kanker-gerelateerde mutaties in zowel $A_{2B}AR$ als A_1AR beïnvloeden de activering van receptoren, en kunnen uiteindelijk de kenmerken van kanker waar adenosine en adenosinereceptoren een sleutelrol spelen veranderen.

Hoofdstuk 7 rapporteert de aanpak voor de identificatie van een stereoselectiviteitshotspot in de herkenning van $A_{2B}AR$ vanuit zowel computationele als experimentele aspecten. Met een $A_{2B}AR$-homologiemodel konden we de selectiviteitshotspot voor stereoselectieve antagonistherkenning voorspellen. Moleculaire modellering suggereerde dat de structurele determinanten van dit selectiviteitsprofiel residu V250[6.51] op $A_{2B}AR$ en (*S*)-ISAM-140 als het actieve stereo-isomeer van het ligand zouden zijn. De enantiomeren van ISAM-140 werden gescheiden en hun absolute configuraties werden eenduidig toegewezen via een combinatie van semipreparatieve chirale HPLC, circulair dichroïsme spectroscopie en röntgenkristallografie. De stereospecifieke bindingsmodus werd vervolgens bevestigd door plaatsgerichte mutagenese-experimenten en radioligandbindingsassays. Hogere affiniteit van (*S*)-ISAM-140 werd verkregen op $A_{2B}AR$ en een gedeeltelijk herstelde affiniteit voor beide stereo-isomeren werd waargenomen op de L249V[6.51] $A_{2A}AR$-mutant (de $A_{2B}AR$-achtige mutatie). Dit effect werd verklaard op basis van structuur-energiemodellering via

rigoureuze vrije-energieverstoringsberekeningen (FEP).

De algemene conclusies uit de resultaten van de afzonderlijke experimentele hoofd-stukken worden in detail besproken in **hoofdstuk 8**. Dit hoofdstuk biedt ook toekom-stperspectieven en uitdagingen die uit het onderzoek beschreven in dit proefschrift naar voren komen.

List of publications

Part of this thesis:

Wang X, Jespers W, de Waal JJ, Wolff KAN, de Uden L, IJzerman AP, van Westen GJP, Heitman LH. *Cancer-related somatic mutations alter adenosine A$_1$ receptor pharmacology – a focus on mutations in the loops and C-terminus*. FASEB J **2022**, 36:e22358. Doi: 10.1096/fj.202200203RR.

Wang X, Jespers W, Wolff KAN, Buytelaar J, IJzerman AP, van Westen GJP, Heitman LH. *Cancer-related somatic mutations in transmembrane helices alter adenosine A$_1$ receptor pharmacology.* Molecules **2022**, 27(12):3742. Doi: 10.3390/molecules27123742.

Wang X, van Westen GJP, IJzerman AP, Heitman LH. *G protein-coupled receptors and their mutations in cancer – a focus on adenosine receptors.* GPCRs as Therapeutic Targets Manuscript in press.

Wang X, van Westen GJP, Heitman LH, IJzerman AP. *G protein-coupled receptors expressed and studied in yeast. The adenosine receptor as a prime example.* Biochem Pharmacol **2021,** 187:114370. Doi: 10.1016/j.bcp.2020.114370.

Wang X*, Jespers W*, Prieto-Díaz R*, Majellaro M, IJzerman AP, van Westen GJP, Sotelo E, Heitman LH, Gutiérrez-de-Terán H. *Identification of V6.51L as a selectivity hotspot in stereoselective A$_{2B}$ adenosine receptor antagonist recognition*. Sci Rep **2021,** 11:14171. Doi: 10.1038/s41598-021-93419-x.

*These authors contributed equally.

Wang X*, Jespers W*, Bongers B, Habben Jansen MCC, Stangenberger CM, Dilweg MA, Gutiérrez-de-Terán H, IJzerman AP, Heitman LH, van Westen GJP. *Characterization of cancer-related somatic mutations in the adenosine A$_{2B}$ receptor.* Eur J Pharmacol. **2020,** 880:173126. Doi: 10.1016/j.ejphar.2020.173126.

*These authors contributed equally.

Not part of this thesis:

Doornbos MLJ, <u>Wang X</u>, Vermond SC, Peeters L, Pérez-Benito L, Trabanco A, Lavreysen H, María Cid J, Heitman LH, Tresadern G, IJzerman AP. *Covalent allosteric probe for the metabotropic glutamine captoror 2: design, synthesis, and pharmacological characterization*. J Med Chem. **2019,** 62:223-233. Doi: 10.1021/acs.jmedchem.8b00051.

Bongers B, Gorostiola González M, <u>Wang X</u>, van Vlijmen HWT, Jespers W, Gutiérrez-de-Terán H, Ye K, IJzerman AP, Heitman LH, van Westen GJP. *Pan-cancer in silico analysis of somatic mutations in G protein-coupled receptors: the effect of evolutionary conservation and natural variance*. Manuscript in preparation.

Feng C, <u>Wang X</u>, Jespers W, Liu R, Zamarbide Losada SD, Gorostiola González M, van Westen GJP, Danen EHJ, Heitman LH. *The impact of cancer-related mutations on ligand binding at the adenosine A_{2A} receptor and its function*. Manuscript submitted.

Beerkens BLH, <u>Wang X</u>, Avgeropoulou M, Adistia LN, van Veldhoven JPD, Jespers W, Liu R, Heitman LH, IJzerman AP, van der Es D. *Development of subtype-selective covalent ligands for the adenosine A_{2B} receptor by tuning the reactive group*. RSC Med Chem, manuscript in press.

Oral and poster communications:

2020-May LACDR Spring Symposium, oral communication

2019-Oct FIGON DMD, Leiden, the Netherlands, poster presentation

2018-Oct FIGON DMD Ede, the Netherlands, oral communication (selected poster abstract)

2017-May LACDR Spring Symposium, poster presentation (best poster prize)

Curriculum Vitae

Xuesong Wang was born on January 6th, 1992 in Xi'an, Shaanxi and grew up in Zhuhai, Guangdong, China. After graduating from the No.1 High School of Zhuhai in 2010, she started her study in pharmaceutical science at the China Pharmaceutical University and obtained her bachelor degree. In 2014, she moved to the Netherlands and followed the master's program of Biopharmaceutical Sciences at Leiden University. During her master study, she performed a 9-month internship at the Division of Pharmacology, of the Leiden Academic Centre for Drug Research (LACDR), under supervision of Dirk-Jan van den Berg and Prof. Dr. Elizabeth de Lange. The project focused on the influence of P-glycoprotein and multidrug resistance protein mediated blood-brain-barrier transport on the brain distribution of the antineoplastic etoposide. After her first internship, she performed a second 6-month internship at the Division of Medicinal Chemistry, under supervision of Dr. Maarten Doornbos and Prof. Dr. Laura Heitman. There, she worked on a project focused on the characterization of potential covalent allosteric modulators for the metabotropic glutamate receptor 2, which resulted in a published research article.

In 2016, she was sponsored by the China Scholarship Council (CSC) to perform her PhD research at the Division of Drug Discovery and Safety (former Division of Medicinal Chemistry), LACDR under supervision of Prof. Dr. Laura Heitman, Prof. Dr. Gerard van Westen and Prof. Dr. Ad IJzerman. Her project focused on the characterization of (cancer-related) mutations in adenosine receptors on ligand binding and receptor activation. Throughout her PhD, she presented the work described in this thesis several times at various national and international conferences, including the FIGON Dutch Medicine Day (2017 – 2019). In 2018, she was awarded the 1st poster prize at the LACDR Spring Symposium. From 2020 to 2021, she worked as the educational support at the same division. As of December 2021, she works as a postdoctoral researcher under supervision of Prof. Dr. Bob van de Water and Dr. Sylvia Le Dévédec.

Acknowledgments

The work presented in this thesis would not have been possible without the contributions and support of many different people. I'm deeply grateful to everyone I have collaborated with for their input that enabled my PhD work to reach the current state.

In particular, I would like to thank Ad, Laura and Gerard for their endless patience, encouragement, inspiration and trust throughout not only my PhD study, but ever since I started in our research group as a master student. I have had many supervisors since I started at Leiden University, my daily supervisors Dirk-Jan and Maarten during my master, and as a PhD candidate, Ad, Laura and Gerard. You all have taught me different things. Thank you for your constructive criticism, practical input, guiding hand and insightful advice.

I would like to thank all my colleagues and students for their company throughout this scientific journey. To my students, especially my master students Carolien, Just, Kim, Mariangela, Liedeke and Jill, who have greatly contributed to parts of this thesis and gave me their great inspiration to work on these projects. To my collaborators, Willem, Brandon, Hugo and Eddy, who have broadened my vision and greatly facilitated my research projects. To my officemates, Indira, Julia, Anna, Huub, Jara and Tamara for their persistent invitations for coffee breaks and interesting scientific discussions. To Thea, Henk, Rongfang and Cas, for the steady support in the lab. Special thanks to many great people, Daan, Jaco, Maarten, Marina, Lance, Xue, Chenlin, Bert, Majlen, Tasia and Yao for all the fun and distress activities. To the MedChem beach volleyball team, Lindsey, Sebastian, Hein and Olivier for all the great winning or losing moments. To Lisa, Natalia and Lia, for sharing many animal pictures which brought up some non-scientific discussions alongside scientific work.

Finally, I would like to thank my beloved family and friends. To my best friends, Yuhanyang, Junyan, Yin, Meiling and Wenbin for their endless encouragement from six time zones away. To my boyfriend, Ka Chun, for his understanding, patience and support since we have met. To my parents for their long-term encouragement and support during the trip to my dream for many years.

And to all the people that I may have forgotten, as acknowledgements can never be complete.